University of São Paulo
"Luiz de Queiroz" College of Agriculture

Assessing carbon dynamics of irrigated and rainfed potato (*Solanum tuberosum* L.) cropping systems in the Andean hillside landscape

Fabio Ernesto Martínez Maldonado

Thesis presented, to obtain the degree of Doctor in Science. Area: Agricultural Systems Engineering

Piracicaba
2023

Fabio Ernesto Martínez Maldonado
Agricultural Engineer, M.Sc., Agricultural Sciences major on Crop Physiology

Assessing carbon dynamics of irrigated and rainfed potato (*Solanum tuberosum* L.) cropping systems in the Andean hillside landscape

versão revisada de acordo com a Resolução CoPGr 6018 de 2011

Advisor:
Prof. Dr. **FÁBIO RICARDO MARIN**

Thesis presented to obtain the degree of Doctor in Science. Area: Agricultural Systems Engineering

Piracicaba
2023

Dados Internacionais de Catalogação na Publicação
DIVISÃO DE BIBLIOTECA – DIBD/ESALQ/USP

Martínez Maldonado, Fabio Ernesto

Assessing carbon dynamics of irrigated and rainfed potato (*Solanum tuberosum* L.) cropping systems in the Andean hillside landscape / Fabio Ernesto Martínez Maldonado. - - versão revisada de acordo com a Resolução CoPGr 6018 de 2011. - - Piracicaba, 2023.

132 p.

Tese (Doutorado) - - USP / Escola Superior de Agricultura “Luiz de Queiroz”.

1. Batata 2. Balanço de carbono 3. Eddy covariance 4. Up-scaling 5. Fator de acoplamento 6. Omega I. Título

DEDICATION

To my parents Ernesto and Martha.
To my sister Gina and my nephews Sofia and Joshua
To my little brother, Nico, to whom I owe the new north (Yes, it was possible)
To my life partner, Zahara Lucia
To Yairu and Quynde
To the father
To the protective mother
To agricultural sciences
To the Latin American peasants

ACKNOWLEDGMENTS

To Professor Fábio Marin for all his guidance, support, and knowledge transmitted. For his example of scientific rigor and above all the trust placed in me.

To Dra. Angela Castaño, for her generosity, guidance, and patience. Thank you for opening the possibility of this research and area of knowledge, especially thanks for the friendship, trust, and total support in my process.

To Gerardo Goez, for his friendship, his friendship, and always a great deal of support.

To Zahara Lasso, for her unconditional love and support throughout the development of this thesis. Her support in the most difficult moments was decisive.

To my parents, for your constant love and support. Overall, thanks, Mom.

To José Molina, Elías Silva, Duván Ocampo, Laura Torres, Douglas Gómez, and Gustavo Araujo for their support in the field experiments and their valuable friendship.

To Rafael Gómez my friend, for his advice, company, and family hug. To Mónica Fuentes, for her unconditional support. Thanks, guys.

To the Colombian Corporation for Agricultural Research (AGROSAVIA) for the trust, sponsorship, and support of this research.

To the “Luiz de Queiroz" College of Agriculture ESALQ, University of São Paulo, for opening its doors to me and allowing me to grow professionally and academically.

To the Sistema de Información Agroclimática del cultivo de la papa en la región de Cundinamarca Colombia (SIAP) proyect and its researchers.

To the Fondo de Ciencia, Tecnología e Innovación del Sistema General de Regalías, administered by the Fondo Nacional de Financiación para Ciencia, Tecnología e Innovación—Francisco José de Caldas, Program Colombia BIO, Gobernación de Cundinamarca and Ministerio de Ciencia, Tecnología e Innovación (MINCIENCIAS), for the project funding.

To Colfuturo, for the scholarship loan.

To Defensa, Pedro Arteaga, Javier Pilpud, Iván Callejas, Leonardo Comba, Zahara Lasso, and James Torres for helping me set academic life to music

To Music and Poetry for supporting academic work

To life and the father for the possibility of these years as a doctoral student
To Nico, for showing me new layers of life.

EPIGRAPH

“Extraño
el abreviado arrullo del cortijo
su grieta soterrada
fundando algún silbido contra viento.
No se fue conmigo
el alma
quedo impresa en las paredes
zurcida como un muérdago en tu alfombra
rasgada por los niños anteriores.
Me pregunto
sí usarás las tristeza
como vistazos del silencio
¿sientes la humedad en equilibrio
por mi ausencia?
los tránsitos del día
están colgados del futuro
como un parpado gigante
a veces
de la mirada
ausentan tu memoria .”.

FABIO MARTINEZ (Delirio-fragmento)

CONTENTS

RESUMO

Avaliação da dinâmica do carbono em sistemas de cultivo de batata (*Solanum tuberosum* L.) irrigado e de sequeiro na região da encosta andina

Devido ao fato de que a batata tem baixas emissões de gases de efeito estufa e um baixo potencial de aquecimento global, a agricultura global de batata é vista como parte do futuro da agricultura climaticamente inteligente. No entanto, a contribuição da batata para a mitigação pelo sequestro de CO_2 ainda é pouco estudada. A batata "andina" é cultivada tanto em campos industriais irrigados quanto em sistemas de sequeiro e, como resultado, a produtividade e a capacidade de sumidouro de carbono podem ser diferentes. Atualmente, há uma falta de estudos de troca de carbono na atmosfera da cultura que permitam conhecer a atividade sumidouro ou fonte das batatas sob esses regimes hídricos. Por conta disso, esta pesquisa teve como objetivo investigar a dinâmica dos fluxos de carbono em sistemas de cultivo de batata irrigada e de sequeiro (*Solanum tuberosum* L.) na região da encosta andina. Um sistema de correlação de turbilhões (EC) foi usado para estudar a saldo de trocas do ecossistema (NEE), produção primária bruta (GPP) e respiração do ecossistema (R_{eco}) em relação à disponibilidade de água. Devido aos fluxos de água e carbono serem sistemas fortemente acoplados, a influência da disponibilidade de água sobre o NEE foi explorada através do estudo das interações dos fluxos de água e carbono. Além disso, como o GPP é o principal impulsionador do sequestro de carbono, uma proposta de up-scaling baseada em curvas fotossintéticas de resposta à luz é proposta para estimar a GPP como uma alternativa quando as medições de EC não estão disponíveis. A cultura da batata de sequeiro foi uma fonte de CO_2 (NEE positivo) principalmente devido ao baixo crescimento, alto desacoplamento água-carbono e menor capacidade de assimilação. Os locais de cultivo de batata irrigada foram sumidouros de CO_2 (NEE mais negativo) e tiveram grandes magnitudes de GPP, indicando que a irrigação é uma importante prática de mitigação. Os modelos multicamadas reproduziram corretamente o comportamento do GPP da batata quando comparado com as medições de EC, indicando que o passagem de escala ("*upscaling*") é uma alternativa confiável para a estimativa do GPP.

Palavras-chave: Batata, Balanço de carbono, Eddy covariance, Up-scaling, Fator de acoplamento, Omega

ABSTRACT

Assessing carbon dynamics of irrigated and rainfed potato (*Solanum tuberosum* L.) cropping systems in the Andean hillside landscape

Because potatoes have low agricultural emissions and a lower average global warming potential, global potato agriculture is viewed as part of a climate-smart agricultural future. However, the contribution of potatoes to mitigation by CO_2 sequestration remains little studied. "Andean" potato is cultivated in both industrial irrigated fields and rainfed systems, as a result, productivity and carbon sink capability could be quite different. Currently, there is a lack of crop-atmosphere carbon exchange studies to know the sink or source activity of potatoes under those water regimes. On this account, this research aimed to investigate carbon fluxes dynamics of irrigated and rainfed potato (*Solanum tuberosum* L.) cropping systems in the Andean hillside landscape. Specifically, an Eddy covariance tower was used to study the response of net ecosystem exchange (NEE), gross primary production (GPP), and ecosystem respiration (R_{eco}) to water availability on potato agroecosystems. Due to water and carbon fluxes are tightly coupled systems, the influence of water availability on NEE was explored by studying water and carbon fluxes interactions. Furthermore, owing to GPP is the main driver of land carbon sequestration, an up-scaling proposal based on photosynthetic light-response curves is proposed for estimating GPP as an alternative when EC measurements are not available. The rainfed potato crop was a CO_2 source (positive NEE) mainly due to low growth, biomass development, high water-carbon decoupling, and lower assimilation capacity. The irrigated potato crop sites were a CO_2 sink (had the most negative NEE) and had large magnitudes of GPP during the crop growth, indicating that irrigation is an important mitigation practice. Multilayer models correctly reproduced the behavior of potato GPP when compared to EC measurements, indicating that Upscaling is a reliable alternative.

Keywords: Potato, Carbon budget, Eddy covariance, Up-scaling, Coupling index, Omega

.

1. INTRODUCTION

According to Agrimonde (Scenarios and Challenges for Feeding the World in 2050), the increasing rate of agricultural production will be considerably lower than in previous decades, with an estimate of 1.15% per year for the period 2003-2050 (Paillard et al., 2014a). By then, more than 9 billion people will have to be fed, 3 billion more than in 2000, and 6 billion more than in 1960 (FAO, 2015). In order to feed this population, contemporary agriculture faces challenges such as increasing productivity with the least possible impact on natural resources, soil, the atmosphere, and surface and subsurface waters (Lobell et al., 2009). To cover food demand in 2050, FAO estimates that agriculture will have to produce almost 50% more food, fodder, and biofuel than was produced in 2012. However, feeding the world without changes in the atmospheric composition is no easy feat. Agriculture covers 12.6% of the earth's surface (Oertel et al., 2016) and contributes with 10–14% of total greenhouse gases (GHGs) (Jansson et al., 2021), where CO_2 has the highest contribution (65%) to global emissions (Bhattacharyya et al., 2021; IPCC, 2014; Rodas-Zuluaga et al., 2021). The increase in the atmospheric CO_2 concentration, and its exceedingly long-term permanency and accumulating behavior have raised concerns given its relationship with global mean temperature and climate change (Bhattacharyya et al., 2021; Lynch et al., 2021). In consequence, limiting the impact of climate change to 1.5 ^{o}C by reaching net-zero carbon dioxide emissions globally around 2050 is the main Paris Agreement goal. The world is required to stay within the cumulative carbon budget of 570 Gt CO_2 and sequester 0.1 Gt CO_2 annually by 2030 and 2.3 Gt CO_2 annually by 2050 (Ahmed et al., 2020). This picture emerges requiring major changes for agriculture which paradoxically can contribute to both climate change and its mitigation (Martínez-Maldonado et al., 2021a). In the words of the Carbon Cycle Institute, "Agriculture is the one sector that has the ability to transform from a net emitter of CO_2 to a net sequester of CO_2" (The Carbon Cycle Institute, 2020).

Because the priority is to slow down climate change as quickly as possible, strategies such as Smart-climate Agriculture (SCA) (FAO) and low carbon agriculture (LCA) (Carter et al., 2018; Guo et al., 2017a; Norse, 2012; Sá et al., 2017; van Wijk et al., 2020) have been considered by international and national bodies for promoting strategies and policies for low C agricultural growth and address climate change mitigation and adaptation policies (Liu et al., 2021a; Mcdonald et al., 2021). In addition, to enhancing food security and increasing resilience, these strategies focus on increasing mitigation from carbon–efficient food production practices, land-use change, and carbon sinks (Carter et al., 2018; Lipper et al., 2014a; Sá et al., 2017; van Wijk et al., 2020). High CO_2 mitigation could only be achieved through agricultural production systems based on agricultural best management practices; and high C sequestration potential (Sá et al., 2017). In other words, to mitigate it there are two main points to be addressed: reducing CO_2 emissions and increasing CO_2 sequestration (Liu 2022). Either way it will require changing how we farm, and how we manage our natural carbon sinks (Ahmed et al., 2020). The potential of agricultural best management practices towards reducing GHG emissions is estimated at 0.3 to 1.17 Pg C year^{-1} (Lam et al., 2013; Neufeldt et al., 2015) and represents 2.7 to 10.4% of the global GHG emissions (Houghton, 2013; le Quéré et al., 2015; Sá et al., 2017). Carbon Sequestration (CS) is a valuable alternative (Bhattacharyya et al., 2021); agriculture has the potential to sequester soil carbon up to 1 GT year^{-1}, which would reduce around 10% of annual GHG emissions of 8–10 GT year^{-1} (Jansson et al., 2021). However, soil carbon storage is not an infinite solution to reduce carbon emissions, mainly because soils have a defined carbon saturation level (Jansson et al., 2021; Paustian et al., 2019; Six et al., 2002). Vegetation by its side, as a basic biological component of the earth's surface, absorbs CO_2 and releases oxygen through photosynthesis, and can be considered one of the earth's natural carbon sinks (Liu et al., 2021b). The primary carbon exchange between the atmosphere and vegetation incorporates about 123 GT of CO_2 per year into

plant biomass through photosynthesis indicating that vegetation plays a crucial role in carbon sequestration and neutrality. However, to improve the rate at which CO_2 is removed from the atmosphere, sequestration needs enhance sink strength by enhancing photosynthetic efficiency and hence biomass production (Jansson et al., 2021). To do so, efforts can involve expanding the adoption of technologies or agriculture practices to increase carbon storage in agroecosystems, such as irrigation. Irrigated agriculture may be one of the main suitable options to mitigate greenhouse gas emissions and climate change by enhancing agricultural productivity per unit area (Emde et al., 2021; Martin-Gorriz et al., 2021a) and by modifying the metabolic behavior of microbial communities (Emde et al., 2021; Tautges et al., 2019). In one way or another, crop management and agricultural best management practices must generate changes to crops in order to cope with climate change impacts, this is, maintaining sufficient production, but at the same time reducing emissions and increasing carbon sequestration as much as possible, i.e., production systems must be climate-smart (FAO) (Jennings et al., 2020a; Lipper et al., 2014a). The amount of carbon is being absorbed by the biosphere/soil or is flowing into the atmosphere can be assessed by NEE (Wood, 2021a). The NEE is the net difference of photosynthetic carbon uptake (GPP) and the respiration of autotrophs and heterotrophs (R_{eco}) (Verlinden et al., 2013) and provides a useful for identifying and monitoring carbon sinks (Lasslop et al., 2010a, 2010b; Reichstein et al., 2005b; Verlinden et al., 2013; Wood, 2021a). Reductions in NEE (less negative NEE) indicates limitations in the CO_2 sequestration potential of the vegetation, and positive values indicate that the CO_2 is being released into the atmosphere due to greater carbon fluxes from R_{eco}, which will further aggravate the amount of CO_2 emissions and worsen global warming (Liu et al., 2021b).

The contribution of potatoes to the global food supply is increasing; today potato is the third most important food crop for global food security (Campos and Ortiz, 2020; Hill et al., 2021a) and an important agroecosystem for worldwide carbon and GHG balances due to its sizeable, cultivated area (more than 19 million hectares) (CIP, 2022), the increase in its production (more than 374 million metric tons per year) (Devaux et al., 2014), and the extraordinary adaptive range. Regarding climate change, potato yields are likely to increase globally by 2050 due to CO_2 and adaptation benefits. Across climate models, the expected range of yield increases from adaptation is 9–20%, indicating that the impacts of climate change on potatoes are favorable compared to other major crops (Hijmans, 2003; Raymundo et al., 2018). On the other hand, potatoes have comparatively low agricultural emissions (Clune et al., 2017a; Haile-Mariam et al., 2008a; Jennings et al., 2020a; Nemecek et al., 2012a) and a lower average global warming potential than cereals, other vegetables, and fruit crops (Clune et al., 2017a; Jennings et al., 2020a). For instance, CO_2 emissions are lower for potatoes than sweet corn (Haile-Mariam et al., 2008a) and nitrous oxide emissions are lower for potatoes than cereal crops (Flynn et al., 2005). Therefore, given that 1) potato is a low-emission crop (Clune et al., 2017a; Flynn et al., 2005; Haile-Mariam et al., 2008a; Nemecek et al., 2012a), and 2) the projected yield increases with adaptation, global potato agriculture is viewed as part of a climate-smart agricultural future, playing an important role in a sustainable future food system (Jennings et al., 2020a).

Due to the potential of potatoes to contribute to a climate-smart future, there is a growing interest in quantifying the GHG and CO_2 fluxes on potato crop ecosystems, however, to our knowledge, almost all the research has focused mainly on studying the carbon water and energy relationships of European potato varieties. The tetraploid cultivated potato *Solanum tuberosum* is divided into two entities either referred to as sub-species or Cultivar Groups: *S. tuberosum* Chilotanum Group or long day "European" potato and *S. tuberosum* Andigenum Group or short day "Andean" potato (Ghislain et al., 2009a; Raker and Spooner, 2002). "European" potato grows under industrial production systems in temperate latitudes towards the northern hemisphere which has around 50% of the global growing area and the highest potato yield levels worldwide (Birch et al., 2012a; FAO, 2022; Jennings et al., 2020a;

Paredes et al., 2018). "Andean" potato, is distributed from western-south Venezuela to northern Argentina and is cultivated in tropical highlands in both industrial irrigated fields and rainfed systems customary among small-holders farmers (Gervais et al., 2021a; Kassaye et al., 2020).

Regarding research on European potatoes, a meaningful subject is the effect of crop management and rotation cycles on net carbon exchange and evapotranspiration (ET) and how land-management practices (such as irrigation) change the carbon sink of the crop's ecosystem. Likewise, crop site comparisons, monitoring, and quantification of variations in net carbon exchange related to environmental drivers were, as well, other frequent subjects found (Table 1). One of the first studies on potato crops was carried out in 2000 by Hsieh et al. (2000). They described the relationship between footprint, observation height, surface roughness, and atmospheric stability in order to assess turbulent fluxes of momentum, sensible heat, latent heat, and CO_2. Anthoni et al. (2004) calculated annual net ecosystem exchange (NEE) values with the different night-time u* thresholds over a potato crop in Thuringia, Germany. They found that the annual NEE becomes more positive with increasing u*and that the lower respiration rates of potatoes were linked to their lower C assimilation compared to other crops. In Coahuila México, Moreno (2003) found an ET of 6 mm day^{-1} in the maximum foliar development in a potato crop from measurements of latent heat. Coyle et al. (2009) estimated the vertical fluxes of momentum, sensible heat, and the trace-gas over a potato field in central Scotland during the summer of 2006, covering 4 weeks just after rainfall and then in dry sunny weather. From water-vapor flux stomatal conductance of the canopy was estimated to separate the total ozone flux into its stomatal and non-stomatal components. From European effort "The CarboEurope-IP" detailed measurements of NEE are being performed for one or more years to understand and quantify the present terrestrial carbon balance of Europe at the local, regional, and continental scales. The project counts with a database that has been used by many researchers like Aubinet et al. (2001, 2009) who estimated in Lonzée (a node of the Carboeurope) the seasonal NEE, gross primary productivity (GPP), ecosystem respiration (R_{eco}), net primary productivity (NPP), autotrophic respiration, heterotrophic respiration, and net biome production (NBP) in a sugar beet/winter wheat/seed potato/winter wheat rotation cycle. The highest values of GPP and R_{eco} were observed in the winter wheat (16 g C m^2 day^{-1} and 8 g C m^2 day^{-1}, respectively) and the lowest in the potato crop (Potatoes cv. Spunta) (10 g C m^2 day^{-1} and 5 g C m^2 day^{-1}, respectively). Likewise, Moors et al. (2010) studied GPP and R_{eco} from 17 flux sites (3 for potato) and for 45 cropping periods. They found that potatoes show net carbon losses, and that the variation of carbon fluxes for the same crop at different locations is determined by the annual differences in climatic conditions. Another study on potato crop carried out by Ceschia et al. (2010) using the CarboEurope-IP NEE indicates that potatoes are small sources of C and had large positive net ecosystem carbon budget. In Québec, South-eastern, Canada, the evapotranspiration (ET) of a rainfed potato crop (*Solanum Tuberosum* L., cultivar Reba) was quantified using the eddy covariance techniques (EC). The cumulative ET calculated was 331.5 mm, with a daily maximum of 6.5 mm at full coverage. Actual crop coefficients (Kc) varied as ET in the different growing stages, from a mean of 0.63 at vegetative growth to 0.91 at tuber initiation. The authors reported that the water productivity of potatoes under rainfall and water use was 22.1 and 12.1 kg m^{-3}, respectively (Parent and Anctil, 2012).

For one year, the carbon and water flux data at five different agricultural sites were measured by Chi et al. (2016) using the eddy-covariance method. The potato crop site was a CO_2 sink (had the most negative annual NEE of -490 ± 41 g C m^{-2}) and had large magnitudes of CO_2 uptake and emissions during the measurement periods compared to cover crops (mustard and arugula) and spring wheat. In general potato has larger magnitudes of GPP, and R_{eco} values during the main growing season (MGS) than other crops. This higher R_{eco} and GPP of potato were most likely a result of irrigation during the MGS as well as the high carbon uptake capability of potatoes. Meshalkina

et al. (2017) presented data on the carbon balance of the typical grain crop rotation by measuring CO_2 fluxes from eddy covariance stations (EC) for four years. They reported that in potato crop, the NEE showed a range of 50-100 g C m^{-2} per year. In the same year, in Lonzée Terrestrial Observatory (Belgium), continuous eddy-covariance measurements of CO_2 fluxes, water vapor and energy, and regular biomass samplings were performed over three complete rotation cycles (sugar beet/winter wheat/seed potato/winter wheat) (Buysse et al., 2017). The potato crop presented the lowest net C sequestration (NEE) mainly due to a shorter number of days of active vegetation, slower growth and biomass development resulting from a precocious harvest and the crop's lower assimilation capacity. The authors reported a higher sensitivity to drought that could be related to both the shallow root system and management practices. Meshalkina et al. (2018) calculated the cumulative NEE, R_{eco}, and GPP to determine the carbon balance for crop rotations, finding carbon losses for all the studied agroecosystems, in particular for fields with potato plants, the losses achieve - 307 g C m^{-2} $year^{-1}$.

Table 1. Studies about mass, energy and water fluxes in potato crop using the Eddy Covariance methodology.

Autors	Location	Subjects	Variables
Hsieh et al. (2000)	Taipei, Taiwan	To establish a field testing of a model for estimating scalar flux footprint in thermally stratified atmospheric surface layer flows	Turbulent fluxes of momentum, sensible heat (H), latent heat (L), and CO_2
Anthoni et al. (2004)	Thuringia, Germany	Differences in seasonal NEE patterns between crop sites	Net Ecosystem Exchange (NEE) of CO_2, ecosystem respiration at 10°C (R_{10})
Moreno (2007)	Coahuila, México	To quantify evapotranspiration (ET) of a rainfed potato crop	Fluxes of sensible heat (H), latent heat (L) and soil heat (G)
Aubinet et al. (2009)	Brussels, Belgium	To measure net carbon fluxes exchanged by crops, estimating carbon sequestration during rotation cycles. To compare carbon budgets of different crops. To measure the impact of climate and management activities on assimilation, respiration and global sequestration. To analyze of the importance of respiration and assimilation over the carbon balance	Fluxes of CO2, water vapor and sensible heat (H), Net Ecosystem Exchange (NEE) of CO_2 , Total Ecosystem Respiration (TER), Gross primary production (GPP), Net Primary Productivity (NPP) and Net Biome Production (NBP)
Coile et al. (2009)	Edinburgh, Scotland	To estimate the total flux of ozone and water-vapor, stomatal influence of ozone	Turbulent fluxes of momentum, sensible heat (H), and the trace-gas (ozone flux)
Moors et al. (2010)	17 sites across Europe. Sites were part of the CarboEurope flux network (see http://www.carboeurope.org/).	To estimate the variability in CO_2 emissions of different crops at the same location and the variation in CO_2 emissions of the same crop at different locations	Net Ecosystem Exchange (NEE) of CO_2, Gross primary production (GPP), Reco
Ceschia et al. (2010)	17 sites across Europe. Sites were part of the CarboEurope flux network (see http://www.carboeurope.org/).	To study the variability of Net Ecosystem Production (NEP) and assessment of the effect of management on the NECB	Net Ecosystem Exchange (NEE) of CO2, Net Ecosystem Production (NEP), number of days of active vegetation cover (NDAV), Gross primary production (GPP)
Parent and Anctil (2012)	Québec, Canada	To quantify evapotranspiration (ET) of a rainfed potato crop	Fluxes of water vapor, flux density of sensible (H) and latent heat (L), energy balance closure
Chi (2016)	Pullman, Washington, USA	To analyze the differences in carbon and water budgets between no-till and conventional tillage cropping systems, low- vs. high- rainfall zones, as well as irrigated vs. non-irrigated agricultural ecosystems. To study the impacts of meteorological conditions and management practices on carbon. Source/sink identification for agricultural ecosystems.	Net Ecosystem Exchange (NEE) of CO_2, Gross primary production (GPP), Reco, main growing season (MGS), evapotranspiration (ET), and sensible heat flux (H), energy balance closure
Buysse et al. (2017)	Brussels, Belgium	To determine the inter-annual variability of carbon fluxes based on meteorological influence. To compare the carbon budget over rotations, between and among the crop types. To quantify the crop response to weather conditions and evaluate the impact of some management practices on crop CO_2 emissions	Fluxes of CO2, water vapor and sensible heat (H), Net Ecosystem Exchange (NEE) of CO_2, Total Ecosystem Respiration (TER), Gross primary production (GPP), Net Primary Productivity (NPP), Net Biome Production (NBP), Rd response to Temperature, photosynthesis rate response to DPV
Meshalkina et al. (2017)	Moscow, Russia.	To estimate carbon balance for potato crop rotation	Net Ecosystem Exchange (NEE) of CO_2, Reco
Meshalkina et al. (2018)	Moscow, Russia.	To estimate carbon balance for the agroecosystems with potato	Water vapor and CO_2 fluxes, Net Ecosystem Exchange (NEE) of CO_2, Gross primary production (GPP), Reco

The foregoing shows an interesting degree of progress in the knowledge of the carbon fluxes of European potato varieties. However, around half of the global potato harvest comes from developing countries (Birch et al., 2012a; Hill et al., 2021a; Mackay, 2009) and "Andean" potatoes. Although, Andean potatoes are the primary source of income for thousands of small-scale producers and the most crucial staple food in the maintenance of food security and nutritional status (Hill et al., 2021a; Mosquera Vásquez et al., 2017a), very little has been said about their CO_2 fluxes and carbon balances. Yet, production and productivity of Andean potatoes are constrained by frequent and severe drought episodes (Gervais et al., 2021a; Kassaye et al., 2020) due to the uncertainty in precipitation patterns (Quiroz et al., 2018a), since more than half of the potato farms are cultivated under rainfed conditions. For example, in Cundinamarca (Colombia), in 2019, 36.7% of the total Diacol capiro cultivar planted area was developed with irrigation, while 63.3% of the total area potato production had no irrigation (DANE, 2019). In those rainfed areas, drought could affect the rates of carbon uptake generated by GPP and carbon release caused by Reco (Meir et al., 2008; van der Molen et al., 2011). A depression of the rate of carbon uptake could occur (Ciais et al., 2005a; Law et al., 2000; Pereira et al., 2007; Reichstein et al., 2002; Schwalm et al., 2010; Zhou et al., 2013) and carbon sink capability could be reduced (NEE less negative). However, there is a lack of crop-atmosphere carbon exchange studies to know the sink or source capacity of Andean potatoes under those water regimes.

The influence of water availability on NEE must be explored through the study of water and carbon fluxes interactions. I agree with Nelson et al. (2018) that Photosynthesis and transpiration are so closely related that knowledge and assumptions about one are required to understand the other. Water and carbon fluxes are tightly coupled systems (Brunsell and Wilson, 2013a; Díaz et al., 2022a; Gentine et al., 2019; van Dijke et al., 2020a) due to the shared stomatal path of water vapor and CO_2 exchange during photosynthesis (Gentine et al., 2019; Lombardozzi et al., 2012a). Likewise, the essential ET-GPP tradeoff determines the productivity potential of an ecosystem (Bonan and Doney, 2018; Díaz et al., 2022a; Law et al., 2002a, 2000; Luke Smallman and Williams, 2019). In potatoes, the interrelationship between carbon and water cycles remains unknown. To the best of my knowledge, there have been no water-carbon coupled studies that provide information to understand how water availability modulates the sink or source behavior of potatoes.

The GPP is the largest carbon flux from the atmosphere to the biosphere in the world. Coupled with water and energy, is the axis of the functioning of worldwide ecosystems. GPP drives the global carbon cycle (Houghton, 2013) and ecosystem functions, such as respiration and growth, therefore provide the basis of food, fiber, wood, and energy for all life on earth (Beer et al., 2010; Chen et al., 2019; Melnikova and Sasai, 2020; Zhang et al., 2019). Due to GPP is one of the major processes controlling land-atmosphere CO_2 exchange, and the main driver of land carbon sequestration, plays a pivotal role in the global carbon balance, contributing to climate mitigation: GPP is the major mechanism of terrestrial ecosystems to potentially offset anthropogenic CO_2 emissions (Anav et al., 2015; Beer et al., 2010; Chen et al., 2019; Guanter et al., 2014; Zhang et al., 2019).

However, terrestrial GPP is the most variable component in the carbon cycle over time and space (Anav et al., 2015; Xia et al., 2015; Zhang et al., 2019), and is driven by a wide range of biotic and abiotic factors operating by changes in vegetation phenology and physiology (Xia et al., 2015). Hence, understanding GPP patterns and variability is critical to developing accurate predictions of climate–carbon cycle feedback (Anav et al., 2015; Chen et al., 2019; Xia et al., 2015). Though quantification of GPP is a major subject in global climate change studies (Anav et al., 2015), its dynamics and responses to the changing environment remain poorly understood (Anav et al., 2015; Campbell et al., 2017; Melnikova and Sasai, 2020; Zhang et al., 2019). In the last few years have been achieved great advances in quantifying the spatio-temporal patterns of GPP with ground, atmospheric, and space observations

(Anav et al., 2015; Melnikova and Sasai, 2020). The eddy covariance (EC) technique has been recognized as the most efficient method for measuring fluxes of energy, CO_2, other GHG gases, and water between the terrestrial bio-sphere and the atmosphere, on an ecological scale (Baldocchi, 2001). The EC method allows that GPP can be inferred from direct and continuous measurements of net carbon exchange (NEE) of CO_2 at the ecosystem scale (Campioli et al., 2016; Lasslop et al., 2010a; Papale et al., 2006a). Through relatively simple models parameterized with the NEE measurements, separation of ecosystem respiration (R_{eco}) and GPP from NEE is typically made (Melnikova and Sasai, 2020; Perez-Priego et al., 2018; Reichstein et al., 2005b). Previous potatoes GPP estimations using the EC method have reported high carbon and relatively larger magnitudes of potato GPP than other crop sites. Nonetheless, there is a lack of detailed information about carbon balances and key factors that control GPP related to water availability and management. Additionally, the available studies were carried out for "European" potato varieties in non-tropical conditions, which may imply different biophysical and eco-physiological responses of the growing agroecosystems to climate drivers.

Even though eddy covariance (EC) measurements provide accurate and reliable information about GPP at the ecosystem level, flux measurements are often not available in many places. The EC data set relies upon the characteristics and available area for measurements. As an alternative for estimating GPP, local information can be built into a model based on up-scaling in situ observations, which is then applied globally (Beer et al., 2010). Andean potatoes are grown primarily in the middle to higher elevations of the Andes throughout the mountain's Andean countries. Most mountain potato agricultural systems include valley floors and high plains, as well as steep hillsides (Mateo et al., n.d.). Under these growing conditions, where satellite remote sensing and the EC don't have a chance, upscaling strategies gain great importance for estimating GPP. However, there are currently no studies on potato GPP upscaling processes as an alternative to the inherent limitations of methodologies like EC.

Given the importance of potato as a climate smart option and for worldwide carbon and GHG balances, this research aimed to investigate carbon fluxes dynamics of irrigated and rainfed potato (*Solanum tuberosum* L.) cropping systems in the Andean hillside landscape. In the first chapter "**Responses in the coupling of carbon and water vapor exchanges of irrigated and rainfed Andean potato (*Solanum tuberosum* L. subsp. andigenum) agroecosystems"** we studied the close link between carbon and water fluxes to understand the response of NEE and its components GPP and R_{eco} to water availability. The magnitudes of NEE and its components (GPP and R_{eco}) were quantified; as well as the impact of water deficit periods on carbon and water vapor fluxes and the role of leaf area in controlling these fluxes, and finally the ET-GPP coupling and inherent water use efficiency IWUE in irrigated and rainfed potato crops is studied and quantified. In the second chapter **"Gross Primary Production of Rainfed and Irrigated Potato (*Solanum tuberosum* L.) in the Colombian Andean Region Using Eddy Covariance Technique"**, the variation of the GPP was studied in greater depth to understand the differences in GPP between rainfed and irrigated systems, and how were the differences in GPP related to differences in crop growth. The third chapter **"Upscaling Gross Primary Production from Leaf to Canopy for Potato Crop (*Solanum tuberosum* L.)"** is a GPP up-scaling proposal based on the light profile within the canopy and photosynthetic light-response curves (An–I curves). Both big-leaf and multilayer upscaling strategies for potato canopy were assessed in order to provide a useful and validated alternative to the EC technique that could be extrapolated to other potato cultivars to obtain canopy GPP estimations from infra-red gas analyzer (IRGA) measurements. Finally, the fourth chapter **"Analytical approach to relate evapotranspiration, canopy-atmosphere coupling level and water deficit sensitivity"** is a broad review that, based on the theoretical analysis of the omega coefficient, proposed an alternative view of the decoupling factor under conditions of water deficit.

References

Ahmed, J., Almeida, E., Aminetzah, D., Denis, N., Henderson, K., Katz, J., Kitchel, H., Mannion, P., 2020. Agriculture and climate change Reducing emissions through improved farming practices.

Anav, A., Friedlingstein, P., Beer, C., Ciais, P., Harper, A., Jones, C., Murray-Tortarolo, G., Papale, D., Parazoo, N.C., Peylin, P., Piao, S., Sitch, S., Viovy, N., Wiltshire, A., Zhao, M., 2015. Spatiotemporal patterns of terrestrial gross primary production: A review. Reviews of Geophysics. https://doi.org/10.1002/2015RG000483

Anthoni, P.M., Knohl, A., Rebmann, C., Freibauer, A., Mund, M., Ziegler, W., Kolle, O., Schulze, E.D., 2004. Forest and agricultural land-use-dependent CO_2 exchange in Thuringia, Germany. Glob Chang Biol 10, 2005–2019. https://doi.org/10.1111/j.1365-2486.2004.00863.x

Aubinet, M., Chermanne, B., Vandenhaute, M., Longdoz, B., Yernaux, M., Laitat, E., 2001. Long term carbon dioxide exchange above a mixed forest in the Belgian Ardennes. Agric For Meteorol 108, 293–315. https://doi.org/10.1016/S0168-1923(01)00244-1

Aubinet, M., Moureaux, C., Bodson, B., Dufranne, D., Heinesch, B., Suleau, M., Vancutsem, F., Vilret, A., 2009. Carbon sequestration by a crop over a 4-year sugar beet/winter wheat/seed potato/winter wheat rotation cycle. Agric For Meteorol 149, 407–418. https://doi.org/10.1016/j.agrformet.2008.09.003

Baldocchi, D., 2001. Assessing Carbon Balance: Problems and Prospects of Covariance Techniques.

Beer, C., Reichstein, M., Tomelleri, E., Ciais, P., Jung, M., Carvalhais, N., Rödenbeck, C., Arain, M.A., Baldocchi, D., Bonan, G.B., Bondeau, A., Cescatti, A., Lasslop, G., Lindroth, A., Lomas, M., Luyssaert, S., Margolis, H., Oleson, K.W., Roupsard, O., Veenendaal, E., Viovy, N., Williams, C., Woodward, F.I., Papale, D., 2010. Terrestrial gross carbon dioxide uptake: Global distribution and covariation with climate. Science (1979) 329, 834–838. https://doi.org/10.1126/science.1184984

Bhattacharyya, S.S., Leite, F.F.G.D., Adeyemi, M.A., Sarker, A.J., Cambareri, G.S., Faverin, C., Tieri, M.P., Castillo-Zacarías, C., Melchor-Martínez, E.M., Iqbal, H.M.N., Parra-Saldívar, R., 2021. A paradigm shift to CO_2 sequestration to manage global warming – With the emphasis on developing countries. Science of the Total Environment. https://doi.org/10.1016/j.scitotenv.2021.148169

Birch, P.R.J., Bryan, G., Fenton, B., Gilroy, E.M., Hein, I., Jones, J.T., Prashar, A., Taylor, M.A., Torrance, L., Toth, I.K., 2012. Crops that feed the world 8: Potato: Are the trends of increased global production sustainable? Food Secur 4, 477–508. https://doi.org/10.1007/s12571-012-0220-1

Bonan, G.B., Doney, S.C., 2018. Climate, ecosystems, and planetary futures: The challenge to predict life in Earth system models. Science (1979). https://doi.org/10.1126/science.aam8328

Brunsell, N.A., Wilson, C.J., 2013. Multiscale Interactions between Water and Carbon Fluxes and Environmental Variables in A Central U.S. Grassland. Entropy 15, 1324–1341. https://doi.org/10.3390/e15041324

Buysse, P., Bodson, B., Debacq, A., de Ligne, A., Heinesch, B., Manise, T., Moureaux, C., Aubinet, M., 2017. Carbon budget measurement over 12 years at a crop production site in the silty-loam region in Belgium. Agric For Meteorol 246, 241–255. https://doi.org/10.1016/j.agrformet.2017.07.004

Campbell, J.E., Berry, J.A., Seibt, U., Smith, S.J., Montzka, S.A., Launois, T., Belviso, S., Bopp, L., Laine, M., 2017. Large historical growth in global terrestrial gross primary production. Nature 544, 84–87. https://doi.org/10.1038/nature22030

Campioli, M., Malhi, Y., Vicca, S., Luyssaert, S., Papale, D., Peñuelas, J., Reichstein, M., Migliavacca, M., Arain, M.A., Janssens, I.A., 2016. Evaluating the convergence between eddy-covariance and biometric methods for assessing carbon budgets of forests. Nat Commun 7, 1–12. https://doi.org/10.1038/ncomms13717

Campos, H., Ortiz, O., 2020. The potato crop: Its agricultural, nutritional and social contribution to humankind, The Potato Crop: Its Agricultural, Nutritional and Social Contribution to Humankind. https://doi.org/10.1007/978-3-030-28683-5

Carter, S., Arts, B., Giller, K.E., Golcher, C.S., Kok, K., de Koning, J., van Noordwijk, M., Reidsma, P., Rufino, M.C., Salvini, G., Verchot, L., Wollenberg, E., Herold, M., 2018. Climate-smart land use requires local solutions, transdisciplinary research, policy coherence and transparency. Carbon Manag 9, 291–301. https://doi.org/10.1080/17583004.2018.1457907

Ceschia, E., Béziat, P., Dejoux, J.F., Aubinet, M., Bernhofer, C., Bodson, B., Buchmann, N., Carrara, A., Cellier, P., di Tommasi, P., Elbers, J.A., Eugster, W., Grünwald, T., Jacobs, C.M.J., Jans, W.W.P., Jones, M., Kutsch, W., Lanigan, G., Magliulo, E., Marloie, O., Moors, E.J., Moureaux, C., Olioso, A., Osborne, B., Sanz, M.J., Saunders, M., Smith, P., Soegaard, H., Wattenbach, M., 2010. Management effects on net ecosystem carbon and GHG budgets at European crop sites. Agric Ecosyst Environ 139, 363–383. https://doi.org/10.1016/j.agee.2010.09.020

Chen, S., Huang, Y., Gao, S., Wang, G., 2019. Impact of physiological and phenological change on carbon uptake on the Tibetan Plateau revealed through GPP estimation based on spaceborne solar-induced fluorescence. Science of the Total Environment 663, 45–59. https://doi.org/10.1016/j.scitotenv.2019.01.324

Chi, J., Waldo, S., Pressley, S., O'Keeffe, P., Huggins, D., Stöckle, C., Pan, W.L., Brooks, E., Lamb, B., 2016. Assessing carbon and water dynamics of no-till and conventional tillage cropping systems in the inland Pacific Northwest US using the eddy covariance method. Agric For Meteorol 218–219, 37–49. https://doi.org/10.1016/j.agrformet.2015.11.019

Ciais, P., Reichstein, M., Viovy, N., Granier, A., Ogée, J., Allard, V., Aubinet, M., Buchmann, N., Bernhofer, C., Carrara, A., Chevallier, F., de Noblet, N., Friend, A.D., Friedlingstein, P., Grünwald, T., Heinesch, B., Keronen, P., Knohl, A., Krinner, G., Loustau, D., Manca, G., Matteucci, G., Miglietta, F., Ourcival, J.M., Papale, D., Pilegaard, K., Rambal, S., Seufert, G., Soussana, J.F., Sanz, M.J., Schulze, E.D., Vesala, T., Valentini, R., 2005. Europe-wide reduction in primary productivity caused by the heat and drought in 2003. Nature 437, 529–533. https://doi.org/10.1038/nature03972

CIP, 2022. Hechos y Cifras sobre la Papa [WWW Document]. URL www.cipotato.org

Clune, S., Crossin, E., Verghese, K., 2017. Systematic review of greenhouse gas emissions for different fresh food categories. J Clean Prod 140, 766–783. https://doi.org/10.1016/j.jclepro.2016.04.082

Coyle, M., Nemitz, E., Storeton-West, R., Fowler, D., Cape, J.N., 2009. Measurements of ozone deposition to a potato canopy. Agric For Meteorol 149, 655–666. https://doi.org/10.1016/j.agrformet.2008.10.020

DANE, 2019. Boletin Tenico Encuesta Nacional Agropecuaria (ENA) 2019-I. Boletín Técnico 8, 1–38.

Devaux, A., Kromann, P., Ortiz, O., 2014. Potatoes for Sustainable Global Food Security. Potato Res 57, 185–199. https://doi.org/10.1007/s11540-014-9265-1

Díaz, E., Adsuara, J.E., Martínez, Á.M., Piles, M., Camps-Valls, G., 2022. Inferring causal relations from observational long-term carbon and water fluxes records. Sci Rep 12. https://doi.org/10.1038/s41598-022-05377-7

Emde, D., Hannam, K.D., Most, I., Nelson, L.M., Jones, M.D., 2021. Soil organic carbon in irrigated agricultural systems: A meta-analysis. Glob Chang Biol 27, 3898–3910. https://doi.org/10.1111/gcb.15680

FAO, 2022. FAOSTAT, FAO Statistical Databases [WWW Document]. FAO Statistical Databases.

FAO, 2015. The future of food and agriculture: Trends and challenges, Food and Agriculture Organization of the United Nations.

Flynn, H.C., Smith, J., Smith, K.A., Wright, J., Smith, P., Massheder, J., 2005. Climate- and crop-responsive emission factors significantly alter estimates of current and future nitrous oxide emissions from fertilizer use. Glob Chang Biol 11, 1522–1536. https://doi.org/10.1111/j.1365-2486.2005.00998.x

Gentine, P., Green, J.K., Guérin, M., Humphrey, V., Seneviratne, S.I., Zhang, Y., Zhou, S., 2019. Coupling between the terrestrial carbon and water cycles - A review. Environmental Research Letters 14. https://doi.org/10.1088/1748-9326/ab22d6

Gervais, T., Creelman, A., Li, X.Q., Bizimungu, B., de Koeyer, D., Dahal, K., 2021. Potato Response to Drought Stress: Physiological and Growth Basis. Front Plant Sci 12, 1–10. https://doi.org/10.3389/fpls.2021.698060

Ghislain, M., Núñez, J., Herrera, M.D.R., Spooner, D.M., 2009. The single Andigenum origin of Neo-Tuberosum potato materials is not supported by microsatellite and plastid marker analyses. Theoretical and Applied Genetics 118, 963–969. https://doi.org/10.1007/s00122-008-0953-6

Guanter, L., Zhang, Y., Jung, M., Joiner, J., Voigt, M., Berry, J.A., Frankenberg, C., Huete, A.R., Zarco-Tejada, P., Lee, J.E., Moran, M.S., Ponce-Campos, G., Beer, C., Camps-Valls, G., Buchmann, N., Gianelle, D., Klumpp, K., Cescatti, A., Baker, J.M., Griffis, T.J., 2014. Global and time-resolved monitoring of crop photosynthesis with chlorophyll fluorescence. Proc Natl Acad Sci U S A 111. https://doi.org/10.1073/pnas.1320008111

Guo, R., Zhao, Y., Shi, Y., Li, F., Hu, J., Yang, H., 2017. Low carbon development and local sustainability from a carbon balance perspective. Resour Conserv Recycl 122, 270–279. https://doi.org/10.1016/j.resconrec.2017.02.019

Haile-Mariam, S., Collins, H.P., Higgins, S.S., 2008. Greenhouse Gas Fluxes from an Irrigated Sweet Corn (Zea mays L.)–Potato (Solanum tuberosum L.) Rotation . J Environ Qual 37, 759–771. https://doi.org/10.2134/jeq2007.0400

Hijmans, R.J., 2003. The Effect of Climate Change on Global Potato Production, Amer J of Potato Res.

Hill, D., Nelson, D., Hammond, J., Bell, L., 2021. Morphophysiology of Potato (Solanum tuberosum) in Response to Drought Stress: Paving the Way Forward. Front Plant Sci 11, 1–19. https://doi.org/10.3389/fpls.2020.597554

Houghton, R.A., 2013. The Contemporary Carbon Cycle, in: Treatise on Geochemistry: Second Edition. Elsevier Inc., pp. 399–435. https://doi.org/10.1016/B978-0-08-095975-7.00810-X

Hsieh, C.I., Katul, G., Chi, T.W., 2000. An approximate analytical model for footprint estimation of scalar fluxes in thermally stratified atmospheric flows. Adv Water Resour 23, 765–772. https://doi.org/10.1016/S0309-1708(99)00042-1

IPCC, 2014. Climate Change 2014 Part A: Global and Sectoral Aspects, Climate Change 2014: Impacts, Adaptation, and Vulnerability. Part A: Global and Sectoral Aspects. Contribution of Working Group II to the Fifth Assessment Report of the Intergovernmental Panel on Climate Change.

Jansson, C., Faiola, C., Wingler, A., Zhu, X.G., Kravchenko, A., de Graaff, M.A., Ogden, A.J., Handakumbura, P.P., Werner, C., Beckles, D.M., 2021. Crops for Carbon Farming. Front Plant Sci 12. https://doi.org/10.3389/fpls.2021.636709

Jennings, S.A., Koehler, A.K., Nicklin, K.J., Deva, C., Sait, S.M., Challinor, A.J., 2020. Global Potato Yields Increase Under Climate Change With Adaptation and CO_2 Fertilisation. Front Sustain Food Syst 4. https://doi.org/10.3389/fsufs.2020.519324

Kassaye, K.T., Yilma, W.A., Fisha, M.H., Haile, D.H., 2020. Yield and water use efficiency of potato under alternate furrows and deficit irrigation. International Journal of Agronomy 2020. https://doi.org/10.1155/2020/8869098

Lam, S.K., Chen, D., Mosier, A.R., Roush, R., 2013. The potential for carbon sequestration in Australian agricultural soils is technically and economically limited. Sci Rep 3. https://doi.org/10.1038/srep02179

Lasslop, G., Reichstein, M., Papale, D., Richardson, A., Arneth, A., Barr, A., Stoy, P., Wohlfahrt, G., 2010a. Separation of net ecosystem exchange into assimilation and respiration using a light response curve approach: Critical issues and global evaluation. Glob Chang Biol 16, 187–208. https://doi.org/10.1111/j.1365-2486.2009.02041.x

Lasslop, G., Reichstein, M., Papale, D., Richardson, A., Arneth, A., Barr, A., Stoy, P., Wohlfahrt, G., 2010b. Separation of net ecosystem exchange into assimilation and respiration using a light response curve approach: Critical issues and global evaluation. Glob Chang Biol 16, 187–208. https://doi.org/10.1111/j.1365-2486.2009.02041.x

Law, B.E., Falge, E., Gu, L., Baldocchi, D.D., Bakwin, P., Berbigier, P., Davis, K., Dolman, A.J., Falk, M., Fuentes, J.D., Goldstein, A., Granier, A., Grelle, A., Hollinger, D., Janssens, I.A., Jarvis, P., Jensen, N.O., Katul, G., Mahli, Y., Matteucci, G., Meyers, T., Monson, R., Munger, W., Oechel, W., Olson, R., Pilegaard, K., Paw, K.T., Thorgeirsson, H., Valentini, R., Verma, S., Vesala, T., Wilson, K., Wofsy, S., 2002. Environmental controls over carbon dioxide and water vapor exchange of terrestrial vegetation, Agricultural and Forest Meteorology.

Law, B.E., Williams, M., Anthoni, P.M., Baldocchi, D.D., Unsworth, M.H., 2000. Measuring and modelling seasonal variation of carbon dioxide and water vapour exchange of a Pinus ponderosa forest subject to soil water deficit. Glob Chang Biol 6, 613–630. https://doi.org/10.1046/j.1365-2486.2000.00339.x

le Quéré, C., Moriarty, R., Andrew, R.M., Canadell, J.G., Sitch, S., Korsbakken, J.I., Friedlingstein, P., Peters, G.P., Andres, R.J., Boden, T.A., Houghton, R.A., House, J.I., Keeling, R.F., Tans, P., Arneth, A., Bakker, D.C.E., Barbero, L., Bopp, L., Chang, J., Chevallier, F., Chini, L.P., Ciais, P., Fader, M., Feely, R.A., Gkritzalis, T., Harris, I., Hauck, J., Ilyina, T., Jain, A.K., Kato, E., Kitidis, V., Klein Goldewijk, K., Koven, C., Landschützer, P., Lauvset, S.K., Lefèvre, N., Lenton, A., Lima, I.D., Metzl, N., Millero, F., Munro, D.R., Murata, A., S. Nabel, J.E.M., Nakaoka, S., Nojiri, Y., O'Brien, K., Olsen, A., Ono, T., Pérez, F.F., Pfeil, B., Pierrot, D., Poulter, B., Rehder, G., Rödenbeck, C., Saito, S., Schuster, U., Schwinger, J., Séférian, R., Steinhoff, T., Stocker, B.D., Sutton, A.J., Takahashi, T., Tilbrook, B., van der Laan-Luijkx, I.T., van der Werf, G.R., van Heuven, S., Vandemark, D., Viovy, N., Wiltshire, A., Zaehle, S., Zeng, N., 2015. Global Carbon Budget 2015. Earth Syst Sci Data 7, 349–396. https://doi.org/10.5194/essd-7-349-2015

Lipper, L., Thornton, P., Campbell, B.M., Baedeker, T., Braimoh, A., Bwalya, M., Caron, P., Cattaneo, A., Garrity, D., Henry, K., Hottle, R., Jackson, L., Jarvis, A., Kossam, F., Mann, W., McCarthy, N., Meybeck, A., Neufeldt, H., Remington, T., Sen, P.T., Sessa, R., Shula, R., Tibu, A., Torquebiau, E.F., 2014. Climate-smart agriculture for food security. Nat Clim Chang. https://doi.org/10.1038/nclimate2437

Liu, X., Wang, P., Song, H., Zeng, X., 2021a. Determinants of net primary productivity: Low-carbon development from the perspective of carbon sequestration. Technol Forecast Soc Change 172, 121006. https://doi.org/10.1016/j.techfore.2021.121006

Liu, X., Wang, P., Song, H., Zeng, X., 2021b. Determinants of net primary productivity: Low-carbon development from the perspective of carbon sequestration. Technol Forecast Soc Change 172. https://doi.org/10.1016/j.techfore.2021.121006

Lobell, D.B., Cassman, K.G., Field, C.B., 2009. Crop Yield Gaps: Their Importance, Magnitudes, and Causes. Annu Rev Environ Resour 34, 179–204. https://doi.org/10.1146/annurev.environ.041008.093740

Lombardozzi, D., Levis, S., Bonan, G., Sparks, J.P., 2012. Predicting photosynthesis and transpiration responses to ozone: Decoupling modeled photosynthesis and stomatal conductance. Biogeosciences 9, 3113–3130. https://doi.org/10.5194/bg-9-3113-2012

Luke Smallman, T., Williams, M., 2019. Description and validation of an intermediate complexity model for ecosystem photosynthesis and evapotranspiration: ACM-GPP-ETv1. Geosci Model Dev 12, 2227–2253. https://doi.org/10.5194/gmd-12-2227-2019

Lynch, J., Cain, M., Frame, D., Pierrehumbert, R., 2021. Agriculture's Contribution to Climate Change and Role in Mitigation Is Distinct From Predominantly Fossil CO_2-Emitting Sectors. Front Sustain Food Syst 4. https://doi.org/10.3389/fsufs.2020.518039

Mackay, G., 2009. New Light on a Hidden Treasure. Exp Agric 45, 376–376.

Martínez-Maldonado, F.E., Castaño-Marín, A.M., Góez-Vinasco, G.A., Marin, F.R., 2021. Gross primary production of rainfed and irrigated potato (Solanum tuberosum l.) in the colombian andean region using eddy covariance technique. Water (Switzerland) 13. https://doi.org/10.3390/w13223223

Martin-Gorriz, B., Martínez-Alvarez, V., Maestre-Valero, J.F., Gallego-Elvira, B., 2021. Influence of the water source on the carbon footprint of irrigated agriculture: A regional study in south-eastern Spain. Agronomy 11. https://doi.org/10.3390/agronomy11020351

Mateo, âs, Eng, A., Tapia, M.E., n.d. High mountain environment and farming systems in the Andean Region of Latin America social organization of production a case study of a peasant community in the southern andes : amaru cusco, peru.

Mcdonald, H., Frelih-Larsen, A., Lóránt, A., Duin, L., Andersen, S.P., Costa, G., Bradley, H., 2021. Carbon farming Making agriculture fit for 2030, Study for the committee on Environment, Public Health and Food Safety (ENVI). Luxembourg.

Meir, P., Metcalfe, D.B., Costa, A.C.L., Fisher, R.A., 2008. The fate of assimilated carbon during drought: Impacts on respiration in Amazon rainforests. Philosophical Transactions of the Royal Society B: Biological Sciences 363, 1849–1855. https://doi.org/10.1098/rstb.2007.0021

Melnikova, I., Sasai, T., 2020. Effects of Anthropogenic Activity on Global Terrestrial Gross Primary Production. J Geophys Res Biogeosci 125. https://doi.org/10.1029/2019JG005403

Meshalkina, J., Yaroslavtsev, A., Vassenev, I., 2017. Carbon balance of the typical grain crop rotation in Moscow region assessed by eddy covariance method 19, 12212.

Meshalkina, J.L., Yaroslavtsev, A.M., Vasenev, I.I., Andreeva, I. v., Tihonova, M. v., 2018. Carbon balance assessment by eddy covariance method for agroecosystems with potato plants and oats & vetch mixture on sod-podzolic soils of Russia. IOP Conf Ser Earth Environ Sci 107. https://doi.org/10.1088/1755-1315/107/1/012119

Moors, E.J., Jacobs, C., Jans, W., Supit, I., Kutsch, W.L., Bernhofer, C., Béziat, P., Buchmann, N., Carrara, A., Ceschia, E., Elbers, J., Eugster, W., Kruijt, B., Loubet, B., Magliulo, E., Moureaux, C., Olioso, A., Saunders, M., Soegaard, H., 2010. Variability in carbon exchange of European croplands. Agric Ecosyst Environ 139, 325–335. https://doi.org/10.1016/j.agee.2010.04.013

Moreno, E., 2003. Determinación del consumo de agua por el cultivo de papa con el método de la covarianza eddy 76.

Mosquera Vásquez, T., del Castillo, S., Gálvez, D.C., Rodríguez, L.E., 2017. Breeding Differently: Participatory Selection and Scaling Up Innovations in Colombia. Potato Res 60, 361–381. https://doi.org/10.1007/s11540-018-9389-9

Nelson, J.A., Carvalhais, N., Migliavacca, M., Reichstein, M., Jung, M., 2018. Water-stress-induced breakdown of carbon-water relations: Indicators from diurnal FLUXNET patterns. Biogeosciences 15, 2433–2447. https://doi.org/10.5194/bg-15-2433-2018

Nemecek, T., Weiler, K., Plassmann, K., Schnetzer, J., Gaillard, G., Jefferies, D., García-Suárez, T., King, H., Milà I Canals, L., 2012. Estimation of the variability in global warming potential of worldwide crop production using a modular extrapolation approach. J Clean Prod 31, 106–117. https://doi.org/10.1016/j.jclepro.2012.03.005

Neufeldt, H., Kissinger, G., Alcamo, J., 2015. No-till agriculture and climate change mitigation. Nat Clim Chang. https://doi.org/10.1038/nclimate2653

Norse, D., 2012. Low carbon agriculture: Objectives and policy pathways. Environ Dev 1, 25–39. https://doi.org/10.1016/j.envdev.2011.12.004

Oertel, C., Matschullat, J., Zurba, K., Zimmermann, F., Erasmi, S., 2016. Greenhouse gas emissions from soils—A review. Chemie der Erde 76, 327–352. https://doi.org/10.1016/j.chemer.2016.04.002

Paillard, S., Treyer, S., Dorin, B., 2014. Agrimonde – Scenarios and Challenges for Feeding the World in 2050. springer.

Papale, D., Reichstein, M., Aubinet, M., Canfora, E., Bernhofer, C., Kutsch, W., Longdoz, B., Rambal, S., Valentini, R., Vesala, T., Yakir, D., 2006. Towards a standardized processing of Net Ecosystem Exchange measured with eddy covariance technique: Algorithms and uncertainty estimation. Biogeosciences 3, 571–583. https://doi.org/10.5194/bg-3-571-2006

Paredes, P., D'Agostino, D., Assif, M., Todorovic, M., Pereira, L.S., 2018. Assessing potato transpiration, yield and water productivity under various water regimes and planting dates using the FAO dual Kc approach. Agric Water Manag 195, 11–24. https://doi.org/10.1016/j.agwat.2017.09.011

Parent, A.C., Anctil, F., 2012. Quantifying evapotranspiration of a rainfed potato crop in South-eastern Canada using eddy covariance techniques. Agric Water Manag 113, 45–56. https://doi.org/10.1016/j.agwat.2012.06.014

Paustian, K., Larson, E., Kent, J., Marx, E., Swan, A., 2019. Soil C Sequestration as a Biological Negative Emission Strategy. Frontiers in Climate. https://doi.org/10.3389/fclim.2019.00008

Pereira, J.S., Mateus, J.A., Aires, L.M., Pita, G., Pio, C., David, J.S., Andrade, V., Banza, J., David, T.S., Paço, T.A., Rodrigues, A., 2007. Net ecosystem carbon exchange in three contrasting Mediterranean ecosystems - The effect of drought. Biogeosciences 4, 791–802. https://doi.org/10.5194/bg-4-791-2007

Perez-Priego, O., Katul, G., Reichstein, M., El-Madany, T.S., Ahrens, B., Carrara, A., Scanlon, T.M., Migliavacca, M., 2018. Partitioning Eddy Covariance Water Flux Components Using Physiological and Micrometeorological Approaches. J Geophys Res Biogeosci 123, 3353–3370. https://doi.org/10.1029/2018JG004637

Quiroz, R., Ramírez, D.A., Kroschel, J., Andrade-Piedra, J., Barreda, C., Condori, B., Mares, V., Monneveux, P., Perez, W., 2018. Impact of climate change on the potato crop and biodiversity in its center of origin. Open Agric 3, 273–283. https://doi.org/10.1515/opag-2018-0029

Raker, C.M., Spooner, D.M., 2002. Chilean tetraploid cultivated potato, Solanum tuberosum, is distinct from the Andean populations: Microsatellite data. Crop Sci 42, 1451–1458. https://doi.org/10.2135/cropsci2002.1451

Raymundo, R., Asseng, S., Robertson, R., Petsakos, A., Hoogenboom, G., Quiroz, R., Hareau, G., Wolf, J., 2018. Climate change impact on global potato production. European Journal of Agronomy 100, 87–98. https://doi.org/10.1016/j.eja.2017.11.008

Reichstein, M., Falge, E., Baldocchi, D., Papale, D., Aubinet, M., Berbigier, P., Bernhofer, C., Buchmann, N., Gilmanov, T., Granier, A., Grünwald, T., Havránková, K., Ilvesniemi, H., Janous, D., Knohl, A., Laurila, T., Lohila, A., Loustau, D., Matteucci, G., Meyers, T., Miglietta, F., Ourcival, J.M., Pumpanen, J., Rambal, S., Rotenberg, E., Sanz, M., Tenhunen, J., Seufert, G., Vaccari, F., Vesala, T., Yakir, D., Valentini, R., 2005. On the separation of net ecosystem exchange into assimilation and ecosystem respiration: Review and improved algorithm. Glob Chang Biol 11, 1424–1439. https://doi.org/10.1111/j.1365-2486.2005.001002.x

Reichstein, M., Tenhunen, J.D., Roupsard, O., Ourcival, J.M., Rambal, S., Miglietta, F., Peressotti, A., Pecchiari, M., Tirone, G., Valentini, R., 2002. Severe drought effects on ecosystem CO_2 and H_2O fluxes at three Mediterranean evergreen sites: Revision of current hypotheses? Glob Chang Biol 8, 999–1017. https://doi.org/10.1046/j.1365-2486.2002.00530.x

Rodas-Zuluaga, L.I., Castañeda-Hernández, L., Castillo-Vacas, E.I., Gradiz-Menjivar, A., López-Pacheco, I.Y., Castillo-Zacarías, C., Boully, L., Iqbal, H.M.N., Parra-Saldívar, R., 2021. Bio-capture and influence of CO_2 on the growth rate and biomass composition of the microalgae Botryococcus braunii and Scenedesmus sp. Journal of CO_2 Utilization 43. https://doi.org/10.1016/j.jcou.2020.101371

Sá, J.C. de M., Lal, R., Cerri, C.C., Lorenz, K., Hungria, M., de Faccio Carvalho, P.C., 2017. Low-carbon agriculture in South America to mitigate global climate change and advance food security. Environ Int 98, 102–112. https://doi.org/10.1016/j.envint.2016.10.020

Schwalm, C.R., Williams, C.A., Schaefer, K., Arneth, A., Bonal, D., Buchmann, N., Chen, J., Law, B., Lindroth, A., Luyssaert, S., Reichstein, M., Richardson, A.D., 2010. Assimilation exceeds respiration sensitivity to drought: A FLUXNET synthesis. Glob Chang Biol 16, 657–670. https://doi.org/10.1111/j.1365-2486.2009.01991.x

Six, J., Conant, R.T., Paul, E.A., Paustian, K., 2002. Stabilization mechanisms of soil organic matter: Implications for C-saturation of soils, Plant and Soil.

Tautges, N.E., Chiartas, J.L., Gaudin, A.C.M., O'Geen, A.T., Herrera, I., Scow, K.M., 2019. Deep soil inventories reveal that impacts of cover crops and compost on soil carbon sequestration differ in surface and subsurface soils. Glob Chang Biol 25, 3753–3766. https://doi.org/10.1111/gcb.14762

The Carbon Cycle Institute, 2020. Carbon Farming [WWW Document]. URL http: //www.carboncycle.org/%20carbon-farming/ ((accessed 12.8.22).

van der Molen, M.K., Dolman, A.J., Ciais, P., Eglin, T., Gobron, N., Law, B.E., Meir, P., Peters, W., Phillips, O.L., Reichstein, M., Chen, T., Dekker, S.C., Doubková, M., Friedl, M.A., Jung, M., van den Hurk, B.J.J.M., de Jeu, R.A.M., Kruijt, B., Ohta, T., Rebel, K.T., Plummer, S., Seneviratne, S.I., Sitch, S., Teuling, A.J., van der Werf, G.R., Wang, G., 2011. Drought and ecosystem carbon cycling. Agric For Meteorol 151, 765–773. https://doi.org/10.1016/j.agrformet.2011.01.018

van Dijke, A.J.H., Mallick, K., Schlerf, M., MacHwitz, M., Herold, M., Teuling, A.J., 2020. Examining the link between vegetation leaf area and land-atmosphere exchange of water, energy, and carbon fluxes using FLUXNET data. Biogeosciences 17, 4443–4457. https://doi.org/10.5194/bg-17-4443-2020

van Wijk, M.T., Merbold, L., Hammond, J., Butterbach-Bahl, K., 2020. Improving Assessments of the Three Pillars of Climate Smart Agriculture: Current Achievements and Ideas for the Future. Front Sustain Food Syst. https://doi.org/10.3389/fsufs.2020.558483

Verlinden, M.S., Broeckx, L.S., Zona, D., Berhongaray, G., de Groote, T., Camino Serrano, M., Janssens, I.A., Ceulemans, R., 2013. Net ecosystem production and carbon balance of an SRC poplar plantation during its first rotation. Biomass Bioenergy 56, 412–422. https://doi.org/10.1016/j.biombioe.2013.05.033

Wood, D.A., 2021. Net ecosystem carbon exchange prediction and insightful data mining with an optimized data-matching algorithm. Ecol Indic 124. https://doi.org/10.1016/j.ecolind.2021.107426

Xia, J., Niu, S., Ciais, P., Janssens, I.A., Chen, J., Ammann, C., Arain, A., Blanken, P.D., Cescatti, A., Bonal, D., Buchmann, N., Curtis, P.S., Chen, S., Dong, J., Flanagan, L.B., Frankenberg, C., Georgiadis, T., Gough, C.M., Hui, D., Kiely, G., Li, J., Lund, M., Magliulo, V., Marcolla, B., Merbold, L., Montagnani, L., Moors, E.J., Olesen, J.E., Piao, S., Raschi, A., Roupsard, O., Suyker, A.E., Urbaniak, M., Vaccari, F.P., Varlagin, A., Vesala, T., Wilkinson, M., Weng, E., Wohlfahrt, G., Yan, L., Luo, Y., 2015. Joint control of terrestrial gross primary productivity by plant phenology and physiology. Proc Natl Acad Sci U S A 112, 2788–2793. https://doi.org/10.1073/pnas.1413090112

Zhang, Y., Song, C., Band, L.E., Sun, G., 2019. No Proportional Increase of Terrestrial Gross Carbon Sequestration From the Greening Earth. J Geophys Res Biogeosci 124, 2540–2553. https://doi.org/10.1029/2018JG004917

Zhou, J., Zhang, Z., Sun, G., Fang, X., Zha, T., McNulty, S., Chen, J., Jin, Y., Noormets, A., 2013. Response of ecosystem carbon fluxes to drought events in a poplar plantation in Northern China. For Ecol Manage 300, 33–42. https://doi.org/10.1016/j.foreco.2013.01.007

2. RESPONSES IN THE COUPLING OF CARBON AND WATER VAPOR EXCHANGES OF IRRIGATED, AND RAINFED ANDEAN POTATO (*Solanum tuberosum* L.) AGROECOSYSTEMS

Abstract

We studied the link between carbon and water fluxes to understand the response of net ecosystem carbon exchange (NEE) to water availability conditions of three different potato water regimes cropping systems [full irrigation (FI), deficit irrigation (DI) and rainfed (RF)]. Through the eddy covariance technique, we measured CO_2 and water vapor exchanges and determined surface resistances, omega factor, and inherent water use efficiency (IWUE). Additionally, continuous plant growth determinations of leaf area index (LAI) and specific leaf area (SLA) were made over the three cropping systems. The RF potato was a net carbon source (NEE = 187.21 ± 3.84 g C m^{-2}), while both, FI (NEE= −311.96 ± 12.82 g C m^{-2}) and DI (−17.3 ± 4.6 g C m^{-2}) were a net carbon sink. Greater sink activity is due to high fluxes of gross primary productivity (GPP) [where the GPP > ecosystem respiration (R_{eco})] and evapotranspiration (ET), and the high efficiency in the exchange of carbon and water. Without water limitations, the larger canopy, with greater photosynthetic activity ($GPP/R_{eco} > 2$) as well as with low internal resistance offers a greater area for water and carbon exchange, and the highly coupled and synchronized ET – GPP fluxes are primarily controlled by the radiative environment. The lower sink capacity of the DI potato crop and the carbon source activity from the RF, are consequences of a smaller area for water and carbon exchange due to the smaller canopy, and a low IWUE from decoupled and desynchronized carbon and water exchange caused by unbalanced restrictions on ET and GPP fluxes. Specifically, at DI potato, ET remained at a high rate, while GPP was reduced by means of non-stomatal limitations. In the rainfed potato, vapor pressure deficit (VPD) played a significant role increasing midday canopy resistance (Rc) up to 13 times compared to irrigated sites, when VPD was around 0.8 kPa. In consequence, ET and GPP fluxes decreased together, but GPP decreased more than ET because of stomatal and non-stomatal limitations.

Keywords: NEE, IWUE, ET-GPP coupling, Omega, Potato

2.1. Introduction

Efforts to achieve carbon neutrality and promote low-carbon development require climate-smart agriculture where crops cope with climate change impacts and emit relatively low greenhouse gases (Jennings et al., 2020b; Lipper et al., 2014b; Liu et al., 2021c) such as carbon dioxide (CO_2) (Bouzalakos and Mercedes, 2010; Guo et al., 2017b). Vegetation plays a key role to achieve carbon neutrality through photosynthetic CO_2 sequestration (Guo et al., 2017b; Liu et al., 2021c), therefore, is quite essential to understand how agroecosystems can act as carbon sinks and reduce the carbon flux from land into the atmosphere (Wood, 2021b). Potatoes have comparatively low agricultural emissions compared to other crops (Clune et al., 2017b; Haile-Mariam et al., 2008b; Jennings et al., 2020b; Nemecek et al., 2012b), and one of the lowest average global warming potentials (Clune et al., 2017b; Jennings et al., 2020b). However, though potato is an important crop for food security, and for worldwide carbon and GHG balances (CIP, 2022; Devaux et al., 2014), little is known about its carbon sequestration potential which could be very diverse due to differences in crop management practices, especially in water management.

The net ecosystem carbon exchange (NEE), calculated as the difference between R_{eco} and GPP, reflects the amount of CO_2 captured or emitted by vegetation (Liu et al., 2021c), and provides a means of identifying and monitoring carbon sinks (Fei et al., 2017; Wood, 2021b). Nonetheless, the CO_2, captured by vegetation through photosynthesis, is inherently associated with a water loss that regulates the mass-energy exchanges (Field et al., 1995; Tang et al., 2015). Plants tend to optimize the increase in carbon gain (increase GPP) while minimizing water losses (ET) (Katul et al., 2010a, 2009), resulting in a negative net ecosystem exchange (NEE) and a net gain of CO_2 for the

ecosystem (Díaz et al., 2022b; Scott et al., 2006a). Under drought conditions, water to support GPP is limited and the rate of carbon uptake decreases (Ciais et al., 2005a; Law et al., 2000; Pereira et al., 2007; Reichstein et al., 2002; Schwalm et al., 2010; Zhou et al., 2013). As a result, NEE varies from uptake to emission (Ciais et al., 2005a; Jongen et al., 2011), and the potential of crops to act as carbon sinks could be reduced (Jongen et al., 2011).

Water and carbon fluxes are tightly coupled systems (Brunsell and Wilson, 2013; Díaz et al., 2022; Gentine et al., 2019; van Dijke et al., 2020a), which tend to be synchronized since they share common environmental controls, and the stomatal path of water vapor and CO_2 exchange during photosynthesis (Gentine et al., 2019; Krich et al., 2022; Leuning, 1995; Lin et al., 2015; Lombardozzi et al., 2012b). This essential tradeoff of water (ET) for carbon (GPP) (Díaz et al., 2022b; Law et al., 2002b), and their coupled relationship, could be quantified through water use efficiency (WUE), which connects water and carbon fluxes together and is a key indicator of ecosystem CO_2–water coupling (Ali et al., 2017; Gentine et al., 2019; Hu et al., 2008; Keenan et al., 2013a; Li et al., 2022; Niu et al., 2011; Tang et al., 2015). However, though the WUE concept provides useful information to optimize water and carbon management in crop production (Keenan et al., 2013b; Oo et al., 2023; Xie et al., 2016) the influence of vapor pressure deficit (VPD) on canopy conductance (Monteith, 1986; Wagle et al., 2016) could lead to misinterpretation of carbon uptake and water loss responses to environment (Wagle et al., 2016). Many studies have indicated that WUE is strongly dependent on VPD at daily or hourly time scales (Abbate et al., n.d.; Beer et al., 2009; Herbst et al., 2002; Hu et al., 2008; Linderson et al., 2012; Morén et al., 2001; Tang et al., 2006; Zhou et al., 2015, 2014), and so the alternative concept Inherent Water Use Efficiency (IWUE) was suggested to include the effects of vapor pressure deficit (VPD) on the photosynthesis-transpiration relationship via stomatal conductance (Beer et al., 2009; Bierhuizen and Slatyer, 1965; Launiainen et al., 2011; Zhou et al., 2015, 2014). This approach is an analogy of the leaf level intrinsic water-use efficiency (iWUE), defined as the ratio of the fluxes of net photosynthesis and conductance for water vapor (Beer et al., 2009; Li et al., 2017).

At the ecosystem level, $IWUE = \frac{GPP*VPD}{ET}$, and it can be determined by means of carbon GPP and water ET measurements from the eddy covariance technique, since carbon assimilation is proportional to GPP, and VPD/E is a proxy for canopy conductance (Beer et al., 2009). From IWUE, the stronger linear relationship between GPP*VPD and ET (Beer et al. (2009), has been widely used to comparing diurnal cycles of carbon and water (Nelson et al., 2018b) and to explore carbon and water coupling interactions (Battipaglia et al., 2013a; Grossiord et al., 2014; Leonardi et al., 2012; Loader et al., 2011; Zhou et al., 2014). The IWUE represents the intrinsic link between carbon and water fluxes through stomatal conductance, however the extent of the surface control by stomata, will depend on the degree of decoupling [omega coefficient, (Jarvis and Mcnaughton, 1986)] between the plant canopy and the atmosphere (Steduto and Hsiao, 1998), which in turn, is controlled by VPD and soil water availability. In this sense, accounting for the effect of VPD results in a physiologically more meaningful approach for studying carbon–water interactions.

Photosynthesis and transpiration are closely related that knowledge and assumptions about one are required to understand the other (Nelson et al., 2018b). However, the interrelationship between carbon and water cycles in potatoes crops is not completely understood. To the best of our knowledge, there have been no water-carbon coupled studies that provide information to understand how water availability modulates the carbon sink or source behavior of potatoes. Specifically, research has not explored the mechanism and interactions of carbon and water coupling and its relation to the NEE. The available studies about sink capacity have been carried out for "European" potato (*S. tuberosum* Chilotanum Group), addressing the effect of climate and management on carbon fluxes (NEE, GPP, R_{eco}) independently of water vapor flux (ET) (Aubinet et al., 2009a; Buysse et al., 2017;

Meshalkina et al., 2017, 2018; Moors et al., 2010). Likewise, only one study has reported a relatively high carbon sink capability of irrigated potato fields compared to other rainfed crop sites (Chi et al., 2016b).

Around half of the global potato harvest comes from developing countries (Birch et al., 2012b; Hill et al., 2021b; Mackay, 2009), where the "Andean" potatoes, S. *tuberosum* Andigenum Group (Ghislain et al., 2009b; Raker and Spooner, 2002) are a primary source of income and the most crucial staple food (Hill et al., 2021b; Mosquera Vásquez et al., 2017a). Andean potatoes are cultivated under short days of the tropical highlands in both industrial irrigated fields and rainfed systems customary among small-holders' farmers. We hypothesize that, under well-watered conditions, a tight coupling between GPP and ET fluxes is due to Photosynthetic Photon Flux Density (PPFD)-drive high photosynthesis and evapotranspiration rates, generating the highest IWUE and therefore a larger diurnal sink activity (NEE more negative). In rainfed systems, severe drought episodes could affect the carbon sink capability of potatoes via decoupling between carbon and water fluxes and asynchronous response of GPP and ET. In this paper, we studied the close link between carbon and water fluxes to understand the response of NEE and its components GPP and R_{eco} to water availability. We used carbon and water flux measurements from two industrial production systems and one small-scale rainfed systems to develop the following objectives: (a) quantify magnitudes of NEE and its components (gross primary production, GPP, and ecosystem respiration, R_{eco}) in irrigated and rainfed potato crops, (b) study the impact of water deficit periods on carbon and water vapor fluxes and explore the role of leaf area in controlling these fluxes, and (c) study and quantify ET-GPP coupling and inherent water use efficiency IWUE in irrigated and rainfed potato crops.

2.2. Materials and Methods

2.2.1. Site description

The study area is in a fluvio-lacustrine plain landscape originated from the silting of an old lake that occupied different tectonic depressions formed in the process of lifting the eastern mountain range. The soils have the influence of volcanic ash from the volcanic bodies of the central mountain range and correspond predominantly to Andisol, Inceptisol and Vertisol orders (Service-USDA, 2014). The soils of the terrace relief generally have a depth greater than one meter, however, in the decaying marshes and valleys reliefs, the shallow soils are limited by the water table. The deficit irrigated (DI) cycle was carried out in a 9.5-hectare commercial lot under rain gun sprinkler system and located in the Municipality of Facatativá, Cundinamarca, Colombia (4.80371, -74.28883, ~2573 m above sea level). Irrigation was only scheduled during periods when crop development is normally more sensitive to water stress; vegetative growth and tuberization stages. In the Municipality of Subachoque, Cundinamarca, Colombia (4.888668, -74.18668 ~ 2609 m above sea level), the full irrigated (FI) cycle was performed in a 3.11 hectare commercial lot under a fixed-sprinkler irrigation system. The decision to irrigate the crop was made after identifying soil water deficit using a water balance calculated according to FAO-56 and monitoring the soil tensiometers installed inside crop. The rainfed (RF) cycle was carried out in a 6-hectare lot located in the municipality of Tenjo, Cundinamarca, Colombia (4.87033, -74.1294, ~2572 m above sea level). In all study sites, a flat landscape where the soils have an isomesic texture and the parent material are medium-sized deposits and volcanic ash, and the apparent density is less than 1 g cm^{-3}. The average annual temperature of 12 to 14 °C and an annual supply of rainfall between

500 to 1000 mm distributed in a bimodal way predominate. The June - August and December - February periods are the ones with the lowest rainfall (Martínez-Maldonado et al., 2021a).

2.2.2. Meteorological and eddy covariance measurements

Using an eddy covariance station, net carbon exchange and weather variables inside the experimental fields were continuously recorded. In the DI site, the station was installed on March 19, 2020; in the RF site on August 13, 2020; and in the FI site on February 03, 2021. Measurements presented in this study extend from March 19, 2020, until July 30, 2020, at DI site, August 11 until December 11, 2020, at RF site and from February 02 until June 07 in FI site. The configuration of the eddy covariance EC micrometeorological station used at each evaluation site consisted of main and complementary sensors. The main sensor, the IRGASON, is a system integrated by an open-path gas analyzer (EC 150, Campbell Scientific, Inc., Logan, Utah, USA) and a 3D sonic anemometer (CSAT3A, Campbell Scientific, Inc., Logan, Utah, USA) both operated by a separated electronic module (EC100, Campbell Scientific, Inc., Logan, Utah, USA). EC tower and additional sensor configuration are described by Martínez-Maldonado et al. (2021).

2.2.3. NEE partitioning between gross primary productivity GPP and ecosystem respiration R_{eco}

Negative values represent fluxes from the atmosphere to the surface, while positive values represent fluxes moving from the surface to the atmosphere. Therefore, the ecosystem respiration (R_{eco}) is defined as a positive value, while the gross primary production (GPP) is defined as a negative value. Nighttime values of NEE are equal to R_{eco} due to the absence of photosynthetic activity at night, while diurnal NEE is the algebraic sum of GPP and R_{eco}. The non-linear Mitscherlich light-response function, which parametrizes the NEE against the PPFD was used to partition diurnal NEE (solar global radiation > 1 W m^{-2}) into ecosystem respiration (R_{eco}) and GPP (Falge et al., 2001a; Tagesson et al., 2015a) as follows:

$$NEE = -\left(A_{gmax} + R_d\right) * \left(1 - \exp^{\left(\frac{-\phi * I_{inc}}{A_{gmax} + R_d}\right)}\right) + R_d \quad (1)$$

where Ag_{max} is the CO_2 uptake at light saturation [μ_{mol} (CO_2) m^{-2} s^{-1}]; R_d is the respiration term [μ_{mol} (CO_2) m^{-2} s^{-1}] and ϕ is the quantum efficiency [μ_{mol} (CO_2) μ_{mol} (photon) $^{-1}$] or the initial slope of the light response curve, and I_{inc} is the incident PPFD [μ_{mol} (photon) m^{-2} s^{-1}]. For each day, a set of parameters was calculated through non-linear regression, using a subset of NEE and PPFD data from 7 prior to 7 posterior days (moving window of 14 days). Then, for each diurnal half hour of the same day; modeled GPP was estimated by subtracting R_d from the non-linear Mitscherlich light-response function. R_{eco} was calculated by subtracting modeled GPP from measured NEE. Data post-processing, quality control, gap-filling, energy balance closure, uncertainty and statistical analysis methods followed the procedures described in (Martínez-Maldonado et al., 2021b).

2.2.4. Energy balance closure

Half-hourly time series of Rn, H, LE and G from the three sites were analyzed to assess the EC flux data quality through the energy balance closure. Under ideal conditions, according to the first thermodynamics law, the sum of all energy fluxes is zero. Therefore, the energy balance for the studied systems is given by:

$$H + \lambda E = Rn - G - Gs \quad (2)$$

where H is the sensible heat flux, λE is the latent heat flux, both of which was most directly measured using the eddy covariance (EC) technique, G is the soil heat flux at the surface, and Gs is the soil energy storage term. G and Gs were quantified by two heat-flux plates: soil temperature and soil water content sensors installed at depth of 0-20 cm (Campbell and Norman, 1998a; Chi et al., 2016b).

Daily sums of H, λE, G and Gs were calculated, and a linear regression model was parameterized as follow:

$$H_d + \lambda E_d = \beta_0 + \beta_1 (Rn_d - G_d - Gs_d), \quad (3)$$

where d subscript indicates daily flux sum, β0 is the intercept, and β1 is the slope representing the magnitude of the balance closure.

2.2.5. ET-GPP coupling analysis

2.2.5.1. Inherent Water use efficiency

The IWUE was determined to both, daily and half hour temporal scales following the theoretical approach proposed by Beer et al. (2009) which is based on the intrinsic water-use efficiency (iWUE) concept, defined as the ratio of the fluxes of net photosynthesis and conductance for water vapor (Leonardi et al., 2012):

$$iWUE = \frac{A}{g_{H_2O\,v}} = \frac{g_c * (\Delta c)}{1.6 * g_c} = \frac{\Delta c}{1.6} \quad (4)$$

where 1.6 is the molar diffusivity ratio of CO_2 - H_2O (i.e., $gH_2O = gCO_2 * 1.6$, lighter H_2O molecules diffuse more rapidly than does CO_2) "$1.6*g_c$" is the stomatal conductance for water vapor (Gentilesca et al., 2021a). Approximating at the ecosystem level, the vapor pressure difference Δv is atmospheric VPD, leaf level carbon assimilation *A* is GPP from eddy covariance observations and $g_{H_2O\,v}$ is g' that is solved as:

$$g' = \frac{ET}{1.6 * VPD} \quad (5)$$

where *g'* is the conductance at the ecosystem level proposed by Beer et al. (2009). The usage of marker ' indicates that variables are analyzed at ecosystem level. The inherent water use efficiency (IWUE) was then represented by:

$$IWUE = \frac{GPP}{g'} = \frac{g' * (\Delta c')}{1.6 * g'} = \frac{\Delta c'}{1.6} = \frac{GPP}{1.6 * \left[\frac{ET}{1.6 * VPD}\right]} = \frac{GPP * DPV}{ET} \quad (6)$$

2.2.5.2. Diurnal and daily ET-GPP coupling and synchrony

From equation 6, there is a linear relationship between GPP and ET, adjusted by VPD. To quantify the degree of carbon–water coupling for an individual day, the linear correlation coefficient ET vs GPP*VPD was computed using the half-hourly data (Aguilos et al., 2021; Nelson et al., 2018b; Zhou et al., 2014). The correlation coefficients were determined on both, the daily scale during all crop growth for each site, and the average half-hour for each growth stage "vegetative", "tuberization" and "tuber bulking" for each site. When correlation values are close to unity ($r > 0.85$), the two signals tend to be well coupled and synchronized. In contrast, low correlation values indicate carbon–water decoupling and a poor synchronization of the two fluxes (Nelson et al., 2018b).

2.2.5.3. Coupling between the plant canopy and the atmosphere

The extent to which stomatal and canopy conductance may control water vapor and CO_2 exchange was determined through the decoupling factor omega (Ω) calculated at daily scale using the expression of Jarvis & Mcnaughton (1986):

$$\Omega = \frac{1}{1 + \left[\left(\frac{2Rc}{\left(\frac{S}{\Upsilon} + 2\right)}\right)\right] * Ra} \quad (7)$$

where *Ra* is the aerodynamic resistance of the canopy, *Rc* is the canopy stomatal resistance to vapor diffusion, and Υ is the psychrometric constant. The *Rc* was calculated to both daily and half hour temporal scales by using:

$$Rc = \frac{\rho * cp * VPD}{\Upsilon * LE} + \left(\frac{\Delta}{\Upsilon}\beta - 1\right) * Ra \quad (8)$$

where ρ is the mean air density, cp is the specific heat for air, Υ is the psychrometric constant, Δ is the slope of the saturation vapor pressure-temperature curve calculated at the air temperature T_a, β is the Bowen ratio and *Ra* is the aerodynamic resistance. Finally, *Ra* was calculated to both, daily and half hour temporal scales by:

$$Ra = \frac{\ln\left(\frac{z}{Zo_v}\right)}{u^* K^2} \quad (9)$$

where k is the von Karman constant, u^* is the friction velocity ($m \cdot s^{-1}$), z is the measurement height and z_{ov} is the surface roughness (≅0.01h) for water vapor.

2.2.6. Biological measurements and growth Analysis

From planting and during crop growth, sampling of plants with sequential harvesting was performed. Every 11 or 12 days, ten plants were randomly uprooted for growth analysis after 35, 41, 48, 57, 63, 69, 78, 84, 97, 104, 112, 124, 133, and 147 days post planting (DPP) at DI site; after 25, 37, 47, 54, 65, 75, 85, 98, 105, and 116 DPP at RF site and 33, 46, 57, 70, 80, 96, 110, 122, 135 and 152 DPP, at FI site. The plants were partitioned into four components: green leaves (lamina and petiole), roots, stems, and tubers. The total leaf area and fresh weight of each sample were measured. Plant material was then placed in paper bags and dried in a forced-air drying oven to constant weight at 70 °C. Dry weight data for leaves, roots, stems, and tubers were fitted to nonlinear functions.

Growth and morphological parameters such as specific leaf area (SLA) and leaf area index (LAI) were calculated as outlined by (Hunt, 1990).

$$LAI = \frac{LA}{P} \tag{10}$$

where LA is total leaf area per plant, and P is unit of land area. The SLA measure the density or relative thinness of leaves, which relates the leaves' areas with their dry weight (R Hunt, 1990):

$$SLA = \frac{\left[\left(\frac{LA_1}{LW_1}\right)+\left(\frac{LA_2}{LW_2}\right)\right]}{2} \tag{11}$$

where LW is total leaf dry weight per plant.

2.3. Results

2.3.1. Meteorological Conditions

The average of daily mean PPFD was significantly higher ($p < 0.05$) in the FI site (724.5 ± 216.7 μmol photons m^{-2} s^{-1}) compared to DI (382.45 ± 288.86 μmol photons m^{-2} s^{-1}) and rainfed (567.9 ± 230.7 μmol photons m^{-2} s^{-1}). The average daily maximum vapor pressure deficit (VPD) was higher in the RF site (0.80 KPa ± 0.24) compared to FI (0.73 KPa ± 0.25) and DI(0.59 KPa ± 0.16), while the average daily mean VPD was lower at the DI site (0.29 KPa ± 0.09) compared to FI (0.38 KPa ± 0.12) and RF (0.40 KPa ± 0.16) sites. The accumulated rainfall for the RF site was 229 mm, with a non-uniform time distribution, including events of consecutive dry days followed by high rainfall events, observed by the end of the crop cycle, reaching 98 mm in one week (101 to 107 DPP). The accumulated rainfall for the FI (306 mm) and DI (293 mm) sites were higher and more uniformly distributed, however, at FI site, a drier lapse occurred, from 50–90 days. At the DI site, accumulated rainfall was 306 mm. Low water availability in RF site (SWC < WP) was around 71% of total crop growth days, however, an increase of SWC occurs after 100 days because of higher rain. At the DI site, SWC was closer to the WP level than FC, and was < WP around 40% mainly during initial crop growth days (20 -50 DPP) (Figure 1).

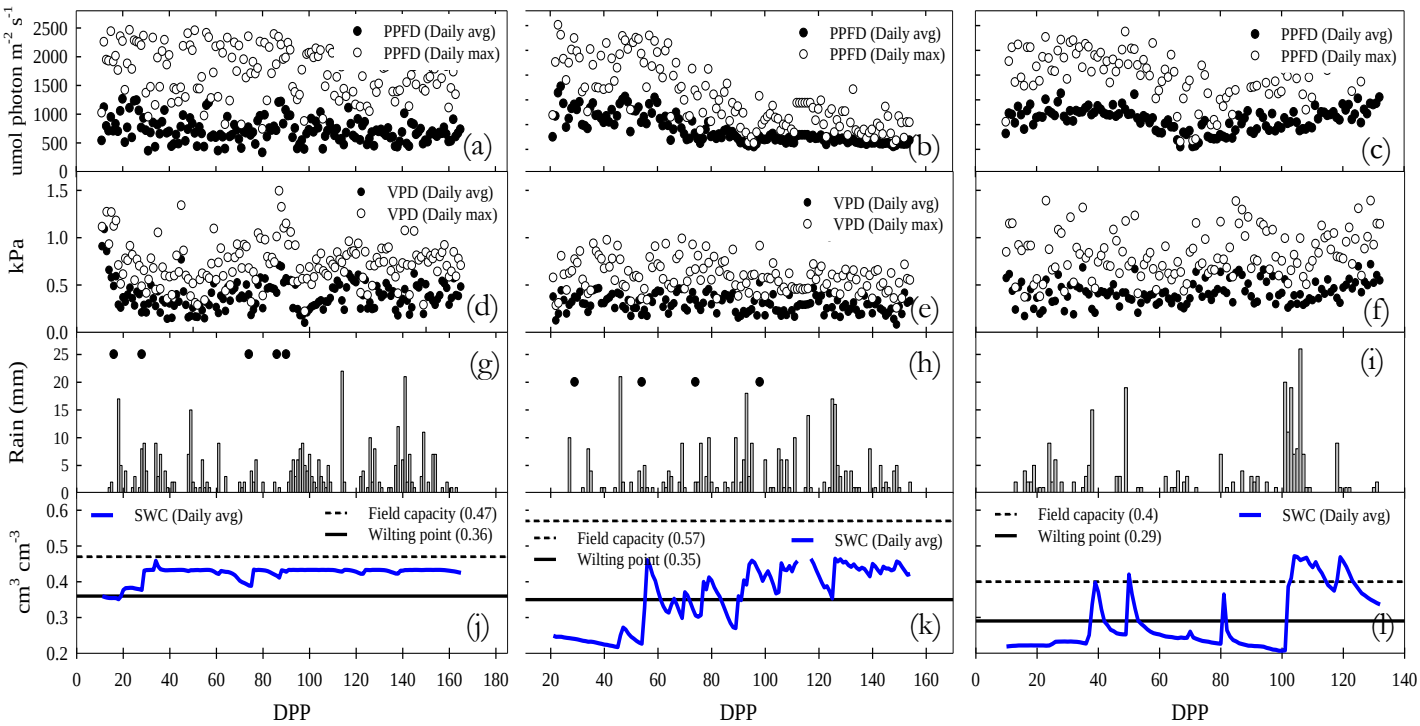

Figure 1. Meteorological measurements for potato crop systems grown under different water management regimes [(a,d,g,j) full irrigation (FI); (b,e,h,k) deficit irrigation (DI); (c,f,i,l) rainfed conditions (RF)]. (a,b,c) photosynthetic active radiation, µmol photons m−2 s−1 (PPFD); (d,e,f) air vapor pressure deficit, kPa (VPD); (g,h,i) rainfall and irrigation times (black dots), mm; (j,kl) soil water content, cm3 cm−3 (SWC), measured at 0–20 cm depth is shown as daily mean values.

2.3.2. Carbon Fluxes of NEE, GPP, and R_{eco}

In the FI site, GPP was the dominant process over the different growth stages, while R_{eco} values were lower and had stable values near 5 g C m^{-2} d^{-1}. Daily GPP and R_{eco} peaked at 13.53 g C m^{-2} d^{-1} and 8.1 g C m^{-2} d^{-1}, respectively, in the tuberization growth stage. NEE values were positive during the first days of the vegetative period, because of the scarce plant cover (GPP close to zero), and during chemical haulm (137 DPP). The NEE negative values decreased rapidly due to the progressive increase of GPP, starting in the vegetative stage when crop emergence occurred, and reaching the most negative values during the tuberization growth stage. As a result, the sink function was strong during the tuberization growth stage, with a daily NEE peak of - 8.35 g C m^{-2} d^{-1}. At DI site, GPP was slightly higher than R_{eco} throughout the growth stages. Compared to the FI site, the GPP values were lower and R_{eco}, higher. They peaked at 10.34 g C m^{-2} d^{-1} and 9.86 g C m^{-2} d^{-1}, respectively, in the tuberization growth stage. Again, NEE fluxes increased as a result of the progressive increase of GPP, however, since the SWC was below the WP level about 41% of the growth cycle, the sink function was weaker than the FI site, with NEE daily peak of - 4.02 g C m^{-2} d^{-1}. In the RF site, the water deficit extended to the vegetative growth and transition phases, during 70% of the cycle. In consequence, R_{eco} dominated the NEE, resulting in a strong daily release of carbon (positive values) during the initial stage of growth. In the tuber stage and most of the tuber bulking, GPP and R_{eco} had similar values and NEE remained at values close to zero until day 120 DPP, where emissions were related to chemical dehaulming (Figure 2).

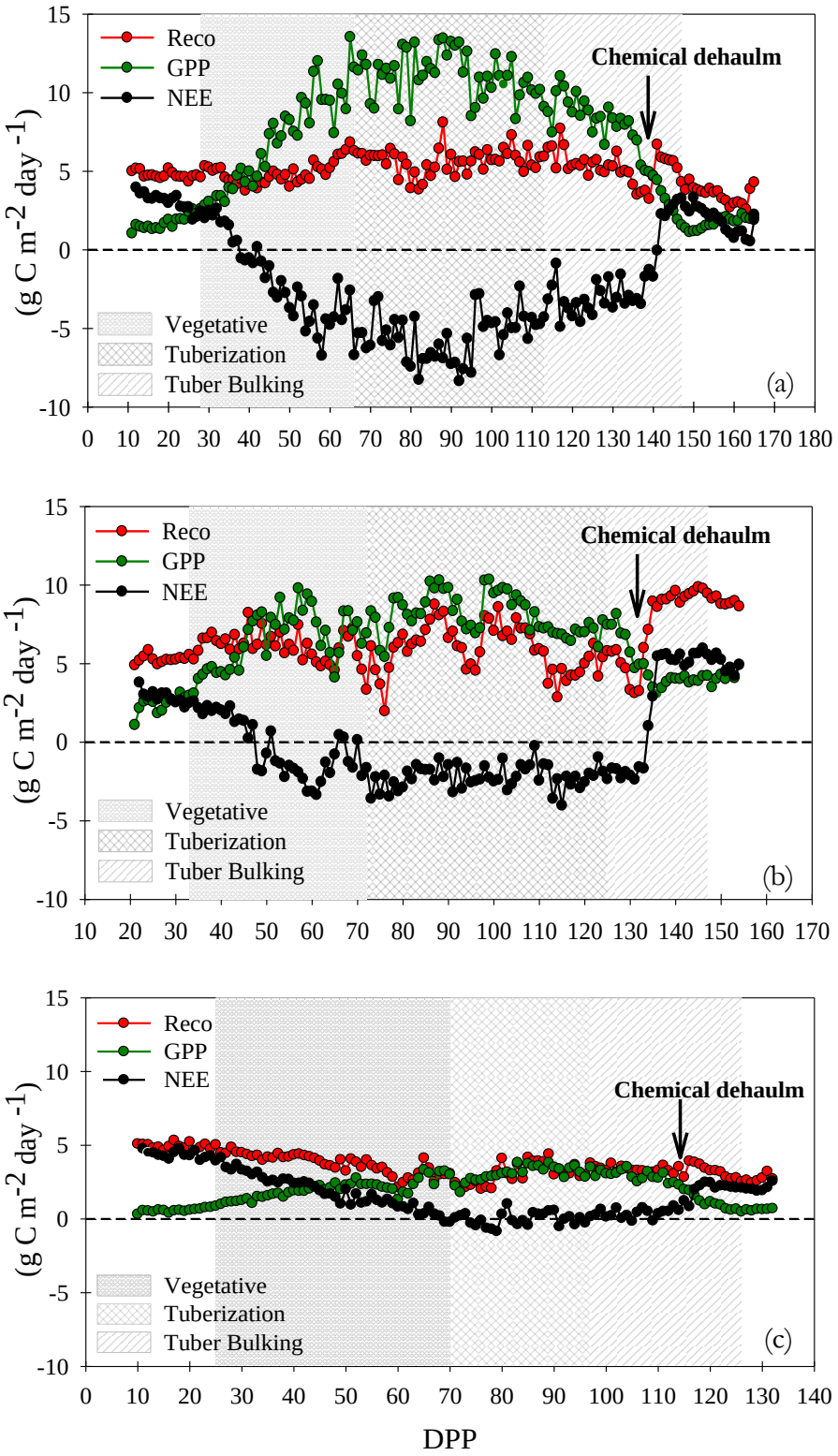

Figure 2. Daily gross primary productivity (GPP), Ecosystem respiration (R_{eco}), and net carbon ecosystem exchange (NEE) during different potato growth stages (vegetative, tuberization, tuber bulking) in three different water regimes (a) full irrigation (FI), (b) deficit irrigation (DI), and (c) Rainfed (RF) conditions.

The differences in the carbon budgets between FI, DI, and RF can be observed in the accumulated NEE, GPP, and R_{eco} (Figure 3). During the initial stages of growth positive values of accumulated NEE were observed in the three measurement sites. However, at the end of the vegetative stage, the FI site was a slight sink of CO_2 with a cumulative NEE of −26 ± 3.47 g C m^{-2} while DI and RF sites were CO_2 sources to the atmosphere (16.91 ± 2.14 g C m^{-2} and 143 ± 5.65 g C m^{-2}, respectively). From the beginning of the tuberization phase, the FI and DI sites were carbon sinks. Nonetheless, the net carbon accumulation at the FI site was greater by -302 g C m^{-2} compared to DI during the tuberization until the end of the tuber bulking stage. The RF site was a CO_2 source to the atmosphere during all growth stages because of its cumulative NEE of 175 ± 3.84 g C m^{-2} at the end of tuber bulking. The effect of chemical haulm is observed as a change in the evolution of the accumulated NEE curve, the daily positive values limit the final balance making it less negative, which is quite evident in the DI site. At the end of the cycle, including haulming emissions, the cumulative NEE at FI, DI and RF was −311.96 ± 12.82, −17.3 ± 4.6 and 187.21 ± 3.84 g C m^{-2}, respectively.

The cumulative GPP was 1087.56 ± 31 g C m^{-2}, 838.69 ± 24 g C m^{-2} and 250.70 ± 7.8 g C m^{-2} for FI, DI and RF, respectively, and the R_{eco} sums were 775.6 ± 19 g C m^{-2}, 821.39 ± 20 g C m^{-2} and 437.92 ± 11 g C m^{-2}. In the FI site, differences in the accumulated values of GPP and R_{eco} begin from the vegetative phase; the GPP values are substantially higher until the end of the evaluation period showing a sigmoidal behavior. Compared to R_{eco}, the cumulative GPP at DI was slightly higher from the 90 ddp in the tuberization growth stage, but it became lower while under chemical haulm practice. In the RF site, the accumulated R_{eco} was higher than GPP during all growth stages (Figure 3).

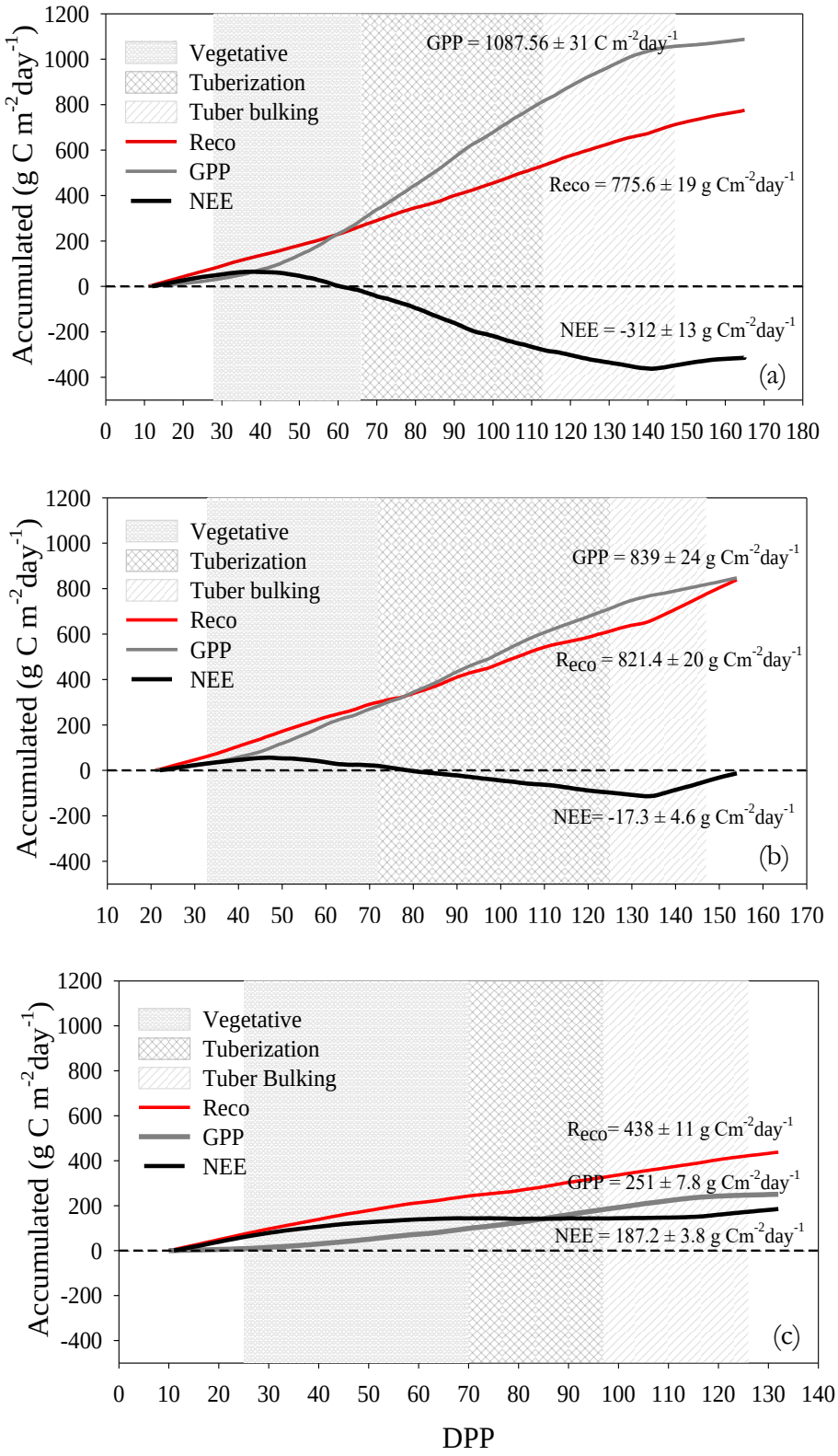

Figure 3. Cumulative gross primary productivity (GPP), Ecosystem respiration (R_{cco}), and Net Carbon Ecosystem Exchange (NEE) during different potato growth stages (vegetative, tuberization, tuber bulking) in three different water regimes (a) full irrigation (FI), (b) deficit irrigation (DI), and (c) Rainfed (RF). Values inside figures correspond to NEE reached at the end of cycle (165 DPP, 152 DPP and 132 DPP for FI, DI and RF, respectively)

2.3.3. Crop development, surface resistance and carbon - water fluxes

In the FI site, the higher LAI (max LAI = 4.3 at 82 DPP) and the decrease of the SLA during the vegetative stage (specifically during accelerated growth, 30 – 50 DPP), imply a greater canopy expansion and a greater assignment of biomass for thicker leaves. At the DI site, the maximum LAI (3.15 at 92 DPP) was similar to that observed at the RF site (3.14 at 78 DPP). For both sites, after reaching max LAI, a strong drop in LAI was observed compared to FI site. The increasing behavior of the SLA during the vegetative growth in the RF site and tuberization in the DI site indicates that the canopy had less thick leaves compared to FI (Figure 4).

An average of 80±14.6% of the net radiation was partitioned to latent heat flux, and its variation was associated with LAI evolution at the FI site. The highest percentage of energy destined for latent heat flux (average of 85.3±16.3%) was observed during the tuberization stage when canopy reached the maximum LAI. In the tuber bulking, the expressive reduction in the latent heat partitioning follows the course of LAI during leaves senescence (Fig. 4a). At the DI site, the energy distribution for LE does not clearly follow the LAI variation and was slightly lower (mean 74 ± 8.89%) compared to FI. During the tuberization stage, at maximum LAI, a slightly lower allocation to latent heat from Rn (76.6 ± 8%) was also observed (Fig. 4b). At the RF site, the Rn distribution for LE during the growth cycle averaged 52 ±16.19%. Likewise, at maximum LAI, the LE allocation only reached 47.3 ±15.8%, being unclear the association between the energy consumption by the latent heat and the variation of LAI (Fig. 4c).

The GPP/R_{eco} relationship allows determining what fraction of the assimilation (GPP) is consumed by the plant or by the heterotrophic activity from soil. Values below 1 take place when the system behaves as a source of CO_2 and there is a predominance of heterotrophic respiration. When GPP/ R_{eco} > 1, the GPP is greater than R_{eco} and the system is storing carbon. At the FI site, R_{eco} was equal to or greater than GPP (GPP/R_{eco} ratio < 1) during the initial crop growth (0 – 38 DPP, low crop cover) and at the end of tuber bulking. From 39 DPP, the GPP/R_{eco} ratio was greater than 1, and their values increased following the LAI pattern until reaching values around 2 Maximum GPP/R_{eco} values (between 2.6 and 2.8), were reached during the maximum LAI in the tuberization stage. At the DI site, GPP/R_{eco} ratio behaves like the FI site. GPP/R_{eco} ratio was less than one, during the initial phases (0 – 50 DPP) and at the end of tuber filling GPP/R_{eco} < 1. However, during tuberization and tuber bulking, the GPP/R_{eco} ratio ranged from 1 to 1.5. In the RF site, during most of the cycle, the GPP/R_{eco} ratio was below 1, and only in the tuberization growth stage the GPP/R_{eco} was > 1 (Figure 4).

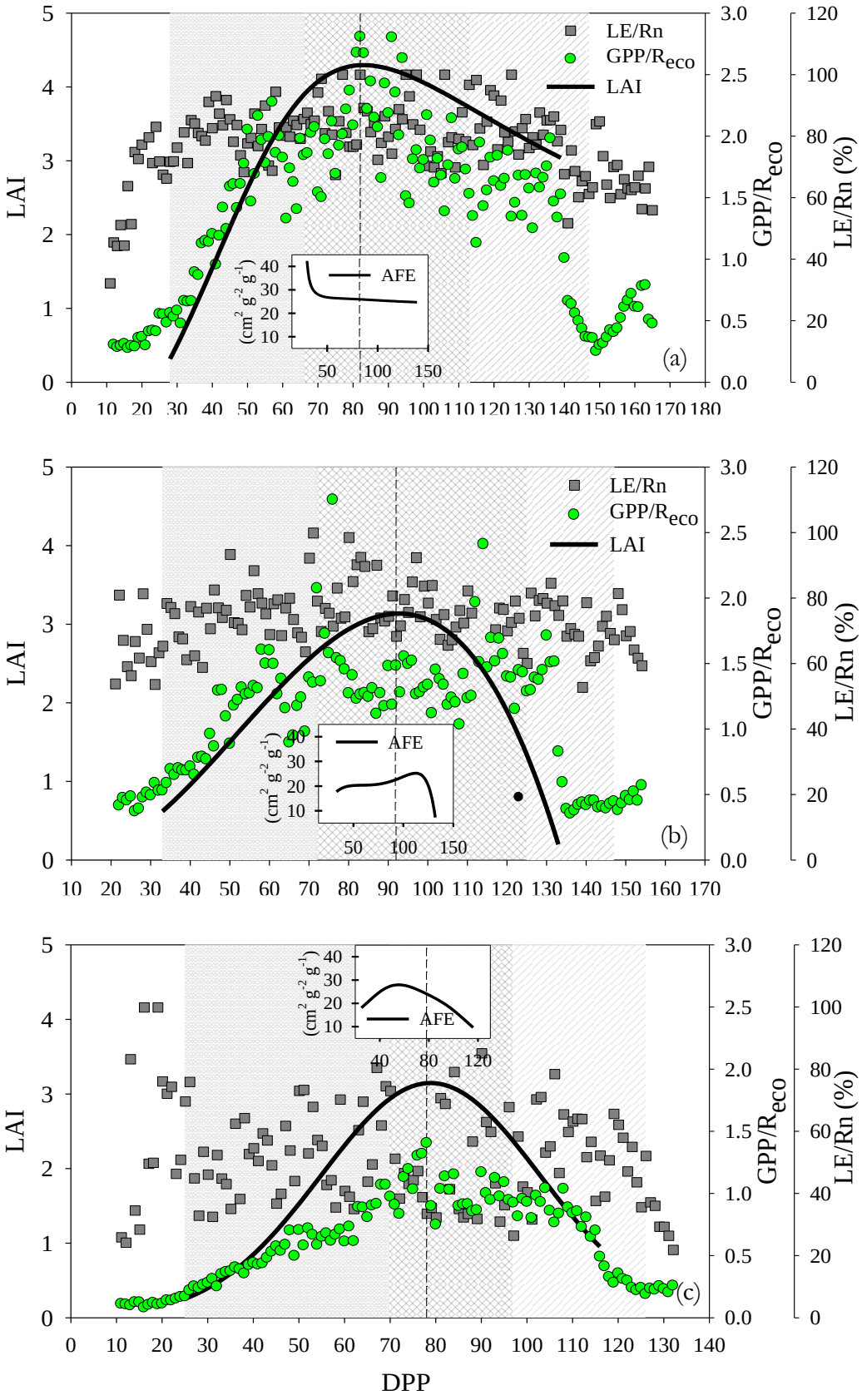

Figure 4. Daily latent heat partitioning (LE/Rn), GPP/R_{eco} ratio, leaf area index (LAI) and specific leaf area, during different potato growth stages (vegetative, tuberization, tuber bulking) in three different water regimes (a) full irrigation (FI), (b) deficit irrigation (DI), and (c) Rainfed (RF) conditions. Dotted perpendicular line indicates maximum LAI.

The diurnal pattern of canopy resistance (Rc) was quite different from that of aerodynamic resistance (Ra). In the FI site, Rc ranged from 17.01 to 75.06 s m^{-1}, with an average of 38.27 (± 12.63) s m^{-1} during the entire growth period. Minimum and maximum Ra were 44.15 s m^{-1} and 146.04 s m^{-1}, respectively, with an average of 90.2 (± 23.13) s m^{-1} (Fig. 5a) The diurnal patterns of Rc and Ra at DI were similar to those in the FI site, varying from 11.15 to 80.42 s m^{-1} and from 37.32 to 112.38 s m^{-1}, respectively and with averages of 32.67 (± 14.86) s m^{-1} and 74.22 (± 18.11) s m^{-1}, respectively (Fig. 5b). However, in the RF site, Rc values strongly increased, and its daily variation was much higher than FI and DI sites, ranging from around 10.36 to 133 s m^{-1}, with an average of 56.07 (± 28.75) s m^{-1}. The daily values and variation of Ra are lower than the other sites, ranging from 36.5 to 114 s m^{-1}, with an average of 64.52 (± 14.66) s m^{-1}. Furthermore, it can be observed that in the RF site Rc was generally higher than Ra reaching values over 100 s m^{-1} during both, vegetative and tuberization stages (Fig. 5c).

The total ET was 297.69 mm for the FI site, 265.05 mm for DI, and 191.38 mm for the RF site. The average daily ET was lower (1.5 mm day^{-1}) for the RF site compared with the DI (2 mm day^{-1}) and FI (1.93 mm day^{-1}). At the FI site in the vegetative stage, the daily sums of ET ranged from 1.05 to 2.8 mm day^{-1} and accumulated ET was and 71 mm, but those values increased during tuberization to an accumulated of 95 mm, and daily sums ranging from 0.97 to 3.2 mm day^{-1}. During Tuber bulking accumulated ET was 50.1 mm while daily ET sums ranged from 1.3 to 3 mm day^{-1}. At the DI site, daily sums of ET ranged from 1.14 to 4 mm, with an accumulated of 87 mm during vegetative growth. The values of daily sums of ET in the tuberization stage were 1.3 to 3.4 mm day^{-1}, and the ET accumulated was 98 mm. The lower values were measured for tuber bulking, when daily sums of ET varied from 1.45 to 2.5 mm day^{-1}, with an accumulated of 46 mm. The RF site had daily sums of ET fluctuating from 0.89 to 3 mm, with an accumulated of 78 mm during vegetative growth. Compared to FI and DI, lower values of daily sums and accumulated ET were measured during the tuberization stage; from 0.78 to 2.3 mm day^{-1}, and 36 mm (almost 60 mm difference to FI and DI), respectively. At the tuber bulking stage, although daily sums (0.6 – 3.3 mm day^{-1}) were similar to FI and DI, lower values were found for accumulated ET (30 mm) (Figure 5).

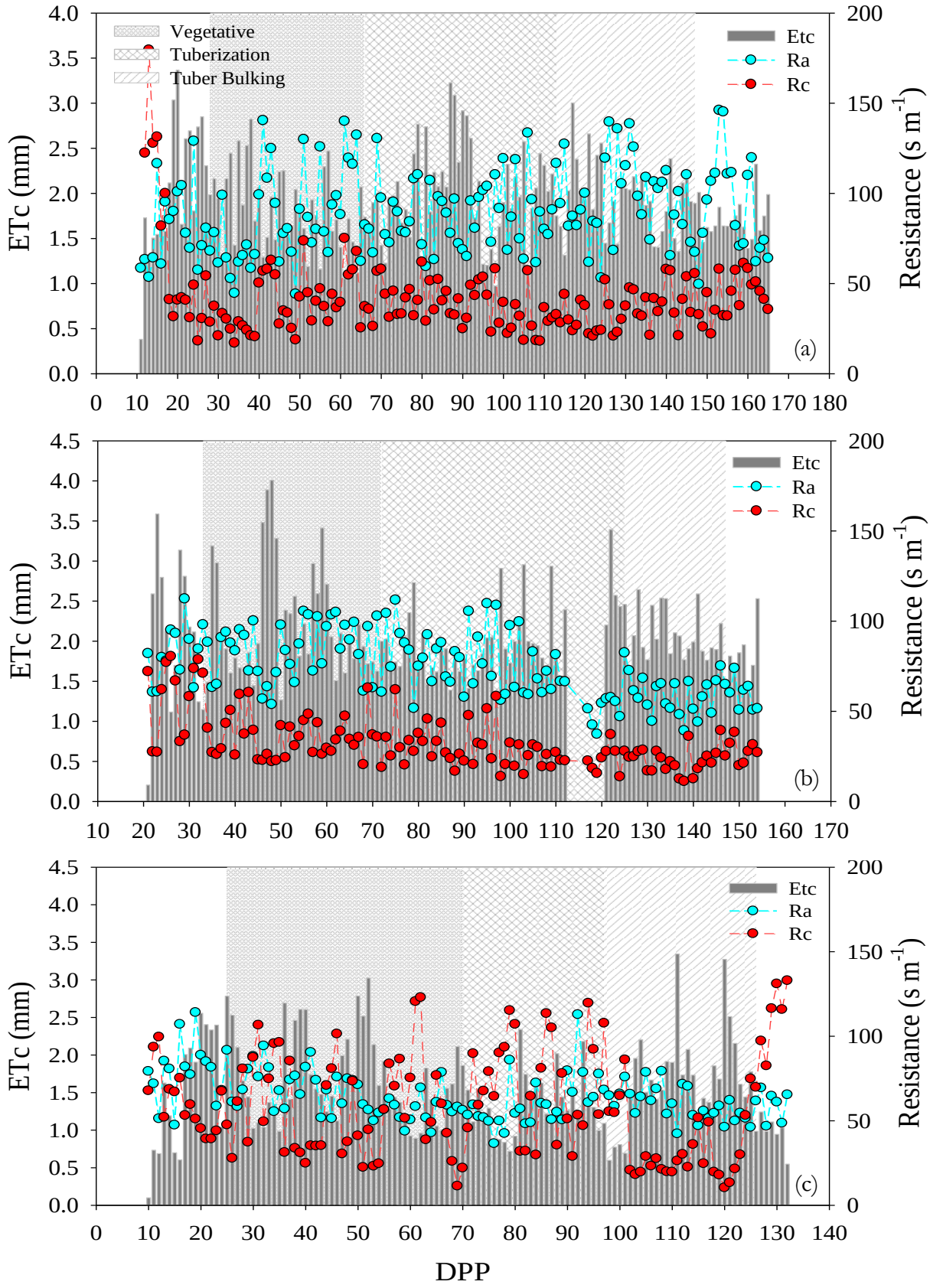

Figure 5. Daily crop evapotranspiration (ETc) and canopy (Rc) and aerodynamic (Ra) resistances, during different potato growth stages (vegetative, tuberization, tuber bulking) in three different water regimes (a) full irrigation (FI), (b) deficit irrigation (DI), and (c) Rainfed (RF) conditions.

2.3.4. Diurnal ET-GPP trends, synchrony and IWUE

Results of the diurnal pattern of vapor pressure deficit (VPD), aerodynamic resistance (Ra), canopy resistance (Rc), ET, and GPP fluxes for FI, DI, and RF sites are presented in Figure 6. The highest daytime carbon and ET fluxes were observed for the FI site, mainly during the tuberization stage (Fig 6b). The GPP showed an increasing trend throughout the day, reaching the highest values around 10:00 – 12:00 (0.83 mg m^{-2} s^{-1}, 1.27 mg m^{-2} s^{-1}, 0.77 mg m^{-2} s^{-1} for vegetative, tuberization, and tuber bulking respectively) after that, it remained constant until 14:00 and then it dropped. The ET had a similar pattern, but peaked at midday (0.11 mm, 0.13 mm, and 0.12 mm for vegetative, tuberization, and tuber bulking respectively) and dropped immediately after. Under FI conditions, the highest sink activity was observed around 10:00 – 12:00, reaching min NEE values of -0.6 mg m^{-2} s^{-1}, -1.025 mg m^{-2} s^{-1}, and -0.59 mg m^{-2} s^{-1} for vegetative, tuberization and tuber bulking respectively. At the DI site, the diurnal patterns of ET and GPP were like FI, but they peaked earlier (around 9:00). Compared to the FI site, daytime ET was similar, but GPP was lower mainly during tuberization (-0.68 mg m^{-2} s^{-1}) and tuber bulking (-0.23 mg m^{-2} s^{-1}) stages (Fig. 6e, 6f). In consequence, the daytime sink activity had a reduction of 34% and 61% for tuberization and tuber bulking respectively, compared to FI NEE values. The RF site had the lowest daytime carbon and ET fluxes. ET peaked values reached at 9:00 during vegetative and tuberization stages were 11% and 31% lower compared to the same stages in the FI site (Fig. 6g, 6h). However, the largest reductions were observed for GPP and NEE fluxes, where the sink activity was reduced by 85%, 73%, and 83% during vegetative, tuberization, and tuber bulking stages, respectively, compared to the same stages in the FI site.

At FI and DI, the VPD increases progressively from 7:00, reaching the highest values around 11:00 – 12:00; max VPD values were near 0.5 kPa, between 0.5 – 0.6 kPa, and 0.4 – 0.6 kPa, for vegetative, tuberization and tuber bulking respectively. In the RF site, an increase of VPD during daytime was observed, reaching maximum values around 12:30 of 0.6 kPa, 0.8 kPa, and 0.72 kPa for vegetative, tuberization, and tuber bulking respectively.

We observed a typical theoretically expected parabolic variation in the diurnal trend of Rc and Ra during all growth stages in both sites (Alves et al., 1998; Irmak and Mutiibwa, 2010; Lin et al., 2020; Monteith and Unsworth, 2013; Perez et al., 2006; Rana et al., 1994). At the FI and DI sites, Rc had high values (> 30 m s^{-1}) in the early morning (5:00 – 8:00), then tend to decrease toless than 15 m s^{-1}, remaining relatively constant from 10:00 to 15:00 After this, Rc increases gradually in the afternoon. The Ra had a diurnal pattern similar to that of Rc and almost does not change among growth stages. However, in both FI and DI sites, values of Ra were higher than Rc, ranging from 40 to 80 m s^{-1}. In the RF site, the diurnal pattern of Rc was different, showing an increasing trend throughout the day and higher values than FI and DI sites. From early morning, Rc increased linearly to its highest values (45 m s^{-1}, 74 m s^{-1}, 32 m s^{-1} for vegetative, tuberization, and tuber bulking respectively) around 13:00 – 14:00 and then dropped. From midday to noon, during the vegetative and tuberization stages, the Ra values were less than or equal to Rc, due to the changes in the diurnal pattern of Rc and a lower Ra (ranging from 30 to 60 m s^{-1}) under RF conditions (Figure 6).

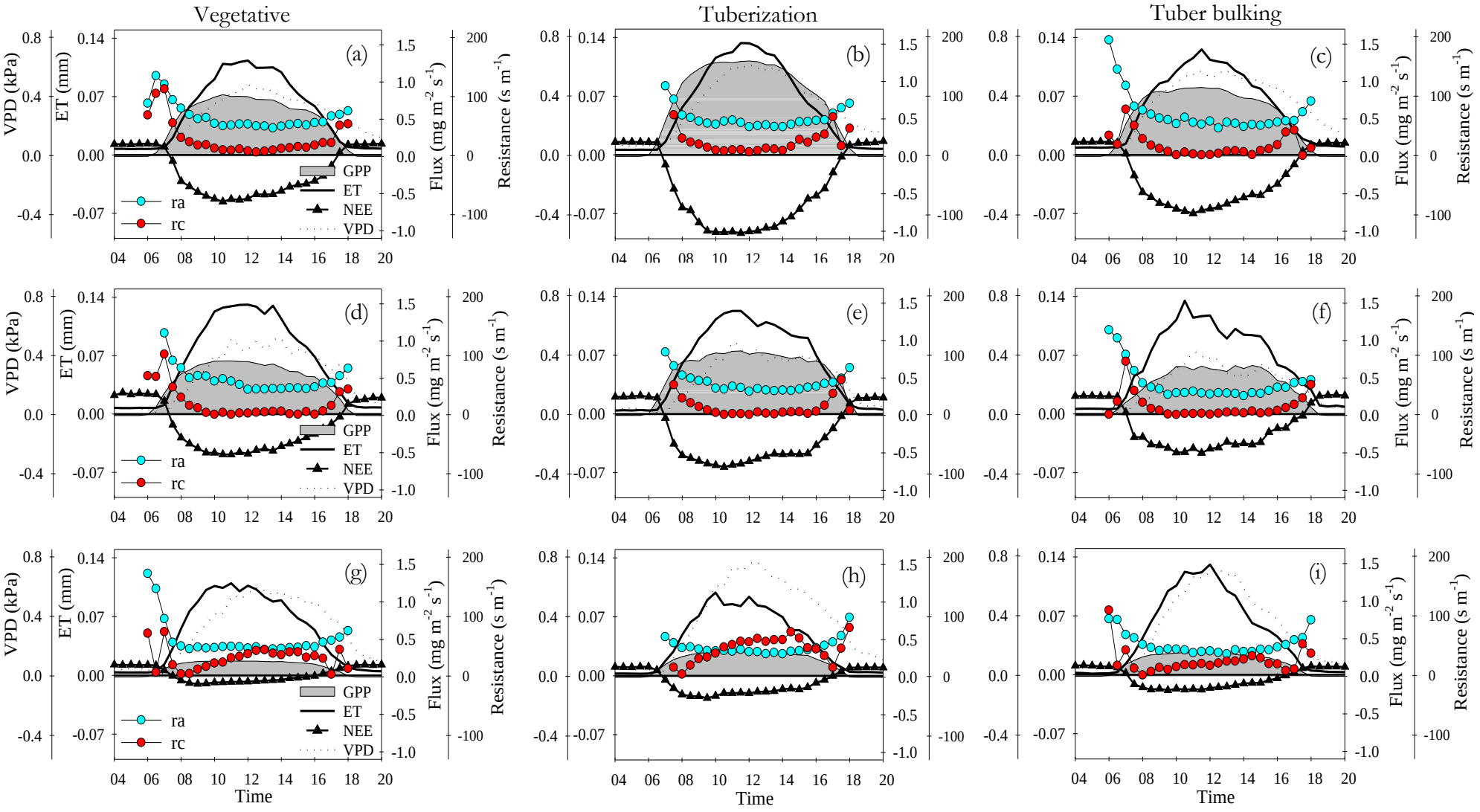

Figure 6. Diurnal half-hourly ET, GPP, VPD, NEE, Ra and Rc, during different potato growth stages (vegetative, tuberization, tuber bulking) in three different water regimes (a,b,c) full irrigation (FI), (d,e,f) deficit irrigation (DI), and (g,h,i) Rainfed (RF) conditions. The diurnal cycle begins at 4:00 h and ends at 20:00 h.

Figure 7, show a comparison between the daily cycles (normalized half-hourly intervals) from sunrise to sunset. At the FI site, the relative fluxes of ET and GPP*VPD were proportional and followed a very close, coupled and synchronized dynamic, thus generating the highest IWUE values. Both ET and GPP*VPD reach their peaks at the same time, around noon. In the morning ET and GPP*VPD closely track the relative changes of both VPD and PPFD. In the afternoon, both fluxes seem to be more in sync with the normalized dynamics of PPFD than with VPD (Fig. 7a, 7b, 7c). At the DI site, the relative fluxes of ET and GPP*VPD are less proportional and synchronized, because the relative flux of GPP*VPD is smaller than ET in the morning. The peaks of both fluxes occured simultaneously around 10-11 am and dropped earlier in the day. The GPP*VPD signal loses synchrony with the normalized values of PPFD and its variation is more coupled with changes in VPD. The normalized flow of ET remains highly synchronized with PPFD during morning and afternoon (Fig. 7d, 7e, 7f). Under RF conditions, the relative fluxes of ET and GPP*VPD were not proportional, decoupled, and poorly synchronized. In the morning hours, the relative flux of GPP*VPD was smaller than ET, however, in the afternoon the dynamic is reversed, and the magnitude of ET relative flux was more restricted than GPP*VPD. The peaks of both fluxes do not coincide since the relative flux of ET reaches its peak earlier than GPP. This time lags between these variables and the differences in the magnitude over day results in high asynchrony and lowest IWUE, compared to FI and DI sites. The relative flux of GPP was exactly coupled to the VPD from morning to 14:00. On the other hand, although the relative flux of ET is highly synchronized with PPFD, discrepancies or less synchrony between ET and PPFD are observed in the afternoon (compared to FI and DI), mainly during vegetative growth and tuberization (Fig. 7g, 7h, 7i)

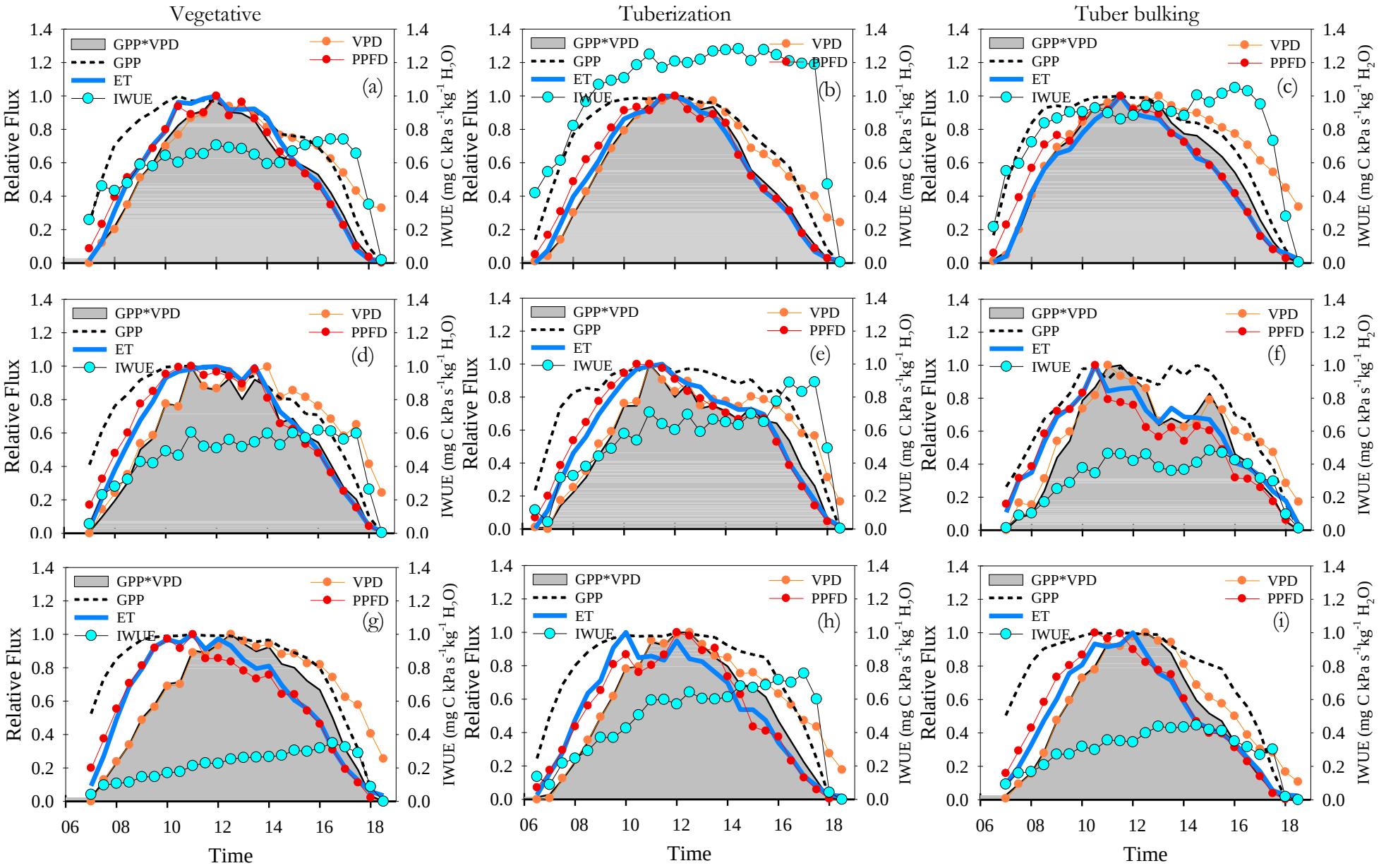

Figure 7. Normalized diurnal variations in half-hourly PPFD, ET, GPP, VPD, GPP*VPD, IWUE during three different potato growth stages (vegetative, tuberization, tuber bulking) in three different water regimes (a,b,c) full irrigation (FI), (d,e,f) deficit irrigation (DI), and (g,h,i) Rainfed (RF) conditions. The diurnal cycle begins at 5:00 h and ends at 19:00 h.

2.3.5. Environmental controls on NEE, GPP, ET, and IWUE-NEE relations

Figure 8 shows the correlations between GPP and ET fluxes with the climatic variables PPFD and VPD, as well as between NEE and IWUE. In the FI site there is a high correlation between GPP*VPD – PPFD and GPP*VPD – VPD, where more than 90% of the GPP*VPD changes are explained by PPFD and VPD (Figure 8). In the DI and RF sites there is a broader response and correlation between GPP*VPD - VPD (Figures 8g, 8h, 8i) than that observed for GPP*VPD – PPFD (Figures 8a, 8b, 8c). The lower correlation and determination coefficients indicate less control of PPFD over GPP*VPD.

The ET and PPFD variables remain highly correlated (Figures 8d, 8e, 8f), while the ET – VPD relationship is lower in all water management conditions (FI, DI, and RF). Compared to the FI and DI sites, the RF site showed an increase in VPD, which results in lower values of ET. While the ET response to PPFD is direct, the ET response to VPD depends on the effect of VPD on canopy conductance. Therefore, a hysteresis effect occurs due to the time lags between these variables, causing lower r and R^2 values. A greater hysteresis effect is observed under RF conditions, indicating a larger delay in the ET response to changes in VPD (Figures 8j, 8k, 8l).

In the FI site, the variables NEE and IWUE are highly linearly correlated and more than 80% of the changes in NEE are explained by IWUE in the three growth stages. In other words, the larger diurnal sink activity was due to the greater ET-GPP coupling represented by higher values of IWUE. It was observed that the highest capture activity (NEE more negative) occurs in high IWUE. At the DI site, there was a lower NEE response to IWUE, mainly at tuberization and tuber bulking, where the main sink activity (more negative NEE) occurs at lower IWUE values compared to FI. At the RF site, we observed the lowest NEE response to IWUE, as well as the lowest r and R^2 at all growth stages (Figures 8m, 8n, 8o). This indicates that in both DI and RF, the lower sink activity was due to the lower ratio between ET and GPP fluxes, represented in a lower IWUE (Figure 8).

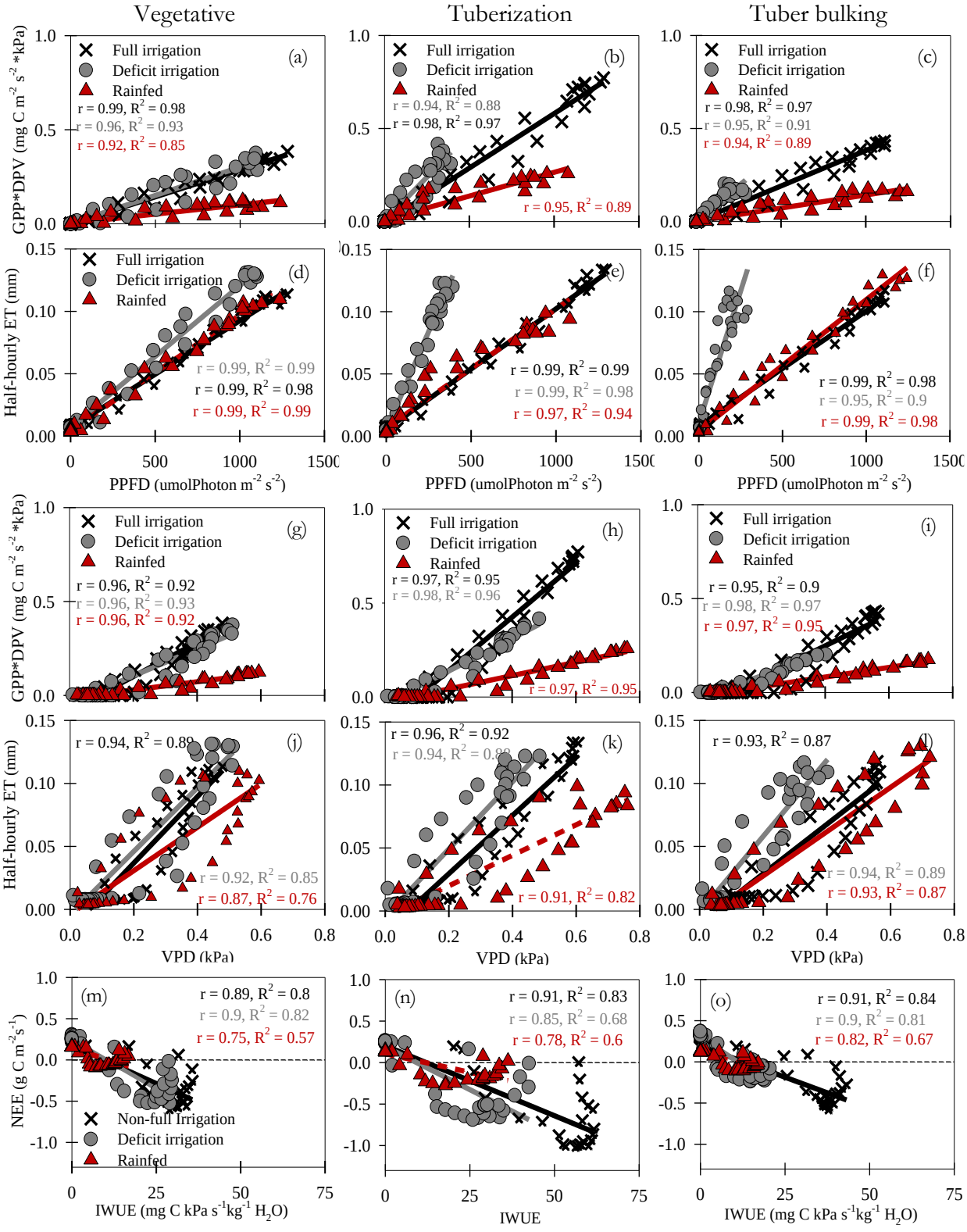

Figure 8. Relationship between GPP*VPD and PPFD, GPP*VPD and VPD, ET and PPFD, ET and VPD, and NEE and IWUE on a diurnal half-hourly basis, during different potato growth stages (vegetative, tuberization, tuber bulking) in three water regimes [full irrigation (FI) deficit irrigation (DI) rainfed conditions (RF)]. Also shown is the correlation coefficient and determination coefficient, and the linear fit between these variables. The p values of all regressions are below the 0.1% significance level.

Logarithmic functions described well the scatter plot between daily means of half-hour GPP versus half-hour ET (Fig. 9) in all sites. The average GPP increases were 0.33, 0.21 and 0.06 mg C m^{-2} s^{-1} per unit of ET mm increase in FI, DI and RF, respectively. On the other hand, the GPP – ET relation increased logarithmically without any clear threshold at the FI site. At the DI and RF sites, the increase of half-hourly GPP shows asymptotic values from 1 and 0.5 mg C m^{-2} s^{-1}, respectively, when half-hourly ET reach values around 0.1 mm and 0.05 mm respectively, indicating no increases of GPP that beyond those ET values. Over the whole crop growth, the individual half-hourly GPP*VPD and ET tend to be well correlated and well coupled ($r = 0.77$, $R^2 = 0.6$) at the FI site. GPP*VPD - ET coupling was slightly lower at the DI site ($r = 0.74$, $R^2 = 0.54$) and the lowest for the RF site ($r = 0.53$, $R^2 = 0.28$). Likewise, the instantaneous IWUE (the slopes of the linear regressions) was greater for the FI site than DI and RF sites, being 4.7, 2.3 and 1.01 mg C kPa s^{-1} kg^{-1} H_2O, indicating an improvement in water use under FI conditions.

The individual half-hourly NEE values were plotted against PPFD, VPD and ET in Figure 9. At the FI site, although all the climatic variables had positive effects on NEE, the carbon sequestration activity had a higher response to both ET and PPFD, compared to VPD. From logarithmic functions, both variables explain around 60% of the NEE variance, and a decrease of - 0.09 and - 0.06 mg C m^{-2} s^{-1} per unit of ET mm and PPFD mmol photons m^{-2} s^{-1}. In the DI site, NEE had a lower response to PPFD; the average decrease of NEE was -0.04 mg C m^{-2} s^{-2} per unit of PPFD mmol photons m^{-2} s^{-1}. While in the FI site, NEE decreased until approximately 1500 mmol photons m^{-2} s^{-1}, in the DI site, NEE decreased linearly to 750 mmol photons m^{-2} s^{-1}, and the main sink activity occurs when PPFD is below 1000 mmol photons m^{-2} s^{-1}. Under RF conditions the response of NEE to environmental conditions was quite reduced. Regarding PPFD, there was no decrease in NEE or sink activity beyond 300 mmol photons m^{-2} s^{-1}. While at the FI and DI sites, the NEE decreased with increasing VPD (until 0.8 kPa approximately) at the RF site, the NEE decreased to around VPD = 0.3 kPa and then, a reduction in sink capacity and positive NEE values accompanied the increase in VPD. The responses of NEE to IWUE differed among sites (Fig. 8). At the FI site, the average NEE became more negative (i.e., larger C sinks) with increasing IWUE, until the maximum carbon sequestration activity near to IWUE = 6 mg C kPa s^{-1} kg^{-1} H_2O. In the DI and RF sites the maximum carbon sequestration activity was near ~2 mg C KPa s^{-1} kg^{-1} H_2O, and ~1 mg C KPa s^{-1} kg^{-1} H_2O respectively. Beyond those IWUE values, there was a substantial reduction in the carbon sequestration activity (Figure 9).

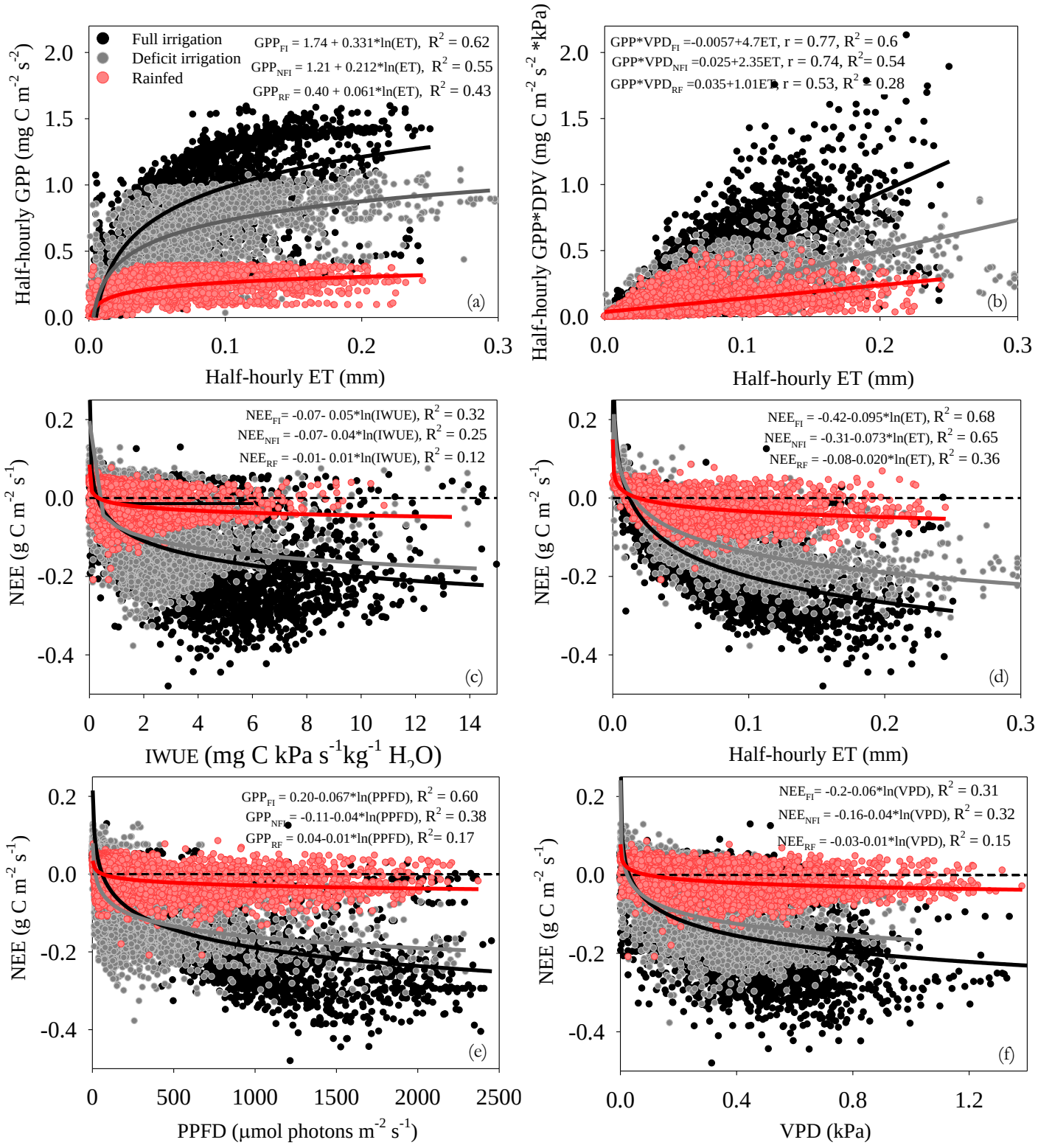

Figure 9. Overall half-hourly relationship between GPP and ET, GPP*VPD and ET, NEE and IWUE, PPFD, ET and VPD in three potato water regimes cropping systems [full irrigation (FI) deficit irrigation (DI) rainfed conditions (RF)]. Also shown is the correlation coefficient, determination coefficient, linear GPP*VPD and ET, and logarithmic functions. The p values of all regressions are below the 0.1% significance level.

2.3.6. ET-GPP coupling and omega

At the FI site, the correlation coefficients were greater than 0.85 for 78% of the 154 crop days, and 14% were between 0.75 and 0.84, indicating that in most of the individual days GPP*VPD and ET fluxes were tightly coupled, proportional, and sync. This constant strong linear relationship among daily GPP, ET, and VPD implies the highest IWUE values found at the FI site. Average high-correlation coefficient of 0.9, and maximum values of IWUE of 22 and 17 mg C kPa day^{-1} kg^{-1} H_2O were found to concur during the tuberization and tuber bulking stages, respectively. Likewise, about 30% of the vegetative stage were slightly GPP*VPD - ET decoupled days ($r \sim 0.66 – 0.84$) coinciding with low (but progressively increasing) IWUE values (Fig. 10a). At the DI and RF sites, only 52% and 41% of the respective correlation coefficients are larger than 0.85 during crop days. Likewise, the IWUE was lower at both sites, compared to the FI site. At the DI site, the highest percentage of uncoupled days ($r \sim 0.55 – 0.84$) were found during the tuberization and tuber bulking stages (48% and 74%, respectively). Correspondingly, the greatest changes of IWUE, with respect to FI, were observed mainly during tuberization and tuber bulking, where the maximum values reached were 14 and 6.5 mg C kPa day^{-1} kg^{-1} H_2O (Fig. 10b). The largest variability in the correlation coefficient was observed at the RF site. Around 74% of vegetative, tuberization stages correlation coefficient for the relation GPP*VPD - ET ranging from 0.3 to 0.84, and 0.48 to 0.84, respectively. The r averages were the lowest ($r= 0.73$ and 0.77 for vegetative, and tuberization, respectively) compared to the FI site. As a result, the RF site had the lowest values of IWUE and occurred during vegetative growth (IWUE < 5 mg C kPa day^{-1} kg^{-1} H_2O) and tuberization (max IWUE = 12 mg C kPa day^{-1} kg^{-1} H_2O) (Fig. 10c).

The degree of coupling between the plant canopy and the atmosphere grounded in omega characterizes the extent to which canopy conductance may control water vapor and CO_2 exchange. The omega values closest to one ($\Omega \sim 0.8 – 0.9$), indicate that in both the FI site and the DI site, the net radiation is the main contributor to the evapotranspiration process therefore, vegetation is completely decoupled from the atmospheric conditions. In the RF site, lower omega values ($\Omega \sim 0.6$) were observed mainly in the vegetative and tuber bulking stages, indicating an increase in coupling, and a greater control of ET by vegetation in terms of surface conductance and VPD (Figure 10).

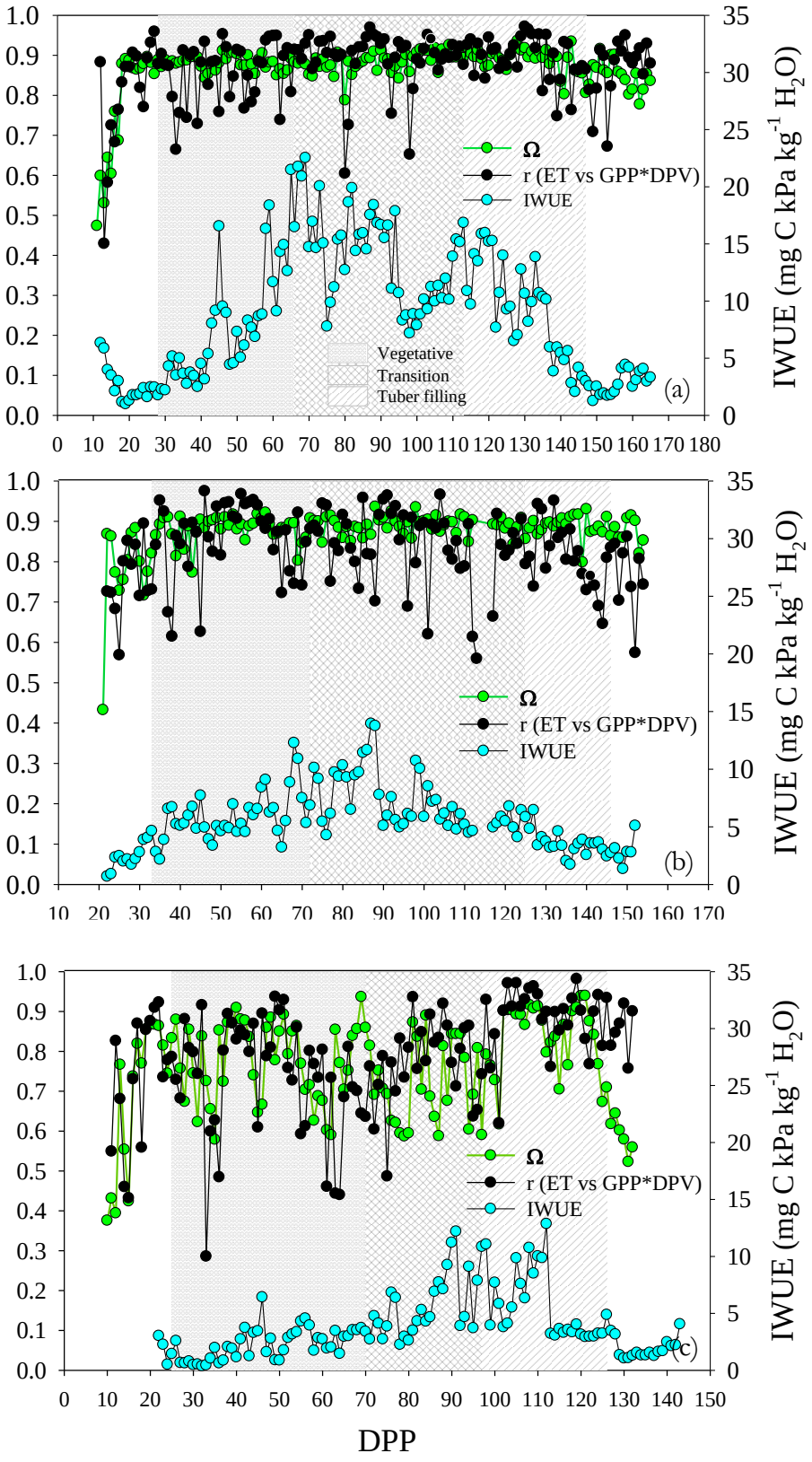

Figure 10. Daily correlation coefficients (r) between GPP*VPD and E, omega coefficient, and IWUE during different potato growth stages (vegetative, tuberization, tuber bulking) in three different water regimes (a) full irrigation (FI), (b) deficit irrigation (DI), and (c) Rainfed (RF) conditions.

2.4. Discussion

2.4.1. Carbon Fluxes of NEE, GPP, and R_{eco}

Under FI conditions, SWC was close to field capacity. Under this well-watered condition potato crop was a carbon sink at the end of the canopy cycle (-362.3 ± 13.15 g C m^{-2}) and after chemical haulm treatment (-312 ± 13 g C m^{-2}). During tuberization occurs 75% of carbon sequestration (-257.287$\pm$ 261 g C m^{-2}) which is expected, since developing tubers are the largest sinks (Oliveira et al., 2021; Viola et al., 2001) and higher carbon fluxes have been observed in this stage (Martínez-Maldonado et al., 2021). At the DI site the carbon sink capacity was reduced by 69% and 95% at the end of the canopy cycle (-113.43 $\pm$ 4.89 g C m^{-2}) and after chemical haulm treatment (-17.3 $\pm$ 4.61 g C m^{-2}) respectively, compared to the FI site. The tuberization stage lost its carbon sink potential by almost 50% and the tuber bulking stage behaves as a CO_2 source. Under the dry conditions of the RF site the crop behaved as a net carbon source to the atmosphere during all growth stages until the end of the canopy (+150.3 $\pm$ 4 g C m^{-2}), emitting even more after the chemical haulm treatment (+187.21 $\pm$ 3.8 g C m^{-2}).

2.4.2. Crop development, surface resistance and carbon - water fluxes

Daily GPP, R_{eco} fluxes, and GPP/R_{eco} ratio indicate a large GPP exceeding R_{eco} during all crop growth in the FI site. The observed GPP/R_{eco} ratio > 2 suggests that autotrophic respiration dominates the carbon fluxes, reflecting an increased physiological activity of the leaves, higher rates of photosynthesis (GPP), and CO_2 sequestration (Cabral et al., 2013; Falge et al., 2002, 2001a; Rana et al., 2016). The scarce difference between GPP and R_{eco}, and the low values of the GPP/R_{eco} ratio at DI site reflect a lower autotrophic activity, and low rates of photosynthesis which are found in drought-stressed ecosystems (Falge et al., 2002). The observed GPP/R_{eco} ratio <1 in almost all growth seasons in the RF site, confirming that the system behaved as a source of CO_2 and carbon fluxes were dominated by heterotrophic respiration due to a very low photosynthetic activity and autotrophic respiration. This means that carbon was mainly consumed by the soil respiration process and less used for the growth and maintenance of plant biomass (Cabral et al., 2013; Falge et al., 2002, 2001a; Goulden et al., 1998; Rana et al., 2016).

Our results indicate a strong influence of growth and canopy development over the energy partitioning and carbon fluxes (Guo et al., 2010; Jia et al., 2014; Kang et al., 2015; Shao et al., 2015; van Dijke et al., 2020a). In the FI site, the LAI was higher than DI and RF sites. The course of the GPP/R_{eco} ratio was in line with the LAI pattern, as well as the increase of the Rn/LE ratio following LAI during tuberization, reaching its highest value at max LAI and falling at almost the same rate. Several authors have reported that LAI is one of the main causes of daily GPP, and ET variations (Gondim et al., 2015; Jongen et al., 2011; Martínez-Maldonado et al., 2021a; Souza et al., 2012). For potato, under well-watered conditions, we reported previously (Martínez-Maldonado et al., 2021a) a synergistic growth of a high LAI and GPP which works as efficient feedback that guarantees canopy growth and high carbon fluxes. Although the highest LAI could be responsible for higher GPP and ET (van Dijke et al., 2020b), the canopy growth affecting carbon and water fluxes also depends on leaf thickness or SLA. Leaf thickening implies longer palisade cells or a higher number of cell layers and therefore higher transpiration efficiency, and increased capacity for area-based photosynthesis (Evans and Poorter, 2001; Vadez et al., 2014; Weraduwage et al., 2015; Wright et al., 1994), and greater photosynthetic rates (Gonzalez-Paleo and Ravetta, 2018; Goorman et al., 2011; Wright et al., 1994). In the FI site, we found a decreasing behavior of the SLA during the first 60 DPP indicating that during the

initial canopy growth, there was a reallocation of biomass to thicker leaves, increasing leaf mass more than leaf area (Weraduwage et al., 2015). Decreasing SLA may imply increasing plant demand for C since more fixed C is required to expand the area of thick leaves than of thin leaves (Gonzalez-Paleo and Ravetta, 2018; Jullien et al., 2009; Weraduwage et al., 2015). In the DI site, the water deficit events during early crop growth changed the morphological characteristics of the canopy, which impacted the course of the GPP/R_{eco} ratio. The significant and faster drop in LAI (from 100 DPP) was accompanied by $GPP/R_{eco} < 1$, which explains tuber bulking as a weaker carbon sink. The increasing SLA during tuberization indicates less carbon requirement for mass increase and lower area-based for photosynthesis, which could partly explain the depression of the GPP/R_{eco} ratio between 80 and 115 DDP.

In the RF site, water deficits occurred beyond 70% of the crop growing season. Reductions in daily GPP and low GPP/R_{eco} ratio during all crop growth may be related to fewer carbon requirements to canopy growth, since lowest LAI values and the increasing behavior of the SLA suggested that the crop had a poorly expanded canopy with thin leaves during all growth stages (Gonzalez-Paleo and Ravetta, 2018; Jullien et al., 2009; Weraduwage et al., 2015; Wright et al., 1994). In potato, water deficit causes a reduction in the expansion of leaves, leading to reduced foliage, reduced canopy, and reduced leaf area index (George et al., 2017; Gervais et al., 2021a, 2021b; Hill et al., 2021b; Howlader & Hoque, 2018; Martínez-Maldonado et al., 2021; Michel et al., 2019; Muthoni & Kabira, 2016; Nasir & Toth, 2022a, 2022b; Obidiegwu et al., 2015; Rodríguez P. et al., 2016). Unlike FI and DI, there was a strong reduction of the LE/Rn ratio at the RF site, indicating that the water vapor flux from the canopy had additional restrictions to those provided by changes in vegetative growth and canopy morphology.

Water and carbon fluxes in plants are linked by stomata (Brunsell and Wilson, 2013b; Díaz et al., 2022b; Gonzalez-Paleo and Ravetta, 2018; Huxman et al., 2004; Scott et al., 2006b; van Dijke et al., 2020b) which is characterized by the canopy resistance (Rc) and represents the bulk resistance to water vapor or mass transfer from leaves (Amer and Hatfield, 2004; Wehr and Saleska, 2021). In our results, at the FI site, higher values of daily ET occurred in lower Rc during all crop growth stages. This expected low canopy resistance under well-watered conditions has been reported by other researchers (Aires et al., 2008; Kumagai et al., 2008; Paulino Junior and Silva von Randow, 2017; Souza et al., 2012). Unlike with López-Olivari et al. (2022), we observed a larger aerodynamic resistance (generally higher than Rc) indicating more importance of Ra in total resistance to water vapor transport. Regarding diurnal patterns, the tendency of the estimated half-hourly Rc had a similar magnitude, along the growth stages. Averaged midday Rc values around 15 s m^{-1} were similar to those reported for potato by Amer & Hatfield (2004) and López-Olivari et al. (2022) and lower than values reported by Kjelgaard & Stockle (2001) (midday Rc values close equal to 40 s m^{-1}). As seen for daily data, diurnal aerodynamic resistance generally was higher than canopy resistance. This large Ra impedes heat transfer as well as water vapor transfer and, therefore, supports the greater evapotranspiration flux (Smith, 1980) observed at the FI site. The highest diurnal ET and GPP fluxes evidenced an intense exchange of carbon and water and consequently a high sink activity (more negative NEE) mainly during tuberization and tuber bulking stages between 07:00 am and noon when the lowest Rc occurred.

At the DI site, Rc and Ra were similar to those found in the FI site. Despite water deficit events, Ra>Rc indicating that ET remains controlled by Ra and less by Rc and water content in the soil (Sutherlin et al., 2019a). Consequently, canopy was less capable to reduce evapotranspiration and avoid water losses (Spinelli et al., 2018a; Fereres and Soriano, 2007; Spinelli et al., 2018b), and ET continues at a high rate while there was a high restriction in the GPP and NEE fluxes. Such decrease in GPP in a low canopy resistance for surface fluxes may have been explained by intra-leaf factors or non-stomatal limitations of photosynthesis (NSL), that could decline the

photosynthetic activity during drought (de La Motte et al., 2020; Nadal-Sala et al., 2021a; Nelson et al., 2018c; Obidiegwu et al., 2015; Xu and Baldocchi, 2004; Yang et al., 2019). NSL has been observed at the ecosystem scale (Jarvis, 1985; Migliavacca et al., 2009; Reichstein et al., 2002) and could include environmental limitations on the photosynthetic pathways (Nelson et al., 2018c), increased mesophyll resistance (de La Motte et al., 2020; Evans, 2021; Flexas et al., 2012), drought-related enzymatic down-regulation (Flexas et al., 2013, 2004; Flexas and Medrano, 2002a; Galmés et al., 2007; Niinemets et al., 2006; Sugiura et al., 2020; Varone et al., 2012a), less total leaf mass, and/or decreasing carbon demand (Fatichi et al., 2014; Nadal-Sala et al., 2021a). In our results, the radiation deficit, and the poorly developed canopy, with less photosynthetic activity and lower autotrophic respiration, constitute the NSL which in turn decreased the GPP.

At FI and DI sites, the diurnal VPD < 0.6 kPa had no effect on canopy resistance because of the irrigated conditions. At the RF site, the VPD > 0.6 kPa indicates that the potato canopy experienced a larger saturation deficit and, as soon as VPD increased, Ra decreased, and Rc increased as the day progressed. The increase of midday Rc was up to 13 times larger than Rc at the FI site when the VPD increased around 0.8 kPa, revealing that under drought conditions, the plants increased the canopy resistance in response to high VPD (Aires et al., 2008; J D N Alves et al., 2022; Silva et al., 2017a; Sutherlin et al., 2019b). Diurnal ET and GPP fluxes were highly restricted in all growth stages suggesting that in potatoes VPD could play a strong role in controlling GPP and ET by means of Rc (Aires et al., 2008). Furthermore, the lower values of ET occurring at higher Rc could be related to the lower partition of energy into LE in the RF site, since the surface energy partitioning into sensible and latent heat depends on surface resistance (Baldocchi et al., 2000; Chen et al., 2009; Kang et al., 2015; Li et al., 2005) and a low LE is necessarily associated to high Rc (Spinelli et al., 2018b). According to Teixeira et al. (2008) VPD exerts negative physiological feedback on ET; while high VPD values increased the gradient of water vapor transport, decreasing LE, at the same time it created an extra barrier on the vapor flow path by closing the stomata, increasing Rc. It should be noted that with the increase of the Rc diurnal GPP was more severely restricted than diurnal ET. This phenomenon, reported by other authors (de La Motte et al., 2020; Nelson et al., 2018c; Spinelli et al., 2018b, 2016; Yang et al., 2019) is explained because while ET is mainly limited by the available energy and secondarily by canopy resistance to vapor transfer, carbon assimilation is primarily limited by canopy resistance, mesophyll conductance, and the rate at which chloroplasts fix carbon (Spinelli et al., 2018b, 2016; Steduto and Hsiao, 1998). On the other hand, the additional non-stomatal limitations of photosynthesis (NSL) under high soil water restriction play a major role in limiting GPP.

2.4.3. Environmental controls on ET-GPP synchrony and NEE-IWUE relations

At the well-watered conditions of the FI site, the diurnal cycles of ET and GPP were proportional and largely synchronized, which is consistent with other studies (Aguilos et al., 2021; Beer et al., 2009; Nelson et al., 2018c). The higher coupling indicates that the amount of carbon that enters the canopy is proportional to water that leaves, and at noon, when the stomata begin to close, carbon and water fluxes decrease by a similar percentage (Gentine et al., 2019; Mallick et al., 2016; Nelson et al., 2018c; van Dijke et al., 2020b). Environmental factors, solar radiation, and vapor pressure deficit (VPD) were highly synchrony and correlated with ET and GPP, suggesting that were important drivers in the short-term diurnal variation of carbon and water fluxes. According to (Grossiord et al., 2014), during periods of optimum soil water supply and non-limiting low VPD, stomata are fully open, and ET increases linearly with VPD. However, in well-watered conditions light is the main driver for photosynthesis and

transpiration (Eamus et al., 2016a, 2016b; Liu et al., n.d., 2021c) since carbon and water exchange increase as more light is intercepted by the canopy (Arkebauer et al., 2009a; Samanta et al., 2020; Wilson et al., 2001). The Ra >Rc condition (at daily and average half-hourly scales) observed at FI site, indicates that evapotranspiration is more strongly controlled by Ra and incoming radiation (Alves et al., 2022b; Irmak & Mutiibwa, 2010; Jarvis, 1985; Jarvis & Mcnaughton, 1986b; Magnani et al., 1998; McNaughton & Jarvis, 1991; Nassif et al., 2019; Spinelli et al., 2016, 2018b). Likewise, we previously demonstrated that GPP had a large response to PPFD due to the high carbon flux at light saturation (95% of asymptote) (Martínez-Maldonado, et al., 2021).

At the DI site, The ET and GPP fluxes become uncoupled, losing synchronization and proportionality mainly in the morning, due to the magnitude of the relative GPP flux being smaller and less synchronized, and correlated with the incoming PPFD. The maximum peaks reached earlier, indicate that the time for intense transpiration activity and water-carbon exchange in the early morning was restricted (almost 2 hours), which constrains the sink activity and IWUE. In this less ET - GPP coupling, stomata are transpiring water but intra-leaf factors and other non-stomatal limitations to photosynthesis are slowing carbon fixation, changing the inherent water use efficiency directly (Beer et al., 2009; Nelson et al., 2018c).

The largest discrepancies between the diurnal relative fluxes of ET and GPP were observed at the RF site. Fluxes were uneven with the advancement of the day, and there was a time lag between their maximum peaks. The course of the GPP was in synchrony and correlated with VPD and unresponsive and less correlated to PPFD, while the diurnal trend of ET was high sync and correlated to PPFD and less sync and correlated to VPD. In our analysis, the high asynchrony and pour coupling are due to the unbalanced constrain for ET and GPP fluxes (affecting GPP > ET) imposed by increases in Rc (in response to higher VPD) and non-stomatal photosynthesis limitations that primarily affect the GPP flux. Therefore, because there was a great restriction in both fluxes (ET and GPP), the IWUE values were the lowest compared to the other measurement sites. A decrease in WUE in response to drought was also found by Migliavacca et al. (2009) and Reichstein et al. (2002).

At the FI site, the synchrony and proportionality of half-hourly ET and GPP fluxes during the growth stages are also reflected in the high correlation between overall half-hour GPP and ET and GPP*VPD and ET. There is a high response of the GPP to ET where more carbon molecules were fixed per water molecule. The carbon assimilation process continues in response to water loss, even at the highest ET, indicating that the crop sustains photosynthetic activity in response to the highest water vapor fluxes, which agrees with Katul et al. (2010b) hypothesis. In the DI and RF sites, the low correlation between half-hour GPP and ET and GPP*VPD and ET indicated an overall decoupling between carbon fluxes. In these sites, a large amount of water vapor was lost for limited CO_2 assimilation, lowering the water use efficiency until behaves asymptotically, meaning that the increases in ET no longer bring additional increases in GPP. In other words, the water cost is increased for the same carbon gain. In this way, after GPP values of 0.5 mg C m^{-2} s^{-2}, respectively at the DI and RF sites, the increases in ET could be considered water losses from the system without productive purposes. This indicates that under water-limiting conditions the crop cannot restrict water losses or maximize its carbon gains.

The influence of IWUE on the NEE can be noted by analyzing Fig. 8 along with Fig. 9. Under the well-watered conditions of the FI site, the high linear correlations between the variation of WUE and NEE (Half-hour diurnal averages of growth phases and overall half-hourly values) indicate that the larger diurnal sink activity was due to the greater ET-GPP coupling represented by higher values of IWUE. This result does support our hypothesis of during well-watered conditions a tight coupling between GPP and ET fluxes due to a PPFD drive - high photosynthesis and evapotranspiration rates, generating the highest IWUE and therefore a larger diurnal sink activity

(NEE more negative). In the DI and RF sites, the lower correlation and response of NEE to IWUE is not only attributed to restrictions and low decoupling of the ET – GPP fluxes, but also to the increases in the R_{eco} flux either by more low autotrophic activity from plants or increased heterotrophic activity from the soil. In other words, the lower number of negative NEE values and the persistent positive values are due to both the low IWUE values and the greater role of R_{eco} in the carbon balance and its impact on NEE. The relationship proposed in the IWUE would only explain the variability of the negative values of the NEE since they are associated with the activity of the GPP.

As a consequence of radiation driving both ET and GPP fluxes, PPFD was the primary driver controlling daytime NEE, accounting for 60% of the variations in overall half-hourly NEE during the growing period. The carbon sequestration increased (NEE gets more negative) at PPFD values beyond 1500 mmol photons m^{-2} s^{-1}. Likewise, the high response of GPP to ET caused NEE to also have a relevant response to ET. At the DI site, the NEE had a lower response to PPFD (NEE decreased linearly around 750 mmol photons m^{-2} s^{-1}) indicating that the lower values of PAR radiation could be the main limiting factor for sink activity. Although lower than in FI, the response of sink activity to ET was high, confirming that despite the deficit events there were no restrictions on ET and the persistent flux of water vapor was the driver of carbon sequestration. In RF, sink activity stalls or saturates at low ET, PPFD, and VPD. The low response to these environmental determinants is due both to the lower GPP and to the fact that the carbon balance is mainly dominated by the high respiration of the ecosystem, due to physiological and biophysical changes previously discussed.

2.4.4. ET-GPP coupling and the omega role

To know whether effectively water and carbon signals were coupled or decoupled under the water availability conditions of the measurement sites, we quantified ET-GPP coupling through the daily correlation coefficients for GPP*VPD vs ET using half-hourly data, and by computing daily $IWUE = GPP * \frac{DPV}{ET}$ from the total daily sums of GP and ET, and average VPD. IWUE has been widely used in numerous studies as a measure of carbon and water coupling (Battipaglia et al., 2013b; Beer et al., 2009; Grossiord et al., 2014; Leonardi et al., 2012; Loader et al., 2011; Zhou et al., 2015, 2014), and since it shows an improved linear relationship among GPP, ET, and VPD the daily correlation coefficient (r) of GPP*VPD vs ET has been used as an indicator for quantify the coupling/decoupling degree between water and carbon fluxes (Aguilos et al., 2021; Beer et al., 2009; Nelson et al., 2018c; Zhou et al., 2015, 2014). However, numerous environmental factors and non-stomatal limitations to carbon assimilation control the photosynthesis/transpiration balance and could affect carbon and water fluxes, causing a carbon–water decoupling (Nelson et al., 2018c; Zhou et al., 2015). For this reason, the decoupling factor omega (Ω) was calculated on a daily scale to know if the ET-GPP decoupling is due to or not to a greater degree of canopy control over carbon and water fluxes and, in this way, understand the source of the associated changes in the IWUE.

In our results, the most of growth days at the FI site had a high daily correlation coefficient for GPP*VPD vs ET > 0.85, indicating that carbon and water fluxes were tightly coupled, and synchronized. High correlations between the two fluxes under well-watered days have been previously reported (Beer et al., 2009; Nelson et al., 2018b). However, we found a greater number of days less coupled during vegetative and ending tuber bulking stage which is explained due to fluxes are less related to the canopy. During the low crop cover and senescence, latent heat flux is supplied mainly by the evaporation from the soil, and carbon fluxes were dominated by heterotrophic respiration where R_{eco} > GPP (Cabral et al., 2013; Falge et al., 2002; Goulden et al., 1998; Rana et al.,

2016). The daily omega ranged from ~0.8 to 0.9 and was close to 0.7 as reported by Brown (1976) for potato, and it is within the range of 0.8 to 0.9 commonly reported in the literature for horticultural crops under no stress (Ferreira, 2017; Jarvis and Mcnaughton, 1986; McNaughton and Jarvis, 1991). The Ω near to 1 implies that ET was more strongly controlled by incoming radiation and less dependent on stomatal conductance and canopy resistance (Jarvis, 1985; P G Jarvis and Mcnaughton, 1986; McNaughton and Jarvis, 1991; Steduto and Hsiao, 1998; Sutherlin et al., 2019b). The less dependence of ET on stomatal conductance is due to the smaller water vapor gradient between the intercellular air space and the epidermal surface of leaves (Steduto and Hsiao, 1998). The leaf surface VPD is different from the air outside of the leaf in its boundary layer (Jarvis, 1985; P G Jarvis and Mcnaughton, 1986), a condition based on Ra > Rc as we found previously in the FI site. The high Ra between leaf surfaces and the air above the canopy indicates a lower diffusivity of water vapor from the leaves that makes ET more coupled with radiation forcing and less dependent on canopy resistance (Jarvis, 1985; P G Jarvis and Mcnaughton, 1986; Zhang et al., 2016). The IWUE increased rapidly at the start of vegetative growth and reaches the maximum values during the tuberization with the maximum LAI. This behavior corroborated with Beer et al. (2009) in herbaceous ecosystems, where LAI and crop growth influence IWUE. The pattern of IWUE suggests that the potato ecosystem became more efficient in its carbon acquisition as the crop growth progressed. In terms of Katul et al. (2010b) increases its capacity to optimize carbon gains to water losses. The lowest cost in water per carbon gain at the FI site can be observed in Figs. 9 where there was a high GPP response to ET changes, even when the effect of VPD was included. This enhanced IWUE may imply an increase in plant transpiration efficiency, and a positive effect on plant carbon balance (Leonardi et al., 2012). As previously discussed in this paper, under favorable water availability conditions, the exchange of water vapor and CO_2 was intense because of the increasing autotrophic activity, larger portions of LE and low canopy resistance to fluxes, and consequently high GPP and evapotranspiration rates (Lambers et al., 2008).

At the DI site, about 50% of the growth period was decoupled and desynchronized ($r< 0.84$). We observed the greatest number of decoupled days during tuberization and tuber bulking, as well as the greatest reductions in IWUE with respect to FI. The daily omega coefficient varies between ~0.8 – 0.9 indicating ET was controlled by the aerodynamic resistance and incoming radiation and less by canopy resistance and VPD (Jarvis, 1985; P G Jarvis and Mcnaughton, 1986). By analyzing together omega, r Pearson and IWUE it can be inferred that the ET - GPP desynchronization and decoupling and the lower efficiency of GPP-ET tradeoff are not due to limitations in ET, nor to a greater canopy control over fluxes. Therefore, the origin of the decoupling and low IWUE could be attributed to non-stomatal limitations in the GPP. This inference is evidenced by the fact that all the results presented in this work point to a great restriction of GPP since during tuberization and tuber bulking there were thinner leaves, a drop in autotrophic respiration, low response, and correlations of GPP to PPFD, and the largest reductions in diurnal and daily carbon fluxes GPP and NEE with respect to FI. We point to the fact that there are no stomatal/surface resistance limitations based on the high omega indicating no changes in Rc and Ra.

At the RF site, on almost all crop days (more than 80%), the ET and GPP fluxes were uncoupled and desynchronized, mainly during vegetative growth and tuberization. However, unlike the DI site, we observed very low values of the correlation coefficient ($r\sim 0.4$) revealing large discrepancies between carbon and water diurnal trends. As a result, the RF site had the lowest reductions in daily IWUE during all crop growth. Omega coefficient (Ω) was lower, and like the correlation coefficient, the lowest values (omega ~ 0.6) were observed mainly in the vegetative and tuber bulking stages. The lower Ω values are indicative that ET is strongly controlled by VPD and Rc (Aires et al., 2008; P G Jarvis and Mcnaughton, 1986; Nassif et al., 2014). However, the higher Rc reducing

evapotranspiration, may restrict photosynthesis more than it restricts ET (Jarvis, 1985; Spinelli et al., 2018b, 2016; Steduto and Hsiao, 1998) as discussed previously. Other researchers have reported a decreasing trend of omega under water deficit caused by an increase in the canopy resistance and a decrease in aerodynamic resistance (de Kauwe et al., 2017; Ferreira, 2017; Paulino Junior and Silva von Randow, 2017; Silva et al., 2017a; Spinelli et al., 2016; Sutherlin et al., 2019b) which agrees with the results presented in this work. Unlike FI and DI sites omega and r, have a similar trend of variation along crop growth. On days where omega and r fall together, the high ET-GPP decoupling is due to a greater extent of canopy control over fluxes in response to higher VPD, causing an unbalance constraint over ET and GPP fluxes, and therefore a very low IWUE. However, as discussed, the restriction on both flows has greater restrictions on GPP due to stomatal and non-stomatal limitations to photosynthesis.

2.5. Conclusions

We investigated the interactions between carbon and water fluxes to understand the response of NEE of three crop systems of Andean potato (*Solanum tuberosum* L. andigenum), growing under contrasting water management conditions. To explore the temporal scales of water and carbon fluxes interactions, we used the inherent water use efficiency (IWUE) approach, which allows study the intrinsic link between carbon and water fluxes through stomatal conductance by means of the eddy covariance technique at the ecosystem level. We quantified water and carbon fluxes, morphological parameters LAI and SLA, canopy and aerodynamic resistances, omega decoupling factor, measures GPP–ET coupling, and IWUE on different time scales to identify differences in the trade-off between carbon uptake and water loss across potato sites and its relation to NEE differences.

Our results indicated that rainfed potato was a net carbon source, while both irrigated systems were a net carbon sink. However, the FI condition showed a carbon sequestration capacity almost 5 times greater than that observed in the DI site

We have shown that a greater sink activity or more negative NEE is due both to the high fluxes of GPP (where the GPP> R_{eco} condition is fulfilled) and ET, as well as to the high efficiency, synchrony, and coupling in the exchange of carbon and water. That is, the higher photosynthetic CO_2 gain per unit of evapotranspired water is related to a high magnitude, proportionality, and synchrony of its diurnal fluxes, which in turn are controlled by the radiative environment and by a canopy with a larger base area for exchange of water and carbon (high LAI and thick leaves), physiologically active (high photosynthetic and respiratory activities), with low internal resistance and highly decoupled from the atmosphere (high omega). This study further shows evidence of how along with canopy growth, the energy consumption for ET (LE), autotrophic respiration, and photosynthetic activity increases, as well as the ability to optimize carbon gains against water losses. The tuberization phase is the most relevant in the carbon sink activity since the completely formed canopy, together with developing tubers, constitute the greatest carbon demand of the crop cycle and thus the highest fluxes of GPP.

Under soil water deficit conditions, the lower sink capacity or carbon source activity is due to limitations in the magnitude of the GPP and ET fluxes and their trade-off efficiency (IWUE). Lower IWUE is a consequence of decoupled and desynchronized carbon and water exchange caused by unbalanced restrictions on ET and GPP fluxes from the stressed canopy. An overall restriction for fluxes is a smaller base area for water and carbon exchange due to limited canopy growth and early senescence. The first unbalanced constraint causing ET-GPP decoupling occurs because ET remained at a high magnitude despite the strong reduction in GPP. GPP decreases by means of non-stomatal effects on canopy assimilation attributed to changes in physiological capacities of photosynthesis reflected

in lower GPP/R_{eco} ratio and a lower response of PPFD. In the longest and most sustained limitation in the SWC, both ET and GPP fluxes decrease together, however, GPP decreases more than ET. On one hand, evapotranspiration was limited by a means of higher Rc in response to high VPD, which greatly impacts carbon assimilation and GPP through stomatal limitations of photosynthesis. On the other hand, GPP reduction is also controlled by non-stomatal limitations reflected in its minimal autotrophic respiration and photosynthetic activity, and high photoinhibition (Martínez-Maldonado et al., 2021) induced by the higher soil water deficit conditions.

The high omega coefficient at the FI site showed that without great limitations or fluctuations of water in the soil, the potato canopy has a greater advantage because of its low surface control on ET and GPP. Water and carbon can freely move in and out, and fluxes are not affected by the stomatal conductance and the water content in the soil. However, this high omega is also disadvantageous under water deficit conditions. Under water deficit conditions of the DI site, the canopy had less capacity to reduce evapotranspiration and avoid water losses. Apparently, the control mechanisms like higher surface resistance to minimize excessive water loss works only in high atmospheric evaporative demand and very low SWC, and although it reduces ET, it has great consequences on GPP.

Through the analysis of both omega and correlation coefficients, we distinguished the possible causes of lower IWUE and the dominance of environmental VPD and PPFD controls of ET and GPP fluxes under the contrasting soil water availability from water management. These variables and their underlying theory could give new information about carbon–water interactions and it can be used as a tool to further understand the impact of drought on potato agroecosystems.

References

Abbate, P.E., Dardanelli, J.L., Cantarero, M.G., Maturano, M., Melchiori, R.J.M., Suero, E.E., n.d. Climatic and Water Availability Effects on Water-Use Efficiency in Wheat.

Aguilos, M., Sun, G., Noormets, A., Domec, J.C., McNulty, S., Gavazzi, M., Prajapati, P., Minick, K.J., Mitra, B., King, J., 2021. Ecosystem productivity and evapotranspiration are tightly coupled in loblolly pine (Pinus taeda l.) plantations along the coastal plain of the southeastern U.S. Forests 12. https://doi.org/10.3390/f12081123

Aires, L.M., Pio, C.A., Pereira, J.S., 2008. The effect of drought on energy and water vapour exchange above a mediterranean C3/C4 grassland in Southern Portugal. Agric For Meteorol 148, 565–579. https://doi.org/10.1016/j.agrformet.2007.11.001

Ali, S., Xu, Y., Ma, X., Ahmad, I., Kamran, M., Dong, Z., Cai, T., Jia, Q., Ren, X., Zhang, P., Jia, Z., 2017. Planting patterns and deficit irrigation strategies to improve wheat production and water use efficiency under simulated rainfall conditions. Front Plant Sci 8. https://doi.org/10.3389/fpls.2017.01408

Alves, I., Perrier, A, Pereira, L.S., Perrier, Alain, 1998. AERODYNAMIC AND SURFACE RESISTANCES OF COMPLETE COVER CROPS: HOW GOOD IS THE "BIG LEAF"?

Alves, J D N, Ribeiro, A., Rody, Y.P., Loos, R.A., 2022. Energy balance and surface decoupling factor of a pasture in the Brazilian Cerrado. Agric For Meteorol 319. https://doi.org/10.1016/j.agrformet.2022.108912

Alves, José Darlon Nascimento, Ribeiro, A., Rody, Y.P., Loos, R.A., 2022. Energy balance and surface decoupling factor of a pasture in the Brazilian Cerrado. Agric For Meteorol 319. https://doi.org/10.1016/j.agrformet.2022.108912

Amer, K.H., Hatfield, J.L., 2004. Canopy resistance as affected by soil and meteorological factors in potato. Agron J 96, 978–985. https://doi.org/10.2134/agronj2004.0978

Arkebauer, T.J., Walter-Shea, E.A., Mesarch, M.A., Suyker, A.E., Verma, S.B., 2009. Scaling up of CO_2 fluxes from leaf to canopy in maize-based agroecosystems. Agric For Meteorol 149, 2110–2119. https://doi.org/10.1016/j.agrformet.2009.04.013

Aubinet, M., Moureaux, C., Bodson, B., Dufranne, D., Heinesch, B., Suleau, M., Vancutsem, F., Vilret, A., 2009. Carbon sequestration by a crop over a 4-year sugar beet/winter wheat/seed potato/winter wheat rotation cycle. Agric For Meteorol 149, 407–418. https://doi.org/10.1016/j.agrformet.2008.09.003

Baldocchi, D., Kelliher, F.M., Black, T.A., Jarvis, P., 2000. Climate and vegetation controls on boreal zone energy exchange. Glob Chang Biol 6, 69–83. https://doi.org/https://doi.org/10.1046/j.1365-2486.2000.06014.x

Battipaglia, G., Saurer, M., Cherubini, P., Calfapietra, C., Mccarthy, H.R., Norby, R.J., Francesca Cotrufo, M., 2013a. Elevated CO_2 increases tree-level intrinsic water use efficiency: Insights from carbon and oxygen isotope analyses in tree rings across three forest FACE sites. New Phytologist 197, 544–554. https://doi.org/10.1111/nph.12044

Battipaglia, G., Saurer, M., Cherubini, P., Calfapietra, C., Mccarthy, H.R., Norby, R.J., Francesca Cotrufo, M., 2013b. Elevated CO_2 increases tree-level intrinsic water use efficiency: Insights from carbon and oxygen isotope analyses in tree rings across three forest FACE sites. New Phytologist 197, 544–554. https://doi.org/10.1111/nph.12044

Beer, C., Ciais, P., Reichstein, M., Baldocchi, D., Law, B.E., Papale, D., Soussana, J.F., Ammann, C., Buchmann, N., Frank, D., Gianelle, D., Janssens, I.A., Knohl, A., Köstner, B., Moors, E., Roupsard, O., Verbeeck, H., Vesala, T., Williams, C.A., Wohlfahrt, G., 2009. Temporal and among-site variability of inherent water use efficiency at the ecosystem level. Global Biogeochem Cycles 23, 1–13. https://doi.org/10.1029/2008GB003233

Bierhuizen, J.F., Slatyer, R.O., 1965. Agricultural Meteorology-Elsevier Publishing Company, Amsterdam-Printed in The Netherlands Effect of atmospheric concentration of water vapour and cos in determining transpiration-photosynthesis relationships of cotton leaves, Agr. Meteorol.

Birch, P.R.J., Bryan, G., Fenton, B., Gilroy, E.M., Hein, I., Jones, J.T., Prashar, A., Taylor, M.A., Torrance, L., Toth, I.K., 2012. Crops that feed the world 8: Potato: Are the trends of increased global production sustainable? Food Secur 4, 477–508. https://doi.org/10.1007/s12571-012-0220-1

Bouzalakos, S., Mercedes, M., 2010. Overview of carbon dioxide (CO_2) capture and storage technology. Developments and Innovation in Carbon Dioxide (CO_2) Capture and Storage Technology 1–24. https://doi.org/10.1533/9781845699574.1

Brown, K.W., 1976. Sugar beet and potatoes, in: Monteith, J.L. (Ed.), Vegetation and the Atmosphere. Academic Press, London, pp. 65–86.

Brunsell, N.A., Wilson, C.J., 2013. Multiscale Interactions between Water and Carbon Fluxes and Environmental Variables in A Central U.S. Grassland. Entropy 15, 1324–1341. https://doi.org/10.3390/e15041324

Buysse, P., Bodson, B., Debacq, A., de Ligne, A., Heinesch, B., Manise, T., Moureaux, C., Aubinet, M., 2017. Carbon budget measurement over 12 years at a crop production site in the silty-loam region in Belgium. Agric For Meteorol 246, 241–255. https://doi.org/10.1016/j.agrformet.2017.07.004

Cabral, O.M.R., Rocha, H.R., Gash, J.H., Ligo, M.A.V., Ramos, N.P., Packer, A.P., Batista, E.R., 2013. Fluxes of CO_2 above a sugarcane plantation in Brazil. Agric For Meteorol 182–183, 54–66. https://doi.org/10.1016/j.agrformet.2013.08.004

Campbell, G.S., Norman, J.M., 1998. An Introduction to Environmental Biophysics, second ed. ed. Springer-Verlag, New York.

Chen, S., Chen, J., Lin, G., Zhang, W., Miao, H., Wei, L., Huang, J., Han, X., 2009. Energy balance and partition in Inner Mongolia steppe ecosystems with different land use types. Agric For Meteorol 149, 1800–1809. https://doi.org/10.1016/j.agrformet.2009.06.009

Chi, J., Waldo, S., Pressley, S., O'Keeffe, P., Huggins, D., Stöckle, C., Pan, W.L., Brooks, E., Lamb, B., 2016. Assessing carbon and water dynamics of no-till and conventional tillage cropping systems in the inland Pacific Northwest US using the eddy covariance method. Agric For Meteorol 218–219, 37–49. https://doi.org/10.1016/j.agrformet.2015.11.019

Ciais, P., Reichstein, M., Viovy, N., Granier, A., Ogée, J., Allard, V., Aubinet, M., Buchmann, N., Bernhofer, C., Carrara, A., Chevallier, F., de Noblet, N., Friend, A.D., Friedlingstein, P., Grünwald, T., Heinesch, B., Keronen, P., Knohl, A., Krinner, G., Loustau, D., Manca, G., Matteucci, G., Miglietta, F., Ourcival, J.M., Papale, D., Pilegaard, K., Rambal, S., Seufert, G., Soussana, J.F., Sanz, M.J., Schulze, E.D., Vesala, T., Valentini, R., 2005. Europe-wide reduction in primary productivity caused by the heat and drought in 2003. Nature 437, 529–533. https://doi.org/10.1038/nature03972

CIP, 2022. Hechos y Cifras sobre la Papa [WWW Document]. URL www.cipotato.org

Clune, S., Crossin, E., Verghese, K., 2017. Systematic review of greenhouse gas emissions for different fresh food categories. J Clean Prod 140, 766–783. https://doi.org/10.1016/j.jclepro.2016.04.082

de Kauwe, M.G., Medlyn, B.E., Knauer, J., Williams, C.A., 2017. Ideas and perspectives: How coupled is the vegetation to the boundary layer? Biogeosciences 14, 4435–4453. https://doi.org/10.5194/bg-14-4435-2017

de La Motte, L.G., Beauclaire, Q., Heinesch, B., Cuntz, M., Foltýnová, L., Šigut, L., Kowalska, N., Manca, G., Ballarin, I.G., Vincke, C., Roland, M., Ibrom, A., Lousteau, D., Siebicke, L., Neiryink, J., Longdoz, B., 2020. Non-stomatal processes reduce gross primary productivity in temperate forest ecosystems during severe edaphic drought: Edaphic drought in forest ecosystems. Philosophical Transactions of the Royal Society B: Biological Sciences 375. https://doi.org/10.1098/rstb.2019.0527

Devaux, A., Kromann, P., Ortiz, O., 2014. Potatoes for Sustainable Global Food Security. Potato Res 57, 185–199. https://doi.org/10.1007/s11540-014-9265-1

Díaz, E., Adsuara, J.E., Martínez, Á.M., Piles, M., Camps-Valls, G., 2022. Inferring causal relations from observational long-term carbon and water fluxes records. Sci Rep 12, 1–12. https://doi.org/10.1038/s41598-022-05377-7

Eamus, D., Huete, A., Yu, Q., 2016a. Modelling Leaf and Canopy Photosynthesis, in: Vegetation Dynamics: A Synthesis of Plant Ecophysiology, Remote Sensing and Modelling. Cambridge University Press., Cambridge, pp. 260–280. https://doi.org/10.1017/cbo9781107286221.011

Eamus, D., Huete, A., Yu, Q., 2016b. Modelling Radiation Exchange and Energy Balances of Leaves and Canopies, in: Vegetation Dynamics: A Synthesis of Plant Ecophysiology, Remote Sensing and Modelling. Cambridge University Press., Cambridge, pp. 244–259. https://doi.org/10.1017/CBO9781107286221.010

Evans, J.R., 2021. Mesophyll conductance: walls, membranes and spatial complexity. New Phytologist. https://doi.org/10.1111/nph.16968

Evans, J.R., Poorter, H., 2001. Photosynthetic acclimation of plants to growth irradiance: The relative importance of specific leaf area and nitrogen partitioning in maximizing carbon gain. Plant Cell Environ 24, 755–767. https://doi.org/10.1046/j.1365-3040.2001.00724.x

F. Kjelgaard, J., O. Stockle, C., 2001. Evaluating surface resistance for estimating corn and potato evapotranspiration with the Penman-Monteith model. Transactions of the ASAE 44, 797. https://doi.org/https://doi.org/10.13031/2013.6243

Falge, E., Baldocchi, D., Olson, R., Anthoni, P., Aubinet, M., Bernhofer, C., Burba, G., Ceulemans, R., Clement, R., Dolman, H., Granier, A., Gross, P., Grünwald, T., Hollinger, D., Jensen, N.O., Katul, G., Keronen, P., Kowalski, A., Lai, C.T., Law, B.E., Meyers, T., Moncrieff, J., Moors, E., Munger, J.W., Pilegaard, K., Rannik, Ü., Rebmann, C., Suyker, A., Tenhunen, J., Tu, K., Verma, S., Vesala, T., Wilson, K., Wofsy, S., 2001. Gap filling strategies for defensible annual sums of net ecosystem exchange. Agric For Meteorol 107, 43–69. https://doi.org/10.1016/S0168-1923(00)00225-2

Falge, E., Baldocchi, D., Tenhunen, J., Aubinet, M., Bakwin, P., Berbigier, P., Bernhofer, C., Burba, G., Clement, R., Davis, K.J., Elbers, J.A., Goldstein, A.H., Grelle, A., Granier, A., Guðmundsson, J., Hollinger, D., Kowalski, A.S., Katul, G., Law, B.E., Malhi, Y., Meyers, T., Monson, R.K., Munger, J.W., Oechel, W., Tha, K., Pilegaard, K., Rannik, Ü., Rebmann, C., Suyker, A., Valentini, R., Wilson, K., Wofsy, S., 2002. Seasonality of ecosystem respiration and gross primary production as derived from FLUXNET measurements, Agricultural and Forest Meteorology.

Fatichi, S., Leuzinger, S., Körner, C., 2014. Moving beyond photosynthesis: From carbon source to sink-driven vegetation modeling. New Phytologist. https://doi.org/10.1111/nph.12614

Fei, X., Jin, Y., Zhang, Y., Sha, L., Liu, Y., Song, Q., Zhou, W., Liang, N., Yu, G., Zhang, L., Zhou, R., Li, J., Zhang, S., Li, P., 2017. Eddy covariance and biometric measurements show that a savanna ecosystem in Southwest China is a carbon sink. Sci Rep 7. https://doi.org/10.1038/srep41025

Ferreira, M.I., 2017. Stress coefficients for soil water balance combined with water stress indicators for irrigation scheduling of woody crops. Horticulturae 3. https://doi.org/10.3390/horticulturae3020038

Field, C.B., Jackson, R.B., Mooney, H.A., 1995. Stomatal responses to increased CO_2: implications from the plant to the global scale. Plant, Celt and Environment 18, 1214–1225. https://doi.org/https://doi.org/10.1111/j.1365-3040.1995.tb00630.x

Flexas, J., Barbour, M.M., Brendel, O., Cabrera, H.M., Carriquí, M., Díaz-Espejo, A., Douthe, C., Dreyer, E., Ferrio, J.P., Gago, J., Gallé, A., Galmés, J., Kodama, N., Medrano, H., Niinemets, Ü., Peguero-Pina, J.J., Pou, A., Ribas-Carbó, M., Tomás, M., Tosens, T., Warren, C.R., 2012. Mesophyll diffusion conductance to CO_2: An unappreciated central player in photosynthesis. Plant Science. https://doi.org/10.1016/j.plantsci.2012.05.009

Flexas, J., Bota, J., Loreto, F., Cornic, G., Sharkey, T.D., 2004. Diffusive and metabolic limitations to photosynthesis under drought and salinity in C3 plants. Plant Biol 6, 269–279. https://doi.org/10.1055/s-2004-820867

Flexas, J., Medrano, H., 2002. Drought-inhibition of photosynthesis in C3 plants: Stomatal and non-stomatal limitations revisited. Ann Bot 89, 183–189. https://doi.org/10.1093/aob/mcf027

Flexas, J., Niinemets, Ü., Gallé, A., Barbour, M.M., Centritto, M., Diaz-Espejo, A., Douthe, C., Galmés, J., Ribas-Carbo, M., Rodriguez, P.L., Rosselló, F., Soolanayakanahally, R., Tomas, M., Wright, I.J., Farquhar, G.D., Medrano, H., 2013. Diffusional conductances to CO_2 as a target for increasing photosynthesis and photosynthetic water-use efficiency. Photosynth Res 117, 45–59. https://doi.org/10.1007/s11120-013-9844-z

Galmés, J., Medrano, H., Flexas, J., 2007. Photosynthetic limitations in response to water stress and recovery in Mediterranean plants with different growth forms. New Phytologist 175, 81–93. https://doi.org/10.1111/j.1469-8137.2007.02087.x

Gentilesca, T., Battipaglia, G., Borghetti, M., Colangelo, M., Altieri, S., Ferrara, A.M.S., Lapolla, A., Rita, A., Ripullone, F., 2021. Evaluating growth and intrinsic water-use efficiency in hardwood and conifer mixed plantations. Trees - Structure and Function 35, 1329–1340. https://doi.org/10.1007/s00468-021-02120-z

Gentine, P., Green, J.K., Guérin, M., Humphrey, V., Seneviratne, S.I., Zhang, Y., Zhou, S., 2019. Coupling between the terrestrial carbon and water cycles - A review. Environmental Research Letters 14. https://doi.org/10.1088/1748-9326/ab22d6

George, T.S., Taylor, M.A., Dodd, I.C., White, P.J., 2017. Climate Change and Consequences for Potato Production: a Review of Tolerance to Emerging Abiotic Stress. Potato Res 60, 239–268. https://doi.org/10.1007/s11540-018-9366-3

Gervais, T., Creelman, A., Li, X.Q., Bizimungu, B., de Koeyer, D., Dahal, K., 2021a. Potato Response to Drought Stress: Physiological and Growth Basis. Front Plant Sci 12, 1–10. https://doi.org/10.3389/fpls.2021.698060

Gervais, T., Creelman, A., Li, X.Q., Bizimungu, B., de Koeyer, D., Dahal, K., 2021b. Potato Response to Drought Stress: Physiological and Growth Basis. Front Plant Sci 12. https://doi.org/10.3389/fpls.2021.698060

Ghislain, M., Núñez, J., Herrera, M.D.R., Spooner, D.M., 2009. The single Andigenum origin of Neo-Tuberosum potato materials is not supported by microsatellite and plastid marker analyses. Theoretical and Applied Genetics 118, 963–969. https://doi.org/10.1007/s00122-008-0953-6

Gondim, P.S. de S., Lima, J.R. de S., Antonino, A.C.D., Hammecker, C., da Silva, R.A.B., Gomes, C.A., 2015. Environmental control on water vapour and energy exchanges over grasslands in semiarid region of brazil. Revista Brasileira de Engenharia Agricola e Ambiental 19, 3–8. https://doi.org/10.1590/1807-1929/agriambi.v19n1p3-8

Gonzalez-Paleo, L., Ravetta, D.A., 2018. Relationship between photosynthetic rate, water use and leaf structure in desert annual and perennial forbs differing in their growth. Photosynthetica 56, 1177–1187. https://doi.org/10.1007/s11099-018-0810-z

Goorman, R., Bartual, A., Paula, S., Ojeda, F., 2011. Enhancement of photosynthesis in post-disturbance resprouts of two co-occurring Mediterranean Erica species. Plant Ecol 212, 2023–2033. https://doi.org/10.1007/s11258-011-9967-2

Goulden, M.L., Wofsy, S.C., Harden, J.W., Trumbore, S.E., Crill, P.M., Gower, T., Fries, T., Daube, B.C., Fan, S., Sutton, D.J., Bazzaz, A., Munger, J.W., 1998. Sensitivity of Boreal Forest Carbon Balance to Soil Thaw. Science (1979) 279, 214–217.

Grossiord, C., Gessler, A., Granier, A., Pollastrini, M., Bussotti, F., Bonal, D., 2014. Interspecific competition influences the response of oak transpiration to increasing drought stress in a mixed Mediterranean forest. For Ecol Manage 318, 54–61. https://doi.org/10.1016/j.foreco.2014.01.004

Guo, H., Zhao, B., Chen, J., Yan, Y., Li, B., Chen, J., 2010. Seasonal changes of energy fluxes in an estuarine wetland of Shanghai, China. Chin Geogr Sci 20, 023–029. https://doi.org/10.1007/s11769-010-0023-2

Guo, R., Zhao, Y., Shi, Y., Li, F., Hu, J., Yang, H., 2017. Low carbon development and local sustainability from a carbon balance perspective. Resour Conserv Recycl 122, 270–279. https://doi.org/10.1016/j.resconrec.2017.02.019

Haile-Mariam, S., Collins, H.P., Higgins, S.S., 2008. Greenhouse Gas Fluxes from an Irrigated Sweet Corn (Zea mays L.)–Potato (Solanum tuberosum L.) Rotation . J Environ Qual 37, 759–771. https://doi.org/10.2134/jeq2007.0400

Herbst, M., Kutsch, W.L., Hummelshøj, P., Jensen, N.O., Kappen, L., 2002. Canopy physiology: interpreting the variations in eddy fluxes of water vapour and carbon dioxide observed over a beech forest Basic and Applied Ecology, Basic Appl. Ecol.

Hill, D., Nelson, D., Hammond, J., Bell, L., 2021a. Morphophysiology of Potato (Solanum tuberosum) in Response to Drought Stress: Paving the Way Forward. Front Plant Sci 11, 1–19. https://doi.org/10.3389/fpls.2020.597554

Hill, D., Nelson, D., Hammond, J., Bell, L., 2021b. Morphophysiology of Potato (Solanum tuberosum) in Response to Drought Stress: Paving the Way Forward. Front Plant Sci. https://doi.org/10.3389/fpls.2020.597554

Howlader, O., Hoque, M., 2018. Growth analysis and yield performance of four potato (Solanum tuberosum L.) Varieties. Bangladesh Journal of Agricultural Research 43, 267–280. https://doi.org/10.3329/bjar.v43i2.37330

Hu, Z., Yu, G., Fu, Y., Sun, X., Li, Y., Shi, P., Wang, Y., Zheng, Z., 2008. Effects of vegetation control on ecosystem water use efficiency within and among four grassland ecosystems in China. Glob Chang Biol 14, 1609–1619. https://doi.org/10.1111/j.1365-2486.2008.01582.x

Hunt, R., 1990. Basic Growth Analysis. London.

Huxman, T.E., Snyder, K.A., Tissue, D., Leffler, A.J., Ogle, K., Pockman, W.T., Sandquist, D.R., Potts, D.L., Schwinning, S., 2004. Rainfall pulses and carbon fluxes in semiarid and arid ecosystems. Oecologia 141, 254–268. https://doi.org/10.1007/s00442-004-1682-4

Irmak, S., Mutiibwa, D., 2010. On the dynamics of canopy resistance: Generalized linear estimation and relationships with primary micrometeorological variables. Water Resour Res 46. https://doi.org/10.1029/2009WR008484

Jarvis, P.G., 1985. Coupling of transpiration to the atmosphere in horticultural crops: the omega factor. Acta Horticulturae 187–205.

Jarvis, P G, Mcnaughton, K.G., 1986. Stomatal Control of Transpiration: Scaling Up from Leaf to Region. Adv Ecol Res 15, 1–49. https://doi.org/10.1016/S0065-2504(08)60119-1

Jarvis, P. G., Mcnaughton, K.G., 1986. Stomatal Control of Transpiration: Scaling Up from Leaf to Region. Adv Ecol Res 15, 1–49. https://doi.org/10.1016/S0065-2504(08)60119-1

Jennings, S.A., Koehler, A.K., Nicklin, K.J., Deva, C., Sait, S.M., Challinor, A.J., 2020. Global Potato Yields Increase Under Climate Change With Adaptation and CO_2 Fertilisation. Front Sustain Food Syst 4. https://doi.org/10.3389/fsufs.2020.519324

Jia, X., Zha, T.S., Wu, B., Zhang, Y.Q., Gong, J.N., Qin, S.G., Chen, G.P., Qian, D., Kellomäki, S., Peltola, H., 2014. Biophysical controls on net ecosystem CO_2 exchange over a semiarid shrubland in northwest China. Biogeosciences 11, 4679–4693. https://doi.org/10.5194/bg-11-4679-2014

Jongen, M., Pereira, J.S., Aires, L.M.I., Pio, C.A., 2011. The effects of drought and timing of rainfall on the inter-annual variation in ecosystem-atmosphere exchange in a Mediterranean grassland. Agric For Meteorol 151, 595–606. https://doi.org/10.1016/j.agrformet.2011.01.008

Jullien, A., Allirand, J.M., Mathieu, A., Andrieu, B., Ney, B., 2009. Variations in leaf mass per area according to N nutrition, plant age, and leaf position reflect ontogenetic plasticity in winter oilseed rape (Brassica napus L.). Field Crops Res 114, 188–197. https://doi.org/10.1016/j.fcr.2009.07.015

Kang, M., Zhang, Z., Noormets, A., Fang, X., Zha, T., Zhou, J., Sun, G., McNulty, S.G., Chen, J., 2015. Energy partitioning and surface resistance of a poplar plantation in northern China. Biogeosciences 12, 4245–4259. https://doi.org/10.5194/bg-12-4245-2015

Katul, G., Manzoni, S., Palmroth, S., Oren, R., 2010a. A stomatal optimization theory to describe the effects of atmospheric CO_2 on leaf photosynthesis and transpiration. Ann Bot 105, 431–442. https://doi.org/10.1093/aob/mcp292

Katul, G., Manzoni, S., Palmroth, S., Oren, R., 2010b. A stomatal optimization theory to describe the effects of atmospheric CO_2 on leaf photosynthesis and transpiration. Ann Bot 105, 431–442. https://doi.org/10.1093/aob/mcp292

Katul, G.G., Palmroth, S., Oren, R., 2009. Leaf stomatal responses to vapour pressure deficit under current and CO_2-enriched atmosphere explained by the economics of gas exchange. Plant Cell Environ 32, 968–979. https://doi.org/10.1111/j.1365-3040.2009.01977.x

Keenan, T.F., Hollinger, D.Y., Bohrer, G., Dragoni, D., Munger, J.W., Schmid, H.P., Richardson, A.D., 2013a. Increase in forest water-use efficiency as atmospheric carbon dioxide concentrations rise. Nature 499, 324–327. https://doi.org/10.1038/nature12291

Keenan, T.F., Hollinger, D.Y., Bohrer, G., Dragoni, D., Munger, J.W., Schmid, H.P., Richardson, A.D., 2013b. Increase in forest water-use efficiency as atmospheric carbon dioxide concentrations rise. Nature 499, 324–327. https://doi.org/10.1038/nature12291

Krich, C., Mahecha, M.D., Migliavacca, M., de Kauwe, M.G., Griebel, A., Runge, J., Miralles, D.G., 2022. Decoupling between ecosystem photosynthesis and transpiration: A last resort against overheating. Environmental Research Letters 17. https://doi.org/10.1088/1748-9326/ac583e

Kumagai, T., Tateishi, M., Shimizu, T., Otsuki, K., 2008. Transpiration and canopy conductance at two slope positions in a Japanese cedar forest watershed. Agric For Meteorol 148, 1444–1455. https://doi.org/https://doi.org/10.1016/j.agrformet.2008.04.010

Launiainen, S., Katul, G.G., Kolari, P., Vesala, T., Hari, P., 2011. Empirical and optimal stomatal controls on leaf and ecosystem level CO_2 and H_2O exchange rates. Agric For Meteorol 151, 1672–1689. https://doi.org/10.1016/j.agrformet.2011.07.001

Law, B.E., Falge, E., Gu, L., Baldocchi, D.D., Bakwin, P., Berbigier, P., Davis, K., Dolman, A.J., Falk, M., Fuentes, J.D., Goldstein, A., Granier, A., Grelle, A., Hollinger, D., Janssens, I.A., Jarvis, P., Jensen, N.O., Katul, G., Mahli, Y., Matteucci, G., Meyers, T., Monson, R., Munger, W., Oechel, W., Olson, R., Pilegaard, K., Paw U H, K.T., Thorgeirsson, H., Valentini, R., Verma, S., Vesala, T., Wilson, K., Wofsy, S., 2002. Environmental controls over carbon dioxide and water vapor exchange of terrestrial vegetation. Agriculture and Forest Meteorology 113, 97–120.

Law, B.E., Williams, M., Anthoni, P.M., Baldocchi, D.D., Unsworth, M.H., 2000. Measuring and modelling seasonal variation of carbon dioxide and water vapour exchange of a Pinus ponderosa forest subject to soil water deficit. Glob Chang Biol 6, 613–630. https://doi.org/10.1046/j.1365-2486.2000.00339.x

Leonardi, S., Gentilesca, T., Guerrieri, R., Ripullone, F., Magnani, F., Mencuccini, M., Noije, T. v., Borghetti, M., 2012. Assessing the effects of nitrogen deposition and climate on carbon isotope discrimination and intrinsic water-use efficiency of angiosperm and conifer trees under rising CO 2 conditions. Glob Chang Biol 18, 2925–2944. https://doi.org/10.1111/j.1365-2486.2012.02757.x

Leuning, R., 1995. A critical appraisal of a combined stomatal-photosynthesis model for C3 plants. Plant, Celt and Environment 18, 339–355. https://doi.org/https://doi.org/10.1111/j.1365-3040.1995.tb00370.x

Li, D., Fang, K., Li, Yingjun, Chen, D., Liu, X., Dong, Z., Zhou, F., Guo, G., Shi, F., Xu, C., Li, Yanping, 2017. Climate, intrinsic water-use efficiency and tree growth over the past 150 years in humid subtropical China. PLoS One 12, 1–19. https://doi.org/10.1371/journal.pone.0172045

Li, S.G., Lai, C.T., Lee, G., Shimoda, S., Yokoyama, T., Higuchi, A., Oikawa, T., 2005. Evapotranspiration from a wet temperate grassland and its sensitivity to microenvironmental variables. Hydrol Process 19, 517–532. https://doi.org/10.1002/hyp.5673

Li, Y., Zhang, X., Shao, Q., Fan, J., Chen, Z., Dong, J., Hu, Z., Zhan, Y., 2022. Community Composition and Structure Affect Ecosystem and Canopy Water Use Efficiency Across Three Typical Alpine Ecosystems. Front Plant Sci 12, 1–14. https://doi.org/10.3389/fpls.2021.771424

Lin, B.S., Lei, H., Hu, M.C., Visessri, S., Hsieh, C.I., 2020. Canopy Resistance and Estimation of Evapotranspiration above a Humid Cypress Forest. Advances in Meteorology 2020. https://doi.org/10.1155/2020/4232138

Lin, Y.S., Medlyn, B.E., Duursma, R.A., Prentice, I.C., Wang, H., Baig, S., Eamus, D., de Dios, V.R., Mitchell, P., Ellsworth, D.S., de Beeck, M.O., Wallin, G., Uddling, J., Tarvainen, L., Linderson, M.L., Cernusak, L.A., Nippert, J.B., Ocheltree, T.W., Tissue, D.T., Martin-StPaul, N.K., Rogers, A., Warren, J.M., de Angelis, P., Hikosaka, K., Han, Q., Onoda, Y., Gimeno, T.E., Barton, C.V.M., Bennie, J., Bonal, D., Bosc, A., Löw, M., Macinins-Ng, C., Rey, A., Rowland, L., Setterfield, S.A., Tausz-Posch, S., Zaragoza-Castells, J., Broadmeadow, M.S.J., Drake, J.E., Freeman, M., Ghannoum, O., Hutley, L.B., Kelly, J.W., Kikuzawa, K., Kolari, P., Koyama, K., Limousin, J.M., Meir, P., da Costa, A.C.L., Mikkelsen, T.N., Salinas, N., Sun, W., Wingate, L., 2015. Optimal stomatal behaviour around the world. Nat Clim Chang 5, 459–464. https://doi.org/10.1038/nclimate2550

Linderson, M.L., Mikkelsen, T.N., Ibrom, A., Lindroth, A., Ro-Poulsen, H., Pilegaard, K., 2012. Up-scaling of water use efficiency from leaf to canopy as based on leaf gas exchange relationships and the modeled in-canopy light distribution. Agric For Meteorol 152, 201–211. https://doi.org/10.1016/j.agrformet.2011.09.019

Lipper, L., Thornton, P., Campbell, B.M., Baedeker, T., Braimoh, A., Bwalya, M., Caron, P., Cattaneo, A., Garrity, D., Henry, K., Hottle, R., Jackson, L., Jarvis, A., Kossam, F., Mann, W., McCarthy, N., Meybeck, A., Neufeldt, H., Remington, T., Sen, P.T., Sessa, R., Shula, R., Tibu, A., Torquebiau, E.F., 2014. Climate-smart agriculture for food security. Nat Clim Chang. https://doi.org/10.1038/nclimate2437

Liu, S., Baret, F., Abichou, M., Manceau, L., Andrieu, B., Weiss, M., Martre, P.M., Manceau, L.L., Martre, P., 2021. Importance of the description of light interception in crop growth models. Plant Physiol 186, 977–997. https://doi.org/10.1093/plphys/kiab113ï

Liu, X., Wang, P., Song, H., Zeng, X., 2021. Determinants of net primary productivity: Low-carbon development from the perspective of carbon sequestration. Technol Forecast Soc Change 172, 121006. https://doi.org/10.1016/j.techfore.2021.121006

Loader, N.J., Walsh, R.P.D., Robertson, I., Bidin, K., Ong, R.C., Reynolds, G., McCarroll, D., Gagen, M., Young, G.H.F., 2011. Recent trends in the intrinsic water-use efficiency of ringless rainforest trees in Borneo. Philosophical Transactions of the Royal Society B: Biological Sciences 366, 3330–3339. https://doi.org/10.1098/rstb.2011.0037

Lombardozzi, D., Levis, S., Bonan, G., Sparks, J.P., 2012. Predicting photosynthesis and transpiration responses to ozone: Decoupling modeled photosynthesis and stomatal conductance. Biogeosciences 9, 3113–3130. https://doi.org/10.5194/bg-9-3113-2012

López-Olivari, R., Fuentes, S., Poblete-Echeverría, C., Quintulen-Ancapi, V., Medina, L., 2022. Site-Specific Evaluation of Canopy Resistance Models for Estimating Evapotranspiration over a Drip-Irrigated Potato Crop in Southern Chile under Water-Limited Conditions. Water (Switzerland) 14. https://doi.org/10.3390/w14132041

Mackay, G., 2009. New Light on a Hidden Treasure. Exp Agric 45, 376–376.

Magnani, F., Leonardi, S., Tognetti, R., Grace, J., Borghetti, M., 1998. Modelling the surface conductance of a broad-leaf canopy: Effects of partial decoupling from the atmosphere. Plant Cell Environ 21, 867–879. https://doi.org/10.1046/j.1365-3040.1998.00328.x

Mallick, Kanishka, Trebs, I., Boegh, E, Mallick, Kaniska, Boegh, Eva, Giustarini, L., Schlerf, M., Drewry, D.T., Hoffmann, L., von Randow, C., Kruijt, B., Araùjo, A., Saleska, S., Ehleringer, J.R., Domingues, T.F., Pierre, J., Ometto, H.B., Nobre, A.D., Leal De Moraes, O.L., Hayek, M., Munger, J.W., Wofsy, S.C., 2016. Canopy-scale biophysical controls of transpiration and evaporation in the Amazon Basin. Hydrol. Earth Syst. Sci 20, 4237–4264. https://doi.org/10.5194/hess-2015-552

Martínez-Maldonado, F.E., Castaño-Marín, A.M., Goez-Vinasco, G.A., Marin, F.R., 2021a. Gross Primary Production of Rainfed and Irrigated Potato (Solanum tuberosum L .) in the Colombian Andean Region Using Eddy Covariance Technique. Water (Switzerland) 13.

Martínez-Maldonado, F.E., Castaño-Marín, A.M., Góez-Vinasco, G.A., Marin, F.R., 2021b. Gross primary production of rainfed and irrigated potato (Solanum tuberosum l.) in the colombian andean region using eddy covariance technique. Water (Switzerland) 13. https://doi.org/10.3390/w13223223

McNaughton, K.G., Jarvis, P.G., 1991. Effects of spatial scale on stomatal control of transpiration. Agric For Meteorol 54, 279–302. https://doi.org/https://doi.org/10.1016/0168-1923(91)90010-N

Meshalkina, J., Yaroslavtsev, A., Vassenev, I., 2017. Carbon balance of the typical grain crop rotation in Moscow region assessed by eddy covariance method 19, 12212.

Meshalkina, J.L., Yaroslavtsev, A.M., Vasenev, I.I., Andreeva, I. v., Tihonova, M. v., 2018. Carbon balance assessment by eddy covariance method for agroecosystems with potato plants and oats & vetch mixture on sod-podzolic soils of Russia. IOP Conf Ser Earth Environ Sci 107. https://doi.org/10.1088/1755-1315/107/1/012119

Michel, A.J., Teixeira, E.I., Brown, H.E., Dellow, S.J., Maley, S., Gillespie, R.N., Richards, K.K., 2019. Water stress responses of three potato cultivars. Agronomy New Zealand 49, 25–37.

Migliavacca, M., Meroni, M., Manca, G., Matteucci, G., Montagnani, L., Grassi, G., Zenone, T., Teobaldelli, M., Goded, I., Colombo, R., Seufert, G., 2009. Seasonal and interannual patterns of carbon and water fluxes of a poplar plantation under peculiar eco-climatic conditions. Agric For Meteorol 149, 1460–1476. https://doi.org/10.1016/j.agrformet.2009.04.003

Monteith, J., Unsworth, M.H., 2013. Principles of Enviromental Physics, Chemical Geology. https://doi.org/10.1016/0009-2541(75)90087-X

Monteith, J.L., 1986. How Do Crops Manipulate Water Supply and Demand? Philos Trans R Soc Lond 316, 245–259.

Moors, E.J., Jacobs, C., Jans, W., Supit, I., Kutsch, W.L., Bernhofer, C., Béziat, P., Buchmann, N., Carrara, A., Ceschia, E., Elbers, J., Eugster, W., Kruijt, B., Loubet, B., Magliulo, E., Moureaux, C., Olioso, A., Saunders, M., Soegaard, H., 2010. Variability in carbon exchange of European croplands. Agric Ecosyst Environ 139, 325–335. https://doi.org/10.1016/j.agee.2010.04.013

Morén, A.S., Lindroth, A., Grelle, A., 2001. Water-use efficiency as a means of modelling net assimilation in boreal forests. Trees - Structure and Function 15, 67–74. https://doi.org/10.1007/s004680000078

Mosquera Vásquez, T., del Castillo, S., Gálvez, D.C., Rodríguez, L.E., 2017. Breeding Differently: Participatory Selection and Scaling Up Innovations in Colombia. Potato Res 60, 361–381. https://doi.org/10.1007/s11540-018-9389-9

Muthoni, J., Kabira, J.N., 2016. Potato Production under Drought Conditions: Identification of Adaptive Traits. International Journal of Horticulture. https://doi.org/10.5376/ijh.2016.06.0012

Nadal-Sala, D., Grote, R., Birami, B., Knüver, T., Rehschuh, R., Schwarz, S., Ruehr, N.K., 2021. Leaf Shedding and Non-Stomatal Limitations of Photosynthesis Mitigate Hydraulic Conductance Losses in Scots Pine Saplings During Severe Drought Stress. Front Plant Sci 12. https://doi.org/10.3389/fpls.2021.715127

Nasir, M.W., Toth, Z., 2022a. Effect of Drought Stress on Potato Production: A Review. Agronomy. https://doi.org/10.3390/agronomy12030635

Nasir, M.W., Toth, Z., 2022b. Effect of Drought Stress on Potato Production: A Review. Agronomy 12. https://doi.org/10.3390/agronomy12030635

Nassif, D.S.P., da Costa, L.G., Vianna, M.D.S., dos Santos Carvalho, K., Marin, F.R., 2019. The role of decoupling factor on sugarcane crop water use under tropical conditions. Exp Agric 55, 913–923. https://doi.org/10.1017/S0014479718000480

Nassif, D.S.P., Marin, F.R., Costa, L.G., 2014. Evapotranspiration and Transpiration Coupling to the Atmosphere of Sugarcane in Southern Brazil: Scaling Up from Leaf to Field. Sugar Tech 16, 250–254. https://doi.org/10.1007/s12355-013-0267-0

Nelson, J.A., Carvalhais, N., Migliavacca, M., Reichstein, M., Jung, M., 2018a. Water-stress-induced breakdown of carbon-water relations: Indicators from diurnal FLUXNET patterns. Biogeosciences 15, 2433–2447. https://doi.org/10.5194/bg-15-2433-2018

Nelson, J.A., Carvalhais, N., Migliavacca, M., Reichstein, M., Jung, M., 2018b. Water-stress-induced breakdown of carbon-water relations: Indicators from diurnal FLUXNET patterns. Biogeosciences 15, 2433–2447. https://doi.org/10.5194/bg-15-2433-2018

Nemecek, T., Weiler, K., Plassmann, K., Schnetzer, J., Gaillard, G., Jefferies, D., García-Suárez, T., King, H., Milà I Canals, L., 2012. Estimation of the variability in global warming potential of worldwide crop production using a modular extrapolation approach. J Clean Prod 31, 106–117. https://doi.org/10.1016/j.jclepro.2012.03.005

Niinemets, Ü., Cescatti, A., Rodeghiero, M., Tosens, T., 2006. Complex adjustments of photosynthetic potentials and internal diffusion conductance to current and previous light availabilities and leaf age in Mediterranean evergreen species Quercus ilex. Plant Cell Environ 29, 1159–1178. https://doi.org/10.1111/j.1365-3040.2006.01499.x

Niu, S., Xing, X., Zhang, Z., Xia, J., Zhou, X., Song, B., Li, L., Wan, S., 2011. Water-use efficiency in response to climate change: From leaf to ecosystem in a temperate steppe. Glob Chang Biol 17, 1073–1082. https://doi.org/10.1111/j.1365-2486.2010.02280.x

Obidiegwu, J.E., Bryan, G.J., Jones, H.G., Prashar, A., 2015. Coping with drought: Stress and adaptive responses in potato and perspectives for improvement. Front Plant Sci 6, 1–23. https://doi.org/10.3389/fpls.2015.00542

Oliveira, J.S., Brown, H.E., Moot, D.J., 2021. Assessing potato canopy growth and development at the individual leaf level to improve the understanding of the plant source–sink relations. N Z J Crop Hortic Sci 49, 325–346. https://doi.org/10.1080/01140671.2021.1879878

Oo, A.Z., Yamamoto, A., Ono, K., Umamageswari, C., Mano, M., Vanitha, K., Elayakumar, P., Matsuura, S., Bama, K.S., Raju, M., Inubushi, K., Sudo, S., Saitoh, N., Hayashida, S., Ravi, V., Ambethgar, V., 2023. Ecosystem carbon dioxide exchange and water use efficiency in a triple-cropping rice paddy in Southern India: A two-year field observation. Science of The Total Environment 854, 158541. https://doi.org/10.1016/j.scitotenv.2022.158541

Paulino Junior, N., Silva von Randow, 2017. Analysis of biological and meteorological controls of evapotranspiration in pristine forests and a pasture site in Amazonia. Revista Ambiente e Agua 12, 179–191. https://doi.org/10.4136/1980-993X

Pereira, J.S., Mateus, J.A., Aires, L.M., Pita, G., Pio, C., David, J.S., Andrade, V., Banza, J., David, T.S., Paço, T.A., Rodrigues, A., 2007. Net ecosystem carbon exchange in three contrasting Mediterranean ecosystems - The effect of drought. Biogeosciences 4, 791–802. https://doi.org/10.5194/bg-4-791-2007

Perez, P.J., Lecina, S., Castellvi, F., Martínez-Cob, A., Villalobos, F.J., 2006. A simple parameterization of bulk canopy resistance from climatic variables for estimating hourly evapotranspiration. Hydrol Process 20, 515–532. https://doi.org/10.1002/hyp.5919

Raker, C.M., Spooner, D.M., 2002. Chilean tetraploid cultivated potato, Solanum tuberosum, is distinct from the Andean populations: Microsatellite data. Crop Sci 42, 1451–1458. https://doi.org/10.2135/cropsci2002.1451

Rana, G., Ferrara, R.M., Vitale, D., D'Andrea, L., Palumbo, A.D., 2016. Carbon assimilation and water use efficiency of a perennial bioenergy crop (Cynara cardunculus L.) in Mediterranean environment. Agric For Meteorol 217, 137–150. https://doi.org/10.1016/j.agrformet.2015.11.025

Rana, G., Katerji, N., Mastrorilli, M., Moujabber, M.E., 1994. Theoretical and Applied Climatology Evapotranspiration and Canopy Resistance of Grass in a Mediterranean Region, Theor. Appl. Climatol.

Reichstein, M., Tenhunen, J.D., Roupsard, O., Ourcival, J.M., Rambal, S., Miglietta, F., Peressotti, A., Pecchiari, M., Tirone, G., Valentini, R., 2002. Severe drought effects on ecosystem CO_2 and H_2O fluxes at three Mediterranean evergreen sites: Revision of current hypotheses? Glob Chang Biol 8, 999–1017. https://doi.org/10.1046/j.1365-2486.2002.00530.x

Rodríguez P., L., Sanjuanelo C., D., Ñústez L., C.E., Moreno-Fonseca, L.P., 2016. Crecimiento y fenología de tres variedades andinas de papa (Solanum tuberosum L.) en estrés hídrico. Agron Colomb 34, 141–154. https://doi.org/10.15446/agron.colomb.v34n2.55279

Samanta, S., Banerjee, S., Mukherjee, A., Patra, P.K., Chakraborty, P.K., 2020. Determining the radiation use efficiency of potato using sunshine hour data: A simple and costless approach. Spanish Journal of Agricultural Research 18, 1–15. https://doi.org/10.5424/sjar/2020182-15561

Schwalm, C.R., Williams, C.A., Schaefer, K., Arneth, A., Bonal, D., Buchmann, N., Chen, J., Law, B., Lindroth, A., Luyssaert, S., Reichstein, M., Richardson, A.D., 2010. Assimilation exceeds respiration sensitivity to drought: A FLUXNET synthesis. Glob Chang Biol 16, 657–670. https://doi.org/10.1111/j.1365-2486.2009.01991.x

Scott, R.L., Huxman, T.E., Cable, W.L., Emmerich, W.E., 2006a. Partitioning of evapotranspiration and its relation to carbon dioxide exchange in a Chihuahuan Desert shrubland. Hydrol Process 20, 3227–3243. https://doi.org/10.1002/hyp.6329

Scott, R.L., Huxman, T.E., Cable, W.L., Emmerich, W.E., 2006b. Partitioning of evapotranspiration and its relation to carbon dioxide exchange in a Chihuahuan Desert shrubland. Hydrol Process 20, 3227–3243. https://doi.org/10.1002/hyp.6329

Service-USDA, U.S.D. of A.N.R.C., 2014. Claves para la Taxonomía de Suelos. Mdp.Edu.Ar 339.

Shao, J., Zhou, X., Luo, Y., Li, B., Aurela, M., Billesbach, D., Blanken, P.D., Bracho, R., Chen, J., Fischer, M., Fu, Y., Gu, L., Han, S., He, Y., Kolb, T., Li, Y., Nagy, Z., Niu, S., Oechel, W.C., Pinter, K., Shi, P., Suyker, A., Torn, M., Varlagin, A., Wang, H., Yan, J., Yu, G., Zhang, J., 2015. Biotic and climatic controls on interannual variability in carbon fluxes across terrestrial ecosystems. Agric For Meteorol 205, 11–22. https://doi.org/10.1016/j.agrformet.2015.02.007

Silva, P.F. da, Lima, J.R. de S., Antonino, A.C.D., Souza, R., de Souza, E.S., Silva, J.R.I., Alves, E.M., 2017. Seasonal patterns of carbon dioxide, water and energy fluxes over the Caatinga and grassland in the semi-arid region of Brazil. J Arid Environ 147, 71–82. https://doi.org/10.1016/j.jaridenv.2017.09.003

Smith, W.K., 1980. Importance of Aerodynamic Resistance to Water Use Efficiency in Three Conifers under Field Conditions. Plant Physiol 65, 132–135. https://doi.org/10.1104/pp.65.1.132

Souza, P.J. de O.P. de, Ribeiro, A., Rocha, E.J.P. da, Farias, J.R.B., Souza, E.B. de, 2012. Sazonalidade no balanço de energia em áreas de cultivo de soja na Amazônia. Bragantia 71, 548–557. https://doi.org/10.1590/S0006-87052012000400013

Spinelli, G.M., Snyder, R.L., Sanden, B.L., Gilbert, M., Shackel, K.A., 2018a. Low and variable atmospheric coupling in irrigated Almond (Prunus dulcis) canopies indicates a limited influence of stomata on orchard evapotranspiration. Agric Water Manag 196, 57–65. https://doi.org/10.1016/j.agwat.2017.10.019

Spinelli, G.M., Snyder, R.L., Sanden, B.L., Gilbert, M., Shackel, K.A., 2018b. Low and variable atmospheric coupling in irrigated Almond (Prunus dulcis) canopies indicates a limited influence of stomata on orchard evapotranspiration. Agric Water Manag 196, 57–65. https://doi.org/10.1016/j.agwat.2017.10.019

Spinelli, G.M., Snyder, R.L., Sanden, B.L., Shackel, K.A., 2016. Water stress causes stomatal closure but does not reduce canopy evapotranspiration in almond. Agric Water Manag 168, 11–22. https://doi.org/10.1016/j.agwat.2016.01.005

Steduto, P., Hsiao, T.C., 1998. Maize canopies under two soil water regimes III. Variation in coupling with the atmosphere and the role of leaf area index. Agric For Meteorol 89, 201–213. https://doi.org/10.1016/S0168-1923(97)00083-X

Sugiura, D., Terashima, I., Evans, J.R., 2020. A decrease in mesophyll conductance by Cell-Wall thickening contributes to photosynthetic downregulation. Plant Physiol 183, 1600–1611. https://doi.org/10.1104/pp.20.00328

Sutherlin, C.E., Brunsell, N.A., de Oliveira, G., Crews, T.E., DeHaan, L.R., Vico, G., 2019a. Contrasting physiological and environmental controls of evapotranspiration over Kernza Perennial crop, annual crops, and C4 and mixed C3/C4 grasslands. Sustainability (Switzerland) 11. https://doi.org/10.3390/su11061640

Sutherlin, C.E., Brunsell, N.A., de Oliveira, G., Crews, T.E., DeHaan, L.R., Vico, G., 2019b. Contrasting physiological and environmental controls of evapotranspiration over Kernza Perennial crop, annual crops, and C4 and mixed C3/C4 grasslands. Sustainability (Switzerland) 11. https://doi.org/10.3390/su11061640

Tagesson, T., Fensholt, R., Cropley, F., Guiro, I., Horion, S., Ehammer, A., Ardö, J., 2015. Dynamics in carbon exchange fluxes for a grazed semi-arid savanna ecosystem in West Africa. Agric Ecosyst Environ 205, 15–24. https://doi.org/10.1016/j.agee.2015.02.017

Tang, J., Bolstad, P. v., Ewers, B.E., Desai, A.R., Davis, K.J., Carey, E. v., 2006. Sap flux-upscaled canopy transpiration, stomatal conductance, and water use efficiency in an old growth forest in the Great Lakes region of the United States. J Geophys Res Biogeosci 111. https://doi.org/10.1029/2005JG000083

Tang, X., Ding, Z., Li, H., Li, X., Luo, J., Xie, J., Chen, D., 2015. Characterizing ecosystem water-use efficiency of croplands with eddy covariance measurements and MODIS products. Ecol Eng 85, 212–217. https://doi.org/10.1016/j.ecoleng.2015.09.078

Teixeira, A.H. de C., Bastiaanssen, W.G.M., Ahmad, M.D., Moura, M.S.B., Bos, M.G., 2008. Analysis of energy fluxes and vegetation-atmosphere parameters in irrigated and natural ecosystems of semi-arid Brazil. J Hydrol (Amst) 362, 110–127. https://doi.org/10.1016/j.jhydrol.2008.08.011

Vadez, V., Kholova, J., Medina, S., Kakkera, A., Anderberg, H., 2014. Transpiration efficiency: New insights into an old story. J Exp Bot 65, 6141–6153. https://doi.org/10.1093/jxb/eru040

van Dijke, A.J.H., Mallick, K., Schlerf, M., MacHwitz, M., Herold, M., Teuling, A.J., 2020a. Examining the link between vegetation leaf area and land-atmosphere exchange of water, energy, and carbon fluxes using FLUXNET data. Biogeosciences 17, 4443–4457. https://doi.org/10.5194/bg-17-4443-2020

van Dijke, A.J.H., Mallick, K., Schlerf, M., MacHwitz, M., Herold, M., Teuling, A.J., 2020b. Examining the link between vegetation leaf area and land-atmosphere exchange of water, energy, and carbon fluxes using FLUXNET data. Biogeosciences 17, 4443–4457. https://doi.org/10.5194/bg-17-4443-2020

Varone, L., Ribas-Carbo, M., Cardona, C., Gallé, A., Medrano, H., Gratani, L., Flexas, J., 2012. Stomatal and non-stomatal limitations to photosynthesis in seedlings and saplings of Mediterranean species pre-conditioned and aged in nurseries: Different response to water stress. Environ Exp Bot 75, 235–247. https://doi.org/10.1016/j.envexpbot.2011.07.007

Viola, R., Roberts, A.G., Haupt, S., Gazzani, S., Hancock, R.D., Marmiroli, N., Machray, G.C., Oparka, K.J., 2001. Tuberization in Potato Involves a Switch from Apoplastic to Symplastic Phloem Unloading, The Plant Cell.

Wagle, P., Xiao, X., Kolb, T.E., Law, B.E., Wharton, S., Monson, R.K., Chen, J., Blanken, P.D., Novick, K.A., Dore, S., Noormets, A., Gowda, P.H., 2016. Differential responses of carbon and water vapor fluxes to climate among evergreen needleleaf forests in the USA. Ecol Process 5. https://doi.org/10.1186/s13717-016-0053-5

Wehr, R., Saleska, S.R., 2021. Calculating canopy stomatal conductance from eddy covariance measurements, in light of the energy budget closure problem. Biogeosciences 18, 13–24. https://doi.org/10.5194/bg-18-13-2021

Weraduwage, S.M., Chen, J., Anozie, F.C., Morales, A., Weise, S.E., Sharkey, T.D., 2015. The relationship between leaf area growth and biomass accumulation in Arabidopsis thaliana. Front Plant Sci 6, 1–21. https://doi.org/10.3389/fpls.2015.00167

Wilson, K.B., Baldocchi, D.D., Hanson, P.J., 2001. Leaf age affects the seasonal pattern of photosynthetic capacity and net ecosystem exchange of carbon in a deciduous forest. Plant Cell Environ 24, 571–583. https://doi.org/10.1046/j.0016-8025.2001.00706.x

Wood, D.A., 2021. Net ecosystem carbon exchange prediction and insightful data mining with an optimized data-matching algorithm. Ecol Indic 124, 107426. https://doi.org/10.1016/j.ecolind.2021.107426

Wright, G.C., Rao, R.C.N., Farquhar, G.D., 1994. Water-use efficiency and carbon isotope discrimination in peanut under water deficit conditions. Crop Sci 34, 92–97. https://doi.org/10.2135/cropsci1994.0011183X003400010016x

Xie, J., Chen, J., Sun, G., Zha, T., Yang, B., Chu, H., Liu, J., Wan, S., Zhou, C., Ma, H., Bourque, C.P.A., Shao, C., John, R., Ouyang, Z., 2016. Ten-year variability in ecosystem water use efficiency in an oak-dominated temperate forest under a warming climate. Agric For Meteorol 218–219, 209–217. https://doi.org/10.1016/j.agrformet.2015.12.059

Xu, L., Baldocchi, D.D., 2004. Seasonal variation in carbon dioxide exchange over a Mediterranean annual grassland in California. Agric For Meteorol 123, 79–96. https://doi.org/10.1016/j.agrformet.2003.10.004

Yang, J., Duursma, R.A., de Kauwe, M.G., Kumarathunge, D., Jiang, M., Mahmud, K., Gimeno, T.E., Crous, K.Y., Ellsworth, D.S., Peters, J., Choat, B., Eamus, D., Medlyn, B.E., 2019. Incorporating non-stomatal limitation improves the performance of leaf and canopy models at high vapour pressure deficit. Tree Physiol 39, 1961–1974. https://doi.org/10.1093/treephys/tpz103

Zhang, Z.Z., Zhao, P., McCarthy, H.R., Zhao, X.H., Niu, J.F., Zhu, L.W., Ni, G.Y., Ouyang, L., Huang, Y.Q., 2016. Influence of the decoupling degree on the estimation of canopy stomatal conductance for two broadleaf tree species. Agric For Meteorol 221, 230–241. https://doi.org/10.1016/j.agrformet.2016.02.018

Zhou, J., Zhang, Z., Sun, G., Fang, X., Zha, T., McNulty, S., Chen, J., Jin, Y., Noormets, A., 2013. Response of ecosystem carbon fluxes to drought events in a poplar plantation in Northern China. For Ecol Manage 300, 33–42. https://doi.org/10.1016/j.foreco.2013.01.007

Zhou, S., Yu, B., Huang, Y., Wang, G., 2015. Daily underlying water use efficiency for AmeriFlux sites. J Geophys Res Biogeosci 120, 887–902. https://doi.org/10.1002/2015JG002947

Zhou, S., Yu, B., Huang, Y., Wang, G., 2014. The effect of vapor pressure deficit on water use efficiency at the subdaily time scale. Geophys Res Lett 41, 5005–5013. https://doi.org/10.1002/2014GL060741

3. GROSS PRIMARY PRODUCTION OF RAINFED AND IRRIGATED POTATO (*Solanum tuberosum* L.) IN THE COLOMBIAN ANDEAN REGION USING EDDY COVARIANCE TECHNIQUE

Abstract

Potato farming is relevant for global carbon balances and greenhouse emissions, of which gross primary productivity (GPP) is one of the main drivers. In this study, the net carbon ecosystem exchange (NEE) was measured using the Eddy Covariance (EC) method in two potato crops, one of them with an irrigation system, the other under rainfed conditions. Accurate NEE partition into GPP and ecosystem respiration (R_{eco}) was carried out by fitting a light response curve. Direct measurements of dry weight and leaf area were performed from sowing to the end of canopy life cycle and tuber bulking. Agricultural drought in the rainfed crop resulted in limited GPP rate, low leaf area index (LAI), and low canopy carbon assimilation response to the photosynthetically active radiation (PAR). Hence, in this crop, there was lower efficiency in tuber biomass gain and NEE sum indicated net carbon emissions to atmosphere (NEE = 154.7 g C m^{-2} ± 30.21). In contrast, the irrigated crop showed higher GPP rate and acted as a carbon sink (NEE = −366.6 g C m^{-2} ± 50.30). Our results show, the environmental and productive benefits of potato crops grown under optimal water supply.

Keywords: Potato crop; Water management; Water deficit; Net ecosystem Carbon exchange; Ecosystem respiration

3.1. Introduction

According to *Agrimonde (Scenarios and Challenges for Feeding the World in 2050)*, the increasing rate of agricultural production will be considerably lower than in previous decades, with an estimate of 1.15% per year for the 2003–2050 period (Paillard et al., 2014b). Hence, more than 9000 million people will have to be fed in 2050 (FAO, 2017); to meet the demand for food in 2050, agriculture will have to produce almost 70% more (Kole, 2020). Potato crops have been increasing their production since 2012, more in the developing world than in developed countries (Ortiz and Mares, 2017). The environmental cost to achieve this purpose could be very high, considering that agriculture is a major contributor to global greenhouse gas (GHG) emissions (Smith et al., 2019). However, agriculture also represents a carbon sink, capturing atmospheric carbon dioxide (CO_2) into the biomass and soil. (Martin-Gorriz et al., 2021b) This is the paradox of agriculture, from the point of view of climate change, which can contribute to both climate change and its mitigation. In terms of mitigation, a key ecosystem process to decrease the atmospheric CO_2 is to remove it from the atmosphere by increasing the vegetation carbon sequestration or uptake (Verma et al., 2005) during photosynthesis, as gross primary productivity (GPP). However, GPP can greatly vary across biomes, as it is strongly influenced by multiple meteorological drivers (Litton and Giardina, 2008). In optimal water availability conditions, the photosynthetic photon flux density (PPFD) is the main factor driving GPP (Rambal et al., 2014). However, under water-limited conditions, Soil Water Content (SWC) deficit leads to a depression of the rate of carbon uptake (Li et al., 2019), hence, reductions in GPP. Under water-limited conditions, an SWC increase could increase GPP, indicating that irrigated agriculture has a potential role as a carbon sink (Rambal et al., 2014). Irrigation systems could slow down the return of stored carbon as CO_2 via respiration and improve the photosynthetic input of carbon (Blom-Zandstra and Verhagen, 2015). However, about 82% of the total agricultural land in the world is under rainfed agricultural systems (Cassman and Wood, 2005), and potato crop fields are no exception. In Colombia (2019), 78% of the total area potato production had no irrigation. These differences in crop water management might imply differences in GPP and CO_2 sink potential that are currently unknown.

Several methods have been used to estimate GPP, using an extrapolating chamber and biometric measurements (Malhi et al., 2009), also canopy process modeling (Wagle et al., 2015). However, the eddy covariance (EC) technique has been recognized as the most efficient method for measuring fluxes of energy, CO_2, other GHG gases, and water between the terrestrial biosphere and the atmosphere, on an ecological scale (Baldocchi, 2003), and at the whole production system level. Previous potato GPP estimations using the EC method in non-tropical conditions have reported high carbon uptake of potatoes and relatively larger magnitudes of GPP than other crop sites (Anthoni et al., 2004b). However, there is a lack of detailed information about carbon balances and key factors that control GPP related to water availability and management. Additionally, the available studies were carried out in non-tropical conditions, which may imply different biophysical and eco-physiological responses of the growing agroecosystems to climate drivers.

Potato is an important agroecosystem for worldwide carbon and GHG balances due to its sizeable cultivated area (more than 19 million hectares) (Centro Internacional de la Papa (CIP), 2017) and its extraordinary adaptive range. In Colombia and the world, potato is the primary source of income of thousands of small-scale producers and the most crucial staple food, playing a significant role in the maintenance of food security and nutritional status (Mosquera Vásquez et al., 2017b).

This study reports CO_2 fluxes and GPP determinations from rainfed and irrigated potato fields in Cundinamarca, Colombia. We hypothesized that the GPP responses are largely determined by the soil water content (SWC) as a direct consequence of irrigation practices. The following questions are addressed in this study: (1) What are the differences in GPP between rainfed and irrigated systems, and how do they impact the NEE? (2) How are the differences in GPP related to differences in crop growth between the two potato production systems?

3.2. Materials and Methods

3.2.1. Site description and crop management

The study was carried out in two sites of the Colombian Andean region, in the western Savanna province of the department of Cundinamarca. The evaluation of the potato rainfed production system (hereinafter Rainfed) was carried out in a 6 hectares (ha) commercial plot (4.87033° N, −74.1294° W; ~2572 m above sea level). The potato irrigated production system (hereinafter Irrigated) was evaluated in a 3.11 ha commercial lot, under a fixed-sprinkler irrigation system (4.888668° N, −74.18668° W; ~2609 m above sea level). Both potato (*Solanum tuberosum* L.) production systems used the Diacol Capiro variety. The sowing date for Rainfed was 1 August 2020, and the sowing date for Irrigated was 22 January 2021. The plant density was 33,333 pl ha^{-1} for both production systems. The two sites are located over a fluvio-lacustrine plain with a flat landscape, an average annual temperature of 12–14 °C, and annual precipitation between the 800–1000 mm bimodally distributed. The June–August and December–February periods have the lowest rainfall, due to the double passage of the Intertropical Convergence Zone (ITCZ). The soil of the two production systems is deep and well-drained, with the presence of volcanic ash corresponding to the Andisol order (Soil Survey Staff, 2014). Potato cultivation can be established at any time of the year due to Colombia's climate offer due to its geographical location. Common practices include sowing vegetative or asexual seeds, foliar and soil fertilization, weed control, hilling (earthing up), insecticide, and fungicide treatment, haulm cutting, chemical dehaulming, and harvesting.

3.2.2. Microclimate and Eddy Covariance (EC) measurements

Net carbon exchange and microclimatic variables were continuously recorded using an Eddy Covariance (EC) tower. In Rainfed, the EC station was installed on 13 August 2020, 12 days post-planting (DPP), while in Irrigated, the EC station was installed on 3 February 2021 (12 DPP). The EC measurements for Rainfed went until the end of the canopy life cycle, 22 November 2020 (113 DPP). The EC measurements for Irrigated went until the end of the canopy life cycle, 9 June 2021 (138 DPP).

The EC tower included an IRGASON with an open-path gas analyzer (EC 150, Campbell Scientific, Inc., Logan, UT, USA) and a 3D sonic anemometer (CSAT3A, Campbell Scientific, Inc., Logan, UT, USA), both are operated by a separated electronic module (EC100, Campbell Scientific, Inc., Logan, UT, USA). Raw data was recorded at a 10 Hz sampling frequency using a high-performance datalogger (CR1000X, Campbell Scientific, Inc., Logan, UT, USA). The tower height for both locations was calculated according to the equation $hEC = Zd + 4\,(hc - Zd)$ (Foken et al., 2012); where, hEC = EC installation height, Zd = zero plane displacement (0.63 m) and hc = average height of the crop (0.9 m). The IRGASON was placed at a 1.7 m height. The IRGASON azimuth was 45° for Rainfed and 175° for Irrigated, corresponding to the prevailing wind directions recorded by the sonic anemometer, three weeks before starting evaluations.

The following sensors were also installed: a Net Radiometer, to measure the incoming and outgoing short-wave and long-wave radiation (Rn), NR-LITE2 (Kipp & Zonen B.V., Delft, The Netherlands) at a height of 2 m, three sensors for the measurement of photosynthetically active radiation (PAR) (CS310, Apogee Instruments, Inc., Logan, UT, USA) positioned at a height of 0.5, 1, and 2.2 m; a pyranometer sensor (CS301, Apogee Instruments, Inc., Logan, UT, USA) at a height of 2 m that measures the total incident radiation; two temperature (Tair) and a relative humidity air sensor (HR) installed at a height of 1 and 2 m, respectively (HygroVUE™ 10, Campbell Scientific, Inc., Logan, UT, USA); two multiparameter smart sensors (CS655, Campbell Scientific, Inc., Logan, UT, USA) installed at a depth of 9 cm and 15 cm to monitor soil volumetric water content (SWC), bulk electrical conductivity, and soil temperature, and four type E thermocouples (TCAV-Averaging Soil Thermocouple Probe, Campbell Scientific, Inc., Logan, UT, USA). Soil heat flux density, G (W m^{-2}), was obtained using the average value between the measurements of two HFP01 sensors (Hukseflux Thermal Sensors B.V., Delftechpark, Delft, The Netherlands), installed 88 cm apart at a depth of 8 cm. Climatic data were recorded every 5 min and averages were integrated on a half-hourly basis. Precipitation data were collected every day using a rain gauge connected to a datalogger (Oregon Scientific, Inc., Tualatin, OR USA) at the height of 2 m.

3.2.3. Biometric measurements

The sampling of plants using sequential harvesting was performed after sowing, during the crop growth, every eleven or twelve days. Ten randomly selected plants were uprooted for growth analysis after 25, 37, 47, 54, 65, 75, 85, 98, 105, and 116 DPP in Rainfed; and 33, 46, 57, 70, 80, 96, 110, 122, 135, and 152 DPP in Irrigated. The total leaf area and fresh weight of each sample were measured. Plant material was placed in paper bags and dried in a forced-air drying oven to constant weight at 70 °C. Total dry weight (DW) and tubers dry weight (TDW) were fitted to the logistic growth model, as follows:

$$DW(t) = \frac{a_1}{1 + b_1 e^{-c_1 t}}\,, TDW(t) = \frac{a_2}{1 + b_2 e^{-c_2 t}} \quad (1)$$

where $a_1,\ b_1,\ c_1$ are the model parameters for DW, a_2, b_2, c_2 are the model parameters for TDW, and t is DPP.

The leaf area index (LAI) and the absolute growth rate (AGR) were calculated as indicated in (Roderick Hunt, 1990). Leaf area duration (LAD) for each growth stage was calculated by integration of individual LAD values obtained, as follows:

$$LAD = \frac{LAI_{i+1} + LAI_i}{2} (t_{i+1} - t_i) \quad (2)$$

3.2.4. Data processing and quality control

Raw data time series were recorded at 10 Hz, as well as corrected fluxes of CO_2. Latent heat and sensible heat were calculated on a half-hourly basis, using the EasyFlux® CRBasic software (Campbell Scientific, Inc., Logan, UT, USA), installed in the CR1000X datalogger. The corrections and procedures applied to the data were despike, filter high-frequency time series data, coordinate rotation using planar fit method (Wilczak et al., 2001), frequency corrections using co-spectra (Moncrieff et al., 1997), correction for air density fluctuations using (Webb et al., 1980), data quality classifications (QC) (Foken et al., 2012), and calculation of footprint characteristics (Kljun et al., 2015; Kormann and Meixner, 2001).

Further postprocessing of fluxes included fetch filter (removing records in which fetch 90 was larger than the upwind distance from the tower to the edge of the area of study), outlier detection and removal was done using the MAD method (Papale et al., 2006b), and a QC filter, where only the records with QC < 6 were kept (Foken et al., 2012).

3.2.5. Gap-filling methods

After applying the data filters, the diurnal gaps accounted for 35% of Rainfed and 54% of Irrigated. The gap-filling for both EC and meteorological data was performed in R (R Core Team, 2021), according to the algorithm described in (Reichstein et al., 2005a), considering the covariation of the fluxes with the meteorological variables and their temporal autocorrelations.

3.2.6. NEE partitioning

Negative values represent fluxes from the atmosphere to the surface, while positive values represent fluxes moving from the surface to the atmosphere. Therefore, the ecosystem respiration (R_{eco}) is defined as a positive value, while the gross primary production (GPP) is defined as a negative value. Nighttime values of NEE are equal to R_{eco} due to the absence of photosynthetic activity at night, while diurnal NEE is the algebraic sum of GPP and R_{eco}. The non-linear Mitscherlich light-response function (Equation (3)) parametrized NEE against the photosynthetically active radiation PAR and was the method used to partition diurnal NEE (Global radiation > 1 W m^{-2}) into R_{eco} and GPP (Falge et al., 2001c; Tagesson et al., 2015b).

$$NEE = -(F_{csat} + R_d) * \left(1 - e^{\left(\frac{-\propto * PAR_{inc}}{F_{csat}+R_d}\right)}\right) + R_d \quad (3)$$

where F_{csat} is the CO_2 uptake at light saturation (μmol CO_2 m^{-2} s^{-1}), R_d is the respiration term, and a is the quantum efficiency (μmol CO_2 μmol^{-1} photons) or the initial slope of the light response curve. At each day, a set of parameters was calculated using non-linear regression on a subset of NEE and PAR_{inc} data within a moving window of 15 days centered on each day. Then, for each diurnal half an hour of the same day, the GPP was estimated by subtracting R_d from the non-linear Mitscherlich light-response function, and R_{eco} was calculated by subtracting the estimated GPP from the measured NEE.

3.2.7. Uncertainty and statistical analysis

The uncertainty associated to random sampling errors and gap-filling procedures was determined using a Monte Carlo simulation with 100 iterations (Richardson and Hollinger, 2007). For each iteration, the starting point was the gap-free dataset in which gaps were randomly inserted in the same proportion as the original data. Random noise was added to the remaining data, simulating random error, which is known to follow a double exponential distribution with parameter $\sigma(\delta)$ depending on the magnitude of NEE (Equation (4)) (Richardson et al., 2006).

$$\sigma(\delta) = \begin{cases} 0.62 + 0.63NEE, NEE > 0 \\ 1.42 - 0.19NEE, NEE < 0 \end{cases} \quad (4)$$

Each of the datasets with synthetic gaps and noise was passed through the gap-filling and NEE partition procedures described above, and sums of gap-filled NEE, GPP, and R_{eco} were calculated. Then, uncertainty for each half-hourly flux was calculated as the confidence interval for the mean of the 100 obtained values. The mean of the 100 sums of each flux was obtained, and cumulative uncertainty was determined as the confidence interval of the sums of NEE, GPP, and R_{eco}, with $\alpha = 0.05$.

3.2.8. Energy balance closure

The plausibility of EC flux data was evaluated through the energy balance closure. Under ideal conditions, according to the first thermodynamics law, the sum of all energy fluxes is zero. Therefore, the energy balance for the studied systems is given by:

$$H + \lambda E = Rn - G - Gs \quad (5)$$

where H is the sensible heat flux, λE is the latent heat flux, both of which were most directly measured using the eddy covariance (EC) technique, G is the soil heat flux at the surface, and Gs is the soil energy storage term. G and Gs were quantified by two heat-flux plates: soil temperature and soil water content sensors installed at a depth of 0–20 cm (Campbell and Norman, 1998b; Chi et al., 2016c). Daily sums of H, λE, G and Gs were calculated, Band a linear regression model was parametrized as follow:

$$H_d + \lambda E_d = \beta_0 + \beta_1(Rn_d - G_d - Gs_d) \quad (6)$$

where *d* subscript indicates daily flux sum, β_0 is the intercept, and β_1 is the slope representing the magnitude of the balance closure.

3.3. Results

3.3.1. Meteorological conditions

Figure 1 shows microclimate behavior for Rainfed and Irrigated. PAR was observed on both sites mainly as diffuse radiation, which was evident because of variations over time. This is typical for the study area, characterized by high cloud cover. The average of daily mean PAR was significantly higher ($p < 0.05$) in Irrigated (724.5 ± 216.7 μmol photons m^{-2} s^{-1}) compared to Rainfed (567.9 ± 230.7 μmol photons m^{-2} s^{-1}). Nevertheless, the average daily mean (Tmean) and the maximum air temperature (Tmax) were higher in Rainfed (Tmean: 16.80 °C ± 0.92, Tmax: 20.32 °C ± 1.29) than in Irrigated (Tmean: 16.51°C ± 1.02, Tmax: 19.73 °C ± 1.23). The average daily maximum vapor pressure deficit (DPV) was higher in Rainfed (0.80 KPa ± 0.24) compared to Irrigated (0.73 KPa ± 0.25), while the average daily mean DPV did not show a significant difference in Rainfed (0.40 KPa ± 0.12) and Irrigated (0.38 KPa ± 0.16).

Low water availability in Rainfed (SWC < WP) was the determinant for solar radiation to be directed more for air heating than evapotranspiration (Campbell and Norman, 1998b). The accumulated precipitation for Rainfed was 229 mm, with a non-uniform time distribution, including events of consecutive dry days and high precipitations, observed by the end of the crop cycle, reaching 98 mm in one week (101 to 107 DPP). The accumulated precipitation for Irrigated (306 mm) was higher and more uniformly distributed, however, a drier lapse occurred, from 13 March to 22 April 2021 (50–90 DPP). The decision to irrigate the crop was made after identifying soil water deficit using a water balance calculated according to FAO-56 (Allen et al., 1998) and monitoring the soil tensiometers installed inside each plot.

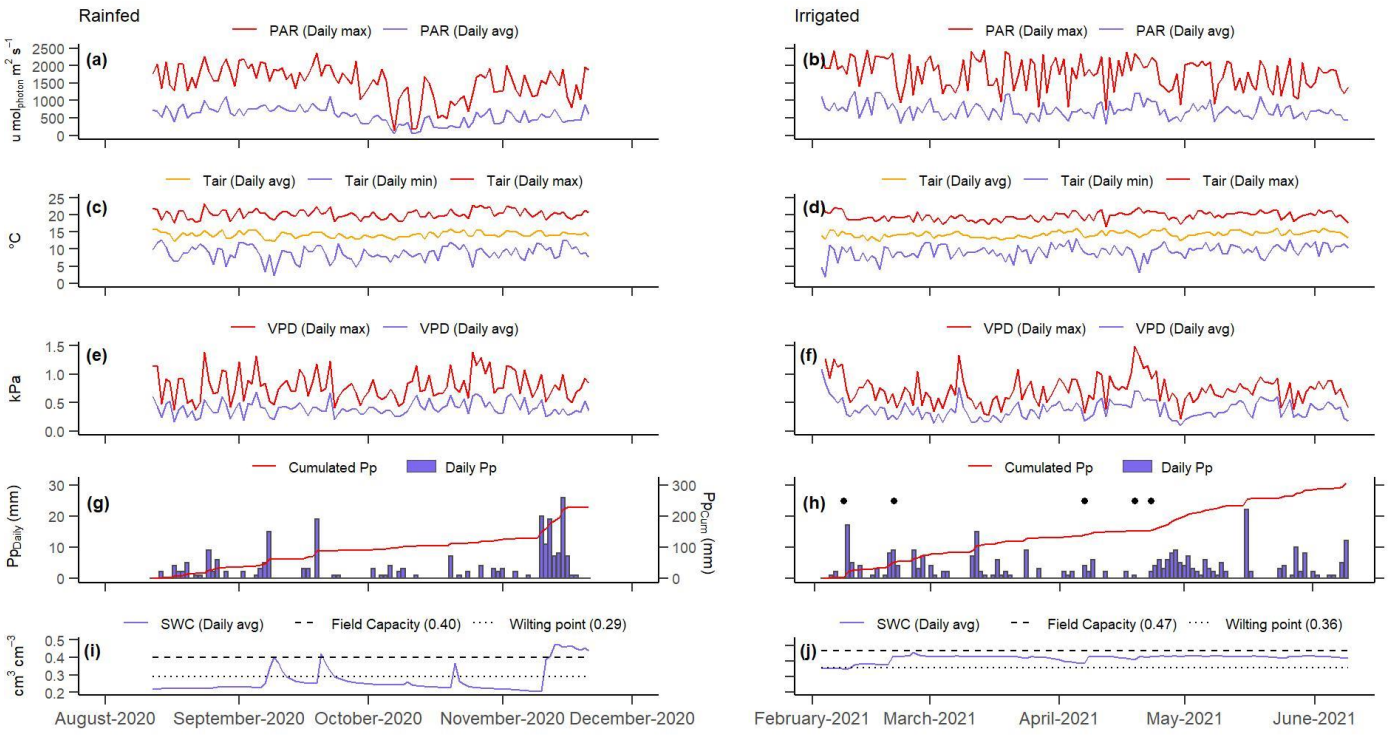

Figure 1. Meteorological measurements for Rainfed (12 August–22 November 2020) and Irrigated (3 February–9 June 2021). (**a**,**b**) photosynthetic active radiation, µmol photons m^{-2} s^{-1} (PAR); (**c**,**d**) air temperature, °C (Tair); (**e**,**f**) vapor pressure deficit, kPa (VPD); (**i**,**j**) soil water content, cm^3 cm^{-3} (SWC), measured at 0–20 cm depth, are shown as daily mean values; (**g**,**h**) daily and cumulated precipitation, mm (Pp), is shown as daily sum, black dots indicate irrigation times.

3.3.2. Energy balance closure and uncertainty

The slope of the regression between the energy fluxes (H + LE) and the available energy (Rn-G-Gs) (Figure 2) indicates an energy balance closure of 0.84 for Rainfed and 0.72 for Irrigated. These values are consistent with several studies made more than two decades ago, which concluded that the range of suitable ratios of the linear regression slope lies between 0.7 and 1 (Callañaupa Gutierrez et al., 2021; Mauder et al., 2020; Wilson et al., 2002). In this study, the imbalance may be mainly attributed to nighttime low turbulence conditions, as has been found in previous studies (Mauder et al., 2020; Wilson et al., 2002).

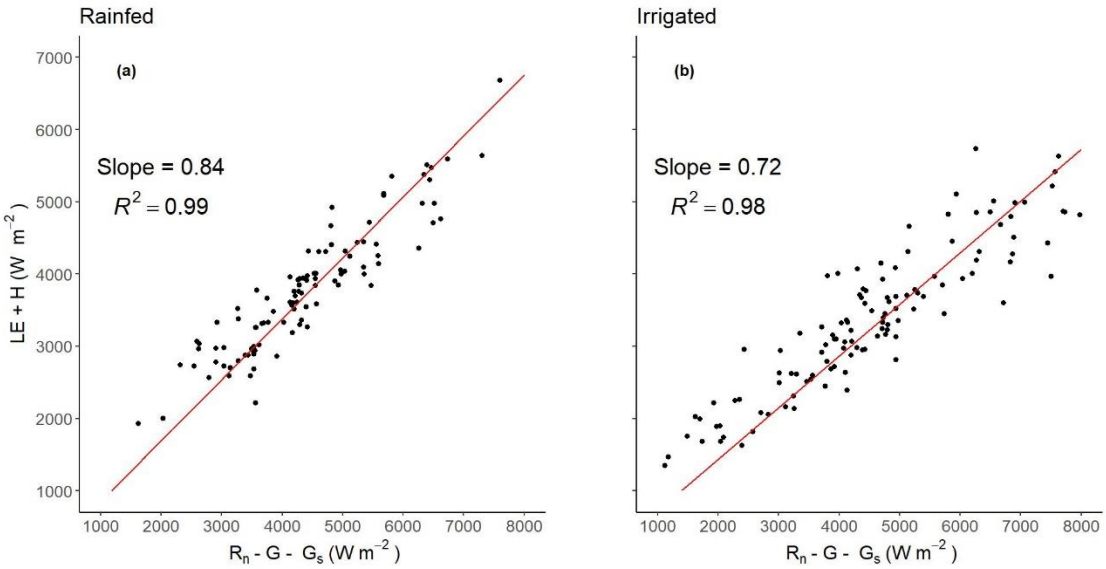

Figure 2. Energy balance closure for (**a**) Rainfed and (**b**) Irrigated sites.

3.3.3. Carbon fluxes, daily averages, maximums, and sums of NEE, GPP, and R_{eco} in the different growth stages for non-irrigated and irrigated crops

Table 1 shows the behavior of fluxes throughout the growth stages. In Rainfed, the sum of NEE from sowing to tuber bulking had a positive value, indicating CO_2 emissions to the atmosphere (154.7 g C m^{-2} ± 30.21). In contrast, Irrigated behaved as a CO_2 sink (sum of NEE = −366.6 g C m^{-2} ± 50.30). In Rainfed, the daily NEE average was negative and close to zero during the tuberization stage (−0.03 g C m^{-2} d^{-1} ±0.29). Irrigated had negative NEE daily means and sums in all stages, except during sprouting, which can be explained by the absence of aerial biomass in potato plants.

Table 1. Mean, maximum, and sum of carbon fluxes throughout growth stages at Rainfed and Irrigated.

[a] Carbon Fluxes		Sprouting		Vegetative		Tuberization		Tuber Bulking	
		Rainfed	Irrigated	Rainfed	Irrigated	Rainfed	Irrigated	Rainfed	Irrigated
NEE	Mean	4.39 (±0.39)	2.92 (±0.30)	1.93 (±0.27)	−1.96 (±0.34)	−0.03 (±0.29)	−5.55 (±0.46)	0.35 (±0.27)	−3.02 (±0.39)
	Max.	4.13 (±0.37)	1.95 (±0.30)	−0.30 (±0.30)	−7.07 (±0.50)	−0.52 (±0.30)	−8.36 (±0.50)	−0.26 (±0.28)	−4.82 (±0.44)
	sum	57.04 (±5.11)	46.7 (±4.80)	88.8 (±12.5)	−76.6 (±13.3)	0.72 (7.80)	−260.9 (±21.82)	5.67 (±4.38)	−75.6 (±9.83)
GPP	Mean	−0.60 (±0.06)	−1.77 (±0.01)	−2.06 (±0.03)	−6.88 (±0.15)	−3.20 (±0.08)	−11.3 (±0.28)	−3.01 (±0.07)	−8.47 (±0.19)
	Max.	−0.80 (±0.05)	−2.61 (±0.02)	−3.46 (±0.09)	−13.4 (±0.34)	−3.87 (±0.11)	−13.8 (±0.37)	−3.57 (±0.09)	−11.16(±0.29)
	sum	−7.82 (±0.75)	−28.28 (±0.09)	−94.8 (±1.19)	−268 (±6.02)	−86.4 (±2.17)	−529.9 (±13.05)	−48.2 (±1.14)	−211.8 (±4.860)
R_{eco}	Mean	4.99 (±0.34)	4.69 (±0.31)	3.99 (±0.25)	4.91 (±0.19)	3.23 (±0.21)	5.72 (±0.19)	3.37 (±0.20)	5.45 (±0.20)
	Max.	5.26 (±0.38)	5.06 (±0.36)	4.97 (±0.31)	6.29(±0.16)	4.26 (±0.19)	7.75(±0.16)	3.80 (±0.18)	7.38 (±0.18)
	sum	64.9 (±4.36)	75.04 (±4.89)	184 (±11.3)	191.5 (±7.33)	87.1 (±5.63)	268.9 (±8.77)	53.9 (±3.24)	136.2 (±4.96)

[a] Carbon flux unit for mean, maximum, and sum are g C m^{-2} d^{-1}, g C m^{-2} d^{-1}, and g C m^{-2}, respectively for NEE, GPP, and R_{eco}. Negative values indicate carbon fixation by the crop from the atmosphere and positive emissions by the ecosystem.

In general, the highest values for each flux were found during the tuberization stage on both crops. Nevertheless, in Rainfed, the highest R_{eco} was observed during the vegetative stage. GPP in Irrigated (−1043.6 g C m^{-2} d^{-1} ± 23.96) was 4.37 times higher than in Rainfed (−239.9 g C m^{-2} d^{-1} ± 5.33), and R_{eco} was 1.71 times higher in Irrigated than in Rainfed, due to the larger amount of respiration contributed by the higher aerial biomass in Irrigated.

3.3.4. Dynamics of daily and accumulated Gross Primary Production—GPP

Daily and accumulated GPP were greater in Irrigated compared to Rainfed throughout the crop growth. In Irrigated, the maximum GPP accumulation rate (MGAR) (11.92 Kg C ha^{-1} d^{-1}) occurred at 88 DPP, when the accumulated GPP was 551.38 Kg C ha^{-1}. In Rainfed, the MGAR was 3.29 Kg C ha^{-1} d^{-1}, at 90 DPP, when the accumulated GPP was 166.45 Kg C ha^{-1}. After reaching the MGAR until the end of the canopy life cycle, the accumulated GPP was also higher in Irrigated (492.2 Kg C ha^{-1}) than in Rainfed (73.45 Kg C ha^{-1}), which indicates that there was a generalized depletion of the GPP under no irrigation conditions (Figure 3).

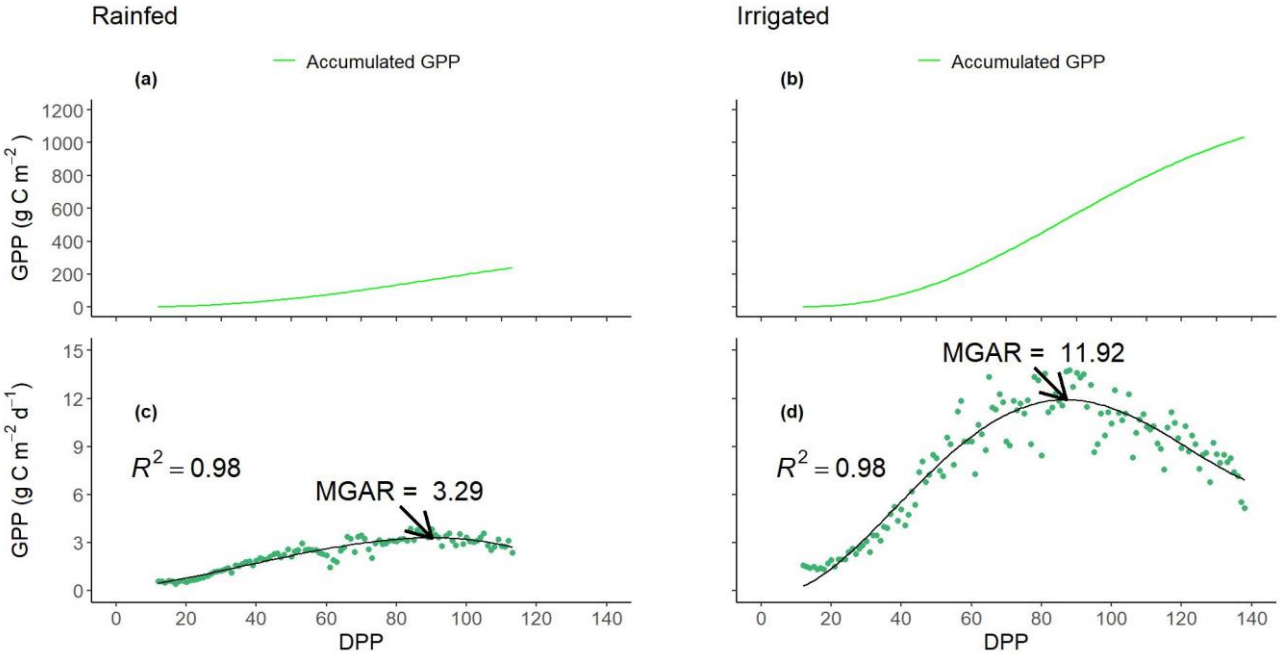

Figure 3. Accumulated and daily gross primary productivity (GPP) in (**a**) Rainfed and (**b**) Irrigated, and maximum GPP accumulation rate (MGAR) in (**c**) Rainfed, and (**d**) Irrigated potato crop. The black arrow indicates the point of MAGR (maximum GPP accumulation rate).

Variations of the half-hourly GPP mean throughout the day and across growth stages were observed on each evaluation site. In Irrigated, there were higher carbon fixing rates through the day (half-hourly GPPs) for all growth stages. Tuberization stage rates increased progressively along the day, reaching a maximum of 1.30 ± 0.19 mg CO_2 m^{-2} s^{-1} between 9 and 13 h. In vegetative and tuber bulking stages, half-hourly GPP maximums (0.83 ± 0.37 mg CO_2 m^{-2} s^{-1} y 0.96 ± 0.18 mg CO_2 m^{-2} s^{-1}, respectively) were also found between 9 and 13 h, however, they were not significatively different ($p > 0.05$). In Rainfed, half-hourly GPPs were lower in the sprouting and vegetative

stages compared to the tuberization and tuber bulking stages. At each growth stage, GPP values between 9 and 16 h were constant and did not exceed 0.35 mg CO_2 m^{-2} s^{-1} (Figure 4). Figure 5 shows the behavior of GPP as a response to the incident PAR. In Irrigated, the incident PAR and growth stages influenced half-hourly GPPs, while in Rainfed, there was no evidence of difference among growth stages. PAR Saturation was defined as the PAR value in GPP that reaches 95% of asymptote. In Irrigated, PAR saturation values were 1494 μmol photons m^{-2} s^{-1}, 1439 μmol photons m^{-2} s^{-1}, 1454 μmol photons m^{-2} s^{-1}, and 1543 μmol photons m^{-2} s^{-1}. GPPs at PAR saturation were 0.21 mg CO_2 m^{-2} s^{-1}, 0.88 mg CO_2 m^{-2} s^{-1}, 1.41 mg CO_2 m^{-2} s^{-1}, and 1.09 mg CO_2 m^{-2} s^{-1} for sprouting, vegetative, tuberization, and tuber bulking stages, respectively. In Rainfed, light saturation occurred at lower values (1522 μmol photons m^{-2} s^{-1}, 354 μmol photons m^{-2} s^{-1}, 225 μmol photons m^{-2} s^{-1}, and 576 μmol photons mm^{-2} s^{-1} for sprouting, vegetative, tuberization and tuber bulking, respectively), and GPPs at PAR saturation did not exceed 0.34 mg CO_2 mm^{-2} s^{-1} in any growth stage.

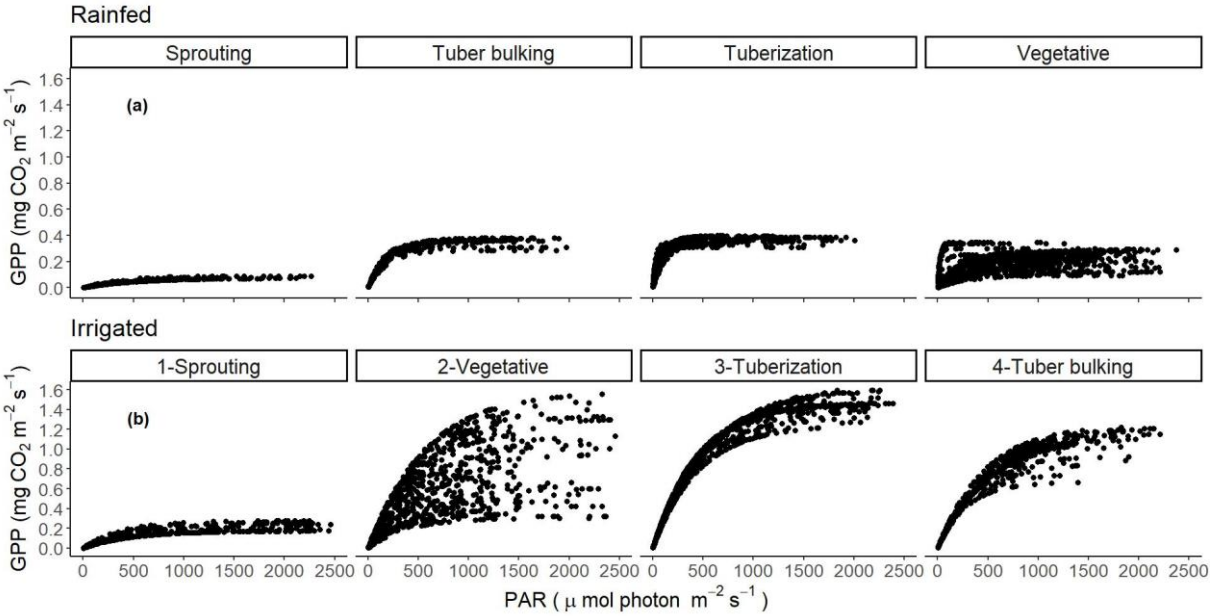

Figure 4. Half-hourly variation of gross primary production (GPP) of (**a**) Rainfed and (**b**) Irrigated potato crop in four different growth stages (sprouting, vegetative, tuberization, tuber bulking). Half-hourly averages are plotted. Vertical bars indicate the standard deviation.

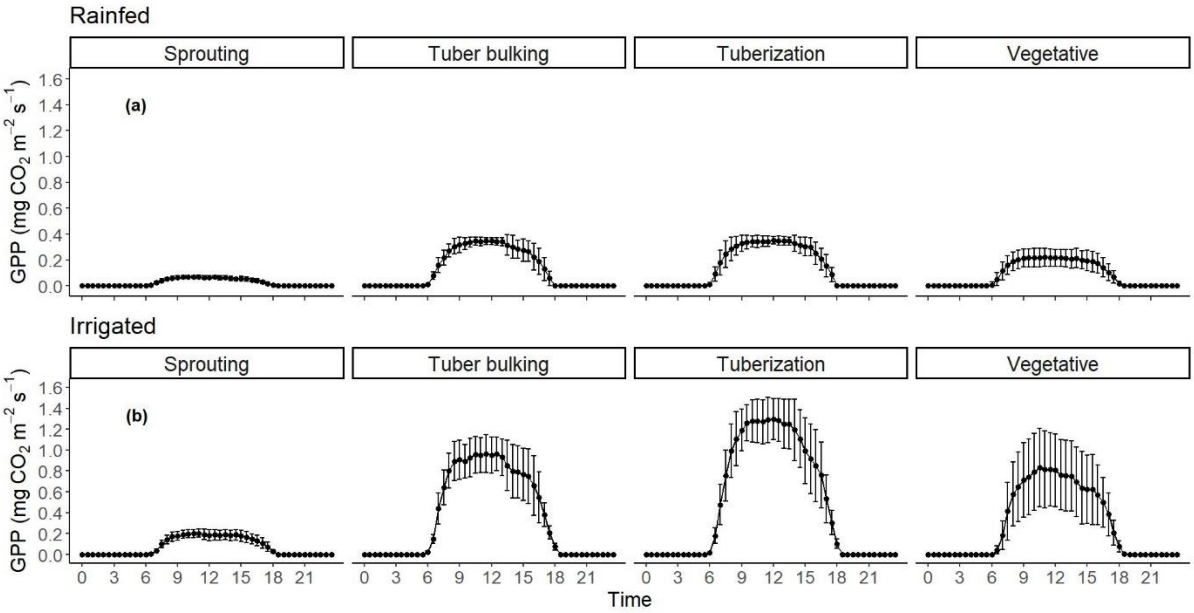

Figure 5. Half-hourly gross primary production (GPP) Versus incident PAR in four different growth stages (sprouting, vegetative, tuberization, tuber bulking) in (**a**) Rainfed and (**b**) Irrigated potato crop.

3.3.5. GPP and growth relationships

The LAI showed a phase of accelerated increase from sprouting to around 80 DDP, when the LAI maximums were reached. The maximum LAI in Irrigated (4.7) was 23.9% higher than in Rainfed (3.5). In Irrigated, the daily GPP had the same trend as LAI, increasing up to 115 kg C ha^{-1} d^{-1}, when the LAI reached its maximum, then decreased to values around 70 kg C ha^{-1} d^{-1} by the end of tuber bulking stage. In Rainfed, the daily GPPs had lower values compared to Rainfed, therefore, the daily GPP did not show the same trend as the LAI. On the day when the LAI was maximum, the daily GPP showed a maximum value of 38.7 kg C ha^{-1} d^{-1} (Figure 6).

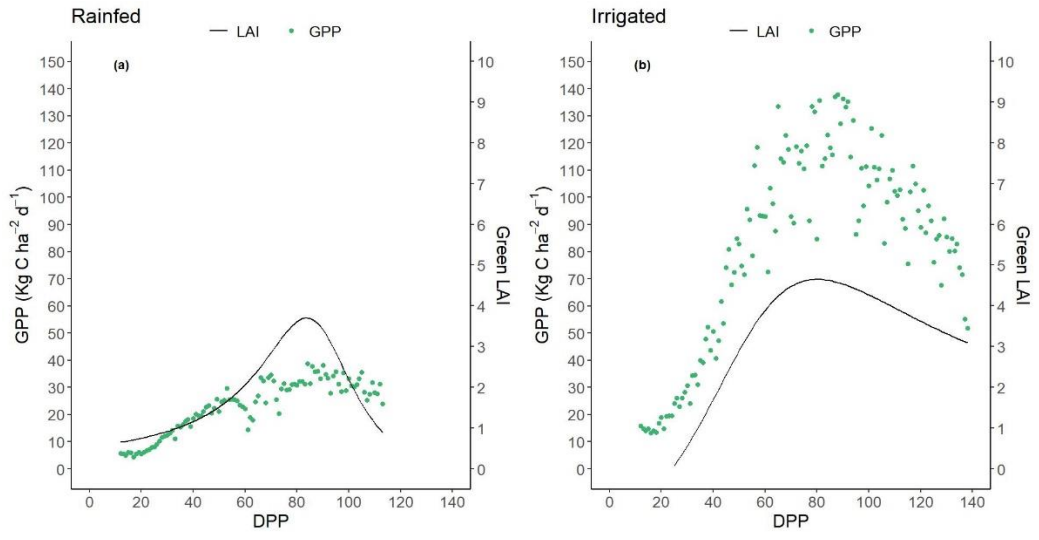

Figure 6. Gross primary productivity (GPP) and leaf area index (LAI) versus days post planting (DPP) in (**a**) Rainfed and (**b**) Irrigated potato crop.

In Irrigated, the plants reached an averaged maximum DW and TDW of 1103 g and 1004 g, respectively. AGR increased progressively until 114 DPP (when the crop reached 82% of the canopy life cycle) with a maximum of 20.95 g d^{-1}. From 115 to 138 DPP, the daily dry biomass accumulation rate decreased progressively until a minimum value of 0.05 g d^{-1}. In Rainfed, DW and TDW values were lower than in Irrigated. Averaged maximum DW and TDW were 256.8 g and 186.8 g, respectively. Maximum AGR (5.25 g d^{-1}) was observed 72 DPP, when the crop reached 64% of the canopy life cycle. From 73 DPP to 113 DPP (the end of the canopy life cycle), AGR dropped to 1.94 g d^{-1} (Figure 7).

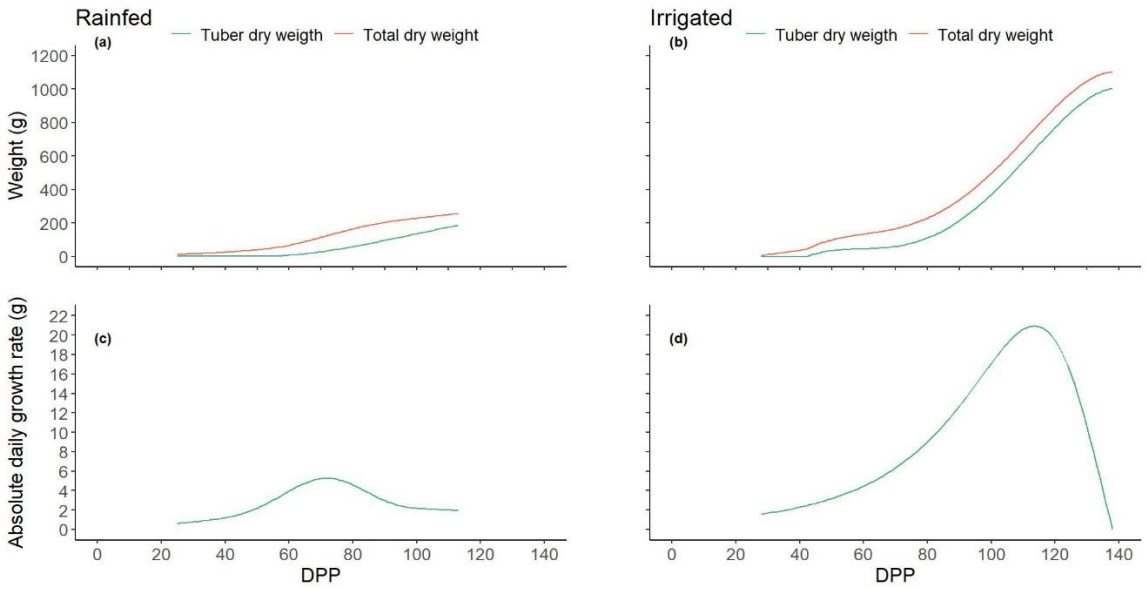

Figure 7. Dry weight (DW) and tuber dry weight (TDW) in (**a**) Rainfed and (**b**) Irrigated; absolute growth rate (AGR) in (**c**) Rainfed and (**d**) Irrigated.

Higher leaf area durations (LAD) were observed in Irrigated, compared to Rainfed. In Irrigated, LAD was 1.3, 1.5, and 3 times LAD in Rainfed for vegetative, tuberization, and tuber bulking stages, respectively (Table 2).

Table 2. Leaf area duration days in Rainfed and Irrigated, classified by growth stage.

Growth Stage	Rainfed (Days)	Irrigated (Days)
Vegetative	67.95	89.11
Tuberization	78.73	117.03
Tuber Bulking	29.25	85.52

3.4. Discussion

Water management practices are an important factor for GPP gain or loss in productive systems, particularly in crops grown under rainfed conditions, where there are inherent limitations related to drought-induced GPP losses (Chen et al., 2021). Our results show that GPP in Irrigated was 337.5% higher than in Rainfed (with a difference of 803.7 g C m^{-2}), and the sum of NEE was negative (sink) in Irrigated and positive (source) in Rainfed, which evidences the influence of soil water conditions on carbon dynamics (Fu et al., 2020; Şaylan et al., 2011). In Irrigated, the SWC was kept close to field capacity, while in Rainfed, the SWC was, most of the time, below the easily

available water and even below the wilting point. The conditions described for Rainfed are related to agricultural drought (Labedzki and Bąk, 2014), which is compatible with a higher VPD max, a higher T mean, and a higher T max than in Irrigated.

In general, half-hourly GPPs were intricately linked to the carbon demand in each of the growth stages, reaching maximums of daily sums of GPP in the tuberization stage, around 90 DPP for both, Irrigated and Rainfed. For each of the growth stages, averaged half-hourly GPPs were significantly greater compared to Rainfed ($p < 0.05$), which agrees with drought-induced GPP losses reported in potato crops by (Aubinet et al., 2009b; Ruidisch et al., 2015) and in other species (Berninger, 1997; Chen et al., 2021; Ciais et al., 2005b; Doughty et al., 2018; Dufranne et al., 2011; Fu et al., 2020; Geruo et al., 2017; Stocker et al., 2019; Van der Molen et al., 2011; Xie et al., 2020).

Half-hourly GPP variation throughout the day is associated with incident PAR (Aubinet et al., 2009b; Emmel et al., 2020; Gitelson and Gamon, 2015; Zhao and Lüers, 2012); such variation has also been reported for potatoes (Quan, 2021; Zhao and Lüers, 2012). In this study, an asymptotic exponential curve of GPP Vs. PAR was fitted on each growth stage, which shows that carbon flux at PAR saturation (95% of asymptote) was greater in Irrigated than in Rainfed ($p < 0.05$), with PAR values around 1450 μmol m^{-2} s^{-1} in Irrigated and 250 μmol m^{-2} s^{-1} in Rainfed.

The mean PAR in Irrigated was higher throughout the crop growth than in the rainfed site. However, although there is a lower PAR in rainfed, this condition does not affect the response of the GPP, due to saturation of the photosynthesis transduction phase occurring at low PAR values. This results in a restricted carbon fixing, which may be attributed to the fact that in a highly water-restricted scenario, non-stomatal restrictions depend on the severity of the water stress (Kamanga et al., 2018a), which are related to reduced mesophyll conductance, and photochemical and enzymatic constraints (Varone et al., 2012b). At this point, the injury of the photosynthetic apparatus, destruction of chlorophyll components, disorganization of chloroplast's ultrastructure and enzyme inactivation, and photo-inhibition (Li et al., 2007a; Mafakheri et al., 2010a) cause a permanent decline in carbon assimilation (Kamanga et al., 2018a; Li et al., 2007a). These non-stomatal limitations were also reported for potato crops in (Beauclaire et al., 2021) at the Lonzée Terrestrial Observatory.

Variations in GPP with respect to LAI were evident along growth stages related to LAI evolution and canopy formation. The highest GPP data dispersion was observed in the vegetative stage, when there was a progressive canopy growth, with the presence of leaves of different ages, and therefore, with differences in light use efficiency. Conversely, in the tuberization stage, when the maximum LAI is reached, the canopy is homogeneous and fully formed, which reflects in the lower data dispersion.

Several authors have reported LAI as one of the main causes of daily GPP variation (Duursma et al., 2009; Ramezani et al., 2020; Wang et al., 2019). In Irrigated, daily GPP dynamics showed the same trend as LAI, evidencing that there exists an efficient feedback regulation mechanism between GPP and LAI, where carbon fluxes are mainly destined to GPP, which guarantees canopy growth and expansion. The canopy, in turn, is highly functional to photosynthetic processes increasing GPP since, in addition to a larger leaf area, the leaves do not show irreversible limitations for carbon assimilation, have a high response to PAR, and greater duration of the leaf area. Conversely, In Rainfed, there was no correspondence between GPP and LAI trends. In this case, the available leaf area is less efficient for photosynthesis, the crop shows early senescence, and is barely functional for GPP growth. In this sense, reference (Aubinet et al., 2009b) reported that reductions in daily GPP evolution during crop growth may be related to leaf senescence and reduced LAI.

LAI functionality and its relationship with GPP can be observed in the growth analysis carried out in both study sites. In Irrigated, synergistic growth of LAI and GPP allowed higher efficiency for DW and TDW gain. Before reaching the maximum LAI (tuberization stage, 81 DPP), all the plant organs are in active growth, so there are higher carbon requirements and a higher available leaf area to fix it. After the maximum LAI, carbon allocation favors tuber bulking over other organs. In Rainfed, GPP and LAI limitations resulted in lower DW and TDW, resulting in less time for active growth, cell division, and expansion. Early decrease of AGR and canopy senescence indicate low carbon demand and fewer organs (stems and leaves) acting as reservoirs, which contribute to the lack of synergy between daily GPP and LAI.

3.5. Conclusions

Reliable results regarding carbon fluxes in two potato crop sites under intertropical conditions in Colombia were obtained using the Eddy Covariance method. The crops, under very different soil water content, were evaluated from sowing to tuber bulking. Gross primary productivity was closely linked to water availability for plants. In irrigated potato, GPP was 337.5% greater than in rainfed potato, with low precipitations, which results in big differences in the net carbon ecosystem exchange (NEE) by the end of each crop cycle. The Irrigated crop acted as an atmospheric carbon sink (NEE = -366.6 g C $m^{-2} \pm 50.30$), while the rainfed crop behaved as a source (NEE = 154.7 g C $m^{-2} \pm 30.21$), which is related to the differences in PAR at light saturation in rainfed (225 μmol m^{-2} s^{-1}) and in irrigated at the tuberization stage (1450 μmol m^{-2} s^{-1}). Consequently, in the rainfed crop, there was a low carbon destination to the structures and organs forming the plants, resulting in a reduction of the total dry matter and tuber yield. Our results show the environmental and productive benefits of potato crops grown under optimal water supply, becoming a fundamental basis to further studies evaluating the effects of other crop practices on carbon dioxide emissions.

References

Allen, R.G., Pereira, L.S., Raes, D., Smith, M., 1998. FAO Irrigation and Drainage Paper No. 56 - Crop Evapotranspiration. https://doi.org/D05109

Anthoni, P.M., Knohl, A., Rebmann, C., Freibauer, A., Mund, M., Ziegler, W., Kolle, O., Schulze, E.D., 2004. Forest and agricultural land-use-dependent CO_2 exchange in Thuringia, Germany. Glob Chang Biol 10, 2005–2019. https://doi.org/10.1111/j.1365-2486.2004.00863.x

Aubinet, M., Moureaux, C., Bodson, B., Dufranne, D., Heinesch, B., Suleau, M., Vancutsem, F., Vilret, A., 2009. Carbon sequestration by a crop over a 4-year sugar beet/winter wheat/seed potato/winter wheat rotation cycle. Agric For Meteorol 149, 407–418. https://doi.org/10.1016/j.agrformet.2008.09.003

Baldocchi, D.D., 2003. Assessing the eddy covariance technique for evaluating carbon dioxide exchange rates of ecosystems: past, present and future. Glob Chang Biol 9, 479–492. https://doi.org/10.1046/j.1365-2486.2003.00629.x

Beauclaire, Q., Gourlez, L., Motte, D., Bernard, H., Bernard, L., 2021. Proofs of non-stomatal limitations of potato photosynthesis during drought by using in-situ eddy covariance data. https://doi.org/10.5194/egusphere-egu2020-5183

Berninger, F., 1997. Effects of drought and phenology on GPP in Pinus sylvestris: A simulation study along a geographical gradient. Funct Ecol 11, 33–42. https://doi.org/10.1046/j.1365-2435.1997.00051.x

Blom-Zandstra, G., Verhagen, J., 2015. Potato production systems in different agro ecological regions and their relation with climate change. Wageningen Research Report 614 614, 32.

Callañaupa Gutierrez, S., Segura Cajachagua, H., Saavedra Huanca, M., Flores Rojas, J., Silva Vidal, Y., Cuxart, J., 2021. Seasonal variability of daily evapotranspiration and energy fluxes in the Central Andes of Peru using eddy covariance techniques and empirical methods. 1. Callañaupa Gutierrez, S.; Segura Cajachagua, H.; Saavedra Huanca, M.; Flores Rojas, J.; Silva Vidal, Y.; Cuxart, J. Seasonal variability of daily evapotranspiration and energy fluxes in the Central Andes of Peru using eddy covariance techniques and emp 261. https://doi.org/10.1016/j.atmosres.2021.105760

Campbell, G.S., Norman, J.M., 1998. An Introduction to Environmental Biophysics, Second. ed, Journal of Environment Quality. Springer, Pullman, WA. https://doi.org/10.2134/jeq1977.00472425000600040036x

Cassman, K.G., Wood, S., 2005. Chapter 26 Cultivated Systems, in: Millennium Ecosystem Assessment: Global Ecosystem Assessment Report on Conditions and Trends. World Research Institute, Washington DC, EE.UU, pp. 741–789.

Centro Internacional de la Papa (CIP), 2017. Hechos y cifras sobre la papa.

Chen, S., Huang, Y., Wang, G., 2021. Detecting drought-induced GPP spatiotemporal variabilities with sun-induced chlorophyll fluorescence during the 2009/2010 droughts in China. Ecol Indic 121, 107092. https://doi.org/10.1016/j.ecolind.2020.107092

Chi, J., Waldo, S., Pressley, S., O'Keeffe, P., Huggins, D., Stöckle, C., Pan, W.L., Brooks, E., Lamb, B., 2016. Assessing carbon and water dynamics of no-till and conventional tillage cropping systems in the inland Pacific Northwest US using the eddy covariance method. Agric For Meteorol 218–219, 37–49. https://doi.org/10.1016/j.agrformet.2015.11.019

Ciais, P., Reichstein, M., Viovy, N., Granier, A., Ogée, J., Allard, V., Aubinet, M., Buchmann, N., Bernhofer, C., Carrara, A., Chevallier, F., De Noblet, N., Friend, A.D., Friedlingstein, P., Grünwald, T., Heinesch, B., Keronen, P., Knohl, A., Krinner, G., Loustau, D., Manca, G., Matteucci, G., Miglietta, F., Ourcival, J.M., Papale, D., Pilegaard, K., Rambal, S., Seufert, G., Soussana, J.F., Sanz, M.J., Schulze, E.D., Vesala, T., Valentini, R., 2005. Europe-wide reduction in primary productivity caused by the heat and drought in 2003. Nature 437, 529–533. https://doi.org/10.1038/nature03972

Doughty, R., Xiao, X., Wu, X., Zhang, Y., Bajgain, R., Zhou, Y., Qin, Y., Zou, Z., McCarthy, H., Friedman, J., Wagle, P., Basara, J., Steiner, J., 2018. Responses of gross primary production of grasslands and croplands under drought, pluvial, and irrigation conditions during 2010–2016, Oklahoma, USA. Agric Water Manag 204, 47–59. https://doi.org/10.1016/j.agwat.2018.04.001

Dufranne, D., Moureaux, C., Vancutsem, F., Bodson, B., Aubinet, M., 2011. Comparison of carbon fluxes, growth and productivity of a winter wheat crop in three contrasting growing seasons. Agric Ecosyst Environ 141, 133–142. https://doi.org/10.1016/j.agee.2011.02.023

Duursma, R.A., Kolari, P., Permki, M., Pulkkinen, M., Mkel, A., Nikinmaa, E., Hari, P., Aurela, M., Berbigier, P., Bernhofer, C., Grnwald, T., Loustau, D., Mlder, M., Verbeeck, H., Vesala, T., 2009. Contributions of climate, leaf area index and leaf physiology to variation in gross primary production of six coniferous forests across Europe: A model-based analysis. Tree Physiol 29, 621–639. https://doi.org/10.1093/treephys/tpp010

Emmel, C., D'Odorico, P., Revill, A., Hörtnagl, L., Ammann, C., Buchmann, N., Eugster, W., 2020. Canopy photosynthesis of six major arable crops is enhanced under diffuse light due to canopy architecture. Glob Chang Biol 26, 5164–5177. https://doi.org/10.1111/gcb.15226

Falge, E., Baldocchi, D., Olson, R., Anthoni, P., Aubinet, M., Bernhofer, C., Burba, G., Ceulemans, R., Clement, R., Dolman, H., Granier, A., Gross, P., Keronen, P., Kowalski, A., Ta Lai, C., Law, B.E., Meyers, T., Moncrieff, J., Moors, E., Munger, W., Pilegaard, K., Rannik, Ü., Rebmann, C., Suyker, A., Tenhunen, J., Tu, K., Verma, S., Vesala, T., Wilson, K., Wofsy, S., 2001. Gap filling stratergies for defansible annual sums of net ecosystem exchange. Agric For Meteorol 107, 43–69. https://doi.org/10.1016/S0168-1923(00)00225-2

FAO, 2017. The future of food and agriculture Trends and challenges. FAO - Food and Agriculture Organization of the United Nations, (ed)., Roma, Italy.

Foken, T., Leuning, R., Oncley, S.R., Mauder, M., Aubinet, M., 2012. Corrections and Data Quality Control, in: A Practical Guide to Measurement and Data Analysis. Springer ScienceCBusiness Media B.V. 2012, Bayreuth, Germany, pp. 85–131. https://doi.org/10.1007/978-94-007-2351-1

Fu, Z., Ciais, P., Bastos, A., Stoy, P.C., Yang, H., Green, J.K., Wang, B., Yu, K., Huang, Y., Knohl, A., Šigut, L., Gharun, M., Cuntz, M., Arriga, N., Roland, M., Peichl, M., Migliavacca, M., Cremonese, E., Varlagin, A., Brümmer, C., Gourlez De La Motte, L., Fares, S., Buchmann, N., El-Madany, T.S., Pitacco, A., Vendrame, N., Li, Z., Vincke, C., Magliulo, E., Koebsch, F., 2020. Sensitivity of gross primary productivity to climatic drivers during the summer drought of 2018 in Europe: Sensitivity of GPP to climate drivers. Philosophical Transactions of the Royal Society B: Biological Sciences 375. https://doi.org/10.1098/rstb.2019.0747

Geruo, A., Velicogna, I., Kimball, J.S., Du, J., Kim, Y., Colliander, A., Njoku, E., 2017. Satellite-observed changes in vegetation sensitivities to surface soil moisture and total water storage variations since the 2011 Texas drought. Environmental Research Letters 12. https://doi.org/10.1088/1748-9326/aa6965

Gitelson, A.A., Gamon, J.A., 2015. The need for a common basis for defining light-use efficiency: Implications for productivity estimation. Remote Sens Environ 156, 196–201. https://doi.org/10.1016/j.rse.2014.09.017

Hunt, R., 1990. BASIC GROWTH ANALYSIS. Academic Division of Unwin Hyman Ltd, London, England. https://doi.org/DOl: 10.1007/978-94-010-9117-6

Kamanga, R.M., Mbega, E., Ndakidemi, P., 2018. Drought Tolerance Mechanisms in Plants: Physiological Responses Associated with Water Deficit Stress in Solanum lycopersicum. Advances in Crop Science and Technology 06, 1–8. https://doi.org/10.4172/2329-8863.1000362

Kljun, N., Calanca, P., Rotach, M.W., Schmid, H.P., 2015. A simple two-dimensional parameterisation for Flux Footprint Prediction (FFP). Geosci Model Dev 8, 3695–3713. https://doi.org/10.5194/gmd-8-3695-2015

Kole, C., 2020. Genomic designing of climate-smart cereal crops, Genomic Designing of Climate-Smart Cereal Crops. Springer Nature Switzerland AG 2020, New Delhi, India. https://doi.org/10.1007/978-3-319-97415-6

Kormann, R., Meixner, F.X., 2001. An analytical footprint model for non-neutral stratification. Boundary Layer Meteorol 99, 207–224. https://doi.org/DOI:10.1023/A:1018991015119

Labedzki, L., Bąk, B., 2014. Meteorological and agricultural drought indices used in drought monitoring in Poland: a review. Meteorology Hydrology and Water Management 2, 13.

Li, W., Zhang, S., Shan, L., 2007. Responsibility of non-stomatal limitations for the reduction of photosynthesis-response of photosynthesis and antioxidant enzyme characteristics in alfalfa (Medicago sativa L.) seedlings to water stress and rehydration. Front Agric China 1, 255–264. https://doi.org/10.1007/s11703-007-0044-5

Li, X., Ramírez, D.A., Qin, J., Dormatey, R., Bi, Z., Sun, C., Wang, H., Bai, J., 2019. Water restriction scenarios and their effects on traits in potato with different degrees of drought tolerance. Sci Hortic 256. https://doi.org/10.1016/j.scienta.2019.05.052

Litton, C.M., Giardina, C.P., 2008. Below-ground carbon flux and partitioning: Global patterns and response to temperature. Funct Ecol 22, 941–954. https://doi.org/10.1111/j.1365-2435.2008.01479.x

Mafakheri, A., Siosemardeh, A., Bahramnejad, B., Struik, P.C., Sohrabi, E., 2010. Effect of drought stress on yield, proline and chlorophyll contents in three chickpea cultivars. Aust J Crop Sci 4, 580–585.

Malhi, Y., Aragão, L.E.O.C., Metcalfe, D.B., Paiva, R., Quesada, C.A., Almeida, S., Anderson, L., Brando, P., Chambers, J.Q., da Costa, A.C.L., Hutyra, L.R., Oliveira, P., Patiño, S., Pyle, E.H., Robertson, A.L., Teixeira, L.M., 2009. Comprehensive assessment of carbon productivity, allocation and storage in three Amazonian forests. Glob Chang Biol 15, 1255–1274. https://doi.org/10.1111/j.1365-2486.2008.01780.x

Martin-Gorriz, B., Martínez-Alvarez, V., Maestre-Valero, J.F., Gallego-Elvira, B., 2021. Influence of the Water Source on the Carbon Footprint of Irrigated Agriculture: A Regional Study in South-Eastern Spain. Agronomy 11, 351. https://doi.org/10.3390/agronomy11020351

Mauder, M., Foken, T., Cuxart, J., 2020. Surface-Energy-Balance Closure over Land: A Review, Boundary-Layer Meteorology. Springer Netherlands, Garmisch- Partenkirchen, Germany. https://doi.org/10.1007/s10546-020-00529-6

Moncrieff, J.B., Massheder, J.M., De Bruin, H., Elbers, J., Friborg, T., Heusinkveld, B., Kabat, P., Scott, S., Soegaard, H., Verhoef, A., 1997. A system to measure surface fluxes of momentum, sensible heat, water vapour and carbon dioxide. J Hydrol (Amst) 188–189, 589–611. https://doi.org/10.1016/S0022-1694(96)03194-0

Mosquera Vásquez, T., Del Castillo, S., Gálvez, D.C., Rodríguez, L.E., 2017. Breeding Differently: Participatory Selection and Scaling Up Innovations in Colombia. Potato Res 60, 361–381. https://doi.org/10.1007/s11540-018-9389-9

Ortiz, O., Mares, V., 2017. The Historical, Social, and Economic Importance of the Potato Crop. Compendium of Plant Genomes 1–10. https://doi.org/10.1007/978-3-319-66135-3_1

Paillard, S., Treyer, S., Dorin, B., 2014. Agrimonde – Scenarios and Challenges for Feeding the World in 2050, First. ed. Springer Netherlands, Dordrecht. https://doi.org/10.1007/978-94-017-8745-1

Papale, D., Reichstein, M., Aubinet, M., Canfora, E., Bernhofer, C., Kutsch, W., Longdoz, B., Rambal, S., Valentini, R., Vesala, T., Yakir, D., 2006. Towards a standardized processing of Net Ecosystem Exchange measured with eddy covariance technique: Algorithms and uncertainty estimation. Biogeosciences 3, 571–583. https://doi.org/10.5194/bg-3-571-2006

Quan, N., 2021. Greenhouse gas exchange above potato and pea fields in the lower fraser valley in British Columbia, Canada. THE UNIVERSITY OF BRITISH COLUMBIA.

R Core Team, 2021. R: A language and environment for statistical computing. URL http://www.R-project.org/.

Rambal, S., Lempereur, M., Limousin, J.M., 2014. How drought severity constrains GPP and its partitioning among carbon pools in a <i>Quercus ilex</i> coppice? Biogeosciences Discussions 11, 8673–8711. https://doi.org/10.5194/bgd-11-8673-2014

Ramezani, M.R., Massah Bavani, A.R., Jafari, M., Binesh, A., Peters, S., 2020. Investigating the leaf area index changes in response to climate change (case study: Kasilian catchment, Iran). SN Appl Sci 2, 1–11. https://doi.org/10.1007/s42452-020-2290-6

Reichstein, M., Falge, E., Baldocchi, D., Papale, D., Aubinet, M., Berbigier, P., Bernhofer, C., Buchmann, N., Gilmanov, T., Granier, A., 2005. On the separation of net ecosystem exchange into assimilation and ecosystem respiration : review and improved algorithm. Glob Chang Biol 11, 1424–1439. https://doi.org/10.1111/j.1365-2486.2005.001002.x

Richardson, A.D., Hollinger, D.Y., 2007. A method to estimate the additional uncertainty in gap-filled NEE resulting from long gaps in the CO 2 flux record. Agric For Meteorol 147, 199–208. https://doi.org/10.1016/j.agrformet.2007.06.004

Richardson, A.D., Hollinger, D.Y., Burba, G.G., Davis, K.J., Flanagan, L.B., Katul, G.G., Munger, J.W., Ricciuto, D.M., Stoy, P.C., Suyker, A.E., Verma, S.B., Wofsy, S.C., 2006. A multi-site analysis of random error in tower-based measurements of carbon and energy fluxes. Agric For Meteorol 136, 1–18. https://doi.org/10.1016/j.agrformet.2006.01.007

Ruidisch, M., Nguyen, T.T., Li, Y.L., Geyer, R., Tenhunen, J., 2015. Estimation of annual spatial variations in forest production and crop yields at landscape scale in temperate climate regions. Ecol Res 30, 279–292. https://doi.org/10.1007/s11284-014-1208-4

Şaylan, L., Kimura, R., Munkhtsetseg, E., Kamichika, M., 2011. Seasonal variation of carbon dioxide fluxes over irrigated soybean (Glycine max L.). Theor Appl Climatol. https://doi.org/10.1007/s00704-011-0470-4

Smith, L.G., Kirk, G.J.D., Jones, P.J., Williams, A.G., 2019. The greenhouse gas impacts of converting food production in England and Wales to organic methods. Nat Commun 10, 1–10. https://doi.org/10.1038/s41467-019-12622-7

Soil Survey Staff, 2014. Keys to Soil Taxonomy, 12th ed, Book. USDA-Natural Resources Conservation Service, Washington DC, EE.UU.

Stocker, B.D., Zscheischler, J., Keenan, T.F., Prentice, I.C., Seneviratne, S.I., Peñuelas, J., 2019. Drought impacts on terrestrial primary production underestimated by satellite monitoring. Nat Geosci 12, 264–270. https://doi.org/10.1038/s41561-019-0318-6

Tagesson, T., Fensholt, R., Cropley, F., Guiro, I., Horion, S., Ehammer, A., Ardo, J., 2015. Dynamics in carbon exchange fluxes for a grazed semi-arid savanna ecosystem in West Africa. Agric Ecosyst Environ 205, 15–24. https://doi.org/10.1016/j.agee.2015.02.017

Van der Molen, M.K., Dolman, A.J., Ciais, P., Eglin, T., Gobron, N., Law, B.E., Meir, P., Peters, W., Phillips, O.L., Reichstein, M., Chen, T., Dekker, S.C., Doubková, M., Friedl, M.A., Jung, M., van den Hurk, B.J.J.M., de Jeu, R.A.M., Kruijt, B., Ohta, T., Rebel, K.T., Plummer, S., Seneviratne, S.I., Sitch, S., Teuling, A.J., van der Werf, G.R., Wang, G., 2011. Drought and ecosystem carbon cycling. Agric For Meteorol 151, 765–773. https://doi.org/10.1016/j.agrformet.2011.01.018

Varone, L., Ribas-Carbo, M., Cardona, C., Gallé, A., Medrano, H., Gratani, L., Flexas, J., 2012. Stomatal and non-stomatal limitations to photosynthesis in seedlings and saplings of Mediterranean species pre-conditioned and aged in nurseries: Different response to water stress. Environ Exp Bot 75, 235–247. https://doi.org/10.1016/j.envexpbot.2011.07.007

Verma, S.B., Dobermann, A., Cassman, K.G., Walters, D.T., Knops, J.M., Arkebauer, T.J., Suyker, A.E., Burba, G.G., Amos, B., Yang, H., Ginting, D., Hubbard, K.G., Gitelson, A.A., Walter-Shea, E.A., 2005. Annual carbon dioxide exchange in irrigated and rainfed maize-based agroecosystems. Agric For Meteorol 131, 77–96. https://doi.org/10.1016/j.agrformet.2005.05.003

Wagle, P., Xiao, X., Suyker, A.E., 2015. Estimation and analysis of gross primary production of soybean under various management practices and drought conditions. ISPRS Journal of Photogrammetry and Remote Sensing 99, 70–83. https://doi.org/10.1016/j.isprsjprs.2014.10.009

Wang, J., Xiao, X., Bajgain, R., Starks, P., Steiner, J., Doughty, R.B., Chang, Q., 2019. Estimating leaf area index and aboveground biomass of grazing pastures using Sentinel-1, Sentinel-2 and Landsat images. ISPRS Journal of Photogrammetry and Remote Sensing 154, 189–201. https://doi.org/10.1016/j.isprsjprs.2019.06.007

Webb, E.K., Pearman, G.I., Leuning, R., 1980. Correction of flux measurements for density effects due to heat and water vapour transfer. Quarterly Journal of the Royal Meteorological Society. https://doi.org/10.1002/qj.49710644707

Wilczak, J.M., Oncley, S.P., Stage, S.A., 2001. Sonic anemometer tilt correction algorithms 127–150.

Wilson, K., Goldstein, A., Falge, E., Aubinet, M., Baldocchi, D., Berbigier, P., Bernhofer, C., Ceulemans, R., Dolman, H., Field, C., Grelle, A., Ibrom, A., Law, B.E., Kowalski, A., Meyers, T., Moncrieff, J., Monson, R., Oechel, W., Tenhunen, J., Valentini, R., Verma, S., 2002. Energy balance closure at FLUXNET sites. Agric For Meteorol 113, 223–243. https://doi.org/10.1016/S0168-1923(02)00109-0

Xie, X., Li, A., Tan, J., Jin, H., Nan, X., Zhang, Z., Bian, J., Lei, G., 2020. Assessments of gross primary productivity estimations with satellite data-driven models using eddy covariance observation sites over the northern hemisphere. Agric For Meteorol 280, 107771. https://doi.org/10.1016/j.agrformet.2019.107771

Zhao, Lüers, 2012. Improved determination of daytime net ecosystem exchange of carbon dioxide at croplands. Biogeosciences Discussions 9, 2883–2919. https://doi.org/10.5194/bgd-9-2883-2012

4. UPSCALING GROSS PRIMARY PRODUCTION FROM LEAF TO CANOPY FOR POTATO CROP (*Solanum tuberosum* L.)

Abstract

Estimating gross primary production (GPP) is important to understand the land–atmosphere CO_2 exchange for major agroecosystems. Eddy covariance (EC) measurements provide accurate and reliable information about GPP, but flux measurements are often not available. Upscaling strategies gain importance as an alternative to the limitations of the use of the EC. Although the potato provides an important agroecosystem for worldwide carbon balance, there are currently no studies on potato GPP upscaling processes. This study reports two GPP scaling-up approaches from the detailed leaf-level characterization of gas exchange of potatoes. Multilayer and big leaf approaches were applied for extrapolating chamber and biometric measurements from leaf to canopy. Measurements of leaf area index and photosynthesis were performed from planting to the end of the canopy life cycle using an LP-80 ceptometer and an IRGA Li-Cor 6800, respectively. The results were compared to concurrent measurements of surface–atmosphere GPP from the EC measurements. Big-leaf models were able to simulate the general trend of GPP during the growth cycle, but they overestimated the GPP during the maximum LAI phase. Multilayer models correctly reproduced the behavior of potato GPP and closely predicted both: the daily magnitude and half-hourly variation in GPP when compared to EC measurements. Upscaling is a reliable alternative, but a good treatment of LAI and the photosynthetic light-response curves are decisive factors to achieve better GPP estimates. The results improved the knowledge of the biophysical control in the carbon fluxes of the potato crop.

Keywords: carbon flux; gross primary productivity; upscaling; eddy covariance method

4.1. Introduction

Gross primary production (GPP) is a key ecosystem process that decreases the atmospheric carbon dioxide (CO_2) concentration (Arkebauer et al., 2009b; Suyker et al., 2005; Teubner et al., 2019) CO_2 flux information (Arkebauer et al., 2009b) is necessary to improve the knowledge of the potential of ecosystems to grow and mitigate climate change (Wagle et al., 2017, 2015). Although eddy covariance (EC) measurements provide accurate and reliable information about carbon and energy balances at the ecosystem level, flux measurements are often not available in many places (Jiang et al., 2014). Therefore, different methodologies are needed to estimate GPP based on extrapolations of chamber and biometric measurements and the canopy upscaling process using readily measurable meteorological and environmental variables (Malhi et al., 2009; Martínez-Maldonado et al., 2021c; Wagle et al., 2015).

Upscaling the GPP from leaf to canopy is challenging because of the large micro-environment [light, temperature, vapor pressure deficit (VPD)] variability within plant canopies at both the vertical and horizontal dimensions (Eamus et al., 2016c; Ran et al., 2017). A common strategy to represent carbon uptake during gross primary production (GPP) is through photosynthetic light use efficiency models based on photosynthetic light-response curves and light distribution through the canopy (Arkebauer et al., 2009b; Goudriaan, 1986; Hoyaux et al., 2008; Monsi et al., 2005; Moureaux et al., 2008; Raulier et al., 1999; Waldo et al., 2016), assuming that light is the primary driver of vertical variation in photosynthesis (Bonan et al., 2021). Nevertheless, canopy estimates require additional features such as light distribution through the canopy, canopy structure (mean leaf angle and leaf area index), and vertical profiles of weather variables within and above the crop (Eamus et al., 2016c, 2016d).

Scaling methods vary with different complexity from the simplest one-big leaf (Chen and Dudhia, 2001; Jarvis, 1995; Lloyd et al., 1995; Luo et al., 2018; Pleim and Xiu, 1995), to two-big leaf models (De Pury and Farquhar, 1997; Luo et al., 2018; Wang and Leuning, 1998) and multilayer models (Chen et al., 2020; Kobayashi et al., 2012; Liu et al., 2020; Meyers and Hollinger, 2004; Ran et al., 2017). The big leaf model is a representation of a canopy as a

single giant leaf (Eamus et al., 2016d), which can be parameterized under a tractable mathematical solution at the canopy level (Raulier et al., 1999). In most plant species, the photosynthetic system is bulked in the upper layer of the canopy, and light decreases faster in horizontal canopies than in vertical ones (Monsi et al., 2005). Since the leaves in the potato canopy have a horizontal tendency (Campbell, 1990; Campbell and Norman, 1998b), an approach that treats vegetation as a big leaf where the canopy GPP predictions are proportional to the photosynthesis of topmost unshaded leaves (Raulier et al., 1999) could be useful. However, since the canopy is arbitrarily represented by a single leaf, it treats sunlit and shaded leaves within the canopy equally. In other words, the model assumes that there is no uncertainty introduced by ignoring the shaded fraction of the canopy, which results in an overestimation of flux rates (De Pury and Farquhar, 1997; Luo et al., 2018; Raulier et al., 1999; Wang and Leuning, 1998).

In the multilayer model, the canopy is divided into *n* layers and light intensity declines with depth into the canopy as a function of the leaf area index (Bonan, 2015; Eamus et al., 2016d). Consequently, canopy photosynthesis is calculated separately for each layer. In general, multilayer models consider variations in the light level within the canopy, leaf inclination, and other leaf aspects as well as the variation of air temperature, wind speed, humidity, and CO_2 concentration (Eamus et al., 2016d; Hoyaux et al., 2008; Luo et al., 2018). The model calculates the net photosynthetic rate (An) for each layer, using the absorptance and the respective layer's leaf area (Arkebauer et al., 2009b; Eamus et al., 2016d; Luo et al., 2018; Norman et al., 1991).

Several researchers have attempted to evaluate the performance of different upscaling schemes with flux measurements (for wheat, shrublands, broadleaf, Amazonian, and conifer forests) (Arkebauer et al., 2009b; Medlyn et al., 2003; Mercado et al., 2006; Sprintsin et al., 2012), and have shown that the big-leaf approach matches overestimate or underestimate EC measurements (Hoyaux et al., 2008; Moureaux et al., 2008; Sprintsin et al., 2012). Other studies have demonstrated the improved accuracy of multilayer models for GPP calculations (Hoyaux et al., 2008; Moureaux et al., 2008; Sprintsin et al., 2012). Potatoes are critical for the food security of people across South America, Africa, and Asia, feeding more than one billion people worldwide (Jennings et al., 2020c; Quiroz et al., 2018b). It is the 4th most important crop in terms of global production (Velez Betancourt, 2020), since more than 19 million hectares are cultivated around the world, making potatoes an important agroecosystem for worldwide carbon and greenhouse gas (GHG) balances (Campos and Ortiz, 2019; Mosquera Vásquez et al., 2017b; Velez Betancourt, 2020). However, despite the importance of potatoes, there are currently no studies on potato GPP upscaling processes as an alternative to the limitations inherent to EC techniques to obtain GPP contributions to the net ecosystem exchange.

This study aimed to test big-leaf and multilayer upscaling strategies for potato canopy GPP estimation. Our scaling proposal is based on the light profile within the canopy and photosynthetic light-response curves (An–I curves). The analytical solution uses models of photosynthesis such as the nonrectangular hyperbola and exponential model to describe light-driven photosynthesis in conjunction with Beer's law for the canopy light profile. The scaled-up estimates of canopy GPP were compared to concurrent measurements of surface–atmosphere GPP from the EC technique. To our knowledge, this study is the first to investigate upscaling strategies for potato canopy GPP estimation using EC data. This upscaling proposal might provide a useful and validated alternative to the EC technique and could be extrapolated to other potato cultivars to obtain canopy GPP estimations from infra-red gas analyzer (IRGA) measurements.

Specifically, the study reports the performance of two GPP scaling-up modeling approaches from the detailed leaf-level characterization of the gas exchange of potatoes. We addressed the following specific questions in

our study: (1) what are the differences in the upscaled GPP between the two approximations? (2) why do these differences occur? (3) which model is the closest to the GPP obtained from the EC data?

4.2. Materials and Methods

4.2.1. Site description

This study was conducted in the Colombian Andean Region, Western Savanna Province of the department of Cundinamarca. The potato (*Solanum tuberosum* L. Diacol Capiro Cultivar) cropping system was planted in a 3.11 hectare (ha) commercial plot, under a fixed-sprinkler irrigation system, located in the municipality of Subachoque (4.888668 N, −74.18668 W; ~2609 m asl). The crop was sown on 22 January 2021, with a plant density of 33333 pl ha^{-1}. The site was located over a fluvio-lacustrine plain with a flat landscape, with an average annual temperature ranging from 12 to 14 °C and an annual precipitation from 800 to 1000 mm with a bimodal distribution. The June–August and December–February periods have the lowest rainfall (Martínez-Maldonado et al., 2021c) due to the double passage of the Intertropical Convergence Zone (ITCZ). The soils are deep and well drained with the presence of volcanic ash and correspond to the Andisol order (Soil Survey Staff, 2014).

4.2.2. Microclimate and Eddy Covariance (EC) measurements

Net carbon exchange and microclimatic variables were continuously recorded using the EC technique. The equipment was installed on 3 February 2021 (12 days post planting, DPP), and the measurements were taken until the end of the canopy life cycle on 9 June 2021 (138 DPP). The EC tower included an IRGASON with an open-path gas analyzer (EC 150, Campbell Scientific, Inc., Logan, UT, USA) and a 3D sonic anemometer (CSAT3A, Campbell Scientific, Inc., Logan, UT, USA). Both are operated by a separate electronic module (EC100, Campbell Scientific, Inc., Logan, UT, USA). The EC tower and additional sensor configuration are described by (Martínez-Maldonado et al., 2021c).

4.2.3. NEE partitioning

The non-linear Mitscherlich light-response function, which parametrizes the net ecosystem exchange (NEE) against the photosynthetic photon flux density (PPFD), was used to partition diurnal NEE (solar global radiation > 1 W m^{-2}) into ecosystem respiration (R_{eco}) and GPP (Falge et al., 2001b; Tagesson et al., 2015c) as follows:

$$NEE = -\left(A_{gmax} + R_d\right) * \left(1 - \exp^{\left(\frac{-\phi * I_{inc}}{A_{gmax} + R_d}\right)}\right) + R_d \quad (1)$$

where Ag_{max} is the CO_2 uptake at light saturation [μ_{mol} (CO_2) m^{-2} s^{-1}]; R_d is the respiration term [μ_{mol} (CO_2) m^{-2} s^{-1}]; and ϕ is the quantum yield efficiency [μ_{mol} (CO_2) μ_{mol} (photon) $^{-1}$], i.e., the initial slope of the photosynthetic light-response curve, and I_{inc} is the incident PPFD [μ_{mol} (photon) m^{-2} s^{-1}].

For each day, a set of parameters was calculated through non-linear regression, using a subset of NEE and PPFD data within a centered moving window of 14 days. For each diurnal half-hour of the same day, GPP was estimated by subtracting R_d from the non-linear Mitscherlich light-response function. R_{eco} was calculated by subtracting the modeled GPP from the measured NEE. Data postprocessing, quality control, gap-filling, energy balance closure, uncertainty, and statistical analysis methods were applied, following the procedures described in (Martínez-Maldonado et al., 2021c).

4.2.4. Leaf-level measurements

At the leaf scale, we used an infrared gas analyzer IRGA LICOR 6800 IRGA system (LI-COR Biosciences, Lincoln, Nebraska, USA) to measure 1) the net photosynthetic rate at leaf scale (A_n) [μ_{mol} (CO_2) m^{-2} s^{-1}] as a function of PPFD, ranging from 50 to 2000 μ_{mol} (photon) m^{-2} s^{-1} (An–I curves); and 2) An–I curves were recorded in three strata of the plant canopy: the upper stratum (topmost unshaded leaves), the middle stratum, and the low stratum (bottommost shaded leaves). Measurements were taken at 28, 36, 41, 52, 66, 71, 77, 91, 105, 117, and 130 days post planting (DPP) between 9:00 and 11:00 am in three plants. On the same days, the accumulated leaf area index (LAI) was also determined for each layer of the plant canopy in 15 randomly selected plants using an ACCUPAR LP-80 ceptometer (METER Group, Inc., Pullman, WA, USA) with an external Apogee SQ110 PPFD sensor from 0 to 4000 μmol (photon) m^{-2} s^{-1} and 80 probe PPFD sensors at the measurement bar. LAI data for the three canopy layers (upper, middle, and low) were fitted to third-degree and fourth-degree polynomial regressions.

Leaf insertion angles were determined using a compass and protractor, marking the leaf inclination angle. Subsequently, an analysis of the distribution of foliar angles was carried out according to (Campbell, 1990; Wang and Jarvis, 1988) to determine the mean density angle (MDA) and the value of the ratio of the horizontal to vertical axis of the ellipsoid or parameter *x* using the following equation:

$$x = 1.7433025 + \left(\frac{162.22048}{MDA}\right) \quad (2)$$

The extinction coefficient (K) between 8:00 and 17:30 h was estimated from the ellipsoidal equation (Campbell, 1990) that relates the variation of K with the vertical and horizontal projections of the canopy elements (parameter *x*) and the zenith angle ψ:

$$K = \frac{\sqrt{x^2 + tan^2\,\psi}}{x + 1.774\,(x + 1.182)^{-0.733}} \quad (3)$$

4.2.5. Upscaling approaches

The upscaled canopy GPP was based on light-use-efficiency models. The photosynthetic light-response curves (An–I curves) were fitted to three different and well described mathematical models like rectangular hyperbola-based models: (1) Michaelis–Menten as in Baly and Smith (Baly, 1935),(Smith, 1936); (2) hyperbolic tangent-based models (Jassby and Platt, 1976); and (3) exponential-based models (Webb et al., 1974). The

mathematical models that better fit the An–I curve data obtained in the field measurements were determined via sum of squared residuals (SSR) comparison (Lobo et al., 2013). Models with the lowest SSR were found in Baly (Baly, 1935), Smith (Smith, 1936) and Webb (Webb et al., 1974), and they have basically the following structure:

$$A_n = \frac{\Phi * I * A_{gmax}}{\Phi * I + A_{gmax}} - R_d \quad (4)$$

Michaelis–Menten function (Baly) (Baly, 1935)

$$A_n = \frac{\Phi * I * A_{gmax}}{\sqrt{\Phi_{(Io)}^2 * I^2 + A_{gmax}^2}} - R_d \quad (5)$$

Michaelis–Menten type function (Smith) (Smith, 1936)

$$A_n = \left\{ A_{gmax} \left[1 - \exp\left(\frac{\Phi * I}{A_{gmax}} \right) \right] \right\} - R_d \quad (6)$$

Exponential type function (Webb) (Webb et al., 1974)

where A_n is the net photosynthetic rate [μ_{mol} (CO_2) m^{-2} s^{-1}]; A_{gmax} is the light-saturated gross photosynthetic rate [μ_{mol} (CO_2) m^{-2} s^{-1}]; R_d is the dark respiration rate [μ_{mol}(CO_2) m^{-2} s^{-1}]; I is the photosynthetic photon flux density PPFD [μ_{mol} (photon) m^{-2} s^{-1}] and Φ is the quantum yield of assimilation [μ_{mol} (CO_2) μ_{mol} (photon) $^{-1}$]. The light-saturated gross photosynthetic rate (A_{gmax}) and quantum yield of assimilation (Φ) data obtained from the light-use-efficiency models and for each canopy stratum (upper, middle, and low) were fitted to third-degree and fourth-degree polynomial regressions to describe their behavior during canopy growth over time.

4.2.6. Modeling schemes for Gross Primary Production of the Canopy (GPP_{can})

Big-Leaf Approach (BL)

The gross primary production of the canopy (GPP_{can}) was integrated over the canopy using a rectangular hyperbola base function (Michaelis–Menten type model), where light intensities within a canopy were calculated using a negative exponential function with a canopy light extinction coefficient (k) (Bonan, 2019, 2015; Eamus et al., 2016c). The total net carbon uptake integrated over the canopy is:

$$GPP_{can} = \frac{A_{gmax}}{K} ln \frac{\Phi * K * I + A_{gmax}}{(\Phi * I * K * e^{-KLAI}) + A_{gmax}} \quad (7)$$

where GPP_{can} is the gross primary production of the canopy [μ_{mol} (CO_2) m^{-2} s^{-1}]; A_{gmax} is the light-saturated gross photosynthetic rate [μ_{mol} (CO_2) m^{-2} s^{-1}] of the topmost unshaded leaves; I is the photosynthetic photon flux density PPFD [μ_{mol} (photon) m^{-2} s^{-1}]; K is the extinction coefficient; and Φ is the quantum yield of assimilation [μ_{mol}(CO_2) μ_{mol} (photon)$^{-1}$]. The values of the asymptotic estimate of the maximum gross photosynthetic rate (A_{gmax}) [μ_{mol} (CO_2) m^{-2} s^{-1}] and the quantum yield Φ [μ_{mol} (CO_2) μ_{mol} (photon) $^{-1}$] were obtained from the fitted rectangular hyperbola-based models Baly (Baly, 1935) and Smith (Smith, 1936) (Figure 1).

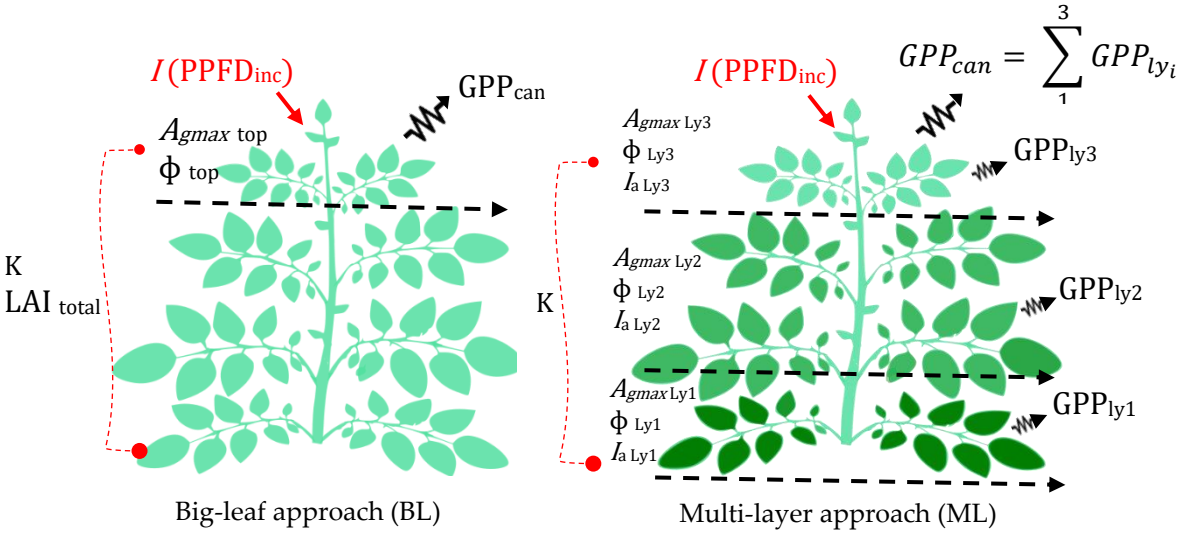

Figure 1. Schematic descriptions of the GPP_{can} upscaling models Big-leaf (BL) and Multilayer (ML).

Multilayer Approach (ML)

In this approach, the value of GPP_{can} was estimated from an extrapolation scheme based on Michaelis–Menten (rectangular hyperbola-based model) of Smith [51] and exponential Mitscherlich (Webb) (Webb et al., 1974) applied to three different layers of the canopy.

The canopy was divided in three layers, upper stratum (topmost unshaded leaves), middle stratum, and low stratum (bottommost shaded leaves), each one with defined LAI values. The leaf area index for each layer was obtained by the difference in leaf area index at the two heights bounding the layers. Thus, $LAI_i = LAI'_i - LAI'_{i-1}$, where LAI'_i is the LAI- ACCUPAR LP-80 measurement beneath the i_{th} layer. For n layers, $LAI'_n \equiv LAI$.

The leaf gross assimilation (Gi) was computed for each layer by introducing the description of the incident and absorbed PPFD in each layer in the Michaelis–Menten (Smith) (Smith, 1936) and Mitscherlich (Webb) (Webb et al., 1974) functions:

$$G_{i\,Smith} = \frac{\Phi_i * I_{ai} * A_{gmax_i}}{\sqrt{\Phi_i{}^2 * I_{ai}{}^2 + A_{gmax_i}{}^2)}} \quad (8)$$

$$G_{i\,Webb} = \left\{A_{gmax_i}\left[1 - \exp\left(\frac{\Phi_i * I_{ai}}{A_{gmax_i}}\right)\right]\right\} \quad (9)$$

where G_i is leaf gross assimilation; A_{gmax} is light-saturated gross photosynthetic rate [$\mu_{mol}(CO_2)$ m^{-2} s^{-1}] for the layer *i*; Φ is the quantum yield of assimilation for the layer *i* [$\mu_{mol}(CO_2)$ μ_{mol} (photon)$^{-1}$]. A_{gmax} and Φ are parameters estimated from the mathematical models Michaelis–Menten (Smith) (Smith, 1936) and Mitscherlich (Webb) (Webb et al., 1974). I_{ai} is the absorbed PPFD [μ_{mol} (photon) m^{-2} s^{-1}] for each layer, computed using Beer's law and the approach by Monsi et al. (Monsi et al., 2005)and Sellers et al. (Sellers et al., 1992):

$$I_{ai} = I * (1 - e^{-K\,LAI_i}) \quad (10)$$

where LAI_i is the leaf area index for each layer; *I* is the incident PPFD [μ_{mol} (photon) m^{-2} s^{-1}] above the canopy (measured every 30 min by the EC station) for the top layer, or the transmitted PPFD irradiance (I_{ti}) from cumulated leaf area index (LAI_c) of the layers above the layer *i* estimated by:

$$I_{ti} = I * e^{-KLAIc} \quad (11)$$

The gross primary production for each canopy layer (GPP_{ly}) was computed every 30 min by multiplying G_i by the canopy scaling factor, as shown in Equation (13) (Bonan, 2019, 2015)

$$GPP_{ly_i} = G_i * \left\{\frac{1 - e^{-KLAIi}}{K}\right\} \quad (12)$$

Then, the gross primary production of the entire canopy (GPP_{can}) was estimated by summing the contribution of each layer (Figure 1):

$$GPP_{can} = \sum_{1}^{3} GPP_{ly_i} \quad (13)$$

4.2.7. Accuracy assessment

The model's goodness of fit was evaluated using RMSE. Complementary accuracy assessment was made through the variation of regression data around the 1:1 line.

4.3. Results

4.3.1. Meteorological conditions

The daily mean PPFD was 724.5 ± 216.7μ_{mol} (photon) m^{-2} s^{-1}. The average daily mean temperature (Tmean) and the maximum air temperature (Tmax) were 16.51 °C ± 1.02 and 19.73 °C ± 1.23, respectively. The average daily maximum vapor pressure deficit (VPD) was 0.73 kPa ± 0.25 and the average irrigated daily mean VPD was 0.38 kPa ± 0.16. The accumulated rainfall was 306 mm, uniformly distributed, but including the relatively drier period from 13 March to 22 April 2021 (50–90 DPP). The soil water content (SWC) was near to field capacity in almost all the crop growth cycles (Figure 2).

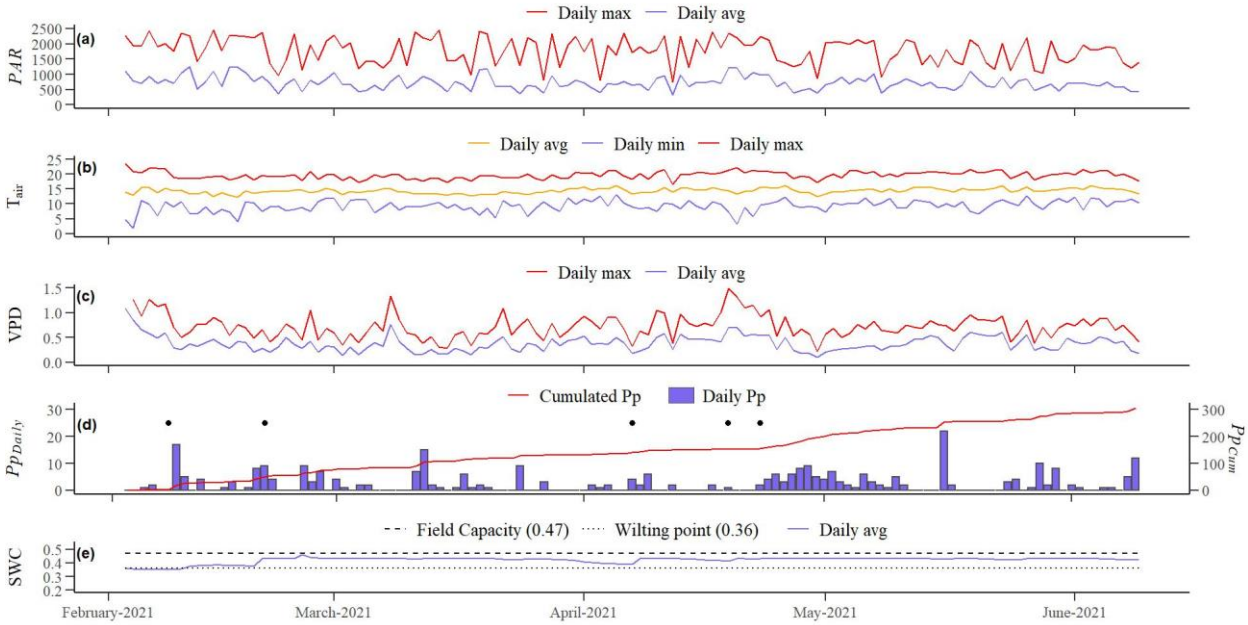

Figure 2. Meteorological variables observed along the experiment (from 3 February to 9 June 2021). (**a**) average and maximum daily photosynthetic active radiation (PPFD, μ_{mol} (photon) m^{-2} s^{-1}); (**b**) average, maximum, and minimum air temperature (Tair, °C); (**c**) average and maximum daily vapor pressure deficit (VPD, kPa); (**d**) daily and cumulated precipitation (Pp, mm), shown as daily sum, black dots indicate irrigation times; (**e**) soil water content, (SWC, cm^3 cm^{-3}), measured at 0–20 cm depth, shown as daily mean values.

4.3.2. Leaf Area Index (LAI) evolution

LAI is defined as the sum of the photosynthetically active leaf surfaces divided by the soil surface occupied by canopy and is the basic variable for relating the radiation intercepted by the canopy to the total incident radiation. The total LAI increased in an accelerated way, from the initial phase of crop growth to around 80 DPP, when the LAI peak reached 4.65. The accumulated LAI in the middle stratum had the same trend, increasing up to a maximum of 3.43 at 73 DPP. The LAI measured in the upper stratum remained around unity throughout the entire growth period of the crop (Figure 3)

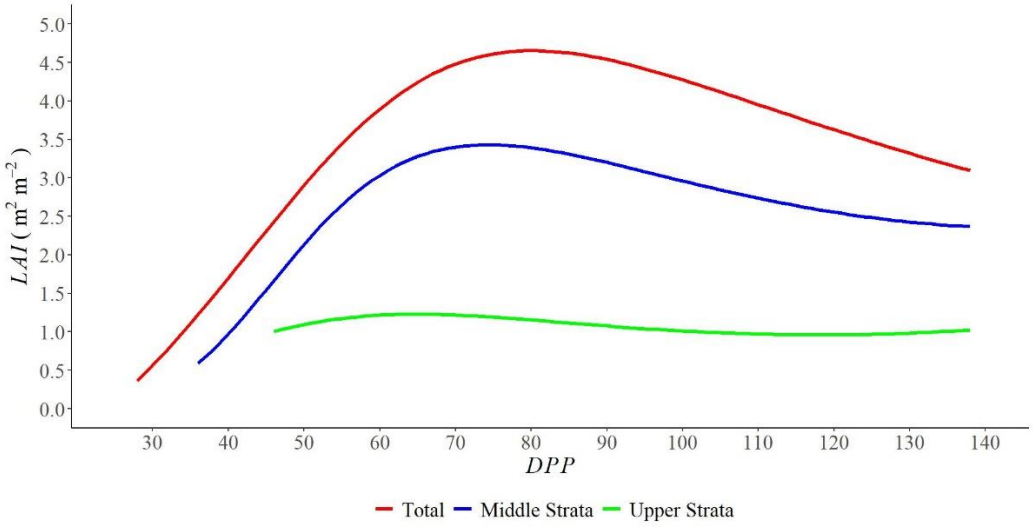

Figure 3. Accumulated leaf area index (LAI) through plant canopy, upper stratum (topmost unshaded leaves), middle stratum, and total of potatoes (*Solanum Tuberosum* L. Var. Diacol capiro) versus days post planting (DPP).

4.3.3. Photosynthetic behavior through the canopy

The response of the net assimilation rate to the incident photosynthetic photon flux density (PPFD) varied with canopy depth and leaf age. The leaves of the upper stratum presented the highest carbon assimilation (*An*) responses to PPFD. The largest *An* response to an incident PPFD was observed between 71 and 91 DPP. Maximum values around 23 μmol (CO_2) m^{-2} s^{-1} were obtained with PPFD higher than 900 μ_{mol} (photon) m^{-2} s^{-1} (Figure 4a). The middle leaves had a lower response of net photosynthetic rate (*An*) to photosynthetic photon flux density than the upper stratum leaves. The highest responses of *An* to PPFD were observed between 71 and 77 DPP. In this canopy position, *An* leaf values of around 20 μmol (CO_2) m^{-2} s^{-1} were obtained with a PPFD greater than 800 μmol (photon) m^{-2} s^{-1} (Figure 4b). The bottom leaves presented a limited (maximum average 9.7 μmol (CO_2) m^{-2} s^{-1}) net photosynthetic rate response to PPFD in all evaluated dates. Although the highest response to PPFD was observed between 77 and 105 DPP, the highest possible assimilation values (*An* < 15 μmol (CO_2) m^{-2} s^{-1}) were obtained at low PPFD values (500 μmol (photon) m^{-2} s^{-1}) (Figure 4c). The declining tendency in net photosynthetic responses to PPFD was observed with leaf aging and canopy depth. The measured light response of *An* declined from the top (young and unshaded leaves) to the basal (old and most shaded leaves) within the potato canopy. Likewise, the net photosynthetic responses to PPFD were lower when canopy age was greater than 117 DPP in all canopy strata, revealing the impact of leaf age on potato leaf photosynthetic traits (Figure 4).

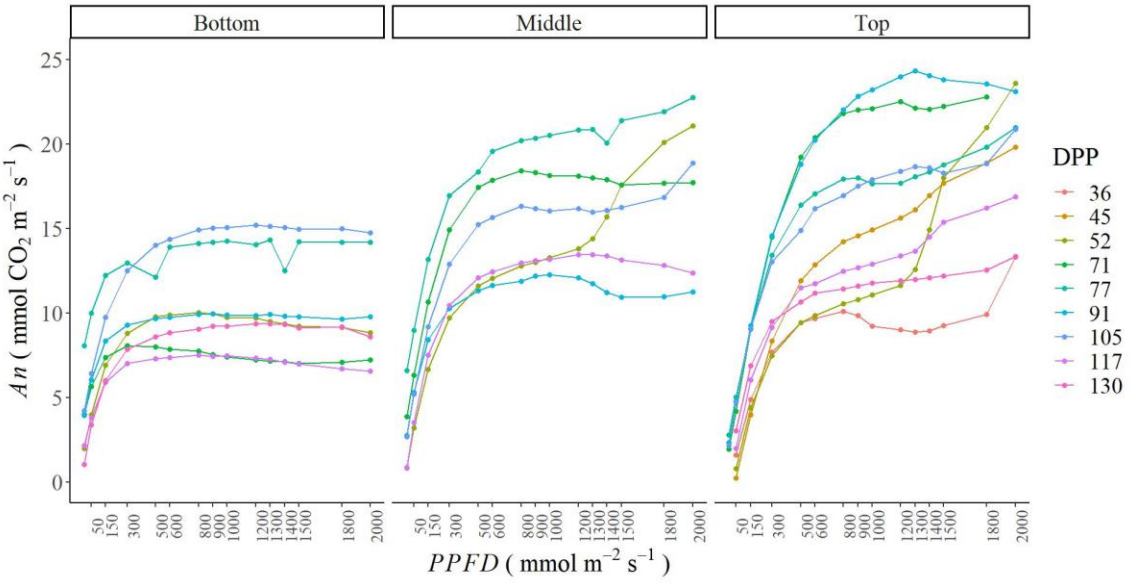

Figure 4. Measured response of net photosynthetic rate (An) for potato (*Solanum Tuberosum* L. Var. Diacol capiro) to photosynthetic photon flux density (PPFD) at different days post planting (DPP) on the bottommost shaded leaves (**left**), middle leaves (**center**), and the topmost unshaded leaves (**rigth**) of potatoes (*Solanum Tuberosum* L. Var. Diacol capiro).

The three models represented the variation of the photosynthetic traits with leaf aging and canopy depth well. The measured light-saturated net photosynthetic rate (A_{gmax}) and quantum yield of assimilation (Φ) reached their maximum at full canopy development, around the maximum LAI stage (60–90 DPP), and then declined gradually as leaves senesced (Figure 5). Regarding canopy leaf position, the three models showed an A_{gmax} declination from the top to the bottom of the canopy, where the lowest carbon assimilation rates at light saturation were observed. In contrast, by comparison with upper canopy leaves, values for Φ in the lower canopy were higher. The parameters A_{gmax} and Φ calculated throughout Michaelis–Menten (Smith) (Smith, 1936) and Mitscherlich (Webb) (Webb et al., 1974) models showed a similar trend and values for the three canopy strata. The values of A_{gmax} and Φ obtained from Michaelis–Menten (Baly) (Baly, 1935) were higher and varied over a wider range. In addition, they presented variations in their behavior, easily observed in the leaves of the middle and lower canopy strata (Figure 5).

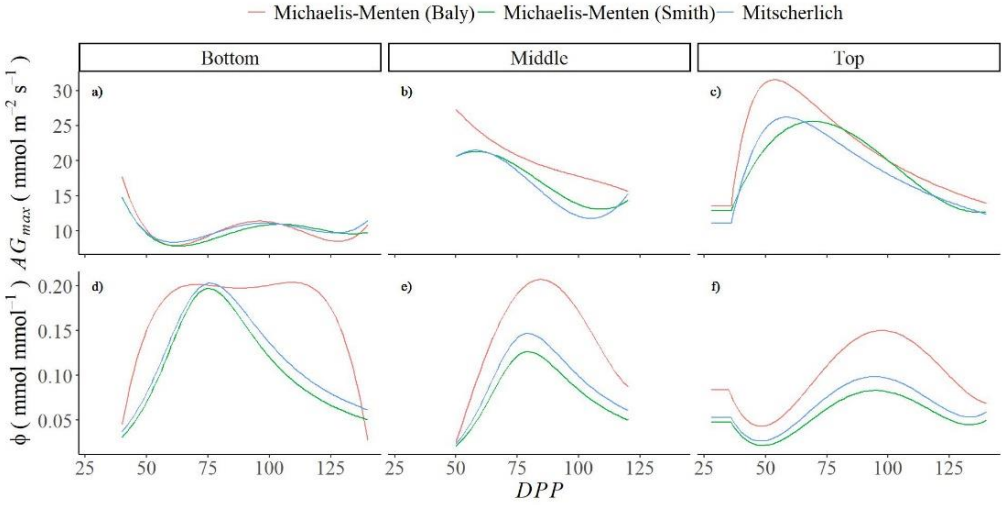

Figure 5. Parameters of light-saturated gross photosynthetic rate (A_{gmax}) and quantum yield of assimilation (Φ) for the topmost unshaded leaves (c, f, respectively), middle stratum leaves(b, e, respectively), and the bottommost shaded leaves (a, d, respectively) of potato (*Solanum Tuberosum* L. Var. Diacol capiro) calculated by the rectangular hyperbola Michaelis—Menten type function, Smith (Smith, 1936) and Baly (Baly, 1935), and by an exponential Mitscherlich function (Webb et al., 1974).

4.3.4. GPP up scaling

The measured EC GPP shows a progressive increase from 28 DPP until a maximum GPP (500 kg C ha^{-1} day^{-1}) occurred at 88 DPP. From 90 to 138 DPP, the daily GPP decreased progressively until a minimum value of 200 kg C ha^{-1} day^{-1}. Multilayer (ML) models correctly reproduce the behavior of potato GPP over time as well as the magnitude of the maximum values that occur around 90 DPP. In the ML Michaelis–Mentem (Smith) model (Smith, 1936), the GPP was underestimated between 36 and 66 DPP (measured GPP was up to 170% higher) and between 87 and 117 DPP (measured GPP was 50% higher). The multilayer model-based Mitscherlich (Webb) function (Webb et al., 1974) underestimates the GPP during most of the cycle. The greatest differences were in the period between 28 and 65 DPP and 95 to 117 DPP. The Big-leaf (BL) Michaelis–Mentem (Smith) model (Smith, 1936) underestimates the GPP mainly between 28–70 DPP. After this period, however, GPP values were close to the measured GPP. The maximum GPP reached is 50% greater than the one measured with the EC tower. However, BL models overestimated GPP, mainly during the maximum LAI phase (80–90 DPP) (Figure 6).

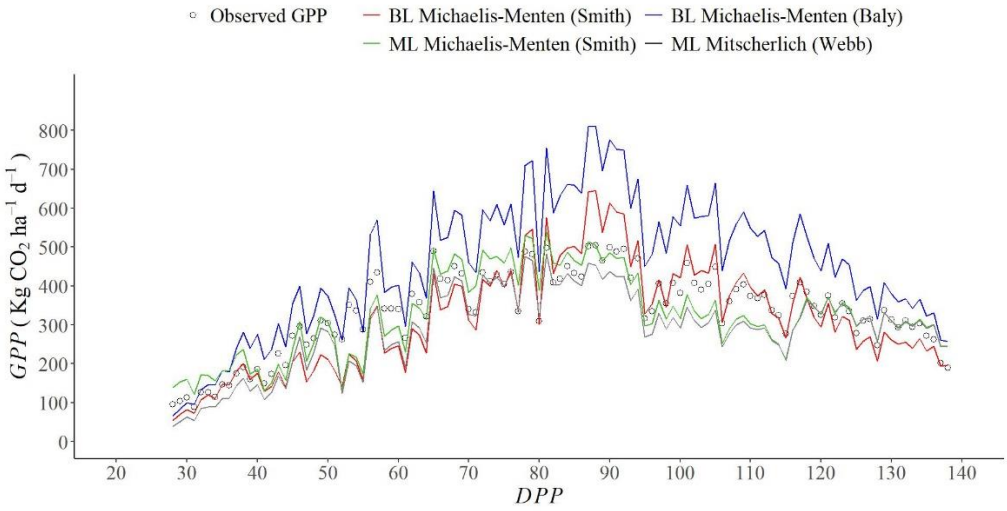

Figure 6. Daily gross primary production (GPP) estimated with the scaling up Big-Leaf—BL (red, blue solid lines) and Multilayer—ML (green, black solid lines) models and Eddy Covariance—EC measurements (open circles), Vs. days post planting (DPP).

The modeled and measured GPP showed variations of the half-hourly GPP mean throughout the day and across growth stages (Figure 7). In the tuberization stage, GPP measured rates increased progressively throughout the day, reaching a maximum of 1.30 ± 0.19 mg CO_2 m^{-2} s^{-1} between 9 to 13 h. In this stage, the ML Michaelis–Menten (Smith) model (Smith, 1936) predicted the measured values more closely than the other models. In the vegetative and tuber bulking stages, half-hourly GPP maximums (0.83 ± 0.37 mg CO_2 m^{-2} s^{-1} and 0.96 ± 0.18 mg CO_2 m^{-2} s^{-1}, respectively) were also found between 9 and 13 h. Again, the GPP predicted by the ML Michaelis–Menten (Smith) model (Smith, 1936) was closer to the measured values. The BL Michaelis–Menten (Baly) model (Baly, 1935) overestimates the half-hourly GPP in all stages (Figure 7).

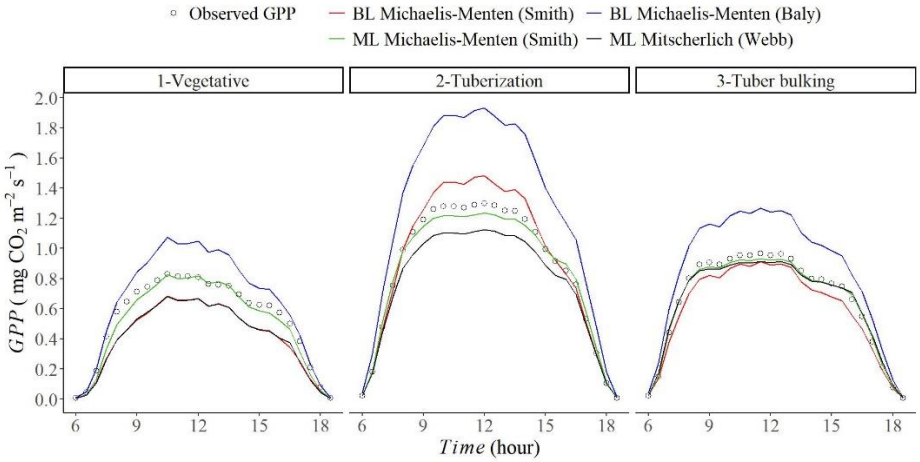

Figure 7. Half-hourly variation of gross primary production (GPP) estimated with the scaling up Big-leaf—BL (red and blue lines) and Multilayer–ML (green and yellow lines) models and with eddy covariance measurements (black line) in three different growth stages (vegetative, tuberization, tuber bulking) of potatoes (*Solanum Tuberosum* L. Var. Diacol capiro). Half-hourly averages are plotted.

Figure 8 shows day-to-day variations of GPP measured (obtained by the eddy covariance technique) versus the big-leaf and multilayer models. In general, the correlation coefficient r showed that the modeled and

measured GPP values had a strong linear correlation. The RMSE value was higher for BL models than ML models, indicating a lower performance and hence less accuracy for BL models. Most of the ML GPP modeled vs GPP measured data are closely distributed around the 1:1 line. This greater closeness of the multilayer models' scatter plot of the predicted value to the 1:1 line indicates a better accuracy than BL models (Figure 8a,b). The ML Michaelis–Menten (Smith) (Smith, 1936) based model had the highest accuracy due to its lowest RMSE (0.131) obtained, followed by the multilayer model based on the Mitscherlich (Webb) (Webb et al., 1974) function (RMSE = 0.155). Likewise, the daily variability in GPP is more accurately captured by the ML Michaelis–Menten (Smith) (Smith, 1936) model due to the linear regression showing the smallest deviation from the 1:1 line (Figure 8b).

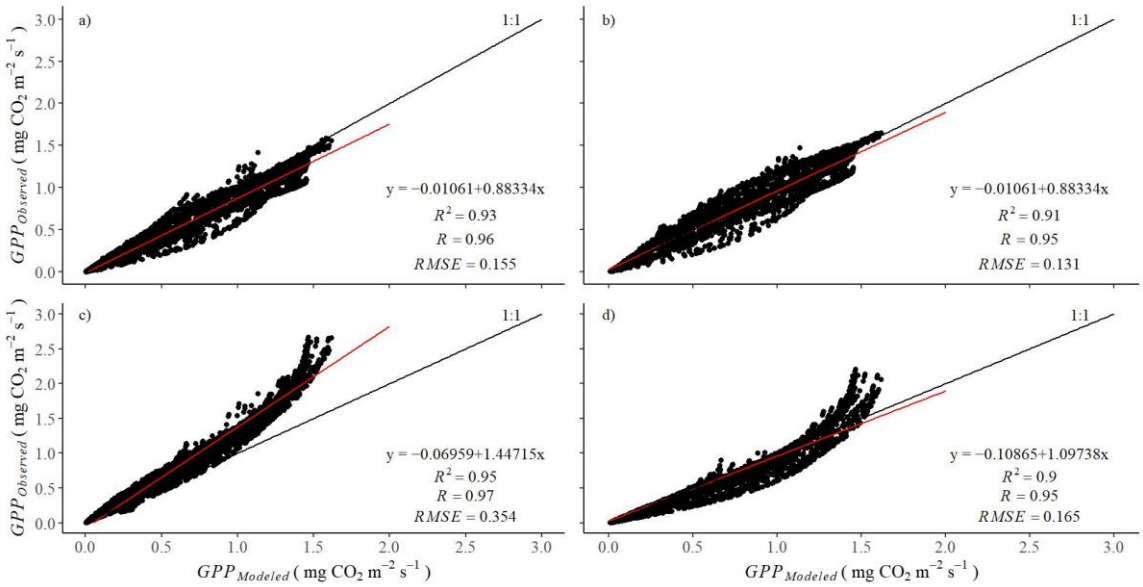

Figure 8. One-to-one comparison of the measured gross primary production (GPP) and the GPP simulated by (**a**) multilayer Mitscherlich (Webb), (**b**) multilayer Michaelis–Menten (Smith), (**c**) big-leaf Michaelis–Menten (Baly), and (**d**) big-leaf Michaelis–Menten (Smith) approaches. Equations, root mean squared error (RMSE), determination and correlation coefficients (R^2) are inserted inside graphs.

4.4. Discussion

The measured GPP has a close relationship with the carbon requirements of each crop growth stage. The maximum daily GPP and half-hourly GPP occur in the tuberization stage and maximum LAI (close to 90 DPP). The behavior of modeled data is consistent with our hypothesis: the big-leaf models overestimate the GPP, specifically during the period of maximum LAI and tuberization stage. Even though multilayer models tend to underestimate the GPP, they better described the daily GPP behavior, and their maximum values were close to the daily GPP and half-hourly GPP values determined by the EC station. Previous studies have shown that the big leaf approach overestimates EC measurements (De Pury and Farquhar, 1997). In particular, de Pury et al.(De Pury and Farquhar, 1997) concludes that the performance of the big leaf model is strongly affected by the LAI and reports an overestimation of 50% in the GPP during the maximum LAI.

Big leaf assumes that the canopy has the same photosynthetic behavior. It has an inability to consider the variation in the CO_2 assimilation of the leaves along the canopy, especially the shaded leaves, which have differences in photosynthetic capacity. This model assumes that the entire canopy is a single unshaded leaf located at the canopy

top (with an evident greater photosynthetic capacity) (Sprintsin et al., 2012). Therefore, the increase in the amount of foliage with these characteristics resulted in overestimations of the maximum LAI. In contrast, with the ML approach, the canopy is separated into layers with different light environments and photosynthetic capacities. In the maximum LAI, the topmost unshaded layer remains constant, and the remaining LAI is distributed between the intermediate and lower layers. Our results indicate that multilayer models performed better than big-leaf models at simulating GPP (as evidenced by ML RMSE being lower than BL RMSE). Some other researchers have also found better performance of ML models compared to BL models in maize and forests (Arkebauer et al., 2009b; Medlyn et al., 2003). However, including several canopy layers for studying light interactions through the canopy requires more detailed input data. In our study for the big-leaf models, we used just 30 min data of PPFD and the zenith angle, and the extinction coefficient was used to define the PPFD attenuation through the canopy in a single LAI layer. In the multilayer models, in addition to daily data of the zenith angle and incident PPFD, transmitted and absorbed radiation in each canopy layer were computed, as well as the evolution of A_{gmax}, quantum yield of assimilation (Φ), and LAI in three different layers during growth was determined.

The main difference is the treatment of the LAI in each approach. In potatoes, Martinez-Maldonado et al. (Martínez-Maldonado et al., 2021c) demonstrated that the evolution of daily GPP is linked to the behavior of the LAI. Furthermore, a direct effect of changes in canopy architecture on simulated productivity has been shown (Sprintsin et al., 2012). This effect is not only linked to the number of photosynthetic leaves but also to the variability in the photosynthetic capacity throughout the canopy. Not all the leaves along the canopy behave like those of the upper stratum. There was a gradient in the photosynthetic capacity within the canopy depending on the age of the leaf, its position in the canopy, and its light environment. In this study, the photosynthetic behavior through the canopy showed that the leaf photosynthesis responses to PPFD, the light-saturated net photosynthetic rate (A_{gmax}), and the quantum yield of assimilation (Φ) of the middle and bottom layers of the canopy were highly different from the upper unshaded leaves. Therefore, each stratum contributed in a different way to the total assimilation of the canopy and this contribution changes during the crop growth cycle.

The upscaling performance depends on the choice of the photosynthetic light-response curves (An–I curves). In the present study, the modeling of the GPP was achieved based on functions that describe and interpret the photosynthetic light responses of leaves. This interpretation works based on primary parameters such as light-saturated net photosynthetic rate (A_{gmax}) and quantum yield of assimilation (Φ). For C3 species, the theoretical quantum yield is around 0.1250 μmol (CO_2) μmol(photon)$^{-1}$ (Lobo et al., 2013; Luo et al., 2000; Singsaas et al., 2001) and the maximum value of A_{gmax} ranges from 42 to 59 μmol (CO_2) m^{-2} s^{-1} (Park S, 1991). Although, the functions used for upscaling had below typical C3 A_{gmax} values, the parameters deduced by the classical Michaelis–Mentem (Baly) function were larger (32 μ_{mol} (CO_2) m^{-2} s^{-1} and 0.15 μmol (CO_2) μmol (photon)$^{-1}$), in comparison to maximum values for Michaelis–Mentem (Smith) (25,6 μmol (CO_2) m^{-2} s^{-1} and 0.08 μmol (CO_2) μ_{mol} (photon)$^{-1}$) and for Webb (26.2 μ_{mol} (CO_2) m^{-2} s^{-1} and 0.098 μmol (CO_2) μmol (photon)$^{-1}$). The above indicates that the Baly-based upscaling model overestimated the GPP due to its higher values in the photosynthetic capacity parameters. The Michaelis–Menten (Baly) function, which tends to overestimate the rate of photosynthesis at low and high irradiances, fails to reproduce the decline of photosynthesis at the photoinhibitory region (Fang et al., 2015; Ye and Zhao, 2010; Ye et al., 2021) and overestimates Agmax and quantum yield of assimilation (Φ), which has also been reported in Amazon forest species (dos Santos Junior et al., 2013).

There are inherent limitations of An–I curves to capture the photosynthetic responses of the canopy, mainly for the upper leaves that were never fully light-saturated even under direct sunlight (Figure 2). However, the

GPP calculated based on the parameters deduced from Michaelis–Menten (Smith) (Smith, 1936) and Mitscherlich (Webb) (Webb et al., 1974) in both big-leaf and multilayer approaches was closer to the measured GPP because they saturated at a lower PPFD than the classical Michaelis–Menten (Baly) equation. In this regard, authors such as (Aubinet et al., 2001b; Hoyaux et al., 2008; Moureaux et al., 2006) indicate that the modeling of the GPP from the Mitscherlich exponential function led to more realistic saturation assimilation values. Among the several processes that need to be described in up scaling models, canopy light absorption is essential since it drives the energy available for photosynthesis. Especially in potatoes, the planophile leaves generate a pronounced light gradient with a possible large effect on total GPP that can be estimated using the analytical solution proposed in this work, which is based on light relations in the canopy using simplified models of photosynthesis.

4.5. Conclusions

The results improve the knowledge of biophysical control in carbon fluxes of potato crops and demonstrate the importance of both the characteristics of the canopy (LAI, leaf angle) and the light relationships of the plants in their immediate environment. Therefore, the photosynthetic light-response curve and a good treatment of the LAI are decisive factors in order to get closer GPP determinations. Big-leaf models are simpler and, although they can simulate the general trend of GPP during the growth cycle, they overestimate the GPP during the maximum LAI since they assume that the canopy has the same photosynthetic behavior as the topmost unshaded leaves. The multilayer approaches allow us to understand not only the amount of leaf area available for photosynthesis but also how the photosynthetic capacity is redistributed in a canopy in relation to the age of the leaf, its position in the canopy, and the changing carbon demand during the crop cycle. Based on these results, the multilayer Michaelis–Menten (Smith) based model predicted more closely both the magnitude and the daily and half-hourly variation in GPP of eddy covariance measurements.

Finally, we demonstrated that models describing the net CO_2 assimilation by a plant leaf as a function of an increase in the photosynthetic photon flux density could be useful for potato GPP estimations. However, for future studies improving accuracy in the GPP upscaling requires descriptions that includes exponential profiles of leaf nitrogen and explore canopy chemistry models to scale leaf GPP to canopy.

References

Arkebauer, T.J., Walter-Shea, E.A., Mesarch, M.A., Suyker, A.E., Verma, S.B., 2009. Scaling up of CO_2 fluxes from leaf to canopy in maize-based agroecosystems. Agric For Meteorol 149, 2110–2119. https://doi.org/10.1016/j.agrformet.2009.04.013

Aubinet, M., Chermanne, B., Vandenhaute, M., Longdoz, B., Yernaux, M., Laitat, E., 2001. Long term carbon dioxide exchange above a mixed forest in the Belgian Ardennes. Agric For Meteorol 108, 293–315. https://doi.org/10.1016/S0168-1923(01)00244-1

Baly, E.C.C., 1935. The Kinetics of Photosynthesis. Proceedings the royal society 117, 218–239. https://doi.org/https://doi.org/10.1098/rspb.1935.0026

Bonan, G., 2019. Mathematical Formulation of Biological Flux Rates, in: Climate Change and Terrestrial Ecosystem Modeling. Cambridge University Press, Cambridge, pp. 53–63. https://doi.org/10.1017/9781107339217.005

Bonan, G., 2015. Leaf Photosynthesis and Stomatal Conductance, in: Ecological Climatology. Cambridge: Cambridge University Press., pp. 241–263. https://doi.org/10.1017/cbo9781107339200.017

Bonan, G.B., Patton, E.G., Finnigan, J.J., Baldocchi, D.D., Harman, I.N., 2021. Moving beyond the incorrect but useful paradigm: reevaluating big-leaf and multilayer plant canopies to model biosphere-atmosphere fluxes – a review. Agric For Meteorol 306, 108435. https://doi.org/10.1016/j.agrformet.2021.108435

Campbell, G.S., 1990. Derivation of an angle density function for canopies with ellipsoidal leaf angle distributions. Agric For Meteorol 49, 173–176. https://doi.org/10.1016/0168-1923(90)90030-A

Campbell, G.S., Norman, J.M., 1998. An Introduction to Environmental Biophysics, Second. ed, Journal of Environment Quality. Springer, Pullman, WA. https://doi.org/10.2134/jeq1977.00472425000600040036x

Campos, H., Ortiz, O., 2019. The potato crop: Its agricultural, nutritional and social contribution to humankind, The Potato Crop: Its Agricultural, Nutritional and Social Contribution to Humankind. https://doi.org/10.1007/978-3-030-28683-5

Chen, F., Dudhia, J., 2001. Coupling and advanced land surface-hydrology model with the Penn State-NCAR MM5 modeling system. Part I: Model implementation and sensitivity. Mon Weather Rev 129, 569–585. https://doi.org/10.1175/1520-0493(2001)129<0569:CAALSH>2.0.CO;2

Chen, N., Wang, A., An, J., Zhang, Y., Ji, R., Jia, Q., Zhao, Z., Guan, D., 2020. Modeling Canopy Carbon and Water Fluxes Using a Multilayered Model over a Temperate Meadow in Inner Mongolia. Int J Plant Prod 14, 141–154. https://doi.org/10.1007/s42106-019-00074-4

De Pury, D.G.G., Farquhar, G.D., 1997. Simple scaling of photosynthesis from leaves to canopies without the errors of big-leaf models. Plant Cell Environ 20, 537–557. https://doi.org/10.1111/j.1365-3040.1997.tb00466.x

dos Santos Junior, U.M., de Carvalho Gonçalves, J.F., Fearnside, P.M., 2013. Measuring the impact of flooding on Amazonian trees: Photosynthetic response models for ten species flooded by hydroelectric dams. Trees - Structure and Function 27, 193–210. https://doi.org/10.1007/s00468-012-0788-2

Eamus, D., Huete, A., Yu, Q., 2016a. Modelling Leaf and Canopy Photosynthesis. Vegetation Dynamics. https://doi.org/10.1017/cbo9781107286221.011

Eamus, D., Huete, A., Yu, Q., 2016b. Modelling Radiation Exchange and Energy Balances of Leaves and Canopies. Vegetation Dynamics 0, 244–259. https://doi.org/10.1017/cbo9781107286221.010

Falge, E., Baldocchi, D., Olson, R., Anthoni, P., Aubinet, M., Bernhofer, C., Burba, G., Ceulemans, R., Clement, R., Dolman, H., Granier, A., Gross, P., Grünwald, T., Hollinger, D., Jensen, N.O., Katul, G., Keronen, P., Kowalski, A., Lai, C.T., Law, B.E., Meyers, T., Moncrieff, J., Moors, E., Munger, J.W., Pilegaard, K., Rannik, Ü., Rebmann, C., Suyker, A., Tenhunen, J., Tu, K., Verma, S., Vesala, T., Wilson, K., Wofsy, S., 2001. Gap filling strategies for defensible annual sums of net ecosystem exchange. Agric For Meteorol 107, 43–69. https://doi.org/10.1016/S0168-1923(00)00225-2

Fang, L., Zhang, Shuyong, Zhang, G., Liu, X., Xia, X., Zhang, Songsong, Xing, W., Fang, X., 2015. Application of Five Light-Response Models in the Photosynthesis of Populus × Euramericana cv. 'Zhonglin46' Leaves. Appl Biochem Biotechnol 176, 86–100. https://doi.org/10.1007/s12010-015-1543-0

Goudriaan, J., 1986. A simple and fast numerical method for the computation of daily totals of crop photosynthesis. Agric For Meteorol 38, 249–254.

Hoyaux, J., Moureaux, C., Tourneur, D., Bodson, B., Aubinet, M., 2008. Extrapolating gross primary productivity from leaf to canopy scale in a winter wheat crop. Agric For Meteorol 148, 668–679. https://doi.org/10.1016/j.agrformet.2007.11.010

Jarvis, P.G., 1995. Scaling processes and problems. Plant Cell Environ 18, 1079–1089. https://doi.org/10.1111/j.1365-3040.1995.tb00620.x

Jassby, A.D., Platt, T., 1976. Mathematical formulation of the relationship between photosynthesis and light for phytoplankton. Limnol Oceanogr 21, 540–547. https://doi.org/10.4319/lo.1976.21.4.0540

Jennings, S.A., Koehler, A.K., Nicklin, K.J., Deva, C., Sait, S.M., Challinor, A.J., 2020. Global Potato Yields Increase Under Climate Change With Adaptation and CO_2 Fertilisation. Front Sustain Food Syst 4. https://doi.org/10.3389/fsufs.2020.519324

Jiang, X., Kang, S., Tong, L., Li, F., Li, D., Ding, R., Qiu, R., 2014. Crop coefficient and evapotranspiration of grain maize modified by planting density in an arid region of northwest China. Agric Water Manag 142, 135–143. https://doi.org/10.1016/j.agwat.2014.05.006

Kobayashi, H., Baldocchi, D.D., Ryu, Y., Chen, Q., Ma, S., Osuna, J.L., Ustin, S.L., 2012. Modeling energy and carbon fluxes in a heterogeneous oak woodland: A three-dimensional approach. Agric For Meteorol 152, 83–100. https://doi.org/10.1016/j.agrformet.2011.09.008

Liu, L., Liu, X., Chen, J., Du, S., Ma, Y., Qian, X., Chen, S., Peng, D., 2020. Estimating maize GPP using near-infrared radiance of vegetation. Science of Remote Sensing 2, 100009. https://doi.org/10.1016/j.srs.2020.100009

Lloyd, J., Grace, J., Miranda, A.C., Meir, P., Wong, S.C., Miranda, H.S., Wright, I.R., Gash, J.H.C., McIntyre, J., 1995. A simple calibrated model of Amazon rainforest productivity based on leaf biochemical properties. Plant Cell Environ 18, 1129–1145. https://doi.org/10.1111/j.1365-3040.1995.tb00624.x

Lobo, F. de A., de Barros, M.P., Dalmagro, H.J., Dalmolin, Â.C., Pereira, W.E., de Souza, É.C., Vourlitis, G.L., Rodríguez Ortíz, C.E., 2013. Fitting net photosynthetic light-response curves with Microsoft Excel - a critical look at the models. Photosynthetica 51, 445–456. https://doi.org/10.1007/s11099-013-0045-y

Luo, X., Chen, J.M., Liu, J., Black, T.A., Croft, H., Staebler, R., He, L., Arain, M.A., Chen, B., Mo, G., Gonsamo, A., McCaughey, H., 2018. Comparison of Big-Leaf, Two-Big-Leaf, and Two-Leaf Upscaling Schemes for Evapotranspiration Estimation Using Coupled Carbon-Water Modeling. J Geophys Res Biogeosci 123, 207–225. https://doi.org/10.1002/2017JG003978

Luo, Y., Hui, D., Cheng, W., Coleman, J.S., Johnson, D.W., Sims, D.A., 2000. Canopy quantum yield in a mesocosm study. Agric For Meteorol 100, 35–48. https://doi.org/10.1016/S0168-1923(99)00085-4

Malhi, Y., Aragão, L.E.O.C., Metcalfe, D.B., Paiva, R., Quesada, C.A., Almeida, S., Anderson, L., Brando, P., Chambers, J.Q., da Costa, A.C.L., Hutyra, L.R., Oliveira, P., Patiño, S., Pyle, E.H., Robertson, A.L., Teixeira, L.M., 2009. Comprehensive assessment of carbon productivity, allocation and storage in three Amazonian forests. Glob Chang Biol 15, 1255–1274. https://doi.org/10.1111/j.1365-2486.2008.01780.x

Martínez-Maldonado, F.E., Castaño-Marin, A.M., Góez-Vinasco, G.A., Marin, F.R., 2021. Gross Primary Production of Rainfed and Irrigated Potato (Solanum tuberosum L .) in the Colombian Andean Region Using Eddy Covariance Technique. Water (Basel) 13, 15. https://doi.org/10.3390/w13223223

Medlyn, B., Barrett, D., Landsberg, J., Sands, P., Clement, R., 2003. Conversion of canopy intercepted radiation to photosynthate: Review of modelling approaches for regional scales. Functional Plant Biology 30, 153–169. https://doi.org/10.1071/FP02088

Mercado, L., Lloyd, J., Carswell, F., Malhi, Y., Meir, P., Nobre, A.D., 2006. Modelling Amazonian Forest eddy covariance data: A comparison of big leaf versus sun/shade models for the C-14 tower at Manaus I. Canopy photosynthesis. Acta Amazon 36, 69–82. https://doi.org/10.1590/s0044-59672006000100009

Meyers, T.P., Hollinger, S.E., 2004. An assessment of storage terms in the surface energy balance of maize and soybean. Agric For Meteorol 125, 105–115. https://doi.org/10.1016/j.agrformet.2004.03.001

Monsi, M., Saeki, T., Schortemeyer, M., 2005. On the factor light in plant communities and its importance for matter production. Ann Bot 95, 549–567. https://doi.org/10.1093/aob/mci052

Mosquera Vásquez, T., Del Castillo, S., Gálvez, D.C., Rodríguez, L.E., 2017. Breeding Differently: Participatory Selection and Scaling Up Innovations in Colombia. Potato Res 60, 361–381. https://doi.org/10.1007/s11540-018-9389-9

Moureaux, C., Debacq, A., Bodson, B., Heinesch, B., Aubinet, M., 2006. Annual net ecosystem carbon exchange by a sugar beet crop. Agric For Meteorol 139, 25–39. https://doi.org/10.1016/j.agrformet.2006.05.009

Moureaux, C., Debacq, A., Hoyaux, J., Suleau, M., Tourneur, D., Vancutsem, F., Bodson, B., Aubinet, M., 2008. Carbon balance assessment of a Belgian winter wheat crop (Triticum aestivum L.). Glob Chang Biol 14, 1353–1366. https://doi.org/10.1111/j.1365-2486.2008.01560.x

Norman, J.M., Welles, J.M., McDermitt, D.K., 1991. Estimating canopy light-use and transpiration efficiencies from leaf measurements. LICOR Application Note 105 18.

Park S, N., 1991. Achievable productivities of certain CAM plants: basis for high values compared with C3 and C4 plants. Neew Phytologys 119, 183–205. https://doi.org/doi.org/10.1111/j.1469-8137.1991.tb01022.x

Pleim, J., Xiu, A., 1995. Development and testing of a surface flux and planetary boundary layer model for application in mesoscale models. Journal of Applied Meteorology 34, 16–32.

Quiroz, R., Ramírez, D.A., Kroschel, J., Andrade-Piedra, J., Barreda, C., Condori, B., Mares, V., Monneveux, P., Perez, W., 2018. Impact of climate change on the potato crop and biodiversity in its center of origin. Open Agric 3, 273–283. https://doi.org/10.1515/opag-2018-0029

Ran, L., Pleim, J., Song, C., Band, L., Walker, J.T., Binkowski, F.S., 2017. A photosynthesis-based two-leaf canopy stomatal conductance model for meteorology and air quality modeling with WRF/CMAQ PX LSM. J Geophys Res 122, 1930–1952. https://doi.org/10.1002/2016JD025583

Raulier, F., Bernier, P.Y., Ung, C.H., 1999. Canopy photosynthesis of sugar maple (Acer saccharum): Comparing big-leaf and multilayer extrapolations of leaf-level measurements. Tree Physiol 19, 407–420. https://doi.org/10.1093/treephys/19.7.407

Sellers, P.J., Berry, J.A., Collatz, G.J., Field, C.B., Hall, F.G., 1992. Canopy reflectance, photosynthesis, and transpiration. III. A reanalysis using improved leaf models and a new canopy integration scheme. Remote Sens Environ 42, 187–216. https://doi.org/10.1016/0034-4257(92)90102-P

Singsaas, E.L., Ort, D.R., DeLucia, E.H., 2001. Variation in measured values of photosynthetic quantum yield in ecophysiological studies. Oecologia 128, 15–23. https://doi.org/10.1007/s004420000624

Smith, E.L., 1936. Photosynthesis in Relation to Light and Carbon Dioxide. Proc Natl Acad Sci U S A 504–511. https://doi.org/https://doi.org/10.1073/pnas.22.8.504

Soil Survey Staff, 2014. Keys to Soil Taxonomy, 12th ed, Book. USDA-Natural Resources Conservation Service, Washington DC, EE.UU.

Sprintsin, M., Chen, J.M., Desai, A., Gough, C.M., 2012. Evaluation of leaf-to-canopy upscaling methodologies against carbon flux data in North America. J Geophys Res Biogeosci 117, 1–17. https://doi.org/10.1029/2010JG001407

Suyker, A.E., Verma, S.B., Burba, G.G., Arkebauer, T.J., 2005. Gross primary production and ecosystem respiration of irrigated maize and irrigated soybean during a growing season. Agric For Meteorol 131, 180–190. https://doi.org/10.1016/j.agrformet.2005.05.007

Tagesson, T., Fensholt, R., Cropley, F., Guiro, I., Horion, S., Ehammer, A., Ardö, J., 2015. Dynamics in carbon exchange fluxes for a grazed semi-arid savanna ecosystem in West Africa. Agric Ecosyst Environ 205, 15–24. https://doi.org/10.1016/j.agee.2015.02.017

Teubner, I.E., Forkel, M., Camps-Valls, G., Jung, M., Miralles, D.G., Tramontana, G., van der Schalie, R., Vreugdenhil, M., Mösinger, L., Dorigo, W.A., 2019. A carbon sink-driven approach to estimate gross primary production from microwave satellite observations. Remote Sens Environ 229, 100–113. https://doi.org/10.1016/j.rse.2019.04.022

Velez Betancourt, A.F., 2020. Estado del arte de la cadena de valor de la papa en Colombia, in: Cadenas Sostenibles Ante Un Clima Cambiante. La Papa En Colombia. Deutsche Gesellschaft für Internationale Zusammenarbeit (GIZ) GmbH Oficinas, Bogotá, Colombia, p. 102.

Wagle, P., Gowda, P.H., Anapalli, S.S., Reddy, K.N., Northup, B.K., 2017. Growing season variability in carbon dioxide exchange of irrigated and rainfed soybean in the southern United States. Science of the Total Environment 593–594, 263–273. https://doi.org/10.1016/j.scitotenv.2017.03.163

Wagle, P., Xiao, X., Suyker, A.E., 2015. Estimation and analysis of gross primary production of soybean under various management practices and drought conditions. ISPRS Journal of Photogrammetry and Remote Sensing 99, 70–83. https://doi.org/10.1016/j.isprsjprs.2014.10.009

Waldo, S., Chi, J., Pressley, S.N., O'Keeffe, P., Pan, W.L., Brooks, E.S., Huggins, D.R., Stöckle, C.O., Lamb, B.K., 2016. Assessing carbon dynamics at high and low rainfall agricultural sites in the inland Pacific Northwest US using the eddy covariance method. Agric For Meteorol 218–219, 25–36. https://doi.org/10.1016/j.agrformet.2015.11.018

Wang, Y., Leuning, R., 1998. A two-leaf model for canopy conductance , photosynthesis and partitioning of available energy I : Model description and comparison with a multi-layered model 91.

Wang, Y.P., Jarvis, P.G., 1988. Mean leaf angles for the ellipsoidal inclination angle distribution. Agric For Meteorol 43, 319–321. https://doi.org/10.1016/0168-1923(88)90057-3

Webb, W.L., Newton, M., Starr, D., Url, S., 1974. Carbon Dioxide Exchange of Alnus rubra . A Mathematical Model. International association for Ecology 17, 281–291.

Ye, Z., Zhao, Z., 2010. A modified rectangular hyperbola to describe the light-response curve of photosynthesis of Bidens pilosa L. grown under low and high light conditions. Front Agric China 4, 50–55. https://doi.org/10.1007/s11703-009-0092-0

Ye, Z.P., Duan, S.H., Chen, X.M., Duan, H.L., Gao, C.P., Kang, H.J., An, T., Zhou, S.X., 2021. Quantifying light response of photosynthesis: Addressing the long-standing limitations of non-rectangular hyperbolic model. Photosynthetica 59, 185–191. https://doi.org/10.32615/ps.2021.009

5. ANALYTICAL APPROACH TO RELATE EVAPOTRANSPIRATION, CANOPY-ATMOSPHERE COUPLING LEVEL, AND WATER DEFICIT SENSITIVITY

Abstract

The decoupling factor (Ω) reflects the leading mechanisms responsible for canopy transpiration and allows to know the relevance of the control of stomatal or canopy conductance on transpiration (T). The Ω is strongly dependent on water availability and could be a good approach to describe how plants minimize excessive water loss by increasing the dominance of biotic factors that controls ET under water deficit conditions. We provided an overview of how the Ω concept could be broadly used and applied for studying the sensitivity of evapotranspiration and water conservation potential of canopies under water deficit conditions. A decoupling condition indicates that under water deficit, the increase of canopy resistance will not have control over the transpiration. Therefore, a structural context of the canopy where predominantly uncoupled regions will have a lower capacity to reduce evapotranspiration and avoid water losses. Furthermore, because the water deficit, stomatal closure restricts photosynthesis more than transpiration, water use efficiency could be lower in decoupled canopies compared to more coupled ones. Yet, we summarized the characteristics that depict 'structural context' predisposing coupled or decoupled conditions that could indicate the capacity of canopy/crop to reduce excessive water losses and maintain a high assimilation/transpiration relation under water deficit.

Keywords: Transpiration, Water deficit, Vapor pressure deficit, Decoupling factor

5.1. Introduction

Radiation, air temperature, air humidity and wind are meteorological elements involved in determining evaporation and transpiration. Both processes occur simultaneously such as evapotranspiration (ET) and are controlled by biophysical conditions (aerodynamic resistance, stomatal conductance, surface conductance) and crop management (Allen et al., 2006). The amount of water evaporated during evapotranspiration is related to the energy received per unit area in the form of latent heat of vaporization (λE). Therefore, the λE flux (LE) is a direct expression of evapotranspiration where 2.45 MJ per m^2 are required to vaporize 1 kilogram or 1 mm of water (Rosenberg et al., 1983).

The main driving-force of the biophysical interaction between the biosphere and the atmosphere is the radiative energy from solar radiation. Although evapotranspiration is directly linked to this available energy (which is the primary driver of vapor transport), there is a considerable influence of the biotic factors (Nassif et al., 2014; Paulino Junior and Silva von Randow, 2017; Spinelli et al., 2018a). The decoupling factor was proposed by Jarvis and Mcnaughton (1986) and it allows to understand the ability of plant canopy and the atmosphere to exchange momentum, energy, and mass (Steduto and Hsiao, 1998), reflects the dominant mechanisms responsible for the canopy ET, and contributes to explain how evapotranspiration is controlled in vegetated surfaces (Paulino Junior and Silva von Randow, 2017; Sutherlin et al., 2019a). Conceptually, the extreme values of Ω mean are a) $\Omega \rightarrow 1$, implying that the net radiation is the only contributor to the evapotranspiration process and that vegetation is completely decoupled from the atmospheric conditions; b) $\Omega \rightarrow 0$, indicating complete coupling of vegetation with atmospheric vapor pressure deficit (VPD) and wind speed (Marin et al., 2016).

According to Jarvis and Mcnaughton (1986) and McNaughton and Jarvis (1991), Ω describes the sensitivity of evapotranspiration (ET) to biological and environmental controlling factors like radiation, wind speed, vapor pressure deficit, or surface conductance (Zhang et al., 2016). In other words, Ω is an index to assess: 1) whether the evapotranspiration process is mainly controlled by the vegetation in terms of surface conductance or

mainly limited by the energy available (radiation), and 2) how different vegetation types control the evapotranspiration fluxes in land–atmosphere interactions (Paulino Junior and Silva von Randow, 2017; Sutherlin et al., 2019a). Ω represents the magnitude of the coupling effect of the canopy and the aerodynamic conductance in controlling rates of canopy evapotranspiration (Kumagai et al., 2004) and characterizes the extent to which stomatal and canopy conductance may control transpiration (water vapor and CO_2 exchange) (Steduto and Hsiao, 1998). Still, Ω is useful to quantify the relative importance of VPD in controlling the evapotranspiration (Ferreira, 2017; Spinelli et al., 2018a; Sutherlin et al., 2019a).

Under water deficit conditions, the primary survival strategy in plants is to avoid excessive water loss and prevent dehydration. Although the stomatal closure or the increase in canopy resistance is an immediate response, the impact on the reduction of transpiration (for controlling water loss) and its consequence on carbon assimilation depends on the natural degree of coupling of canopies to the atmosphere. Likewise, the natural coupling or uncoupling condition of the different species is conditioned by their biophysical environment and their phenotypic characteristics. This review aims to provide an overview around the decoupling factor (Ω) concept and its potential use to analyze the capacity of the canopy to reduce excessive water losses and the possible impacts on assimilation under water deficit. The following question is addressed in this review: How omega is modulated under water deficit and how impact water vapor and CO_2 exchange?

5.2. Materials and Methods

5.2.1. Data sources and search strategies

This review was conducted according to the PRISMA (Preferred Reporting Items for Systematic Reviews and Meta-Analyses) methodology (Moher et al., 2009) through asking a question, choosing the eligibility criteria and key words, searching the literature, excluding, and selecting the papers, assessing the quality of the articles, extracting the required information, and presenting data. The eligible articles published until 2022 were searched in three databases, including Scopus, ScienceDirect, and Web of Science. The search process was accomplished using the keywords "Omega", "decoupling factor", "water deficit", "evapotranspiration". Additional articles were taken into consideration by hand searching, mainly which are theoretical bases for the subject. Metadata was not used in this review.

5.2.2. Study selection

The papers related to the subject of interest were selected by studying the abstracts and titles. Afterward, the full texts of the selected papers were obtained. The main criteria for including papers were the link between water deficit and Ω, as well as retrospective articles than depict the theoretical approach for ET and its relation to the Ω decoupling factor. We excluded studies that did not link the relation between Ω and ET, or papers that work each one individually. After the exclusion of the irrelevant articles, the remaining papers were reviewed meticulously where a carefully reviewing of titles and abstracts was done. We continued with a full-text checking of the articles related to the main criteria for including. Figure 1 presents the flow diagram for the selection process of papers.

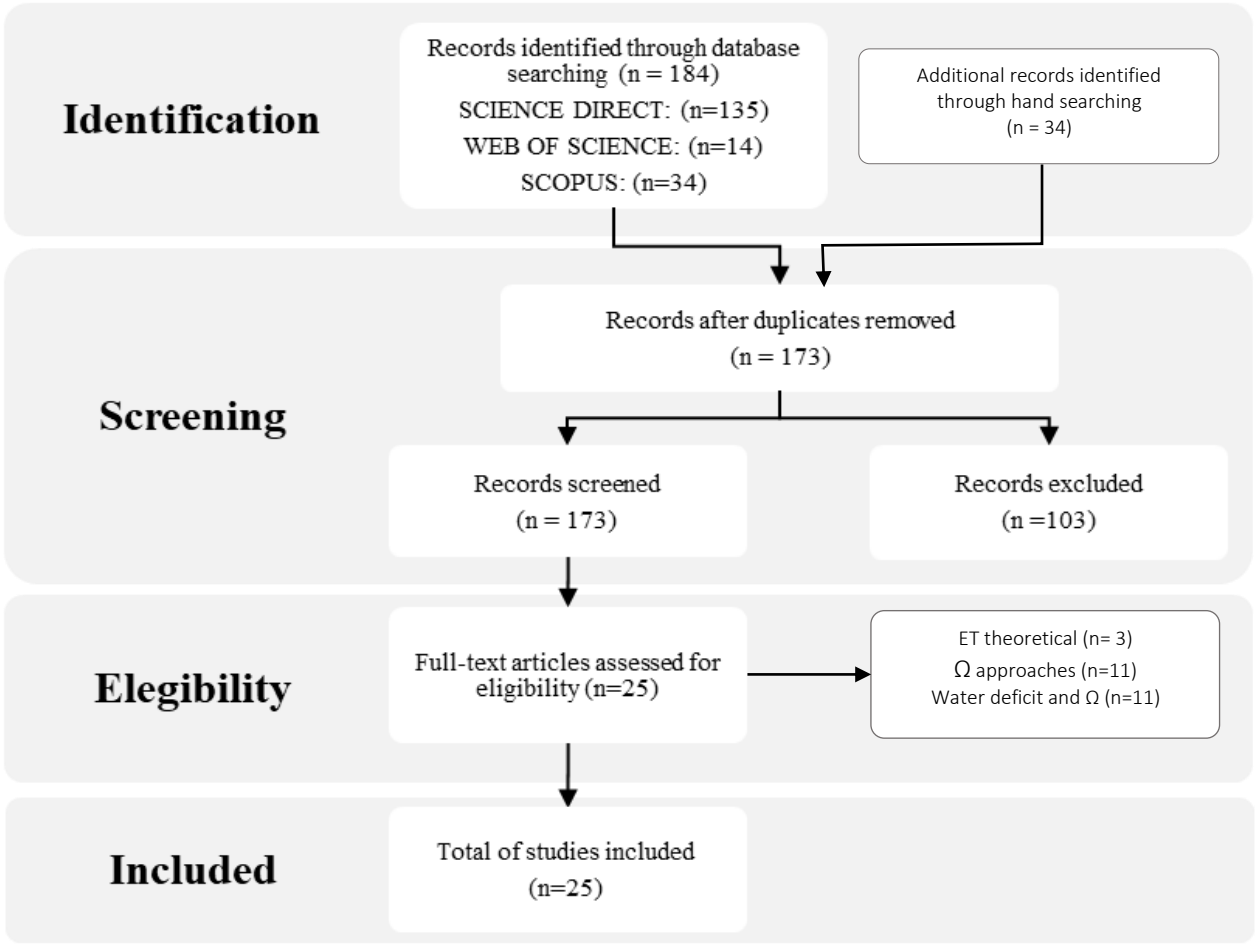

Figure 1. PRISMA flow diagram showing the selection process of papers

5.3. Results

The searches produced 173 records after duplicates were removed. We identified 135 potentially relevant studies in Science Direct, 14 in Web of Science, 34 in SCOPUS, and 34 by hand searching. After reading the full reports, we considered 25 studies. The studies were reported between 1985 and 2022, involving different species. The first reports related to water availability were cited by Jarvis (1985) for soybean and alfalfa. After that, that, some reports were found for grasslands, forests (evergreen broadleaf forests, evergreen oak, lowland dipterocarp forest, rain forest) (Kauwe et al., 2017; Ferreira, 2017; Khatun et al., 2011; Köstner et al., 1992; Nassif et al., 2014; Spinelli et al., 2018; Sutherlin et al., 2019), woody crops, Kernza crop (Sutherlin et al., 2019), sugarcane (Nassif et al., 2014), almond (Spinelli et al., 2018), and maize (Steduto and Hsiao, 1998). Grass species have a greater number of studies on the subject.

Three studies, (Marin, 2021; Monteith, 1965; Penman, 1948) were chosen to develop the theoretical basis of evapotranspiration and as a previous context of **Ω** concept. Fifteen studies (Kauwe et al., 2017; Ferreira, 2017; Jarvis and Mcnaughton, 1986; Jones, 1990; Khatun et al., 2011; Köstner et al., 1992; Marin et al., 2016; Marin and Angelocci, 2011; Marin et al., 2001; Marin, 2021; McNaughton and Jarvis, 1991; Nassif et al., 2014; Spinelli et al., 2018; Steduto and Hsiao, 1998; Sutherlin et al., 2019; Marin et al., 2019) substantiated the conceptual and theoretical meaning of the **Ω**, its sense regarding the link between plant canopy and the atmosphere. In general, studies describe

Ω as an indicator of the dominant mechanisms responsible for the ET of the canopy and a good approach to describe the sensitivity of evapotranspiration to stomatal closure. Eleven studies (Aires et al., 2008; José Darlon Nascimento Alves et al., 2022; de Kauwe et al., 2017; Ferreira, 2017; Jarvis, 1985; Kumagai et al., 2004; Paulino Junior and Silva von Randow, 2017; Silva et al., 2017b; Spinelli et al., 2018a, 2016; Sutherlin et al., 2019a) develop the Ω concept under water deficit conditions. Studies demonstrated how Ω is strongly dependent on water availability, and how its variable value depicted the importance of atmospheric and surface factors in controlling ET.

5.4. Discussion

5.4.1. Evapotranspiration

The process of water evaporation is an "exchange", where a humid surface delivers water vapor in exchange for the heat of the air above said surface (Monteith, 1965). This exchange only works if there are two fundamental components: 1) an energy source providing latent heat of evaporation from the degradation of net radiation (energy component), and 2) a mechanism to remove water vapor. This mechanism is driven both by a sinking force and by the turbulent transport of water vapor (aerodynamic component) (Marin, 2021; Penman, 1948).

In the *aerodynamic component*, evaporation is a mass diffusion process where there is a sink force governed by the gradient flow theory described by (Eq.1):

$$E = (e_{sur} - e_{air}) f(u) \quad (1)$$

where the evaporation rate is related to the difference in the water vapor content, E is the evaporation per unit of time, e_{sur} is the vapor pressure of the evaporating surface, e_{air} is the actual vapor pressure of the surrounding air and *f(u)* is a function of the horizontal wind speed. The difference e_{sur}–e_{air} is the term of the equation that indicates the gradient force directed by the pressure difference between the air and the evaporating surface (Penman, 1948). The main resistance to evaporation from the surfaces is a thin layer of air (1 – 3 mm thick) near the surface where the movement of air is not turbulent and the transport of vapor through this layer occurs by molecular diffusion (sublaminar boundary layer). Penman (1948) parameterized *f(u)* and the result is (Eq.2):

$$E = 0.33(e_{sur} - e_{air}) U_2^{0.76} \quad (2)$$

where e_{air} is the actual vapor pressure of the air at a sufficient height not to be affected by evaporation and U_2 is the air velocity at 2 m.

The *energy component* is based on the concept that the energy for generating water vapor is defined by the energy balance. The shortwave and longwave components of the radiation balance determine the amount of energy available or used for the system. With this amount defined, the way of use or destination of that energy becomes relevant since it can be used mainly for water evaporation or for air heating (Marin, 2021; Penman, 1948) (Eq.3):

$$Rn = LE + H \quad (3)$$

An air mass can be described by its temperature and its vapor pressure. That is, the total heat content is the sum of the sensible heat content (which depends on the temperature) and the latent heat content (which depends on the vapor pressure). A change in latent heat content has an equal and opposite change in sensible heat content. To illustrate the concept, when liquid water carried by an air mass evaporates, there is an increase in the latent heat content in that air mass. Because the evaporation process involves a loss of internal energy, the air will cool down, thus reducing the sensible heat content (Monteith, 1965).

Transport of latent heat (LE) is governed by the vapor pressure gradient (e_{sur}–e_{air}) and the transport of sensible heat (H) is driven by the temperature gradient (T_{sur} – T_{air}). Since these two are the main sinks of the incoming energy, it is useful to define the link between LE and H, in terms of the Bowen relationship: $\beta = \frac{H}{LE}$. which can also be written as pressure and temperature gradients, where Υ is the psychrometric constant (Eq. 4):

$$\beta = \frac{\Upsilon\,(T_{sur}-T_{air})}{(e_{sur}-e_{air})} \tag{4}$$

Where T_{sur} is the surface temperature and T_{air} is the temperature of the air above the surface.

From Bowen ratio, we obtain $H = \beta LE$; replacing *Rn* in the equation, we obtain $Rn = LE + \beta LE$ and, therefore (Eq. 5):

$$LE = \frac{Rn}{(1+\beta)} \tag{5}$$

Replacing the expression for Bowen ratio in terms of pressure and temperature gradients, we obtain (Eq.6):

$$LE = \frac{Rn}{1+\frac{\Upsilon\,(T_{sur}-T_{air})}{(e_{sur}-e_{air})}} \tag{6}$$

By combining the aerodynamic component with the energy component, we obtain (Eq.7) (Penman, 1948):

$$ET = \frac{\mathrm{Rn}\Delta+\mathrm{VPD}\,\Upsilon}{\Delta+\Upsilon} \tag{7}$$

where Δ is the slope of the vapor pressure curve at equilibrium temperature (hPa K^{-1}), γ is the psychrometric coefficient (0.67 hPa K^{-1}), and VPD (e_{sur} – e_{air}) is the air vapor pressure deficit (hPa) which is a function of air temperature and relative humidity.

Monteith (1965) extends Penman's method (1948) to plant surfaces considering aerodynamic and surface resistance factors. Like Penman (1948) he defines an energy component in which latent heat is consumed at a rate of (Eq.8):

$$LE_1 = \frac{\Delta Rn}{\Delta+\gamma} \tag{8}$$

and an aerodynamic component where the evaporation rate from a surface follows the gradient (surface T – T of the surrounding air). This approximation includes the specific heat of the air (*pc*) and the time in which 1 cm^3 of air exchanges heat with 1 cm^2 of surface (*Ra*) (Eq.9):

$$LE_2 = \frac{pc(T_{sur}-T_{air}')}{Ra} = \frac{pcD}{Ra} \tag{9}$$

Therefore, ET is given by Eq.10:

$$ET = LE_1 + LE_2 = \frac{\Delta Rn}{\Delta+\gamma} + \frac{pc\;DPV}{Ra} \tag{10}$$

Considering that, $e_{sur} - e_{air} = \Upsilon(T_{sur} - T_{air})$, the equation can be written as (Eq.11):

$$ET = \frac{\Delta Rn + cp\left[\frac{e_{sur} - e_{air}}{Ra}\right]}{\Delta + \gamma} \quad (11)$$

This equation is analogous to that of Penman (1948). However, Monteith (1965) included the canopy (*Rc*) and aerodynamic resistances (*Ra*) (Marin, 2021). In this approach, the transpiration rate is proportional to the difference between the vapor pressure at the leaf surface (e_{sur}) and the actual vapor pressure of the surrounding air (e_{air}). The term $\frac{e_{sur} - e_{air}}{Ra}$ (external diffusion rate) indicates a potential difference that maintains a current or flow of water vapor that passes through an *external resistance to diffusion "Ra"* present in the air surrounding the leaf. Similarly, the rate of diffusion within the leaf is stated in terms of the gradient between the saturation vapor pressure of the air in contact with the cell walls surrounding the substomatal cavity $e_{s(sub)}$, and the vapor pressure at the surface of the leaf e_{sur}. The term $\frac{e_{s(sub)} - e_{sur}}{Rl}$ (internal diffusion rate), then indicates a potential difference that maintains a flow of water vapor that crosses the internal resistance of the R_l leaf (stoma+cuticle+cell walls, under conditions of water deficit). When the leaves are turgid, with enough water for transpiration, the resistance of the cell walls is zero and the resistance of the stoma is low and much lower than the cuticle. The resistance in this case is due to the stomata, their size and population on the leaf (Monteith, 1965).

When both external and internal diffusion rates are equal (Eq.12):

$$\frac{e_{s\,(sub)} - e_{sur}}{Rl} = \frac{e_{sur} - e_{air}}{Ra} \quad (12)$$

Solving for $e_{s(sub)} - e_{sur}$ we obtain Eq.13:

$$e_{s(sub)} - e_{sur} = \left(1 + \frac{Rl}{Ra}\right)(e_{sur} - e_{air}) \quad (13)$$

where $e_{sur} - e_{air}$ can be replaced by $\frac{e_{s(sub)} - e_{sur}}{(1 + \frac{Rl}{Ra})}$ to alternatively be written as Eq.14:

$$\Upsilon^* = \Upsilon\left(1 + \frac{Rl}{Ra}\right) \quad (14)$$

The psychrometric constant Υ is replaced by Υ^* in the ET equation to obtain the equation of latent heat of transpiration of a leaf or cultivation surface (Monteith, 1965). Finally, the development of the Penman-Monteith equation is obtained (Eq.15):

$$ET = \frac{\Delta Rn + pc\ \rho_{ar}\ [(e_{sur} - e_{air})/Ra]}{\Delta + \Upsilon\,(1 + \frac{Rl}{Ra})} \quad (15)$$

Monteith (1965) extended the concept of resistance from the vegetated surface to a total surface resistance, *Rs*, which describes the resistance to the flow of vapor through the stomata, of the total area of the leaf and the soil surface (Allen et al., 2006; Marin, 2021) where (Eq.16 and Eq.17):

$$\Upsilon^* = \Upsilon\,(1 + \frac{Rs}{Ra}) \text{ and therefore} \quad (16)$$

$$ET = \frac{\Delta Rn + pc\ [(e_{sur} - e_{air})/Ra]}{\Delta + \Upsilon\,(1 + \frac{Rs}{Ra})} \quad (17)$$

5.4.2. Transpiration and decoupling factor

The total flux of water vapor from a crop is the sum of the transpiration of all radiation-intercepting leaves, and the evaporation from the soil surface under the crop. Transpiration plays an important role both because of its contribution to the total flow of water vapor and because of the variety of factors that control it (Monteith, 1965). Transpiration depends on net radiation (*Rn*), vapor pressure deficit (*VPD*), temperature (*T*), wind speed (*u*) and stomatal conductance (*gs*). These variables vary within the canopy and through the atmosphere above the crop surface. Stomatal conductance (*gs*) determines and controls the VPD of the leaf surface directly, however, its relationship with transpiration is not strictly direct (P G Jarvis and Mcnaughton, 1986). The effect of *gs* on transpiration could be direct only if it was considered like a single stoma. In this scenario, a change in the conductance of a single stoma would generate an equal change in the transpiration of that single stoma. Consequently, transpiration would be controlled by the movement of the guard cells and the stomatal geometry. Despite this, the contribution of water vapor from that single stoma would not be enough to modify the VPD gradient of the leaf surface.

At the leaf level, where there is a population of stomata, the relationships between stomatal conductance, foliar VPD, and transpiration are not direct. In the leaf blade, the conductance of the stomata changes in unison, significantly altering the VPD of the leaf surface and generating a change in the water vapor gradient along the leaf boundary layer. In this case, the influence of conductance on transpiration will be determined by the relationship between the VPD of the leaf surface and the external VPD of the air environment beyond the leaf boundary layer. These effects are described by the equation of Jarvis and Mcnaughton (1986) where the sensitivity of transpiration to conductance is given by Eq.18:

$$\frac{dE_l}{E_l} = (1 - \Omega_l) dg_s/g_s \quad \text{and} \quad \frac{dE_c}{E_c} = (1 - \Omega_c) dg_c/g_c \tag{18}$$

In these equations the change in leaf (E_l) and canopy (Ec) transpiration due to a change in stomatal conductance g_s and canopy conductance g_c is estimated. Ω_l and Ω_c are the *leaf and canopy decoupling factors* respectively. This variable describes the degree of coupling of canopies to the atmosphere by depicting how closely the VPD of the leaf surface is related to the air outside the leaf boundary layer. It is a dimensionless value between 0 and 1 that depends on the temperature and the size of the conductance (as they are sites of water evaporation) and the conductance of the leaf boundary layer (which defines the VPD gradient near the leaf surface) (P G Jarvis and Mcnaughton, 1986).

If $\Omega_{l/c} \rightarrow 1$, the conditions at the leaf surface are completely decoupled from the air conditions outside the leaf boundary layer, that is, $VPD_{leaf/canopy}$ and VPD_{amb} are decoupled. Under these conditions there is no effect of stomatal or canopy conductance on transpiration. Stomatal conductance regulates the VPD of the leaf surface, but not transpiration. Transpiration is regulated by the joint effect of net radiation, temperature, the conductance ratio of the foliar boundary layer of the two leaf surfaces (adaxial and abaxial), wind speed, the VPD_{env} (external to the leaf boundary layer). In contrast, when $\Omega_{l/c} \rightarrow 0$, $VPD_{leaf/canopy}$ equals VPD_{env}, the conditions at the leaf surface are fully coupled to the air conditions outside the leaf boundary layer. In this case, the stomatal closure regulates transpiration. At intermediate values of $\Omega_{l/c}$, there is an intermediate control of stomatal conductance in transpiration. If the value of $\Omega_{l/c}$ decreases from 1 to zero, the stomatal conductance control gradually increases. Therefore, transpiration will be regulated by the joint effect of stomatal conductance, net radiation, temperature, conductance ratio of the foliar

boundary layer of the two leaf surfaces (adaxial and abaxial), wind speed and, VPD_{env} (Jarvis and Mcnaughton, 1986; Marin and Angelocci, 2011; Marin, 2021; Nassif et al., 2014).

In the same way, if there are an increase in the sensitivity of transpiration to the control of g_s or g_c the rate of evapotranspiration will be called *imposed evapotranspiration* ET_{imp}. In contrast, if $\Omega_{l/c}$ goes from zero to 1, the sensitivity of transpiration to changes in g_s or total g_c is very low. In this case, the evapotranspiration is called *equilibrium evapotranspiration* ET_{eq} (Jarvis and Mcnaughton, 1986; Marin and Angelocci, 2011; Marin, 2021; Nassif et al., 2014). Therefore, the equation for the dominant mechanisms driving evapotranspiration in terms of surface-atmosphere coupling is (Eq.19):

$$ET = ET_{eq} + (1 - \Omega_c)ET_{imp} \tag{19}$$

This indicates that at the leaf and crop scale, the evapotranspiration response to changes in conductance depends on the Ω factor (Jones, 1990). It is important to note that Ω_c (canopy) will always be larger than Ω_l (leaf) (P G Jarvis and Mcnaughton, 1986).

Authors such as Jarvis and Mcnaughton (1986) and Jones (1990) have reported some typical and unique values for different canopies of unstressed covers such as conifers, tomato, oats, cotton, potatoes, beans, strawberries, citrus, among others. However, these values were calculated for the entire canopy, from measurements of *gs*, or estimated in the mixed layer. More recently Marin et al., 2016; Marin and Angelocci, 2011; Marin et al., 2001; and Nassif et al., 2014 obtained Ω determinations from *gs* measurements through the canopy in exposed and shaded leaves in the upper, middle, and lower part of the canopy throughout the day between 9:00 and 16:00 h in *Citrus latifolia Tanaka* trees, sugarcane, and several other crops. In these studies, the *gs* values were expressed as the canopy resistance to vapor diffusion (*Rc*) and the decoupling factor (Ω) was calculated using the expression of Jarvis and Mcnaughton (1986) (Eq.20):

$$\Omega = \frac{1}{1+\left[\left(\frac{2Rc}{(\frac{S}{\Upsilon}+2)}\right)\right]*Ra} \tag{20}$$

where *Ra* is the aerodynamic resistance of the canopy, and Υ is the psychrometric constant. An alternative equation of the equation is (Eq.21):

$$\Omega = \frac{Ra}{1+\left[\left(\frac{\Upsilon}{s+\Upsilon}\right)\right]*Rc} \tag{21}$$

Equations 20 and 21 show that the decoupling factor (Ω) is a function of *Rc* (1/*gs*) and *Ra* (1/*ga*); if *Rc*/*Ra* is low, Ω is close to 1, and if *Rc*/*Ra* is high, Ω tends to zero. This indicates that Ω is an indicative of the control of these resistances on the evapotranspiration of vegetation. Therefore, the dynamics of vapor transport can be understood by studying Ω.

5.4.3. Structural context of Ω

The decoupling factor (Ω) is not considered a fixed canopy characteristic (Spinelli et al., 2018a, 2016) as it depends on environmental conditions, canopy characteristics, planting arrangements and density, and even plot size (Jones, 1990). Within the same canopy, there may be **Ω** variations, since, along the different strata, there is diversity in leaf distribution, leaf area, leaf density, stomatal density, as well as temperature gradients, VPD and wind speed generated by microenvironments within the canopy (P G Jarvis and Mcnaughton, 1986). **Ω** is also highly dependent on leaf area index (LAI). (Spinelli et al., 2018a) report that in *Prunus dulcis* high LAI were determinants of higher **Ω** values, and that only when senescence caused a fall in LAI a decrease in Ω was observed. The **Ω** also varies with the time of the day, Köstner et al. (1992) reported large variations in the daily pattern in forests and Nassif et al. (2014) reported a daily variation between a range between 0.2 and 0.7 in sugarcane during the wet season. **Ω** has also been shown to depend on wind speed and its effect on *Ra*, as well as on temperature and its relationship with the vapor pressure (Monteith and Unsworth, 2013). These microenvironmental conditions, canopy characteristics, time of day, and environmental conditions make up what is called the "*structural context*" in which a canopy, plant, or leaf is found (P G Jarvis and Mcnaughton, 1986). Other factors such as the presence of windbreaks cause decoupling conditions even in rough crops (Jones, 1990). This because of windbreaks can decrease crop boundary layer conductance (Jarvis, 1985). Consequently, it could be said that the variations in Ω are due to the diversity of *structural contexts* within a canopy of a vegetation cover. This indicates that there are places in the canopy or crop where stomatal control of evapotranspiration predominates and others where evapotranspiration is controlled by the radiative environment and net radiation (Jarvis, 1985; P G Jarvis and Mcnaughton, 1986; Spinelli et al., 2018a, 2016; Sutherlin et al., 2019a).

5.4.4. Decoupling factor Ω dynamics under water déficit

The relationship between water availability and degree of coupling is currently well-known (P G Jarvis and Mcnaughton, 1986; Sutherlin et al., 2019a). Jarvis and Mcnaughton (1986a) observed an increase in coupling ($\Omega \rightarrow 0$) because of water deficit, since the most coupled canopies are more controlled by stomatal conductance and, therefore, by fluctuations of water in soil. Other researchers have reported the increase in the canopy resistance and a decrease in aerodynamic resistance that cause a greater coupling during water deficit events (Aires et al., 2008; José Darlon Nascimento Alves et al., 2022; de Kauwe et al., 2017; Ferreira, 2017; Paulino Junior and Silva von Randow, 2017; Silva et al., 2017b; Spinelli et al., 2018a; Sutherlin et al., 2019a). (Khatun et al., 2011) also found this increased coupling because of water stress in Asian forests. Rana and Katerji (1998) reported that in sorghum canopies under water limited conditions the greater coupling caused ET to depend only on canopy resistance (R_c). In contrast, when there is an increase in SWC and LE, there is an increase in the values of Ω, which indicates a positive correlation between SWC and LE with Ω. In other words, increases in LE occur with a more uncoupled condition ($\Omega \rightarrow 1$) because of lower water deficit thanks to higher SWC (Sutherlin et al., 2019).

During the periods with limiting soil moisture or water deficit, plants reduce the stomatal conductance (g_s) (higher R_s) due to the canopy experiencing a larger saturation deficit (high VPD) and high temperature (Aires et al., 2008; José Darlon Nascimento Alves et al., 2022). In this condition, **Ω** approaches 0, being those low values an indicative that ET is strongly controlled by VPD and g_s (Aires et al., 2008; José Darlon Nascimento Alves et al., 2022;

Ferreira, 2017; Jarvis, 1985). The high coupling to the atmosphere in response to high VPD causes higher surface resistance (*Rs*), a condition that drastically reduces transpiration and canopy ET. This high control of stomatal conductance prevents the excessive losses of water, maintain essential metabolic activities and minimize dehydration caused by high demand of the atmosphere (José Darlon Nascimento Alves et al., 2022; Jarvis, 1985; P G Jarvis and Mcnaughton, 1986; Spinelli et al., 2018a, 2016).

Without great limitations or fluctuations of water in the soil, a canopy can have a greater advantage if it increases the decoupling ($\Omega \rightarrow 1$) since the transpiration is not affected by the stomatal conductance and the water content in the soil (Sutherlin et al., 2019a). When soil moisture decreases, the lower water available and higher VPD could cause mortality in vegetation, therefore, a canopy could have greater advantage in situations of water deficit if it starts to increase coupling ($\Omega \rightarrow 0$), since it would have greater control over water losses by increase surface resistance and the stomata close to retain water (Aires et al., 2008; José Darlon Nascimento Alves et al., 2022; Sutherlin et al., 2019a). However, under severe water deficit there are a dramatic decline in transpiration rate as a result of absolute stomatal closure, whatever the value of Ω (Jarvis, 1985).

But *how much should the conductance change to restrict transpiration under water deficit*? Jarvis and Mcnaughton (1986a) states that in a crop or canopy regions with $\Omega \rightarrow 0$ value (in well-watered conditions), more sensitive reductions in evapotranspiration occur in response to stomatal closure induced by water deficit (Jarvis, 1985) and a *smaller change in conductance is required to restrict evapotranspiration* (due to the dependence of E on *gs*). Therefore, in canopies naturally coupled (due to its "*structural context*"), water deficit has more impact on ET reduction (Ferreira, 2017). In $\Omega \rightarrow 1$ situation, a large decrease would be required in stomatal conductance or a large increase in canopy resistance to restrict evapotranspiration because transpiration is not very sensitive to changes in conductance and is mainly controlled by net radiation. Therefore, as the Ω decrease when water deficit increases, having a decoupled ($\Omega \rightarrow 1$) canopy as high as possible makes that the impact in ET is as low as possible when stomata close (lower *gs*) or canopy resistance (*Rc*) increase (Ferreira, 2017; Jarvis, 1985; Spinelli et al., 2018a). This low sensitivity of transpiration to changes in *gs* and *Rc* indicates that trying to control leaf water potential by manipulating conductance is ineffective. This is one of the reasons why anti-transpiring products have not good results when $\Omega \rightarrow 1$ (Jones, 1990) It could be indicated that in those circumstances that predispose a predominance of stomatal control of transpiration (low Ω values), ET is more sensitive to large changes in soil water content.

5.4.5. The degree of coupling could help to identify the capacity of canopy/crop to reduce excessive water losses under water deficit

The plant's primary necessity is to maintain its water content. In this sense, plants evolved adaptations to survive in a much more coupled environment through developing control mechanisms like stomatal regulation on transpiration. However, such mechanisms are not as effective in a decoupled crop canopy (Jarvis, 1985). Indeed, the potential for water conservation is greater in the more coupled canopies to the atmosphere than in decoupled ones (Fereres and Soriano, 2007; Spinelli et al., 2018a).

The Ω could be functional to determine the sensitivity of evapotranspiration to canopy resistance during water deficit, as demonstrated by Spinelli et al. (2016, 2018) in *Prunus dulcis*. On the other hand, there are certain conditions or "*structural context*" of the vegetation that are typically better able to reduce water losses under drought. A "decoupled" condition means that the canopy/crop can minimally control its transpiration rate via stomatal

regulation (Aires et al., 2008; José Darlon Nascimento Alves et al., 2022; Jarvis, 1985; McNaughton and Jarvis, 1991; Spinelli et al., 2018a). Even under water deficit, stomatal closure response has a low impact on the reduction of ET and a large increase in canopy resistance may result in a marginal reduction in transpiration (Spinelli et al., 2018a, 2016). Therefore, a *structural context* of canopy or crop where predominate uncoupled regions there will be less capacity to reduce evapotranspiration and avoid water losses under water deficit conditions (Spinelli et al., 2018a). On the other hand, in a "highly coupled conditions", canopy resistance control is higher and able to reduce the ET because of stomatal closure immediately limits the excessive losses of water. Therefore, *a structural context* where more coupled regions predominate will have a high capacity to reduce ET and maintain a water-saving strategy under water deficit conditions.

5.4.6. Linking the decoupling factor (Ω) with CO_2 exchange

In conditions of water deficit, the closure of the stomata is the first and main mechanism that limits the loss of water. The cost of stomatal closure is a lower permeability of the leaves to CO_2, which limits the assimilation of Carbon (Brodribb and Holbrook, 2003; Nadal-Sala et al., 2021b). At the beginning of water stress, the decrease in photosynthesis is caused by stomatal limitations (SL) (Kamanga et al., 2018b; Mafakheri et al., 2010b), due to the diffusive resistance of the stomata to the entry of CO_2. Stomata close rapidly, resulting in decreased transpiration and net photosynthesis caused by decreased supply and diffusion of CO_2 to carboxylating enzymes (Flexas and Medrano, 2002b; Galmés et al., 2007; Li et al., 2007b; Mafakheri et al., 2010b). With the progress of water deficit and water stress, the absorption of CO_2 is mainly limited by non-stomatal limitations (NSL) caused by the reduction of mesophyll conductance and photochemical and enzymatic limitations (Galmés et al., 2007; Varone et al., 2012c). As previously indicated, the degree of coupling increases under conditions of water deficit, and such coupling indicates greater control of evapotranspiration by stomatal conductance as a strategy to limit water losses. However, this also indicates lower carbon assimilation. In a decoupled canopy the impact of increasing *Rc* over ET is low but causes SL to photosynthesis. However, the high VPD and the low SWC on which the increase in coupling occurs for reducing ET and minimizing excessive water loss, cause metabolic damage and effects on the plant's primary metabolism related to NSL to photosynthesis. Therefore, the increased coupling under water deficit is directly associated with SL and NSL from plant water stress. From another point of view, in a decoupled canopy under well-watered conditions, ET works as an equilibrium evapotranspiration ET_{eq} which depends only on available radiation. However, under water deficit, when rc increases as a result of an increase of coupling ET starts to work at an imposed evaporation rate ET_{imp}, which depends on the saturation deficit and rc only. This means that, when in a decoupled canopy ET works at an imposed rate, at the same time, the carbon assimilation is limited by both SL and NSL to photosynthesis. Therefore, **Ω** allows not only to know if ET works at ET_{eq} or ET_{imp}, or if canopy increases its control over water vapor flux but recognized possible SL and NSL limitations at the ecosystem level that affects CO_2 assimilation.

Beyond this, the impact on carbon exchange associated with the degree of coupling could be studied in terms of carbon assimilation/transpiration relation or "water use efficiency" (WUE) (Spinelli et al., 2018a, 2016). It is generally accepted that under water deficit, the induced stomatal closure must increase water use efficiency (Rouhi et al., 2007; Spinelli et al., 2018a, 2016). However, in a decoupled canopy stomatal closure may restrict photosynthesis more than it restricts transpiration (Jarvis, 1985; P G Jarvis and Mcnaughton, 1986; Spinelli et al., 2018a, 2016), in consequence WUE could be lower compared to more coupled canopies. A proposed explanation is that in an unstressed "decoupled" canopy, *Rc*/*Ra* is low which means that the stomatal-canopy resistance is relatively

unimportant compared to the larger aerodynamic resistance (Ferreira, 2017; Nassif et al., 2014; Spinelli et al., 2018a, 2016). However, under water deficit conditions, a canopy gets more coupled by *Rc* increases, which causes inherent limitations to CO_2 assimilation. Furthermore, *Ra* decreases, but the aerodynamic resistance for CO_2 is higher than for water vapor due to the 'excess resistance' for CO_2 (Steduto and Hsiao, 1998), which could cause additional limitations for CO_2 fluxes from the turbulent activity of the surface boundary layer.

Considering the points discussed above, we agree Steduto and Hsiao (1998): "*the degree of coupling between the plant canopy and the atmosphere characterizes the extent to which stomatal and canopy conductance may control water vapor and CO_2 Exchange*". Although forests, tree canopies, and tall, rough vegetation are generally considered more closely coupled than pastures or low-growth crops (P G Jarvis and Mcnaughton, 1986; Köstner et al., 1992; Rana and Katerji, 1998; Spinelli et al., 2018a) we try to summarize characteristics that depict '*structural context*' predisposing coupling or decoupling conditions that could indicate the capacity of canopy/crop to reduce excessive water losses and maintain a high assimilation/transpiration relation under water deficit. Table 1 indicates some characteristics that could predispose crops to higher/lower coupling conditions.

Table 1. Structural context of Ω which determines the capacity of canopy/crop to reduce excessive water losses and maintain a high assimilation/transpiration relation under water deficit. Adapted from Jarvis and Mcnaughton (1986)

Low Ω **High capacity of canopy/crop to reduce excessive water losses, higher WUE**	**High Ω** **Low capacity of canopy/crop to reduce excessive water losses, lower WUE**
• Low LAI • Canopy with small leaves • Hypostomatic leaves • Tree-like canopy • Senescence • Leaves more exposed to the wind, from the periphery • Spaced crops • Crop edges • Sunrise and sunset	• LAI large, or increasing • Leaves are large, the larger the blade, the more decoupled it is • Amphiestomatic leaves • Low, smoother canopies • Areas exposed to low wind speed • Continuous canopies • Hours close to noon • Windbreaks around fields

Decoupling indicates low sensitivity of transpiration to canopy resistance. This means that under mild or moderate water deficit events, the stomatal closure, and the increase in the resistance of the canopy (as the first biological response) will not have control over the transpiration, and indirectly over the leaf water potential. This condition causes a low WUE due to the increase in canopy resistance and has a greater restriction in the carbon fluxes than for water vapor. For these reasons, a decoupling condition could be disadvantageous when facing water deficit conditions.

5.5. Conclusions

Nowadays we know that the coupling level increases under conditions of water deficit, causing the ET to depend only on the resistance of the canopy (*Rc*) and this increased coupling could be associated **with stomatal**

limitations of photosynthesis, mainly in presence of mild and moderate water deficit. However, the impact of this greater coupling on CO_2 exchange between canopies with different **Ω** values are still not well understood.

From the central work of McNaughton and Jarvis (1983), the decoupling coefficient **Ω** is a basic measure of the degree of the aerodynamic coupling between plants and the boundary layer. However, its interpretation could go beyond the description of the characteristics of the land surface and the partition between equilibrium or imposed evapotranspiration. This paper shows that it is possible to delineate a '*structural context'* that predisposes high Ω values and a low capacity to get into a water-saving strategy under water deficit conditions. A decoupled canopy has an imbalance in the restrictions of carbon and water fluxes by increases in canopy resistance, being greater for carbon fluxes and having a potentially large impact on gross primary productivity. This decoupling condition could be disadvantageous under water deficit conditions. Therefore, in low and smooth canopies it is important to accurately determine the switch between imposed and equilibrium evapotranspiration and the impact on WUE. This gains relevance for future research in irrigation management related to deficit irrigation in high LAI crops which seeks to impose limited but not severe stress.

Through the analysis of Ω could be studied the environmental controls of ET and GPP fluxes under the contrasting soil water availability. Ω and their underlying theory could give new information about carbon–water interactions. Future studies could be developed to study temporal scales of water and carbon fluxes interactions, and the intrinsic link between carbon and water fluxes through stomatal conductance/canopy resistance at the ecosystem level as well as at the leaf level.

References

Aires, L.M., Pio, C.A., Pereira, J.S., 2008. The effect of drought on energy and water vapour exchange above a mediterranean C3/C4 grassland in Southern Portugal. Agric For Meteorol 148, 565–579. https://doi.org/10.1016/j.agrformet.2007.11.001

Allen, R.G., Pereira, L.S., Dirk, R., Smith, M., 2006. Evapotranspiración del cultivo, Guías para la determinación de los requerimientos de agua de los cultivos, FAO. Roma. https://doi.org/10.1590/1983-40632015v4529143

Alves, J.D.N., Ribeiro, A., Rody, Y.P., Loos, R.A., 2022. Energy balance and surface decoupling factor of a pasture in the Brazilian Cerrado. Agric For Meteorol 319. https://doi.org/10.1016/j.agrformet.2022.108912

Brodribb, T.J., Holbrook, N.M., 2003. Stomatal closure during leaf dehydration, correlation with other leaf physiological traits. Plant Physiol 132, 2166–2173. https://doi.org/10.1104/pp.103.023879

de Kauwe, M.G., Medlyn, B.E., Knauer, J., Williams, C.A., 2017. Ideas and perspectives: How coupled is the vegetation to the boundary layer? Biogeosciences 14, 4435–4453. https://doi.org/10.5194/bg-14-4435-2017

Fereres, E., Soriano, M.A., 2007. Deficit irrigation for reducing agricultural water use. J Exp Bot 58, 147–159. https://doi.org/10.1093/jxb/erl165

Ferreira, M.I., 2017. Stress coefficients for soil water balance combined with water stress indicators for irrigation scheduling of woody crops. Horticulturae 3. https://doi.org/10.3390/horticulturae3020038

Flexas, J., Medrano, H., 2002. Drought-inhibition of photosynthesis in C3 plants: Stomatal and non-stomatal limitations revisited. Ann Bot 89, 183–189. https://doi.org/10.1093/aob/mcf027

Galmés, J., Medrano, H., Flexas, J., 2007. Photosynthetic limitations in response to water stress and recovery in Mediterranean plants with different growth forms. New Phytologist 175, 81–93. https://doi.org/10.1111/j.1469-8137.2007.02087.x

Jarvis, P.G., 1985. Coupling of transpiration to the atmosphere in horticultural crops: the omega factor. Acta Horticulturae 187–205.

Jarvis, P.G., Mcnaughton, K.G., 1986. Stomatal Control of Transpiration: Scaling Up from Leaf to Region. Adv Ecol Res 15, 1–49. https://doi.org/10.1016/S0065-2504(08)60119-1

Jones, H.G., 1990. Physiological Aspects of the Control of Water Status in Horticultural Crops. HortScience 25, 19–25. https://doi.org/10.21273/hortsci.25.1.19

Kamanga, R.M., Mbega, E., Ndakidemi, P., 2018. Drought Tolerance Mechanisms in Plants: Physiological Responses Associated with Water Deficit Stress in Solanum lycopersicum. Advances in Crop Science and Technology 06. https://doi.org/10.4172/2329-8863.1000362

Khatun, R., Ohta, T., Kotani, A., Asanuma, J., Gamo, M., Han, S., Hirano, T., Nakai, Y., Saigusa, N., Takagi, K., Wang, H., Yoshifuji, N., 2011. Spatial variations in evapotranspiration over East Asian forest sites. I. Evapotranspiration and decoupling coefficient. Hydrological Research Letters 5, 83–87. https://doi.org/10.3178/hrl.5.83

Köstner, B.M.M., Schulze, E.D., Kelliher, F.M., Hollinger, D.Y., Byers, J.N., Hunt, J.E., McSeveny, T.M., Meserth, R., Weir, P.L., 1992. Transpiration and canopy conductance in a pristine broad-leaved forest of Nothofagus: an analysis of xylem sap flow and eddy correlation measurements. Oecologia 91, 350–359. https://doi.org/10.1007/BF00317623

Kumagai, T., Saitoh, T.M., Sato, Y., Morooka, T., Manfroi, O.J., Kuraji, K., Suzuki, M., 2004. Transpiration, canopy conductance and the decoupling coefficient of a lowland mixed dipterocarp forest in Sarawak, Borneo: dry spell effects. J Hydrol (Amst) 287, 237–251. https://doi.org/https://doi.org/10.1016/j.jhydrol.2003.10.002

Li, W., Zhang, S., Shan, L., 2007. Responsibility of non-stomatal limitations for the reduction of photosynthesis-response of photosynthesis and antioxidant enzyme characteristics in alfalfa (Medicago sativa L.) seedlings to water stress and rehydration. Front Agric China 1, 255–264. https://doi.org/10.1007/s11703-007-0044-5

Mafakheri, A., Siosemardeh, A., Bahramnejad, B., Struik, P.C., Sohrabi, E., 2010. Effect of drought stress on yield, proline and chlorophyll contents in three chickpea cultivars. Aust J Crop Sci 4, 580–585.

Marin, F.R., 2021. Microclimatología Agrícola: Introdução biofísica da relação planta-atmosfera. FEALQ, Piracicaba.

Marin, F.R., Angelocci, L.R., 2011. Irrigation requirements and transpiration coupling to the atmosphere of a citrus orchard in Southern Brazil. Agric Water Manag 98, 1091–1096. https://doi.org/10.1016/j.agwat.2011.02.002

Marin, F.R., Angelocci, L.R., Nassif, D.S.P., Costa, L.G., Vianna, M.S., Carvalho, K.S., 2016. Crop coefficient changes with reference evapotranspiration for highly canopy-atmosphere coupled crops. Agric Water Manag 163, 139–145. https://doi.org/10.1016/j.agwat.2015.09.010

Marin, F.R., Angelocci, L.R., Righi, E.Z., 2001. Modelo simplificado para estimativa da resistência foliar à difusão de vapor de árvores de lima ácida "Tahiti." Revista Brasileira de Agrometeorologia 9, 227–233.

McNaughton, K.G., Jarvis, P.G., 1991. Effects of spatial scale on stomatal control of transpiration. Agric For Meteorol 54, 279–302. https://doi.org/https://doi.org/10.1016/0168-1923(91)90010-N

Moher, D., Liberati, A., Tetzlaff, J., Altman, D.G., 2009. Preferred reporting items for systematic reviews and meta-analyses: the PRISMA statement. Open Med 3, e123–e130. https://doi.org/10.1136/bmj.b2535

Monteith, J., 1965. Evaporation and enviroment. Symp Soc Exp Biol 19, 205–234.

Monteith, J., Unsworth, M.H., 2013. Principles of Enviromental Physics, Chemical Geology. https://doi.org/10.1016/0009-2541(75)90087-X

Nadal-Sala, D., Grote, R., Birami, B., Knüver, T., Rehschuh, R., Schwarz, S., Ruehr, N.K., 2021. Leaf Shedding and Non-Stomatal Limitations of Photosynthesis Mitigate Hydraulic Conductance Losses in Scots Pine Saplings During Severe Drought Stress. Front Plant Sci 12. https://doi.org/10.3389/fpls.2021.715127

Nassif, D.S.P., Marin, F.R., Costa, L.G., 2014. Evapotranspiration and Transpiration Coupling to the Atmosphere of Sugarcane in Southern Brazil: Scaling Up from Leaf to Field. Sugar Tech 16, 250–254. https://doi.org/10.1007/s12355-013-0267-0

Paulino Junior, N., Silva von Randow, 2017. Analysis of biological and meteorological controls of evapotranspiration in pristine forests and a pasture site in Amazonia. Revista Ambiente e Agua 12, 179–191. https://doi.org/10.4136/1980-993X

Penman, H.L., 1948. Natural evaporation from open water, bare soil and grass. Proceedings of the Royal Society of London 193, 120–145.

Rana, G., Katerji, N., 1998. A Measurement Based Sensitivity Analysis of the Penman-Monteith Actual Evapotranspiration Model for Crops of Different Height and in Contrasting Water Status 149, 141–149.

Rosenberg, N.J., Blad, B.L., Verma, S.B., 1983. Microclimate: the biological environment.

Rouhi, V., Samson, R., Lemeur, R., Damme, P. van, 2007. Photosynthetic gas exchange characteristics in three different almond species during drought stress and subsequent recovery. Environ Exp Bot 59, 117–129. https://doi.org/10.1016/j.envexpbot.2005.10.001

Silva, P.F. da, Lima, J.R. de S., Antonino, A.C.D., Souza, R., de Souza, E.S., Silva, J.R.I., Alves, E.M., 2017. Seasonal patterns of carbon dioxide, water and energy fluxes over the Caatinga and grassland in the semi-arid region of Brazil. J Arid Environ 147, 71–82. https://doi.org/10.1016/j.jaridenv.2017.09.003

Spinelli, G.M., Snyder, R.L., Sanden, B.L., Gilbert, M., Shackel, K.A., 2018. Low and variable atmospheric coupling in irrigated Almond (Prunus dulcis) canopies indicates a limited influence of stomata on orchard evapotranspiration. Agric Water Manag 196, 57–65. https://doi.org/10.1016/j.agwat.2017.10.019

Spinelli, G.M., Snyder, R.L., Sanden, B.L., Shackel, K.A., 2016. Water stress causes stomatal closure but does not reduce canopy evapotranspiration in almond. Agric Water Manag 168, 11–22. https://doi.org/10.1016/j.agwat.2016.01.005

Steduto, P., Hsiao, T.C., 1998. Maize canopies under two soil water regimes III. Variation in coupling with the atmosphere and the role of leaf area index. Agric For Meteorol 89, 201–213. https://doi.org/10.1016/S0168-1923(97)00083-X

Sutherlin, C.E., Brunsell, N.A., de Oliveira, G., Crews, T.E., DeHaan, L.R., Vico, G., 2019. Contrasting physiological and environmental controls of evapotranspiration over Kernza Perennial crop, annual crops, and C4 and mixed C3/C4 grasslands. Sustainability (Switzerland) 11. https://doi.org/10.3390/su11061640

Varone, L., Ribas-Carbo, M., Cardona, C., Gallé, A., Medrano, H., Gratani, L., Flexas, J., 2012. Stomatal and non-stomatal limitations to photosynthesis in seedlings and saplings of Mediterranean species pre-conditioned and aged in nurseries: Different response to water stress. Environ Exp Bot 75, 235–247. https://doi.org/10.1016/j.envexpbot.2011.07.007

Zhang, Z.Z., Zhao, P., McCarthy, H.R., Zhao, X.H., Niu, J.F., Zhu, L.W., Ni, G.Y., Ouyang, L., Huang, Y.Q., 2016. Influence of the decoupling degree on the estimation of canopy stomatal conductance for two broadleaf tree species. Agric For Meteorol 221, 230–241. https://doi.org/10.1016/j.agrformet.2016.02.018

6. GENERAL CONCLUSIONS

Irrigation is an important mitigation practice, due to is an effective means to improve iWUE, minimizing the water cost of carbon gain. Expanding potato irrigation area (where water reserves allow) or using more effective irrigation measures can enhance carbon sequestration in potato fields through enhanced yields and productivity. In irrigated potato systems, photosynthetic carbon input was increased and carbon return through respiration was decreased. Therefore, the carbon sink capacity was increased. The magnitude and dynamics of carbon sequestration observed in the negative values of the NEE is a function of the magnitude and evolution of the GPP in relation to canopy and tuber growth. In general, growth stages have defined the destinations of the GPP in biomass. Tuberization had the greatest carbon sink strength due to its highest GPP values. The vegetative stage is key. The formation of canopy occurs, which will serve as a carbon source organ for the tubers during tuberization and tuber filling. The feedback occurring between canopy and the GPP guarantees carbon for the main sink organs. 2. From the GPP-ET coupling, the higher photosynthetic CO_2 gain per unit of water transpired is related to a high magnitude, proportionality, and synchrony of its diurnal fluxes, which in turn are controlled by the radiative environment, and by a canopy with a larger LAI and thicker leaves, physiologically active (high photosynthetic response to PPFD and high photosynthetic and respiratory activities) and low superficial resistance.

In general, under water deficit, GPP becomes more limited due to canopy increases of Rc (as VPD increases), the very low response to PPFD, and the smallest area, thickness, and duration of the canopy. However, the restriction from Rc to carbon flux is a side effect caused by the restriction to water vapor. Potato is a decoupled (high omega) species and therefore has low control over carbon and water fluxes. The conductance of the canopy regulates through the circadian rhythm or daily regular changes. However, it is not very sensitive to changes in soil water content. The low coupling of canopy to the atmosphere means that it has few possibilities of controlling excessive water losses under water deficit. Apparently, the control mechanisms like higher surface resistance to minimize excessive water loss works only in high atmospheric evaporative demand and very low SWC, and although it reduces ET, it has great consequences on GPP. It could be say that VPD plays a stronger role in controlling carbon and water fluxes when the soil moisture is not adequate, than otherwise and therefore VPD, by means of the omega factor, could be a superior indicator for understanding the response of GPP and ET to drought.

Under water deficit, a decoupled crop ($\Omega \sim 1$) increases its coupling (lowering Ω) because of a high increase in canopy resistance (at high VPD and low SCW) to reduce water vapor flux (ET). However, this increase in canopy resistance can lead to a much greater reduction in carbon uptake. This means that: 1. When in a decoupled canopy stomata close (increasing Rc), the impact in ET is low, but higher for GPP, and this effect on the GPP is called stomatal limitations to photosynthesis (SL). 2. The high atmospheric demands and the low SWC on which the increase in coupling occurs, cause metabolic damage and effects on the plant's primary metabolism related to non-stomatal limitations to photosynthesis (NSL). 3. Both SL and NSL occur at the ecosystem level as a result of increases in canopy coupling to the atmosphere.

From another point of view, in a decoupled canopy under well-watered conditions, ET works as an equilibrium evapotranspiration ET_{eq} which depends only on available radiation. However, under water deficit, when Rc increases as a result of an increase of coupling ET starts to work at an imposed evaporation rate ET_{imp}, which depends on the saturation deficit and Rc only. This means that, when ET works at an imposed rate, at the same time, the carbon assimilation is limited by both stomatal limitations (SL) and non-stomatal limitations (NSL) to photosynthesis. Therefore, Ω allows not only to know if ET works at ET_{eq} or ET_{imp}, or if canopy increases its

control over water vapor flux but recognized possible SL and NSL limitations at the ecosystem level that affects the GPP.

Based on the up-scaling results, it will be possible to alternatively estimate the GPP at the ecosystem level, which is an advantage for the study of the ability to offset emissions of potato crops growing in hillside conditions and in places where there is no it is possible to establish measurements with the EC technique.

The results of this research give novel information about carbon–water relations in potato crops. The used metrics and their underlying theory provide a way to understand the determinants of change in the IWUE and its effect on the NEE.

APPENDIX

Inherent water use efficiency

IWUE was determined following the theoretical approach proposed by Beer et al. (2009). The coupling of carbon assimilation (A) and water losses (E) are based on the gradient flux concept. Following Fick, CO_2 and water fluxes are given by their concentration gradients through the leaves multiplied by a diffusion coefficient (Di), called stomatal conductance (g).

$$A = D_{CO_2} * a * (\Delta c) \quad (1)$$

and $$E = D_{H_2O\,v} * a * (\Delta v) \quad (2)$$

were, DCO_2 and DH_2O are diffusion coefficients of CO_2 and water vapor, respectively; Δc and Δv the difference between ambient and inner leaf partial pressure of carbon dioxide y and water vapor pressure, respectively and a is the cross-sectional area of the stomata.

Being the stomatal conductance

$$g = D_{CO_2} * a \quad (3)$$

we have,

$$A = g_c * (\Delta c) \quad (4)$$

and $$E = (1.6 * g_c) * (\Delta v) \quad (5)$$

were 1.6 is the molar diffusivity ratio of CO_2 - H_2O (i.e., $gH_2O = gCO_2 * 1.6$, lighter H_2O molecules diffuse more rapidly than does CO_2) "1.6*g" is the stomatal conductance for water vapor $g_{H_2O\,v}$ (Gentilesca et al., 2021b; Li et al., 2017).

The intrinsic water-use efficiency (iWUE) ate leaf scale is defined as the ratio of the fluxes of net photosynthesis and conductance for water vapor.

$$iWUE = \frac{A}{g_{H_2O\,v}} = \frac{g_c*(\Delta c)}{1.6*g_c} = \frac{\Delta c}{1.6} \quad (6)$$

At the ecosystem level, the alternative inherent water use efficiency (IWUE) was proposed by (Beer et al., 2009) by approximating the vapor pressure difference Δv to atmospheric VPD assuming equal temperatures of leaves and atmosphere, by approximating the leaf level carbon assimilation A and transpiration E to fluxes of GPP, and ET (soil evapotranspiration is small, and canopy transpiration (T) takes up a large proportion of ET) from eddy covariance observations and, by neglecting aerodynamic resistance.

Therefore, we have that, Eq.4 is now

$$GPP = g' * (\Delta c') \quad (7)$$

and Eq. 5 is $$ET = 1.6 * g' * VPD \quad (8)$$

The usage of marker ´ indicates that variables are analyzed at ecosystem level. Resolving g' at ecosystem level from Eq.4:

$$g' = \frac{ET}{1.6*VPD} \quad (9)$$

Were, g' is the conductance at the ecosystem level proposed by Beer. The inherent water use efficiency (IWUE) is represented by:

$$IWUE = \frac{GPP}{g'} = \frac{g\prime*(\Delta c')}{1.6*g'} = \frac{\Delta c\prime}{1.6} = \frac{GPP}{1.6*\left[\frac{ET}{1.6*VPD}\right]} = \boldsymbol{\frac{GPP*DPV}{ET}} \quad (10)$$